Invest Manitoba
Open for Business

Report of Activities 2023

Manitoba

REPORT OF ACTIVITIES
2023

Manitoba Economic Development, Investment, Trade and Natural Resources
Manitoba Geological Survey

Manitoba

Published by:
Manitoba Economic Development, Investment, Trade and Natural Resources
Manitoba Geological Survey
360–1395 Ellice Avenue
Winnipeg, Manitoba
R3G 3P2 Canada
Telephone: 1-800-223-5215 (General Enquiry)
204-945-6569 (Publication Sales)
Fax: 204-945-8427
Email: minesinfo@gov.mb.ca
Website: manitoba.ca/minerals

ISBN: 978-0-7711-1648-3

This publication is available to download free of charge at manitoba.ca/minerals

Front cover photo:
Manitoba Geological Survey geologists Michelle Gauthier and Jerrold Rentz examine a glaciofluvial deposit in southeastern Manitoba as part of the renewed MGS aggregate resource program (GS2023-14, this volume).

REPORT OF ACTIVITIES 2023

Minister's Message

As Minister of Economic Development, Investment, Trade and Natural Resources, it is my pleasure to present the *Report of Activities 2023*. This publication provides a comprehensive update on geoscience projects and activities conducted by the Manitoba Geological Survey (MGS) over the past year. This year's volume includes 14 reports and five supplementary data repository items, another significant update to Manitoba's geoscience knowledge base.

High quality geoscience data is essential to exploration and mineral resource development, and supports sector investment in our province. MGS research guides mineral exploration activities within established commodity extraction jurisdictions and our frontier areas.

Manitoba's wealth of mineral resources and high potential for new discoveries continues to be a focus of the MGS' geoscientific studies. Our province is home to 29 of the 31 minerals found on Canada's 2021 Critical Minerals List including lithium, graphite, nickel, cobalt, copper and rare-earth elements, six minerals recognized by the Canadian government as having the greatest opportunity to support economic growth and fuel domestic supply chains.

There have been a number of important developments within our provincial mining and exploration sector this past year.

Manitoba's first potash development project began pilot production, led by the Potash and Agri Development Corporation of Manitoba and its equity partner Gambler First Nation.

Recent lithium discoveries in our province sparked excitement and investment interest as global demand for this critical component grows with its use in electric vehicle batteries. Manitoba is also rich in commodities that are integral to the green energy transition, including nickel and cobalt from Thompson, copper and zinc from Snow Lake, and lithium and cesium from Lac du Bonnet.

Manitoba's rich mineral resources and mining framework offer unique advantages to our industries, investors and communities. I encourage you to explore the information found in this report, and connect with our geologists to discuss how their findings can support your exploration interests and make the most of our shared potential and opportunities.

Original signed by

Honourable Jamie Moses

Manitoba Economic Development, Investment, Trade and Natural Resources

Rapport d'activités 2023

Message du ministre

En tant que ministre du Développement économique, de l'Investissement, du Commerce et des Ressources naturelles, je suis heureux de présenter le Rapport d'activités 2023. Cette publication fait le point sur les projets et activités géoscientifiques menés par la Direction des services géologiques du Manitoba (la Direction) au cours de la dernière année. Le recueil de cette année comprend 14 rapports et cinq dépôts de données supplémentaires, ce qui constitue une autre actualisation importante de la base de connaissances géoscientifiques du Manitoba.

Des données géoscientifiques de haute qualité sont essentielles à l'exploration des ressources minérales et à l'exploitation minière, et soutiennent les investissements du secteur dans notre province. Les recherches de la Direction orientent les activités d'exploration minérale dans les zones d'extraction de matières premières établies et dans nos régions pionnières.

La richesse en ressources minérales du Manitoba et le potentiel élevé de nouvelles découvertes continuent d'être au centre des études géoscientifiques de la Direction. Notre province recèle 29 des 31 minéraux figurant sur la liste des minéraux critiques du Canada dressée en 2021, dont le lithium, le graphite, le nickel, le cobalt, le cuivre et les éléments des terres rares, six minéraux reconnus par le gouvernement canadien comme ayant les meilleures chances de soutenir la croissance économique et d'alimenter les chaînes d'approvisionnement nationales.

L'année dernière, le secteur manitobain de la prospection et de l'exploitation minières a connu un certain nombre d'avancées importantes.

Le premier projet d'exploitation de la potasse au Manitoba a commencé sa production pilote, sous la direction de la Potash and Agri Development Corporation of Manitoba et de son partenaire financier, la Première Nation de Gambler.

En outre, les récentes découvertes de lithium dans notre province ont suscité l'enthousiasme et l'intérêt des investisseurs, car la demande mondiale de ce composant essentiel augmente sans cesse en raison de son utilisation dans les batteries des véhicules électriques. Le Manitoba est également riche en matières premières qui font partie intégrante de la transition vers l'énergie verte, notamment le nickel et le cobalt de Thompson, le cuivre et le zinc de Snow Lake, ainsi que le lithium et le césium de Lac du Bonnet.

Cette richesse en ressources minérales et le cadre minier du Manitoba offrent des avantages uniques à nos industries, à nos investisseurs et à nos collectivités. Je vous invite à prendre connaissance des renseignements contenus dans ce rapport et à communiquer avec nos géologues pour discuter de la manière dont leurs conclusions peuvent soutenir vos intérêts en matière d'exploration, afin de tirer le meilleur parti du potentiel et des possibilités qu'offre notre province.

Original signé par

Monsieur Jamie Moses

Ministre du Développement économique, de l'Investissement, du Commerce et des Ressources naturelles

Foreword

On behalf of the Manitoba Geological Survey (MGS), it is my privilege to present the *Report of Activities 2023*—the annual peer-reviewed volume of geoscience project results by the MGS and its partners.

The MGS Branch comprises five sections within the Resource Development Division (RDD): (1) Precambrian Geoscience (Tania Martins, Acting Chief Geologist); (2) Sedimentary Geoscience (Michelle Nicolas, Chief Geologist); (3) Geoscience Data Management (Greg Keller, Manager); (4) the Resource Centre (Peggy Syljuberget, Manager); and (5) Core Library Facilities (Colin Epp, Manager).

The MGS conducts a wide range of investigations throughout Manitoba, including examining exposed bedrock, subsurface and surficial sediments such as sand, gravel, and oil and gas deposits. It also provides geoscience support for the regulatory framework and tenure systems managed by RDD, which includes oil field-pool code designations, geoscientific review of oil and gas licences and applications, borehole licence reviews, aggregate inquiries and land-use designations. The MGS provides foundational data and unbiased technical support to inform government policy, decision-making, mineral exploration, and land-use management by incrementally developing and advancing a detailed understanding of Manitoba's geology and geological processes. The Survey also presents and showcases its work at conferences, workshops and symposiums. Our international presence was impressive this year, including oral and poster presentations on Manitoba's lithium potential at the Society of Economic Geologists in London, United Kingdom, an oral and poster presentation at the International Union for Quaternary Research in Rome, Italy, and an oral presentation on Manitoba's helium potential at the North American Helium Conference in Denver, Colorado.

This year's 14 articles cover a diverse thematic and geographic range, including greenstone belts with Li-Cs-Ta-Ni-Cu-PGE potential, collaborative geoscience projects focusing on critical minerals, re-interpretation of old data using today's knowledge and technologies, geoscience database innovation, and state-of-the-art surficial geoscience. The Survey selected three oil wells in southwestern Manitoba for volatile fraction analysis. The results show high helium values indicative of potential economic concentrations in the Red River and Deadwood formations. Hydrocarbon analysis on the three wells show hydrocarbon systems in the Dawson Bay and Red River formations. Continued research collaboration with universities are highlighted in the work carried out at the Burntwood Lake syenite complex, the regional mapping of the Wekusko Lake pegmatite field, the Cat Lake–Winnipeg River pegmatite field area, and the Quaternary stratigraphic investigations along the Gods and Yakaw rivers. Manitoba's aggregate program is well documented in this year's volume and will serve as a good reference point for where we have been, where we are today and our expectations for future work. I am particularly interested in the multidisciplinary focus on the Bird River domain. This project's focus is on compilation of bedrock geology, the Mineral Deposits Database (MDD) inventory, and a Quaternary study on using surficial materials sampling in glaciated terrains for lithium exploration. Preliminary results show that there are structural emplacement controls at the regional level, and the results from the MDD compilation show spatial distributions that reflect geological controls on mineralization.

One source of valuable archival material is drillcore collected from industry and government. This year, drillcore from Halfway Lake was re-logged to help constrain the affinity of metasedimentary rocks within the Thompson nickel belt stratigraphy. In addition, a project is underway to preserve the drillcore stored outside at the Thompson facilities. In June, July and early August, I carried out a provincial assessment of all the core library facilities, and the state of the core in the northern areas was of great concern. The storage of the core under the elements resulted in the degradation of boxes, and we routinely had to fix, replace and relabel boxes as part of our maintenance of the core facilities. To remedy this, the core boxes were re-stacked, roofed and covered with tarps. A proposal for a five-year rehabilitation and upgrade plan was submitted to save this archival material and preserve it for future generations.

We continue to fill important gaps in the MDD with the addition of 17 000 mineral occurrences focused on the Superior province. A more comprehensive mineral occurrence dataset directly supports land use and related economic development planning (e.g., parks and infrastructure planning within government, MGS project planning, and community economic development strategies). It may trigger renewed interest in exploration in certain areas.

Over the last year, the MGS saw several staff changes. With great sadness, I announced that Christian Böhm left the Survey to join the industry. Over his 22 years with the MGS, his contributions were paramount. Christian served as Chief Geologist for the Precambrian Geoscience section and Acting Director for the MGS, and was passionate about representing Manitoba in federal–provincial discussions. Some projects he participated in on behalf of Manitoba include the Pan-Canadian Geoscience Strategy and the Canadian Minerals and Metals Plan. Christian was also a strong champion for the Survey on the Geo-mapping for Energy and Minerals Program and Targeted Geoscience Initiatives. We are grateful for Christian's dedication to the Manitoba public service and wish him all the best in his future endeavours. After Christian's departure, Tania Martins was appointed Acting Chief Geologist for the Precambrian Geoscience section.

We continued to build capacity by hiring Timothy Gereta as our new Resource Centre Coordinator. With Tim joining the team, the Resource Centre was able to re-open to the public and launch the new online catalogue of information on Manitoba's geology, mineral and petroleum resources. The Geoscience Data Management Unit added two GIS specialists, Austin Martin and Ben Wheadon, and Grace Dick as a System Analyst. We also welcomed Jerrold Rentz as our new Aggregate Geologist, and welcomed back Pamela Fulton-Regula to the Survey after her acting status as Manager of Tenure Services concluded.

The production of the Report of Activities and a wealth of other MGS publications is only possible with the dedicated efforts of all geologists, GIS specialists, lab technicians, summer students and administrative and Corporate Services staff. I offer a special mention to Colin Epp and Paul Belanger for the extra warehouse hours they put in providing expediting support and meticulous maintenance of our equipment this year, and I know the industry would also join me in thanking both for their support in accessing our core library facilities. Bob Davie and his team from RnD Technical provided outstanding professional technical editing services, and Craig Steffano managed report production and publication layout. I sincerely thank every one of the MGS team for their valuable contributions.

Tafa Kennedy, Ph.D., P.Geo.

Director, Manitoba Geological Survey

Avant-propos

J'ai l'honneur de présenter, au nom de la Direction des services géologiques du Manitoba (la Direction), le Rapport d'activités 2023, un recueil annuel examiné par les pairs compilant les résultats de projets géoscientifiques exécutés par la Direction et ses partenaires.

La Direction, au sein de la Division du développement des ressources (la Division), se compose de cinq sections : (1) la Section du Précambrien (Tania Martins, géologue en chef par intérim); (2) la Section de la géologie sédimentaire (Michelle Nicolas, géologue en chef); (3) la Section de la gestion des données géoscientifiques (Greg Keller, gestionnaire); (4) la Section du centre de ressources (Peggy Syljuberget, gestionnaire); et (5) la Section des installations de stockage de carottes de forage (Colin Epp, gestionnaire).

La Direction mène, dans tout le Manitoba, un vaste éventail d'études qui incluent l'examen du substratum rocheux exposé, des matériaux en subsurface et des sédiments superficiels, comme le sable, le gravier, et les dépôts de pétrole et de gaz. Elle fournit également un soutien géoscientifique en ce qui concerne le cadre de réglementation et les régimes fonciers gérés par la Division, ce qui inclut l'attribution de codes aux champs et aux gisements de pétrole, l'examen géoscientifique des permis et des demandes de permis d'exploitation de pétrole et de gaz, l'examen des permis de forage, les requêtes concernant les agrégats et les affectations du sol. La Direction fournit des données fondamentales et un soutien technique impartial à l'appui des politiques et de la prise de décision gouvernementales, de l'exploration minière et d'un aménagement judicieux du territoire en approfondissant progressivement la compréhension de la géologie et des processus géologiques du Manitoba. La Direction des services géologiques du Manitoba présente également ses travaux dans le cadre de conférences, d'ateliers et de symposiums. Notre présence internationale a été impressionnante cette année; citons notamment des présentations orales et des affiches sur le potentiel du Manitoba en matière de lithium à la Society of Economic Geologists à Londres, au Royaume-Uni, une présentation orale et une affiche à l'International Union for Quaternary Research à Rome, en Italie, et une présentation orale sur le potentiel du Manitoba en matière d'hélium à la North American Helium Conference à Denver, dans le Colorado.

Les 14 articles de cette année couvrent un large éventail thématique et géographique, allant des ceintures de roches vertes présentant un potentiel en Li-Cs-Ta-Ni-Cu-ÉGP aux projets géoscientifiques collaboratifs axés sur les minéraux essentiels, en passant par la réinterprétation d'anciennes données à l'aide des connaissances et des technologies actuelles, l'innovation en matière de bases de données géoscientifiques et les géosciences de surface de pointe. La Direction a sélectionné trois puits de pétrole dans le sud-ouest du Manitoba pour l'analyse des fractions volatiles. Les résultats montrent des valeurs élevées d'hélium indiquant des concentrations économiques potentielles dans les formations de Red River et de Deadwood. L'analyse des hydrocarbures sur les trois puits montre des systèmes d'hydrocarbures dans les formations de Dawson Bay et de Red River. La poursuite de la collaboration avec les universités en matière de recherche est mise en évidence dans les travaux réalisés sur le complexe syénitique du lac Burntwood, la cartographie régionale du champ de pegmatites du lac Wekusko, la zone du champ de pegmatites du lac Cat et de la rivière Winnipeg, et les études stratigraphiques du Quaternaire le long des rivières Gods et Yakaw. Le programme de gestion des carrières d'agrégats du Manitoba est bien documenté dans le recueil de cette année et servira de point de référence pour savoir où nous sommes allés, où nous en sommes actuellement et ce que nous attendons des travaux futurs. Je m'intéresse particulièrement à l'approche multidisciplinaire appliquée au domaine de la rivière Bird. Ce projet se concentre sur la compilation de la géologie du substratum rocheux, l'inventaire de la base de données des gisements minéraux et une étude du Quaternaire sur l'utilisation de l'échantillonnage des matériaux superficiels dans les terrains glaciaires pour l'exploration du lithium. Les résultats préliminaires montrent qu'il existe des contrôles des emplacements structuraux au niveau régional, et les résultats de la compilation de la base de données des gisements minéraux montrent des distributions spatiales qui reflètent les contrôles géologiques sur la minéralisation.

Les carottes de forage obtenues de l'industrie et du gouvernement constituent une source d'archives précieuses. Cette année, les carottes de forage du lac Halfway ont été analysées à nouveau afin de préciser l'affinité des roches métasédimentaires dans la stratigraphie de la ceinture nickélifère de Thompson. De plus, un projet est en cours pour préserver les carottes de forage stockées à l'extérieur des installations de stockage de Thompson. En juin, en juillet et au début d'août, j'ai

procédé à une évaluation provinciale de toutes les installations de stockage de carottes de forage, et l'état de celles des régions nordiques était très préoccupant. L'exposition des carottes de forage aux intempéries a entraîné la dégradation des boîtes, et nous avons dû régulièrement réparer, remplacer et réétiqueter les boîtes dans le cadre de l'entretien des installations de stockage. Pour remédier à cette situation, les boîtes de carottes ont été rempilées, puis couvertes à l'aide d'un toit et de bâches. Une proposition de plan quinquennal de remise en état et de modernisation a été soumise afin de sauver ce matériel d'archives et de le préserver pour les générations futures.

Nous continuons à combler d'importantes lacunes dans la base de données des gisements minéraux avec l'ajout de 17 000 occurrences minérales concentrées dans la province du lac Supérieur. Un ensemble de données plus complet sur les occurrences minérales soutient directement l'aménagement du territoire et la planification du développement économique connexe (par exemple, la planification des parcs et des infrastructures par le gouvernement, la planification des projets de la Direction et les stratégies de développement économique des collectivités). Cette démarche pourrait susciter un regain d'intérêt pour l'exploration de certaines zones.

Au cours de l'année écoulée, la Direction a connu plusieurs changements de personnel. C'est avec une grande tristesse que j'ai annoncé que Christian Böhm a quitté la Direction pour rejoindre l'industrie. Au cours des 22 années qu'il a passées au sein de la Direction, ses contributions ont été considérables. M. Böhm a été géologue en chef de la Section du Précambrien et directeur par intérim de la Direction. Il a également été un représentant passionné du Manitoba dans les discussions fédérales-provinciales. Parmi les projets auxquels il a participé au nom du Manitoba, citons la Stratégie pancanadienne de géoscience et le Plan canadien pour les minéraux et les métaux. Il a également été un important porte-parole de la Direction dans le cadre du Programme de géocartographie de l'énergie et des minéraux et d'Initiatives géoscientifiques ciblées. Nous remercions M. Böhm pour son dévouement à la fonction publique manitobaine et lui souhaitons beaucoup de succès dans ses projets futurs. Après son départ, Tania Martins a été nommée géologue en chef par intérim de la Section du Précambrien.

Nous avons continué à renforcer nos capacités en recrutant Timothy Gereta en tant que nouveau coordonnateur du centre de ressources. Après l'arrivée de M. Gereta dans l'équipe, le centre de ressources a pu rouvrir ses portes au public et lancer le nouveau catalogue en ligne de renseignements sur la géologie et les ressources minérales et pétrolières du Manitoba. Le service de gestion des données géoscientifiques s'est enrichi de deux spécialistes du Système d'information géographique, Austin Martin et Ben Wheadon, et de Grace Dick en tant qu'analyste de systèmes. Nous avons également accueilli Jerrold Rentz en tant que nouveau géologue spécialiste des agrégats, et Pamela Fulton-Regula a réintégré la Direction après avoir été gestionnaire par intérim de la Section de la gestion des droits fonciers.

La production du rapport d'activités, ainsi que d'une multitude d'autres publications de la Direction, ne serait pas possible sans les efforts dévoués de tous les géologues, spécialistes du Système d'information géographique, techniciens de laboratoire, stagiaires d'été et de tout le personnel des services administratifs et ministériels. J'adresse une mention spéciale à Colin Epp et à Paul Belanger pour les heures supplémentaires qu'ils ont consacrées, dans d'entrepôt, à l'assistance à l'expédition et à l'entretien méticuleux de notre équipement cette année, et je sais que l'industrie se joindra à moi pour les remercier tous deux de leur soutien à l'accès à nos installations de stockage de carottes de forage. Bob Davie et son équipe à RnD Technical ont fourni d'excellents services professionnels de révision technique et Craig Steffano a géré la production du rapport et la mise en pages de la publication. Je remercie sincèrement tous les membres de l'équipe de la Direction de leurs précieuses contributions.

La directrice des services géologiques du Manitoba,
Tafa Kennedy, Ph.D., P.Geo.

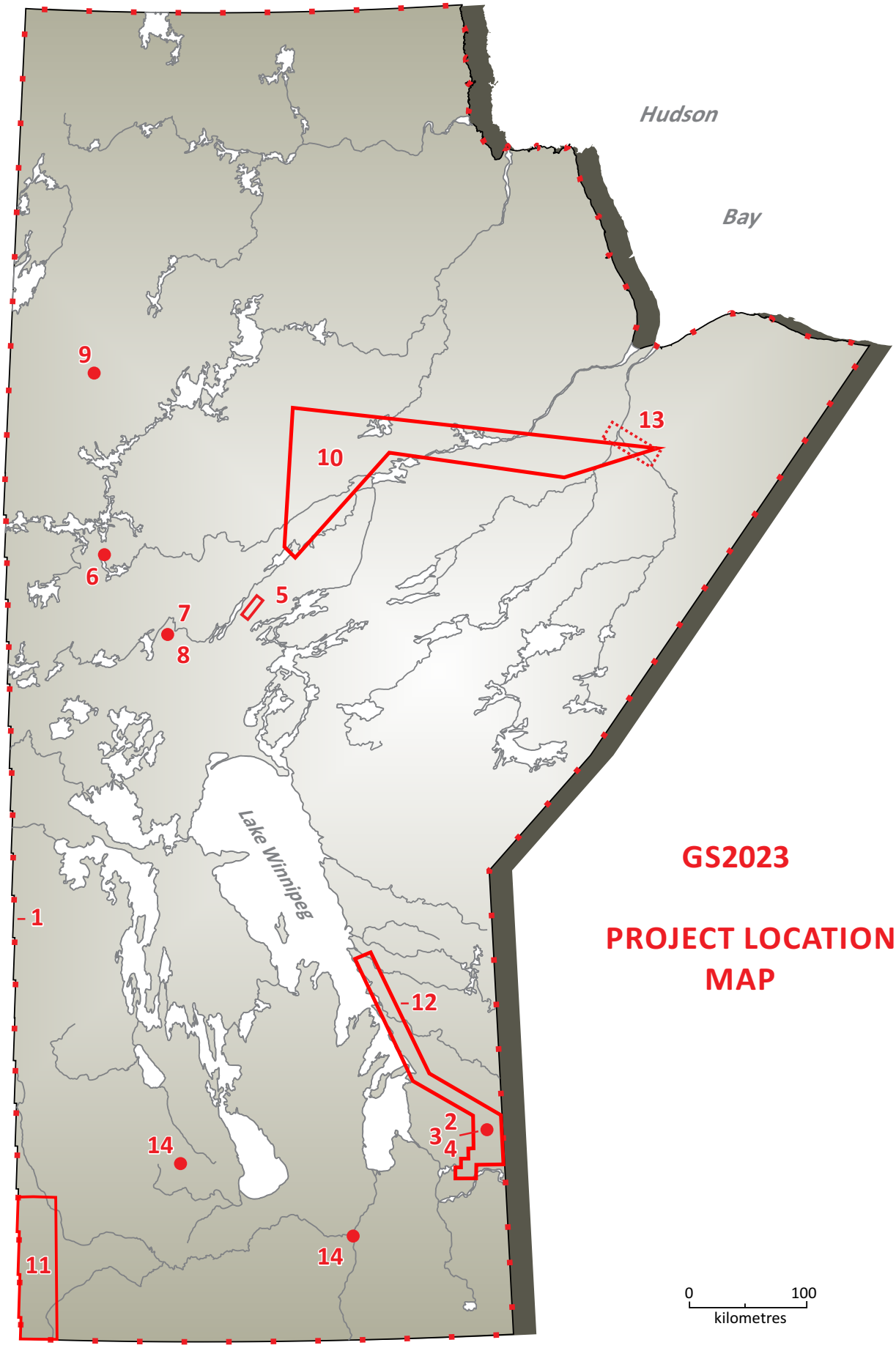
Hudson
Bay
Lake Winnipeg
9
10
13
6
5
7
8
1
12
2
3
4
14
14
11
GS2023
PROJECT LOCATION MAP
0
100
kilometres

Table of Contents

PHANEROZOIC

QUATERNARY

PUBLICATIONS

GS2023-1

Progress report on the Manitoba Mineral Deposits Database

by M.L. Rinne

Summary

The Manitoba Mineral Deposits Database contains data relating to mineral occurrences and deposits throughout the province, including information on critical minerals. Updates to the database during the last year were primarily focused on parts of the Superior province. The latest version includes approximately 17 000 occurrences with location data, and will be provided in GeoFile 5-2023.

In Brief:

- 17,000 mineral occurrences compiled with location data throughout Manitoba
- Most of the 2023 updates were focused on parts of the Superior province
- MDD updates continue to be shared in GeoFile 5

Citation:
Rinne, M.L. 2023: Progress report on the Manitoba Mineral Deposits Database; *in* Report of Activities 2023, Manitoba Economic Development, Investment, Trade and Natural Resources, Manitoba Geological Survey, p. 1–3.

Introduction

The Manitoba Geological Survey (MGS) has been working to update the Mineral Deposits Database (MDD) since 2020. The project rationale and mineral occurrence definitions used for this work are explained in Rinne (2020, 2021, 2022). Specific methods used to help collect mineral occurrence data—including the use of scripts to automate the export of geochemical data tables from scanned PDF files, along with a series of keyword search expressions applied to the main text of industry assessment reports—are described mostly in Rinne (2021). This year's report provides a broad summary of the most recent set of updates to the MDD, followed by an explanation of changes made to allow for faster publication of more preliminary mineral occurrence data.

Results

Since 2020, approximately 35 000 mineral occurrences have been identified in Manitoba, of which nearly half now include preliminary location data. The occurrences with location data are shown in Figure GS2023-1-1, and will also be shared in an updated version of GeoFile 5.

Although new mineral occurrence data have been added from throughout the province, most of the updates during the past year have been focused on parts of the Superior province, where the number of occurrences is now sufficient to resolve the shapes of some greenstone belts and major structures (e.g., Figure GS2023-1-1). For a depiction of the 2023 MDD updates shown at the scale of greenstone belts (and further separated by commodity type), see the report on the Bird River area (Martins et al., 2023).

Changes to the MDD release format

Client requests and feedback helped guide the format of the upcoming MDD release, which has been partially adjusted with the aim of sharing preliminary data more quickly. Compared to last year's release, changes to GeoFile 5 will include the following:

- Partially blank "MDD number" field. Following convention in the previous generation of the MDD (e.g., Conley et al., 2009), the MDD number is a unique identifier assigned to every mineral occurrence in Manitoba. Starting this year, new mineral occurrence numbers are not assigned to new records until other data (especially occurrence locations) have been entered and verified. MDD numbers will be retained for all existing records.
- Partially updated "occurrence classification" field. Occurrence classifications (e.g., mineral occurrence, occurrence with mineral resource estimate, or active mine) have not yet been completed for the more recent mineral occurrence entries, as this requires more information or further review. In addition to a few other fields left partially blank in more recent entries, these columns will be populated as updates continue.
- Addition of a "Surface/subsurface/other" field, in response to helpful feedback and potential-use cases suggested by MGS Quaternary geologists.

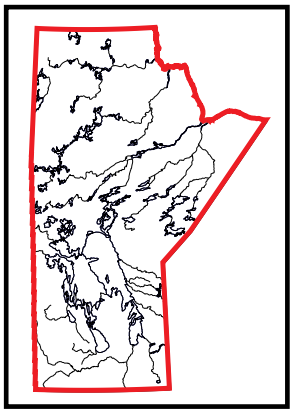

Future plans

Updates to the MDD continue primarily by region, but focus may be directed to specific regions or commodity types as required. Once most of the basic occurrence information has been compiled province-wide, additional information may be appended as necessary. Among the major deposits

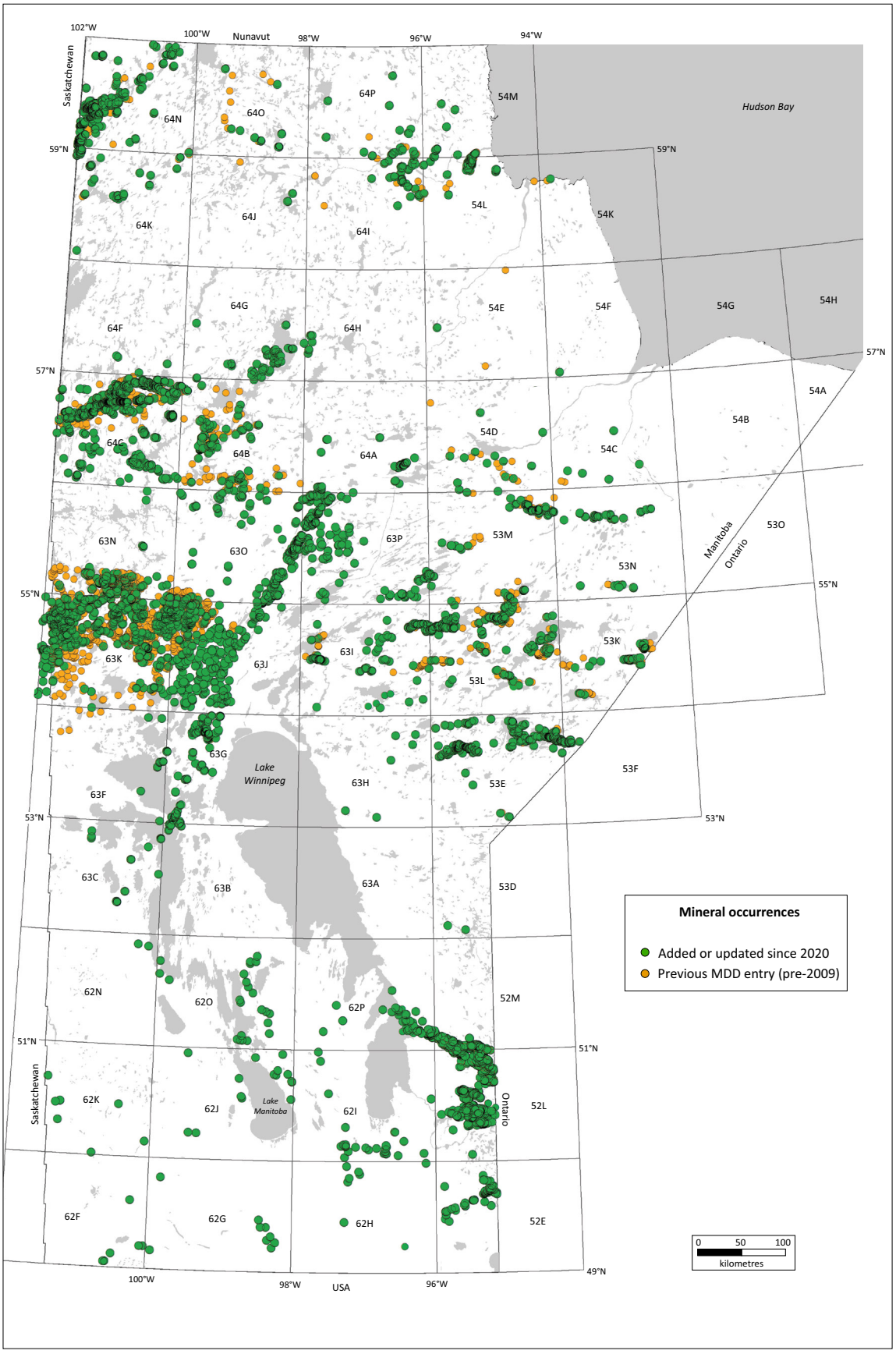

Figure GS2023-1-1: *Map of Manitoba showing mineral occurrences added to the Manitoba Mineral Deposits Database (MDD) since 2020. All of the green points indicated here will be included with relevant data in GeoFile 5-2023, although many are preliminary data that may be changed or removed with further updates.*

and more developed prospects, this will include the addition of a revised mineralization style or deposit model classification that is compatible with nationwide mineral occurrence data standards being developed as part of the Pan-Canadian Geoscience Strategy (National Geological Surveys Committee, 2022).

Economic considerations

Expanding the MDD leads to improved commodity potential assessments, which in turn allows for better-informed land-use plans (such as park development and infrastructure planning), community-focused economic development strategies, and related activities such as geological survey fieldwork plans. In the private sector, mineral occurrence data are key to mineral exploration decisions. The dissemination of new mineral occurrence data can therefore lead to renewed exploration efforts in some parts of Manitoba.

Acknowledgments

Much of the Mineral Deposits Database update project relies on the assistance of students such as J. Janssens and H. Chow from the University of Manitoba, especially in the collection of sample location information. Thanks are also owed to E. Yang and C. Couëslan for their reviews.

References

Conley, G.G., Heine, T.H., Prouse, D.E. and Leskiw, P.D. 2009: Mineral Deposits Database; Manitoba Science, Technology, Energy and Mines, Manitoba Geological Survey.

Martins, T., Rinne, M.L., Breasley, C. and Adediran, H. 2023: Preliminary results from field investigations in the Bird River domain of the Archean Superior province, Manitoba (parts of NTS 52L5, 6, 11, 12); *in* Report of Activities 2023, Manitoba Economic Development, Investment, Trade and Natural Resources, Manitoba Geological Survey, p. 4–13.

National Geological Surveys Committee 2022: Pan-Canadian Geoscience Strategy; URL <https://www.geologicalsurveys.ca/pan-canadian-geoscience-strategy> [September 2023].

Rinne, M.L. 2020: Progress report on updates to the Manitoba Mineral Deposits Database, east-central Manitoba (NTS 53E, F); *in* Report of Activities 2020, Manitoba Agriculture and Resource Development, Manitoba Geological Survey, p. 9–12.

Rinne, M.L. 2021: Updates to the Manitoba Mineral Deposits Database, east-central and northwestern Manitoba (NTS 53E, F, 64J, K, N, O); *in* Report of Activities 2021, Manitoba Agriculture and Resource Development, Manitoba Geological Survey, p. 1–7.

Rinne, M.L. 2022: Updates to the Manitoba Mineral Deposits Database, east-central and northern Manitoba (parts of NTS 53; 54; 64); Manitoba Natural Resources and Northern Development, Manitoba Geological Survey, GeoFile 5-2022, Microsoft® Excel® file.

GS2023-2

Preliminary results from field investigations in the Bird River domain of the Archean Superior province, Manitoba (parts of NTS 52L5, 6, 11, 12)

by T. Martins, M.L. Rinne, C. Breasley[1] and H. Adediran

In Brief:

- The Bird River domain is an area with well-established potential for critical minerals
- Structural and emplacement controls of rare-metal–bearing pegmatites at the regional level were noted
- Results from the Mineral Deposits Database compilation show spatial distributions that reflect geological controls on mineralization

Citation:
Martins, T., Rinne, M.L., Breasley, C. and Adediran, H. 2023: Preliminary results from field investigations in the Bird River domain of the Archean Superior province, Manitoba (parts of NTS 52L5, 6, 11, 12); *in* Report of Activities 2023, Manitoba Economic Development, Investment, Trade and Natural Resources, Manitoba Geological Survey, p. 4–13.

Summary

In 2023, the Manitoba Geological Survey began work on a new compilation and mapping project in the Bird River domain, an area with well-established potential for critical minerals including lithium, cesium, platinum, nickel and chromium. Bedrock geology fieldwork in 2023 was carried out to investigate a number of known rare-element–bearing pegmatites throughout the Cat Lake–Winnipeg River pegmatite field, and also to verify and document various mineral occurrences uncovered during compilation work. Preliminary structural observations indicate that an episode of late lithium mineralization was partly controlled by northeast- or north-northeast-striking sinistral shears. An update on mineral-occurrence data in the Bird River domain is also provided.

Introduction

The Manitoba Geological Survey (MGS) initiated a multidisciplinary geoscientific mapping and compilation project focusing on the Bird River domain of the Superior province of Manitoba, with the Bird River greenstone belt and the Cat Creek–Euclid Lake areas being the focus of the 2023 field season. This report highlights the preliminary results from bedrock mapping. For surficial study results, the reader is referred to Hodder and Martins (2023).

The study area has seen almost 20 years of bedrock mapping activity by the MGS. Projects led by P. Gilbert (e.g., Gilbert, 2006; Gilbert et al., 2008) focused on the southern side of the Bird River domain. Most recently, work by X.M. Yang was focused on the Cat Creek–Euclid Lake area (e.g., Yang et al., 2013; Yang and Houlé, 2020), which is part of the northern side of the Bird River domain. The bedrock-mapping results from these projects were incorporated in the 1:250 000 scale (Manitoba Geological Survey, 2022b) and 1:1 000 000 scale compilation (Manitoba Geological Survey, 2022a) maps, but were not integrated at a smaller regional scale into a seamless geological map.

The Bird River area is also the focus of much interest and exploration activity, particularly related to rare-element–bearing pegmatite bodies and mafic to ultramafic intrusive rocks containing base metals, Cr, Co and platinum-group elements (PGE). Many of these elements are viewed as critical for the economy (Government of Canada, 2021; Government of Manitoba, 2023), so the MGS identified this project as a priority. Given the enormous exploration potential and long history of the region (ongoing for more than 120 years; cf. Tyrrell, 1900), a compilation of mineral occurrences from assessment files and MGS data is also ongoing. The final aim of this bedrock geoscience project is to create a digital ArcGIS product that encompasses all publicly available geological information for the region, together with a compilation release of all the mineral occurrences in the area. The bulk of bedrock geology fieldwork for 2023 was focused around selected pegmatites outcropping in the Bird River greenstone belt area and in the Cat Lake area.

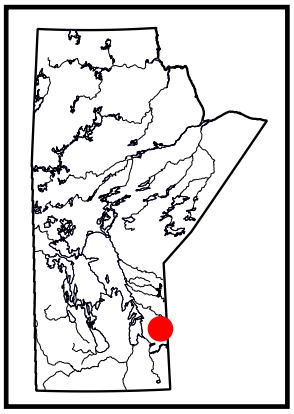

Geological setting

This project focuses on the vast area of the Bird River domain of the Superior province (Figure GS2023-2-1). The Bird River domain is flanked to the north by the English River domain (bounded by the Cat Lake–Euclid Lake fault) and by the Winnipeg River domain to the south (bounded by the Winnipeg River fault). In this report, the domain nomenclature of the Superior province is used as per the domain map in Manitoba Geological Survey (2022a).

An integral part of the Bird River domain is the Bird River greenstone belt (BRGB; Figure GS2023-2-2), an east-trending supracrustal belt that extends for 150 km from Lac du Bonnet in the west to Separation Lake (Ontario) in the east. The BRGB comprises a northern part (Cat Creek–Euclid Lake

[1] Department of Earth, Ocean and Atmospheric Sciences, The University of British Columbia, Vancouver, British Columbia

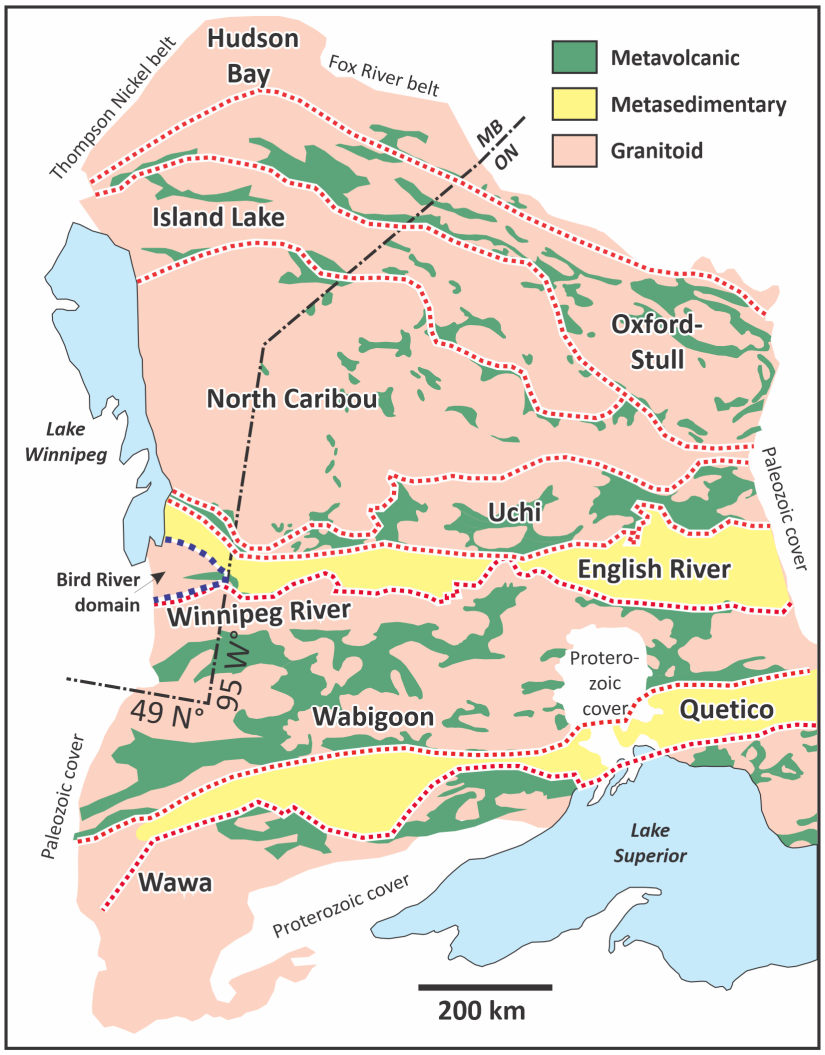

***Figure GS2023-2-1**: Simplified geology of the northwestern Superior province, showing the location of the Bird River domain in Manitoba (blue dashed line). Terrain nomenclature after Percival et al. (2006) and Stott et al. (2010). Bird River domain after Manitoba Geological Survey (2022a). Abbreviations: MB, Manitoba; ON, Ontario.*

area; Yang and Houlé, 2020) and a southern part. The southern part has been subdivided into two geochemically distinct sequences (northern and southern panels), both of which are composed of ca. 2.75–2.72 Ga juvenile, arc-type metavolcanic and associated metasedimentary rocks. These two panels are separated by the Booster Lake formation (<2712 ±17 Ma; Gilbert, 2006), a turbiditic sequence with classic Bouma-type features that is penecontemporaneous with clastic sedimentary rocks of the fluvial-alluvial deposits of the Flanders Lake formation immediately to the east (Gilbert, 2006; Figure GS2023-2-2). The BRGB was historically described as a large synclinal keel (Trueman, 1980; Černý et al., 1981); however, mapping by the MGS has led to a reinterpretation of the volcanostratigraphic framework of this belt (e.g., Gilbert, 2006; Gilbert et al., 2008). For a detailed geological description of the southern part of the BRGB, the reader is referred to work by Gilbert and co-authors (e.g., Gilbert, 2006; Gilbert et al., 2008).

To the north of the southern part of the BRGB, the Bird River domain consists of a granitoid terrane (Maskwa Lake batholith) that contains intrusive phases ranging from 2.85 to 2.73 Ga (Gilbert et al., 2008) and contains the Cat Creek–Euclid Lake area (Figure GS2023-2-2). This northern part of the Bird River domain was interpreted as part of the northern limb of the BRGB by Yang and Houlé (2020). They described the Cat Creek–Euclid Lake area as underlain by a suite of greenstone assemblages formed in a continental-margin setting adjacent to the Mesoarchean Maskwa Lake batholith. The greenstone assemblages consist mainly of mafic–felsic volcanic and related intrusive rocks, and epiclastic and minor volcaniclastic rocks; and mafic–ultramafic layered intrusions. These were intruded by younger phases of tonalite-trondhjemite rocks from a granodiorite suite (i.e., Maskwa Lake batholith II of Yang and Houlé, 2020), late peraluminous granitoid rocks and pegmatites.

Updated mineral occurrence data in the Bird River domain

The Bird River domain is host to a wide range of mineralization styles and critical mineral occurrences, including previously

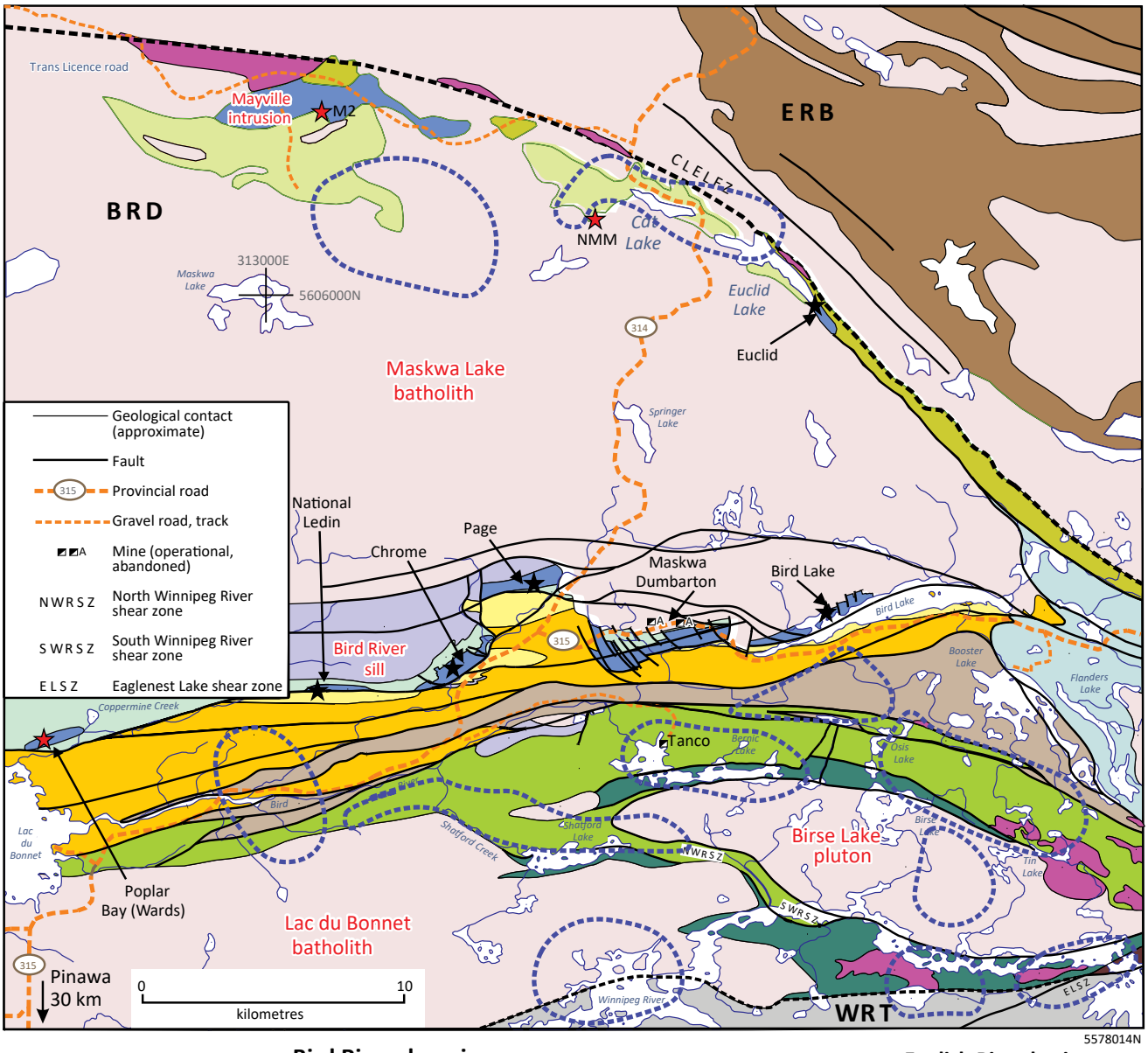

Bird River domain

Intrusive rocks

- S-type granite
- Granite, granodiorite, tonalite
- Gabbro, diorite, quartz diorite
- Pyroxenite, anorthosite, gabbro

Late sedimentary rocks

Flanders Lake formation

- Arenite, polymictic conglomerate

Booster Lake formation

- Greywacke, siltstone

Volcanic and sedimentary rocks

Bird River belt South Panel

Bernic Lake formation

- Heterolithic volcanic breccia, rhyolite, basalt, andesite

Eaglenest Lake formation

- Greywacke, siltstone

Southern MORB-type formation

- Basalt, aphyric; gabbro

Bird River belt North Panel

- Massive to fragmental, mafic to felsic volcanic and sedimentary rocks

Peterson Creek formation

- Massive to fragmental felsic volcanic rocks

Northern MORB-type formation

- Basalt, aphyric; gabbro

Cat Lake area

- Sedimentary and volcanic rocks, related gneiss
- Tholeiitic basalt

English River basin

- Paragneiss, granitoid intrusive rocks, migmatite, pegmatite

Winnipeg River terrane

- Tonalite, granodiorite, granitoid gneiss

- Ni-Cu-PGE deposit/occurrence
- Cr-PGE deposit/occurrence
- Domain or terrane boundary

***Figure GS2023-2-2**: Tectonic assemblages of the Bird River domain, southeastern Manitoba (modified from Gilbert et al., 2008, 2013; Yang et al., 2013). Abbreviations: BRD, Bird River domain; CLELFZ, Cat Lake–Euclid Lake fault zone (indicated by the bold dashed line); ERB, English River basin; M2, Mayville deposit; MORB, mid-ocean–ridge basalt; NMM, New Manitoba mine; WRT, Winnipeg River terrane. Blue dashed lines represent location of the pegmatite groups from the Cat Lake–Winnipeg River pegmatite field (after Černý et al., 1981).*

mined deposits hosted by ultramafic intrusions (e.g., Maskwa, Dumbarton), as well as the currently-producing Tanco mine. As part of this project, recent updates to Manitoba's Mineral Deposits Database (MDD), described by Rinne (2023), were partly targeted to include the Bird River domain. The resulting compilation of new mineral-occurrence data shows spatial distributions that reflect geological controls on mineralization (Figure GS2023-2-3).

The new mineral-occurrence data reveal potentially important features that saw little or no reference in past studies or compilations of the area. Highlights include the following:

- The Little Bear Lake gold occurrences, located in the centre of the Maskwa Lake batholith, trace a belt of gold mineralization approximately 6 km long, with some reported assays of around 300 ppm Au (e.g., Assessment Files 73960, 52L1182, Manitoba Economic Development, Investment,

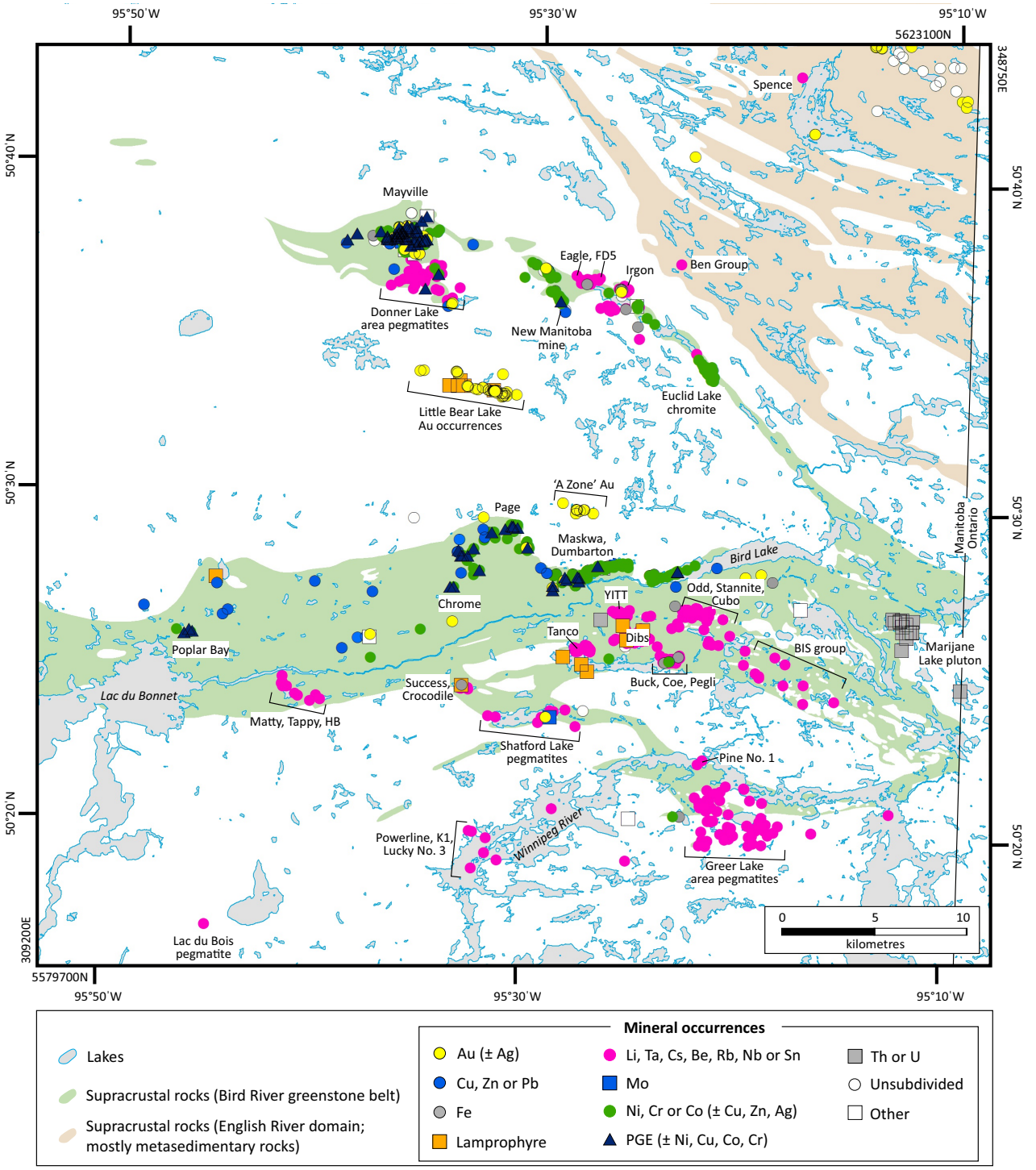

Figure GS2023-2-3: *Simplified map of mineral occurrences in the Bird River area, part of a recent update to the Manitoba Mineral Deposits Database. For clarity, the background geology has been simplified to show only supracrustal-dominant and mafic-intrusive units (i.e., approximate greenstone belt outlines). Corner co-ordinates are in UTM Zone 15 (NAD83).*

Trade and Natural Resources, Winnipeg). An apparently smaller zone of gold mineralization—the "A zone" occurrence—also occurs along a similar eastward trend and could represent an offset of the Little Bear Lake gold trend (Figure GS2023-2-3).

- More comprehensive geochemical data reveal a wider footprint of enrichment in PGE, Ni and other elements around known deposits hosted by mafic to ultramafic intrusions such as Chrome, Maskwa and Mayville.
- Drillcore intersections of lamprophyre dikes were reported by several industry workers in the vicinity of both the Tanco deposit and the Little Bear Lake gold occurrences. Near Little Bear Lake, gold mineralization is reportedly focused along sheared lamprophyre-dike contacts exposed in outcrop (Assessment File 74096). As none of these lamprophyre findings have yet been independently confirmed, they may require further investigation.
- Compiled data show a slightly more widespread distribution of rare-element–bearing pegmatite intrusions than indicated in previous compilations, including two sets of dikes in the English River domain (Figure GS2023-2-3). The Spence pegmatites are weakly uranium-mineralized dikes, perhaps related to later mineralization in the Marijane Lake pluton to the southeast. The Ben Group pegmatites were reported to contain spodumene in several drillcore intersections near or at surface (Assessment File 91309). Such findings would be significant, as they would prove that lithium-bearing pegmatite mineralization extends into the English River domain. An attempt by the MGS geologists to find spodumene reported for the Ben Group dikes in 2023 proved unsuccessful.

Structural observations

Rocks of the Bird River domain were subjected to a complex structural history that has been summarized by several workers, including Duguet et al. (2005), Gilbert et al. (2008), Kremer and Lin (2006) and Kremer (2010). Although regional structural trends vary by location, most workers describe a general sequence of events involving:

1) an early (D_1) episode of north-side-up ductile deformation, resulting in a strong pervasive planar fabric evident in supracrustal outcrops both north and south of the Maskwa Lake batholith;
2) a later (D_2) episode of strike-slip deformation, characterized mostly by northeast-trending sinistral (and south-side-up) shears, and southeast-trending dextral shears; and
3) a possible later (D_2 or D_3?) episode of transpressive deformation, expressed mostly by dextral shears. In the southern part of the BRGB, the later strike-slip events are proposed to have been coeval with the emplacement of at least some pegmatite intrusions at ca. 2640 Ma (Duguet et al., 2005; Gilbert et al., 2008).

Fieldwork in 2023 was undertaken partly to investigate structural controls on pegmatite-dike emplacement and related rare-element mineralization. Preliminary field structural observations throughout the study area revealed features broadly consistent with the early (D_1) foliation and later (D_2 and possibly D_3) strike-slip shears, including a set of dominantly northeast- or north-northeast-trending sinistral shears that are, in places, expressed as a late sinistral spaced cleavage. At the outcrops of the Eagle pegmatite and other pegmatites in the Cat Creek area, rare examples of late lithium mineralization were found to be associated with these late (D_2 or D_3) sinistral brittle-ductile shears (Figure GS2023-2-4). These preliminary findings indicate that late transpressional structures in the Bird River domain were involved in some episode of late lithium remobilization, or possibly later mineralized-pegmatite emplacement.

Detailed pegmatite descriptions

All pegmatite dikes visited during fieldwork were described as belonging to the Cat Lake–Winnipeg River pegmatite field as defined by Černý et al. (1981). This vast pegmatite field has been subdivided into two pegmatite districts (the Cat Lake–Maskwa Lake district and the Winnipeg River district), and subsequently into several different pegmatite groups according to their mineralogy, geochemistry and location (Černý et al., 1981). Martins et al. (2013) presented a summary table of the main characteristics of the different groups of pegmatites within this pegmatite field. The pegmatite outcrops visited and described below were selected by taking into account location, exploration interest and accessibility.

High Grade dike

The High Grade dike is located in the Donner Lake area (part of the Cat Lake–Maskwa Lake district; Figure GS2023-2-3) and was described by both Černý et al., (1981) and Bannatyne (1985). The best exposure visited consists of a 1.5 m wide pegmatite dike intruding pillowed basalt. The dike is oriented roughly north-south and extends for more than 10 m, crosscutting the main foliation in the basalt. Contacts are variable and sharp with the hangingwall (Figure GS2023-2-5a) and irregular and bulbous with the footwall. Black tourmaline occurs in sprays along the dike margin (tourmaline basal sections measure about 0.5 cm with lengths of 1.5 cm). The pegmatite is zoned and is subdivided into a border zone, lepidolite fringe, central zone and core.

The border zone is about 5–7 cm thick (Figure GS2023-2-5a) on both the hangingwall and footwall of the pegmatite dike but better developed on the hangingwall. Main mineralogy is feldspar, quartz, muscovite, cleavelandite (a form of albite) and local apatite. Cleavelandite blades or sprays grew perpendicular to the country rock and can be >7 cm long. The cleavelandite locally extends into the next zone, the lepidolite fringe. The lepidolite fringe is an irregular and discontinuous, 1–3 cm thick lepidolite layer that occurs along the border zone at the hangingwall but

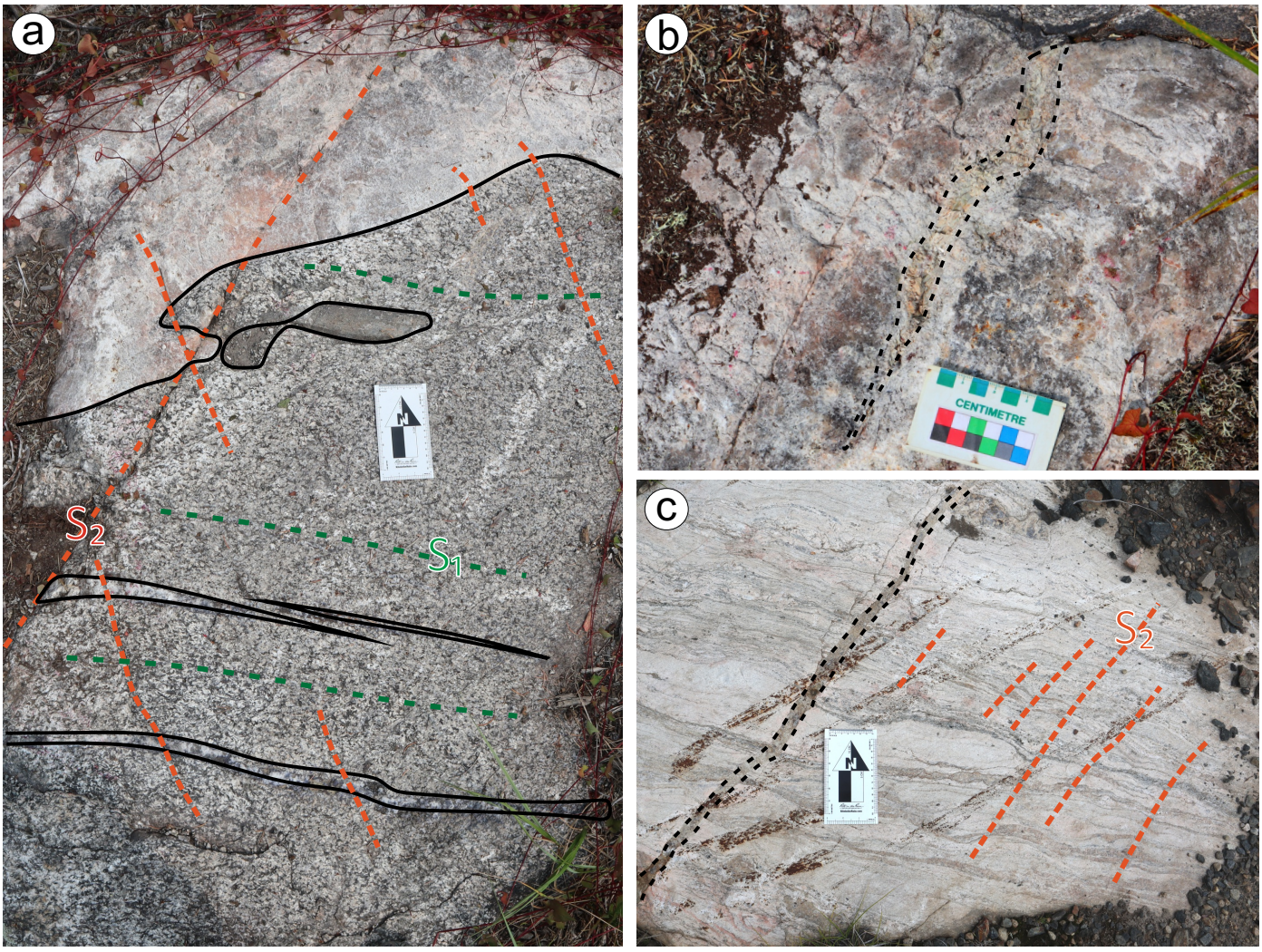

Figure GS2023-2-4: *Outcrop photographs of structural features related to lithium-bearing pegmatites in the northern part of the Bird River greenstone belt, showing:* ***a)*** *Eagle pegmatite (top of image, outlined in black) within a granite overprinted by an early east-striking foliation (S_1) and quartz-holmquistite veins (outlined, bottom of image), with late brittle-ductile shears (labeled S_2) that crosscut both the pegmatite and the quartz veins;* ***b)*** *Eagle pegmatite crosscut by a vein of green spodumene (outlined, centre of image) parallel to north-northeast-striking S_2 shears, located approximately 2 m from the location of panel A;* ***c)*** *late spodumene vein (outlined at centre left) parallel to north-northeast-striking S_2 shears and spaced sinistral cleavage in the pegmatite from the Cat Creek area.*

is not observed at the footwall. This zone is composed mainly of lepidolite, quartz and feldspar.

The central zone is the largest subdivision and makes up almost the entire width of the dike. It contains both aplitic and pegmatitic portions with complex textures and mineralogy, indicating that this is the most fractionated portion of the pegmatite. The aplitic portion is generally very fine grained (almost sugary), white and purple. It consists mainly of lepidolite and albite, with local, medium- to coarse-grained aquamarine. This aplitic portion can be found throughout most of the central zone, except for areas dominated by pegmatitic textures. The pegmatitic section is composed of quartz, albite, spodumene, light pink tourmaline (as locally developed sprays; Figure GS2023-2-5b), various phosphate phases and petalite. Part of this central zone is intensely albitized and probably caused by a later metasomatic event (Figure GS2023-2-5c). This area is chalk white with veins or 'diatreme' of a grey/green-coloured mineral referred to as greenish pollucite alteration, a mixed-layer silicate (Bannatyne, 1985). Petalite in this zone is rimmed by a combination of clay minerals (montmorillonite), tourmaline and phosphate minerals. Local wisps and veinlets of lepidolite, oriented 225°/20°, were also observed in both pegmatitic and aplitic phases. An 8 cm x 25 cm piece of country rock was observed in the central zone.

The core zone developed immediately after the lepidolite fringe and is composed of quartz and massive, blocky feldspar (Figure GS2023-2-5d). Blue tourmaline and beryl (1 cm basal section, 2 cm length) occur locally within this zone.

Eagle, F.D. No. 5 and Tappy pegmatite dikes

The Eagle and F.D. No. 5 pegmatite dikes are located in the Cat Lake–Maskwa Lake district of the Cat Lake–Winnipeg River

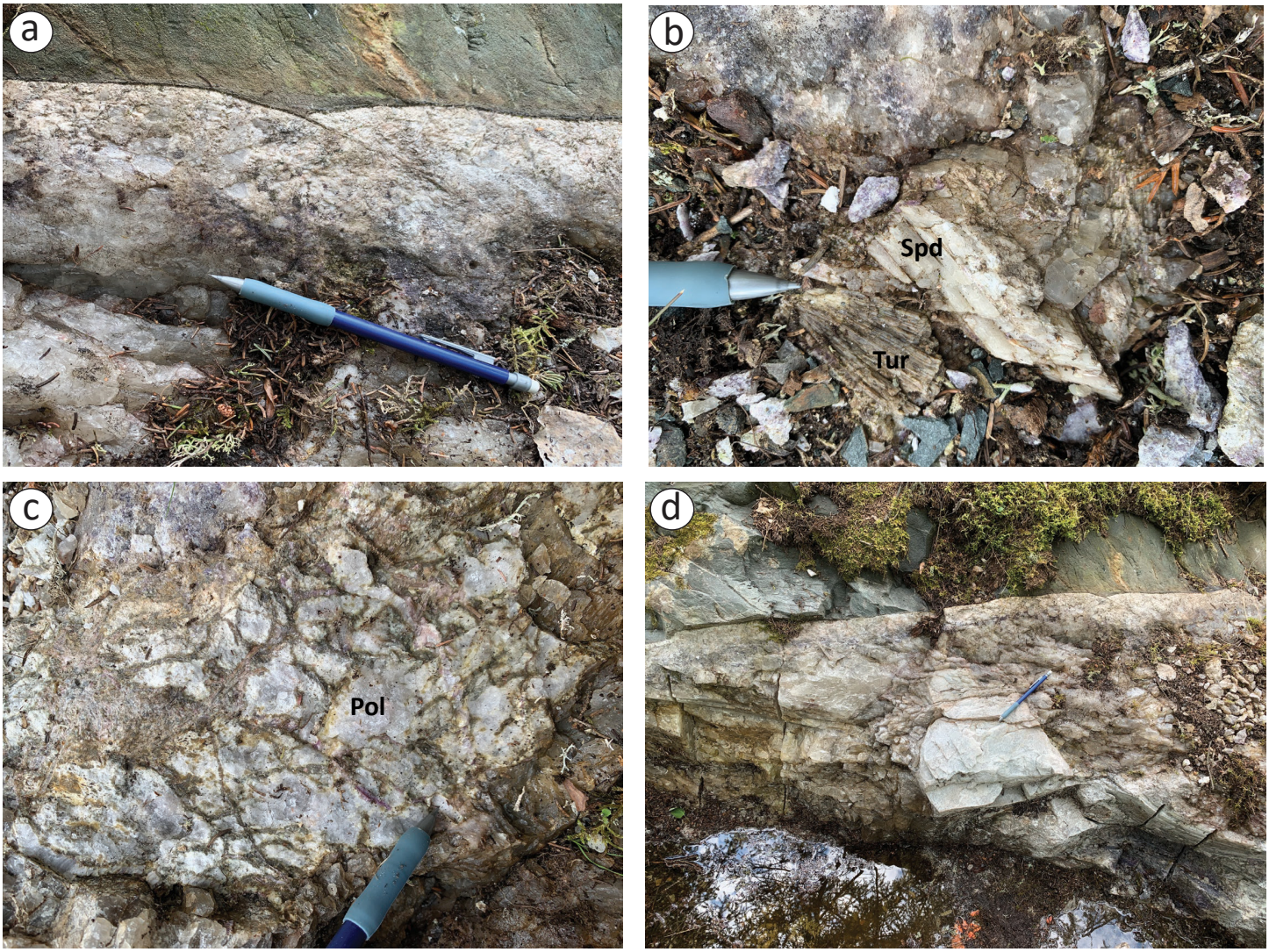

Figure GS2023-2-5*: Outcrop photos of the High Grade dike:* ***a)*** *sharp contact of pegmatite dike with basalt country rock;* ***b)*** *detail of light grey-pink tourmaline (Tur) sprays and spodumene (Spd);* ***c)*** *albitized portion of the central zone with remnants of glassy pollucite (Pol);* ***d)*** *detail of the white blocky feldspar and quartz of the core zone.*

pegmatite field, whereas the Tappy pegmatite is located in the Winnipeg River district (Figure GS2023-2-3). An M.Sc. project was initiated this year at the University of New Brunswick in collaboration with the MGS to map and document these three pegmatite dikes in detail. Refer to Roush et al. (2023) for descriptions of the pegmatite bodies.

YITT-B pegmatite swarm

The YITT-B pegmatite swarm, located northwest of the Tanco mine (Figure GS2023-2-3), was discovered in the late 1980s as a result of regional exploration efforts by the Tantalum Mining Corporation of Canada Ltd. (Assessment File 72418). This exploration work was followed by the research of Anderson (1992) and Anderson et al. (1998), which outlined several zones in the pegmatites, based on textural features and mineral associations: wall zone, intermediate zone (that is subdivided into 1, 2a and 2b subzones) and core zone. Their work also included a detailed mineralogical and paragenetic description of the Yitt-B pegmatite swarm, with descriptions of the following minerals (not listed in order of abundance): quartz, K-feldspar, albite, muscovite, beryl, tourmaline, garnet, columbite-group minerals, cassiterite, phosphates (beusite, triplite, alluaudite, triphylite, phosphophyllite, parascholzite and different varieties of apatite), and sulphides (arsenopyrite löllingite and bismuthinite). Anderson et al. (1998) interpreted the YITT-B pegmatite dikes to be geochemically unique from other pegmatite bodies in the southern part of the Cat Lake–Winnipeg River pegmatite field. The YITT-B pegmatite dikes are enriched in Ta, Nb and Sn, but are very poor in Li, Be, B, P, S and F. The fractionation level of Fe-Mn is considered moderate, whereas the Nb-Ta is evolved. The same authors interpreted the broad geochemical diversity of this pegmatite field to be related to different sources. Specifically, the fertile leucogranites that were parental to the individual pegmatite groups required anatectic melts derived from different lithological sources.

Two outcrops were examined that contained YITT-B pegmatite dikes intruding into cordierite-bearing turbiditic sandstone-mudstone of the Booster Lake formation. In both outcrops the predominant mineral phases are very coarse-grained quartz, K-feldspar, albite and muscovite. In one of the outcrops, an accumulation of quartz about 20 cm thick could be described as a quartz core. In one outcrop, a localized zone of quartz and muscovite intergrowth was interpreted as a greisen. In both outcrops, a very fine grained aplitic unit (saccharoidal texture) of greyish-bluish colour was observed. Albite, quartz, columbite-group minerals, sulphides (possibly arsenopyrite, löllingite and bismuthinite measuring up to 0.5 cm in width) and phosphate phases (predominantly blue apatite) were identified in hand sample.

Coe and Buck claims, pegmatites 7, 8 and 9

The Coe and Buck claims are located at the eastern end of Bernic Lake (Figure GS2023-2-3; Bannatyne, 1985; Lenton, 1979) and consist of a series of pegmatite dikes, of which pegmatites 7, 8 and 9 were mapped in detail. Six major zones were described for pegmatites 7, 8 and 9: 1) a simple pegmatite with chilled margin; 2) a wall zone that consists of quartz, mica and tourmaline in a comb structure; 3) an aplitic zone that hosts a sugary texture of fine-grained feldspar, tourmaline and apatite; 4) intermediate zone 1, a quartz-dominated unit that hosts abundant beryl and phosphate mineralization; 5) intermediate zone 2, a lithium-enriched zone that hosts large 15 cm laths of petalite, which is partially broken down into spodumene and quartz, the spodumene, in turn, being locally broken down into a clay product; and 6) intermediate zone 3, a feldspar-dominated zone containing metre-scale feldspar crystals that are crosscut by veins of albitization. Intermediate zone 3 also contains phosphate-rich bands containing purpurite and apatite.

Pegmatite 7 is a lithium-rich pegmatite dike that intruded foliated pillow basalt (main elongation of pillows is in a northeasterly direction). The intrusion displays bulbous contacts in the western and eastern parts, and brittle contacts in the northern and southern parts. The wall zone hosts quartz, mica and tourmaline parallel to the bulbous country rock contact. Intermediate zone 1 forms the bulk of the intrusion, containing abundant quartz and phosphates such as amblygonite. Intermediate zone 2 is present as a petalite and spodumene mass in the southern part of the intrusion. A separate intrusion, located proximal to pegmatite 7, hosts a granodioritic assemblage and texture (consisting of equigranular orthoclase, quartz and albite).

Pegmatite 8 is exposed along two main outcrops. It has undulatory bulbous contacts with the foliated pillowed basalt and is oriented approximately 098° with a subvertical dip (Figure GS2023-2-6). This pegmatite hosts multiple fragmented xenoliths of basaltic country rock. The xenoliths are surrounded by the wall zone, which is composed of comb-textured mica and quartz in a pink-feldspar groundmass. A distinct band of purpurite and a single crystal of spodumene were identified within intermediate zone 1 (massive quartz zone with abundant amblygonite and beryl). Green mica is common in this pegmatite as accreted clots that appear to be metasomatic in origin (potential late-stage accumulation of hydrous fluid). Cleavelandite is commonly found surrounding the green mica. The northeastern contact of the intrusion is a mix of small-scale fragments of country rock (averaging 2–30 cm).

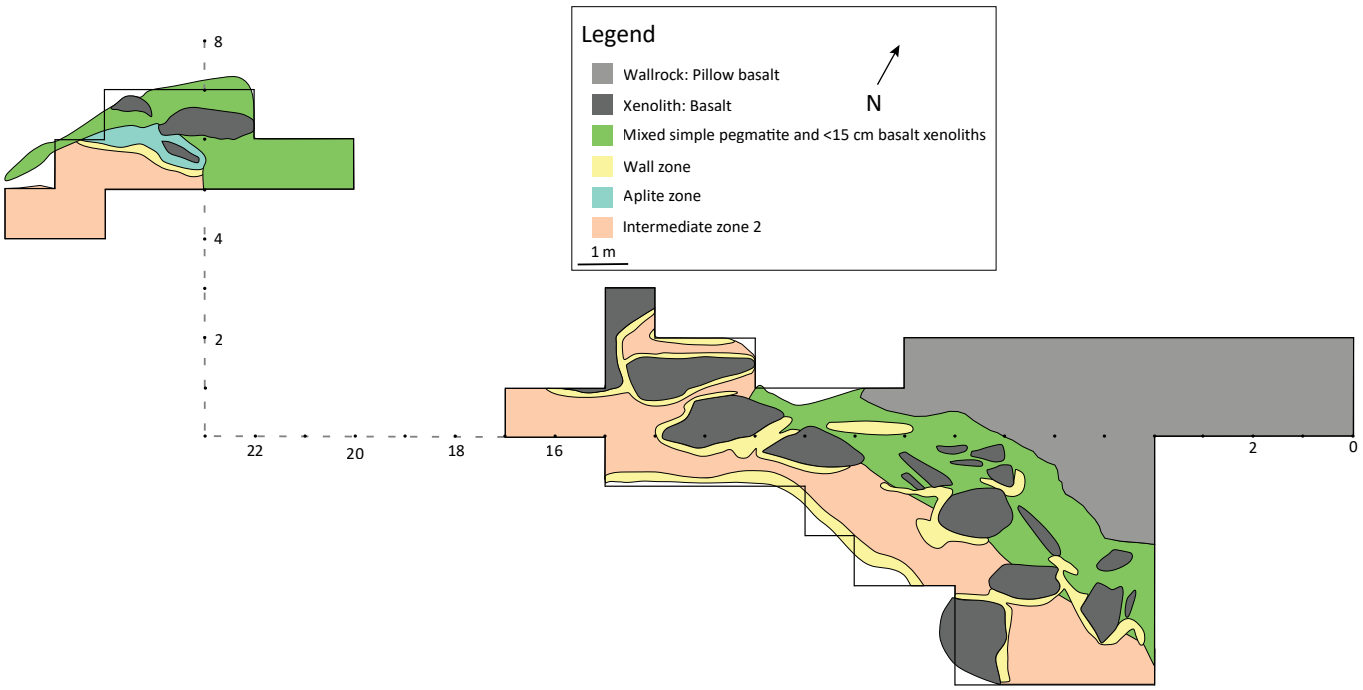

Figure GS2023-2-6*: Sketch of pegmatite 8, part of the Buck group on the eastern shore of Bernic Lake.*

Pegmatite 9 intruded pillowed basalt, which contains abundant holmquistite close to the pegmatite contact. This pegmatite contains a zone of massive metre-scale primary pink orthoclase, termed intermediate zone 3, that was not identified in pegmatites 7 and 8. Intermediate zone 3 also contains clots of green mica and bands enriched in phosphates (70% modal abundances of purpurite and apatite along with an unidentified brown-weathered phosphate phase). Wall-zone rocks are present along the northeastern bulbous contacts of the pegmatite. The wall zone consists of comb-structured mica, quartz and a significant amount of black tourmaline. Intermediate zone 3 (feldspar zone) appears to gradationally change into intermediate zone 1 (quartz zone), which is exposed beneath the cliff outcrop beside the swamp. An offset dike to the west hosts a classic pegmatite zonation of the wall zone transitioning into the aplite zone.

Economic considerations

The Bird River domain of the Archean Superior province in Manitoba is prospective for base metals (nickel, copper, chromium), precious metals (platinum-group elements, gold) and rare elements (e.g., lithium, cesium, tantalum, niobium). A significant number of these elements are now considered critical for Manitoba (Government of Manitoba, 2023) and for Canada (Government of Canada, 2021). Rare-element–bearing pegmatites in particular, such as those of the Cat Lake–Winnipeg River pegmatite field, are becoming increasingly important in the context of a transition to a lower-carbon economy.

Preliminary findings of late, structurally-controlled lithium mineralization in the Cat Lake area imply there may be common structural controls between lode gold and pegmatite dike emplacement in the area. In practical terms, this suggests that some exploration techniques applied to lode gold could be applied to lithium exploration in parts of the Bird River domain. Such techniques could include the detection of controlling structures through mapping and remote-sensing methods (e.g., displacements traced via topographic lineaments, particularly in high-resolution LiDAR data, jogs in landforms or stream trends), followed by targeting of splays, major deflections, zones of likely dilation along regional and secondary shear structures, or targeting of areas where major structures interact with rheological contrasts such as batholith margins.

Manitoba's critical minerals strategy (Government of Manitoba, 2023) highlights the need to provide high-quality geoscience information in support of new critical minerals discoveries. The remarkable extent and variety of critical-mineral occurrences in the Bird River area continues to warrant further data compilation and field investigations in support of this mandate.

Acknowledgments

The logistical support provided by C. Epp and P. Belanger is truly appreciated because, without it, the project could not have gone ahead. Many thanks to H. Chow, J. Bautista (University of Manitoba) and J. Roush (University of New Brunswick) for capable field assistance. Critical reviews by C. Couëslan and X.M. Yang are truly appreciated. RnD Technical provided technical editing and C. Steffano is thanked for layout of the report.

References

Anderson, S.D. 1992: Geochemical and economic evaluation of a pegmatite swarm, Bird River greenstone belt, southeastern Manitoba; B.Sc. thesis, University of Manitoba, Winnipeg, Manitoba.

Anderson, S.D., Černý, P., Halden, N.M., Chapman, R. and Uher, P. 1998: The Yitt-B pegmatite swarm at Bernic Lake, southeastern Manitoba: a geochemical and paragenetic anomaly; The Canadian Mineralogist, v. 36, p. 283–301.

Bannatyne, B. 1985: Industrial minerals in rare-element pegmatites of Manitoba; Manitoba Energy and Mines, Geological Services, Economic Geology Report ER84-1, 96 p.

Černý, P., Trueman, D.L., Ziehlke, D.V., Goad, B.E. and Paul, J. 1981: The Cat Lake–Winnipeg River and the Wekusko Lake pegmatite fields, Manitoba; Manitoba Energy and Mines, Mineral Resources Division, Economic Geology Report ER80-1, 215 p.

Duguet, M., Lin, S., Gilbert, H.P. and Corkery, M.T. 2005: Preliminary results of geological mapping and structural analysis of the Bird River greenstone belt, southeastern Manitoba (NTS 52L5 and 6); *in* Report of Activities 2005, Manitoba Industry, Economic Development and Mines, Manitoba Geological Survey, p. 117–124.

Gilbert, H.P. 2006: Geological investigations in the Bird River area, southeastern Manitoba (parts of NTS 52L5N and 6); *in* Report of Activities 2006, Manitoba Science, Technology, Energy and Mines, Manitoba Geological Survey, p. 184–205.

Gilbert, H.P., Davis, W.D., Duguet, M., Kremer, P.D., Mealin, C.A. and MacDonald J. 2008: Geology of the Bird River Belt, southeastern Manitoba (parts of NTS 52L5, 6); Manitoba Science, Technology, Energy and Mines, Manitoba Geological Survey, Geoscientific Map MAP2008-1, scale 1:50 000.

Gilbert, H.P., Houlé, M.G., Yang, X.M., Scoates, J.S., Scoates, R.F.J., Mealin, C.A., Bécu, V., McNicoll, V. and Galeschuk, C.R. 2013: Mafic and ultramafic intrusive rocks and associated Ni-Cu-(PGE) and Cr-(PGE) mineralization in the Bird River greenstone belt, southeast Manitoba; Geological Association of Canada–Mineralogical Association of Canada, Joint Annual Meeting, Field Trip Guidebook FT-C2; Manitoba Innovation, Energy and Mines, Manitoba Geological Survey, Open File OF2013-7, 51 p.

Government of Canada 2021: Critical minerals; URL <https://www.nrcan.gc.ca/our-natural-resources/minerals-mining/critical-minerals/23414> [August 2023].

Government of Manitoba 2023: The Manitoba critical minerals strategy: driving sustainable growth; URL <https://manitoba.ca/iem/explore/files/criticalmineralsstrategy.pdf> [October 2023].

Hodder, T.J. and Martins, T. 2023: Current Quaternary geology investigations in southeastern Manitoba and implications for mineral exploration (parts of NTS 52L, 62P, 63A); *in* Report of Activities 2023, Manitoba Economic Development, Investment, Trade and Natural Resources, Manitoba Geological Survey, p. 105–119.

Kremer, P.D. 2010: Structural geology and geochronology of the Bernic Lake area in the Bird River greenstone belt, Manitoba: evidence for syn-deformational emplacement of the Bernic Lake pegmatite group; M.Sc. thesis, University of Waterloo, Waterloo, Ontario, 91 p.

Kremer, P.D. and Lin, S. 2006: Structural geology of the Bernic Lake area, Bird River greenstone belt, southeastern Manitoba (NTS 52L6): implications for rare element pegmatite emplacement; *in* Report of Activities 2006, Manitoba Science, Technology, Energy and Mines, Manitoba Geological Survey, p. 206–213.

Lenton P.G. 1979: Mineralogy and petrology of the Buck Claim lithium pegmatite, Bernic Lake, southeastern Manitoba; M.Sc. thesis, University of Manitoba, Winnipeg, Manitoba, 164 p.

Manitoba Geological Survey 2022a: Bedrock geology of Manitoba; Manitoba Natural Resources and Northern Development, Manitoba Geological Survey, Open File OF2022-2, scale 1:1 000 000.

Manitoba Geological Survey 2022b: New edition of the 1:250 000 scale Precambrian bedrock geology compilation map of Manitoba; Manitoba Natural Resources and Northern Development, Manitoba Geological Survey, GeoFile 3-2022.

Martins, T., Kremer, P. and Vanstone, P. 2013: The Tanco mine: geological setting, internal zonation and mineralogy of a world-class rare element pegmatite deposit; Geological Association of Canada–Mineralogical Association of Canada Joint Annual Meeting, Field Trip Guidebook FT-C1; Manitoba Innovation, Energy and Mines, Manitoba Geological Survey, Open File OF2013-8, 17 p.

Percival, J.A., Sanborn-Barrie, M., Skulski, T., Stott, G.M., Helmstaedt, H. and White, D.J. 2006: Tectonic evolution of the western Superior Province from NATMAP and LITHOPROBE studies; Canadian Journal of Earth Sciences, v. 43, p. 1085–1117.

Rinne, M.L. 2023: Progress report on the Manitoba Mineral Deposits Database; *in* Report of Activities 2023, Manitoba Economic Development, Investment, Trade and Natural Resources, Manitoba Geological Survey, p. 1–3.

Roush, J., Martins, T., McFarlane, C.R.M., Rinne, M.L. and Groat, L. 2023: Preliminary examination of the Tappy, Eagle and F.D. No. 5 pegmatites in the Cat Lake–Winnipeg River pegmatite field, southeastern Manitoba (parts of NTS 52L5, 11); *in* Report of Activities 2023, Manitoba Economic Development, Investment, Trade and Natural Resources, Manitoba Geological Survey, p. 20–26.

Stott, G.M., Corkery, M.T., Percival, J.A., Simard, M. and Goutier, J. 2010: Project units 98-006 and 98-007: a revised terrane subdivision of the Superior Province; *in* Summary of Field Work and Other Activities 2010, Ontario Geological Survey, Open File Report 6260, p. 20-1–20-10.

Trueman, D.L. 1980: Stratigraphy, structure, and metamorphic petrology of the Archean greenstone belt at Bird River, Manitoba; Ph.D. thesis, University of Manitoba, Winnipeg, Manitoba, 150 p.

Tyrrell, J.B. 1900: East shore, Lake Winnipeg; Geological Survey of Canada, Annual Report, 1898, v. 11, pt. G.

Yang, X.M. and Houlé, M.G. 2020: Geology of the Cat Creek–Euclid Lake area, Bird River greenstone belt, southeastern Manitoba (parts of NTS 52L11, 12); Manitoba Agriculture and Resource Development, Manitoba Geological Survey, Geoscientific Report GR2020-1, 105 p., 1 map at 1:20 000 scale.

Yang, X.M., Gilbert, H.P. and Houlé, M.G. 2013: Cat Lake–Euclid Lake area in the Neoarchean Bird River greenstone belt, southeastern Manitoba (parts of NTS 52L11, 12): preliminary results of bedrock geological mapping and their implications for geodynamic evolution and metallogeny; *in* Report of Activities 2013, Manitoba Mineral Resources, Manitoba Geological Survey, p. 70–84.

GS2023-3

Exploring use of nitrogen-isotope applications in the study of the magmatic evolution and rare-element ore genesis of pegmatites from southeastern Manitoba (parts of NTS 52L5, 6, 11)

by Y. Chen[1], X.M. Yang and L. Li[1]

In Brief:

- Outcrop and subsurface pegmatite and granitoid samples were collected from four different localities in southeastern Manitoba
- Future work will take place utilizing nitrogen isotope analyses as a novel tool

Citation:
Chen, Y., Yang, X.M. and Li, L. 2023: Exploring use of nitrogen-isotope applications in the study of the magmatic evolution and rare-element ore genesis of pegmatites from southeastern Manitoba (parts of NTS 52L5, 6, 11); *in* Report of Activities 2023, Manitoba Economic Development, Investment, Trade and Natural Resources, Manitoba Geological Survey, p. 14–19.

Summary

Southeastern Manitoba is renowned for its well-preserved Archean cratonic rocks of the Superior province as well as for its substantial economic potential (e.g., critical metal-enriched granitic pegmatites). In the summer of 2023, the Manitoba Geological Survey and the Stable Isotope Geochemistry Laboratory at the University of Alberta initiated a collaborative project to explore the magmatic evolution of the Neoarchean granitoids and pegmatite-related ore genesis in southeastern Manitoba, relying on the use of novel nitrogen-isotope techniques. The results of field sampling conducted in July 2023 are summarized in this report. Outcrop and underground samples were collected from the Tanco lithium-cesium-tantalum–bearing pegmatite, a pegmatite found in the Cat Creek area, the Bird Lake supracrustal-type granitoid and the Lac du Bonnet granitoid. Future work will focus on detailed petrographic, geochemical (especially nitrogen-isotope) and petrogenetic analyses to shed light on the genesis of the Neoarchean granitoids and the spatially related pegmatites, as well as their critical metal-enrichment mechanism.

Introduction

The Bird River domain (BRD) in southeastern Manitoba has long been the subject of geological and economic investigations due to the presence of well-preserved Archean rocks (e.g., the western Superior Neoarchean tonalite-trondhjemite-granodiorite [TTG] suite; Percival et al., 2012; Yang, 2014, 2023; Yang et al., 2019) and the world-class rare-element pegmatite deposit hosting lithium (Li), cesium (Cs) and tantalum (Ta) in the Bernic Lake area (Li-Cs-Ta [LCT] Tanco pegmatite; Černý, 2005). While numerous studies have been carried out on the tectonic evolution of the Superior province (see summary in Yang et al., 2019) and the petrogenesis of the pegmatites from the Bernic Lake pegmatite group (e.g., Stilling et al., 2006), the genesis of the Neoarchean granitoids and the spatially related pegmatites from the Cat Lake–Winnipeg River pegmatite field (Černý et al., 1981) remains unresolved.

Nitrogen (N) is one of the few elements that exists in all reservoirs of the Earth (i.e., the atmosphere, hydrosphere, biosphere, lithosphere and mantle). In the lithosphere, N exists mainly as ammonium (NH_4^+) that can replace potassium (K^+) in the crystal lattice of silicate minerals (Honma and Itihara, 1981) and as NH_4^+/NH_3 or N_2 in hydrothermal fluids (Li et al., 2021). Therefore, N isotopes can potentially serve as a robust tool to trace geological processes (e.g., Li et al., 2014, 2019) and the formation of ore deposits (e.g., orogenic gold deposits; Jia et al., 2003) for the following reasons:

- the significant N isotopic difference between the crust and the mantle
- the large magnitude of isotope fractionation among NH_4^+, NH_3 and N_2 (e.g., Li et al., 2021)
- the close affinity of NH_4^+ to alkali metals (e.g., Honma and Itihara, 1981)
- the fact that NH_3 acts as a complexing agent to enhance heavy metal migration in fluids (e.g., Li et al., 2021)

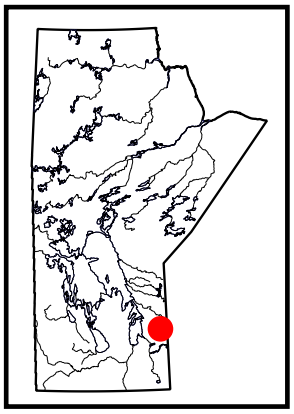

In particular, the pegmatites in southeastern Manitoba are enriched in alkali metals, which provide an excellent opportunity to apply the N-isotope technique to the understanding of the petrogenesis of the Neoarchean granitoids and spatially related LCT pegmatites, and further explore the mechanisms behind the rare-metal enrichment. The use of N isotopes can help tackle three significant scientific issues: 1) the genesis of the Neoarchean TTG suite in southeastern Manitoba; 2) the genesis of the LCT pegmatites in southeastern Manitoba; and 3) the source and rare-metal enrichment processes of the LCT pegmatites.

[1] Department of Earth and Atmospheric Sciences, University of Alberta, 11455 Saskatchewan Drive, Edmonton, Alberta T6G 2E1

As a first step, fieldwork was carried out in July 2023. The general sample characteristics and field relationships recorded at four localities (Tanco LCT pegmatite, Cat Creek pegmatite, Bird Lake supracrustal [S]-type granitoid and Lac du Bonnet granitoid) in southeastern Manitoba are summarized in this report (Figure GS2023-3-1).

Geological background

General geology

Southeastern Manitoba, which is geologically located in the western Superior province, is subdivided into several tectonic elements, including the Uchi domain, English River domain, Bird River domain, Winnipeg River domain and Western Wabigoon domain (Percival et al., 2012; Gilbert et al., 2013; Yang et al., 2019). The Neoarchean BRD, situated between the English River domain and the Western Wabigoon domain, is an east-trending granite-greenstone belt approximately 150 km long extending from Lac du Bonnet, in the west, to Separation Lake (Ontario), in the east (Figure GS2023-3-1; Percival et al., 2006; Gilbert et al., 2008). The supracrustal rocks in the BRD are composed mainly of metavolcanic and metasedimentary rocks and associated synvolcanic intrusive rocks that are separated into two arms by the Mesoarchean Maskwa Lake batholith (Figure GS2023-3-1; Gilbert et al., 2008; Yang and Houlé, 2020). Both the Bird River sill (southern arm) and the Mayville intrusion (northern arm) consist of a series of layered mafic to ultramafic intrusive rocks with a similar age of ca. 2743 Ma, which suggests that they are comagmatic and both part of the Bird River magmatic event (Yang and Houlé, 2020). The later and final stage of mafic magmatism in the BRD is documented by the Maskwa Lake batholith II suite (2726 ±6 Ma; see Wang, 1993), along with granitoids and associated minor gabbroic dikes (Yang and Houlé, 2020). The granitic rocks of the Inconnu plutons and the intrusion at Cat Creek were subsequently emplaced into the belt (Yang and Houlé, 2020). The final stage of BRD magmatism is recorded by the emplacement of the pegmatites along belt-scale faults (Yang and Houlé, 2020).

Numerous granitoid rocks in the BRD have been described in detail (Yang, 2014, 2023; Yang and Houlé, 2020; Yang et al., 2019), including the Maskwa Lake batholith (Bailes et al., 2003), the Marijane Lake pluton, the Birse Lake pluton, the intrusion in the Tin–Osis lakes area and sanukitoid intrusions (Yang, 2014, 2023). The granitoids are defined in part as TTG in the field and represent either the core (i.e., Maskwa Lake batholith I) of the Neoarchean BRD or younger plutons (i.e., Marijane Lake pluton, Birse Lake pluton, intrusion in the Tin–Osis lakes area and sanukitoid intrusions) that have intruded and disrupted the supracrustal rocks of the domain (Yang, 2014, 2023; Yang et al., 2019). Parts of the Marijane Lake pluton, the Birse Lake pluton and the intrusion in the Tin–Osis lakes area are classified as S-type and ilmenite-series granites (Yang, 2014, 2023; Yang et al., 2019). The BRD is also recognized for its LCT pegmatite resources (Černý et al., 1981; Bannatyne, 1985), which are not only spatially related to the S-type granitoids but also considered genetically related to them (Yang, 2014, 2023; Yang et al., 2019).

Tanco LCT pegmatite suite

The Bernic Lake formation in the BRD hosts one of the most economically important and highly fractionated LCT pegmatites in the world (Černý, 2005). The Neoarchean Bernic Lake formation (2724.6 ±1.1 Ma) is dominated by mafic intrusive and volcanic rocks (Gilbert, 2008). The gabbros that host the Tanco LCT pegmatite crystallized at 2723.1 ±0.8 Ma and were subsequently regionally metamorphosed under low-pressure amphibolite-facies conditions (Černý, 2005; Gilbert, 2008; Kremer, 2010). The similar age and close spatial relationship between the Bernic Lake formation and the gabbroic hostrocks indicate that these two units were likely formed during a single magmatic event (Kremer, 2010). The Tanco LCT pegmatite is a bilobate, unexposed intrusion approximately 1520 m long, 1060 m wide and 100 m thick (Černý, 2005). Uranium-lead tantalite (2641 ±3 Ma; Camacho et al., 2012) and zircon (2647.4 ±1.0 Ma; Kremer, 2010) radiometric dating of the pegmatite yielded similar intrusive ages. These ages are consistent with the reactivation of the Bernic Lake shear zone from ca. 2650 to 2640 Ma, facilitating emplacement of the igneous body along the west-trending fault system (Kremer, 2010; Martins et al., 2013). The Tanco LCT pegmatite is granitic and peraluminous in nature, and extremely enriched in economically valuable Li, Cs and Ta (Stilling et al., 2006).

Cat Creek pegmatite suite

The Cat Creek pegmatite suite consists of two main pegmatite bodies and several smaller pegmatite dikes (<20 cm in width), which intruded into a suite of mafic to felsic rocks belonging to the northern arm of the BRD (Yang and Houlé, 2020). Gabbro is the most common hostrock at this location, containing roughly equal proportions of hornblende and plagioclase. The bulk mineral assemblage for this pegmatite is composed of roughly equal proportions of albite and quartz (~40% each, modal abundance), along with minor spodumene and muscovite (~10% each), as well as accessory garnet, apatite and Nb-Ta oxides (~1%).

Samples and field relationships

Outcrop and subsurface samples were collected from four localities in the BRD region of southeastern Manitoba. Brief sample descriptions recorded in the field are presented below.

Tanco LCT pegmatite

The Tanco LCT pegmatite is a highly fractionated pegmatite that is classified as belonging to the LCT family, rare-element class, petalite subtype (Černý and Ercit, 2005). The Tanco pegmatite is composed of nine mineralization zones (Černý, 2005; Stilling et al., 2006). Fist-sized pegmatite samples were collected from the five zones that are currently accessible via the underground mine working faces. The general description of each zone

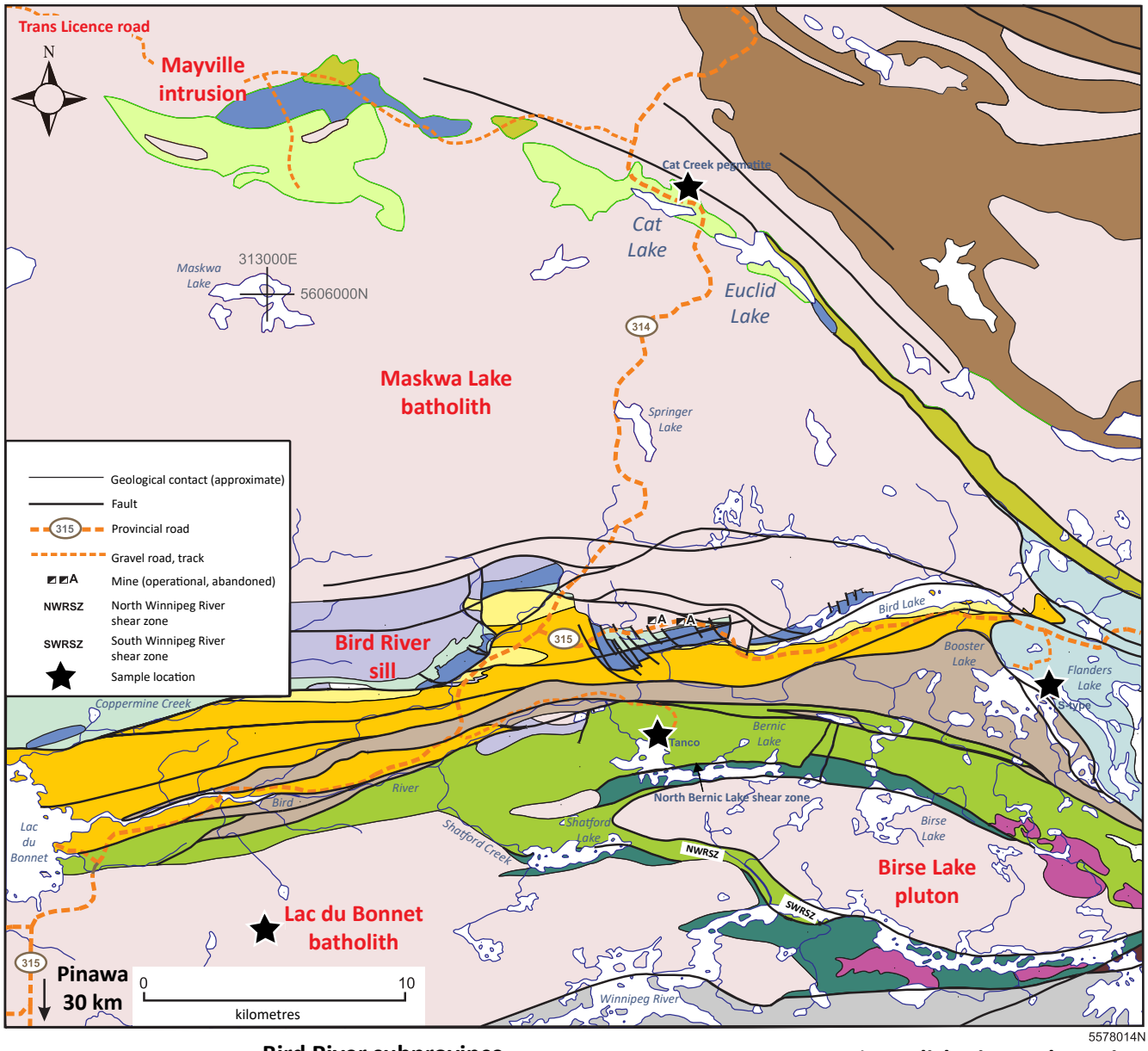

Bird River subprovince

INTRUSIVE ROCKS

- Pegmatite granite
- Granite, granodiorite, tonalite
- Gabbro, diorite, quartz diorite
- Pyroxenite, anorthosite, gabbro

LATE SEDIMENTARY ROCKS

Flanders Lake formation

- Arenite, polymictic conglomerate

Booster Lake formation

- Greywacke, siltstone

VOLCANIC AND SEDIMENTARY ROCKS

BIRD RIVER BELT SOUTH PANEL

Bernic Lake formation

- Heterolithic volcanic breccia, rhyolite, basalt, andesite

Eaglenest Lake formation

- Greywacke, siltstone

Southern MORB-type formation

- Basalt, aphyric; gabbro

BIRD RIVER NORTH PANEL

Diverse arc assemblage

- Massive to fragmental, mafic to felsic volcanic and sedimentary rocks

Peterson creek formation

- Massive to fragmental felsic volcanic rocks

Northern MORB-type formation

- Basalt, aphyric; gabbro

CAT LAKE AREA

- Sedimentary and volcanic rocks, related gneiss
- Tholeiitic basalt

English River subprovince

- Paragneiss, granitoid intrusive rocks, migmatite, pegmatite

Winnipeg River subprovince

- Tonalite, granodiorite, granitoid gneiss

Figure GS2023-3-1: *Regional geology of the Cat Lake–Euclid Lake and Winnipeg River area, southeastern Manitoba, showing the main part of the Bird River greenstone belt between Lac du Bonnet and Flanders Lake, and the northern arm extending as far as the Mayville intrusion (modified from Yang et al., 2013). Abbreviation: MORB, mid-ocean–ridge basalt. All co-ordinates are in UTM Zone 15, NAD83.*

is given below based on field observations as well as literature summaries from Černý (2005) and Stilling et al. (2006).

Zone 20 (wall zone)

The mineralogy of the pegmatite wall zone is mostly megacrystic microcline-perthite, quartz and albite. Minor components of tourmaline, muscovite, lithian muscovite and beryl are evident. The geochemical composition of the wall-zone pegmatite is considered to represent the bulk composition of the Tanco pegmatite (Černý, 2005; Stilling et al., 2006).

Zone 50 (spodumene zone)

The spodumene zone is composed mainly of microcrystalline to megacrystic spodumene and quartz intergrowths with various textures (Breasley et al., 2022). Minor amounts of microcline-perthite, petalite, eucryptite, tantalum oxides, albite and lithian muscovite are present. Xenoliths of amphibolite hostrocks were observed in this zone of the pegmatite, which is of significant economic importance due to the presence of high-grade Li within the Tanco LCT pegmatite.

Zone 70 (quartz zone)

The quartz zone consists of nearly monomineralic quartz. Spodumene xenoliths as well as muscovite veins are commonly observed within the megacrystic quartz. The quartz zone locally has a K-feldspar–rich cap that contains spodumene and quartz intergrowths. The genesis of the quartz zone and its potential role in metal enrichment of the Tanco pegmatite is uncertain.

Zone 80 (pollucite zone)

The pollucite zone consists of nearly monomineralic pollucite. Minor amounts of quartz, spodumene, petalite, muscovite, lepidolite, albite, microcline and apatite can be observed. This zone contains a significant amount of Cs (~75% pure pollucite; Stilling et al., 2006).

Zone 90 (lepidolite zone)

The lepidolite zone is hypothesized to have formed from metasomatism, with purple lithian muscovite replacing primary feldspar (Černý, 2005). Microlite, which is the main Ta-bearing mineral at the Tanco mine, is found intermixed with muscovite and quartz that has replaced microcline (Černý, 2005). The dominant minerals in this zone include lithian muscovite, lepidolite and microcline-perthite, with minor amounts of albite, quartz, beryl, Ta oxides, cassiterite and zircon. This zone is of economic interest due to the high concentrations of Rb and Cs in micas, and the presence of Ta and Nb oxides.

Other pegmatite samples

Samples from a pegmatite in the Cat Creek area were collected for this study. Both the amphibolite hostrock and the pegmatite itself were sampled. In the contact zone, both the amphibolite and pegmatite show varying intensity of shear fabrics, indicating deformation during pegmatite emplacement. The amphibolite hostrock is composed mostly of hornblende and plagioclase, with minor biotite, apatite, epidote and chlorite. The pegmatite is mainly composed of albite, K-feldspar and quartz, with spodumene, tourmaline, muscovite, apatite, garnet and epidote as accessory minerals.

Granitoid samples

Bird Lake S-type granitoid samples were collected along with spatially associated metasedimentary hostrocks (metagreywacke from the Flanders Lake formation; Yang, 2014). The lithology of the S-type granitoid is predominantly medium- to coarse-grained two-mica granite. The sharp contact between the granitoid and hostrock, and the presence of metasedimentary enclaves within the granitoid body, imply that the granitic magma intruded into the metasedimentary hostrock (Figure GS2023-3-2) and potentially assimilated the sedimentary rocks, but this has yet to be determined.

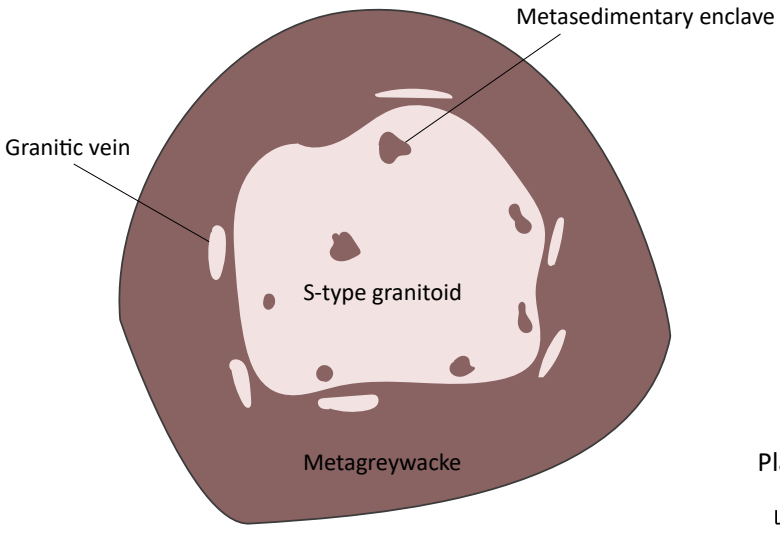

Figure GS2023-3-2: *Schematic illustration of the field relationship between the Bird Lake S-type granitoid and metasedimentary hostrock. Abbreviation: S, supracrustal.*

Samples of the Lac du Bonnet batholith were collected in the Pinawa dam area. The batholith was identified as TTG in the field (Yang, 2014, 2023). The major minerals in these rocks are quartz, K-feldspar and plagioclase, with minor biotite.

Economic considerations

The pegmatites from the Cat Lake–Winnipeg River pegmatite field in southeastern Manitoba are economically significant due to their high contents of rare metals, such as Li, Cs and Ta (Černý, 2005). The increasingly high demands for Li for rechargeable batteries as well as for Cs for drilling fluids make the exploration of pegmatitic resources in Manitoba crucial to the Canadian economy. This project is designed to use the novel N-isotope technique, which is currently one of the best tools to assess the geochemical affinity of alkali metals, to trace the source and enrichment mechanism of Li and Cs. The results are expected to provide insights for greater exploration potential in Manitoba and elsewhere in the Archean Superior province in Canada.

Acknowledgments

The authors thank W. Ezeana and D. Drayson for assistance in the field, and T. Martins and C. Couëslan for constructive reviews of this report. They also thank the Sinomine Tanco team for their support in this project, particularly J. Champagne, W. Wu, J. Zhong, and C. Zhou. The editorial assistance of RnD Technical and report layout by C. Steffano are gratefully acknowledged.

References

Bailes, A.H., Percival, J.A., Corkery, M.T., McNicoll, V.J., Tomlinson, K.Y., Sasseville, C., Rogers, N., Whalen, J.B. and Stone, D. 2003: Geology and tectonostratigraphic assemblages, West Uchi map area, Manitoba/Ontario; Manitoba Industry, Trade and Mines, Open File Report OF2003-1, Geological Survey of Canada, Open File 1522 and Ontario Geological Survey, Preliminary Map P.3461, 1:250 000 scale, URL <https://doi.org/10.4095/213986>.

Bannatyne, B.B. 1985: Industrial minerals in rare-element pegmatites of Manitoba; Manitoba Energy and Mines, Mineral Resources Division, Economic Geology Report ER84-1, 96 p., URL <https://manitoba.ca/iem/info/libmin/ER84-1.pdf> [September 2023].

Breasley, C.M., Martins, T., Linnen, R.L. and Groat, L.A. 2022: Investigating textural and geochemical relations of lithium mineralization in the Tanco pegmatite, southeastern Manitoba (part of NTS 52L6); *in* Report of Activities 2022, Manitoba Natural Resources and Northern Development, Manitoba Geological Survey, p. 25–35, URL <https://manitoba.ca/iem/geo/field/roa22pdfs/GS2022-4.pdf> [September 2023].

Camacho, A., Baadsgaard, H., Davis, D.W. and Černý, P. 2012: Radiogenic isotope systematics of the Tanco and Silverleaf granitic pegmatites, Winnipeg River pegmatite district, Manitoba; The Canadian Mineralogist, v. 50, no. 6, p. 1775–1792.

Černý, P. 2005: The Tanco rare-element pegmatite deposit, Manitoba: regional context, internal anatomy, and global comparisons; *in* Rare-Element Geochemistry and Mineral Deposits, R.L. Linnen and I.M. Samson (ed.), Geological Association of Canada, Short Course Notes, v. 17, p. 127–158.

Černý, P. and Ercit, T.S. 2005: The classification of granitic pegmatites revisited; The Canadian Mineralogist, v. 43, no. 6, p. 2005–2026.

Černý, P., Trueman, D.L., Ziehlke, D.V., Goad, B.E. and Paul, B.J. 1981: The Cat Lake–Winnipeg River and the Wekusko Lake pegmatite fields, Manitoba; Manitoba Department of Energy and Mines, Mineral Resources Division, Economic Geology Report ER80-1, 216 p., URL <https://manitoba.ca/iem/info/libmin/ER80-1.zip> [September 2023].

Gilbert, H.P. 2008: Stratigraphic investigations in the Bird River greenstone belt, Manitoba (part of NTS 52L5, 6); *in* Report of Activities 2008, Manitoba Science, Technology, Energy and Mines, Manitoba Geological Survey, p. 121–138, URL <https://manitoba.ca/iem/geo/field/roa08pdfs/GS-11.pdf> [September 2023].

Gilbert, H.P., Davis, D.W., Duguet, M., Kremer, P.D., Mealin, C.A. and MacDonald, J. 2008: Geology of the Bird River Belt, southeastern Manitoba (parts of NTS 52L5, 6); Manitoba Science, Technology, Energy and Mines, Manitoba Geological Survey, Geoscientific Map MAP2008-1, scale 1:50 000, URL <https://manitoba.ca/iem/info/libmin/MAP2008-1.zip> [September 2023].

Gilbert, H.P., Houlé, M.G., Yang, X.M., Scoates, J.S., Scoates, R.F.J., Mealin, C.A., Bécu, V., McNicoll, V.J. and Galeschuk, C.R. 2013: Mafic and ultramafic intrusive rocks and associated Ni-Cu-(PGE) and Cr-(PGE) mineralization in the Bird River greenstone belt, southeast Manitoba; Geological Association of Canada–Mineralogical Association of Canada, Joint Annual Meeting, May 22–24, 2013, Winnipeg, Manitoba, Field Trip Guidebook FT-C2, Manitoba Innovation, Energy and Mines, Manitoba Geological Survey, Open File OF2013-7, 51 p., URL <https://manitoba.ca/iem/info/libmin/gacmac/OF2013-7_FT-C2.pdf> [September 2023].

Honma, H. and Itihara, Y. 1981: Distribution of ammonium in minerals of metamorphic and granitic rocks; Geochimica et Cosmochimica Acta, v. 45, p. 983–988, URL <https://doi.org/10.1016/0016-7037(81)90122-8>.

Jia, Y., Kerrich, R. and Goldfarb, R. 2003: Metamorphic origin of ore-forming fluids for orogenic gold-bearing quartz vein systems in the North American Cordillera: constraints from a Reconnaissance Study of $\delta^{15}N$, δD, and $\delta^{18}O$; Economic Geology, v. 98, p. 109–123, URL <https://doi.org/10.2113/gsecongeo.98.1.109>.

Kremer, P.D. 2010: Structural geology and geochronology of the Bernic Lake area in the Bird River greenstone belt, Manitoba: evidence for syn-deformational emplacement of the Bernic Lake pegmatite group; M.Sc. thesis, University of Waterloo, Waterloo, Ontario, 91 p.

Li, L., Zheng, Y.-F., Cartigny, P. and Li, J. 2014: Anomalous nitrogen isotopes in ultrahigh-pressure metamorphic rocks from the Sulu orogenic belt: effect of abiotic nitrogen reduction during fluid-rock interaction; Earth and Planetary Science Letters, v. 403, p. 67–78, URL <https://doi.org/10.1016/j.epsl.2014.06.029>.

Li, K., Li, L., Pearson, D.G. and Stachel, T. 2019: Diamond isotope compositions indicate altered igneous oceanic crust dominates deep carbon recycling; Earth and Planetary Science Letters, v. 516, p. 190–201, URL <https://doi.org/10.1016/j.epsl.2019.03.041>.

Li, L., He, Y., Zhang, Z. and Liu, Y. 2021: Nitrogen isotope fractionations among gaseous and aqueous NH_4^+, NH_3, N_2, and metal-ammine complexes: theoretical calculations and applications; Geochimica et Cosmochimica Acta, v. 295, p. 80–97, URL <https://doi.org/10.1016/j.gca.2020.12.010>.

Martins, T., Kremer, P. and Vanstone, P. 2013: The Tanco mine: geological setting, internal zonation and mineralogy of a world-class rare element pegmatite deposit; Geological Association of Canada–Mineralogical Association of Canada, Joint Annual Meeting, May 22–24, 2013, Winnipeg, Manitoba, Field Trip Guidebook FT-C1; Manitoba Innovation, Energy and Mines, Manitoba Geological Survey, Open File OF2013-8, 17 p., URL <https://manitoba.ca/iem/info/libmin/gacmac/OF2013-8_FT-C1. pdf> [September 2023].

Percival, J.A., McNicoll, V. and Bailes, A.H. 2006: Strike-slip juxtaposition of ca. 2.72 Ga juvenile arc and >2.98 Ga continent margin sequences and its implications for Archean terrane accretion, western Superior province, Canada; Canadian Journal of Earth Sciences, v. 43, p. 895–927, URL <https://doi.org/10.1139/e06-039>.

Percival, J.A., Skulski, T., Sanborn-Barrie, M., Stott, G.M., Leclair, A.D., Corkery, M.T. and Boily, M. 2012: Geology and tectonic evolution of the Superior province, Canada; *in* Tectonic Styles in Canada: The LITHOPROBE Perspective, J.A. Percival, F.A. Cook and R.M. Clowes (ed.), Geological Association of Canada, Special Paper 49, p. 321–378.

Stilling, A., Černý, P. and Vanstone, P.J. 2006: The Tanco pegmatite at Bernic Lake, Manitoba. XVI. Zonal and bulk compositions and their petrogenetic significance; The Canadian Mineralogist, v. 44, no. 3, p. 599–623, URL <https://doi.org/10.2113/gscanmin.44.3.599>.

Wang, X. 1993. U-Pb zircon geochronological study of the Bird River greenstone belt, southeastern Manitoba; M.Sc. thesis, University of Windsor, Windsor, Ontario, 96 p.

Yang, X.M. 2014: Granitoid rocks in southeastern Manitoba: preliminary results of reconnaissance mapping and sampling; *in* Report of Activities 2014, Manitoba Mineral Resources, Manitoba Geological Survey, p. 49–63, URL <https://manitoba.ca/iem/geo/field/roa14pdfs/GS-4.pdf> [September 2023].

Yang, X.M. 2023: Progress report on the study of granitoids in Manitoba: petrogenesis and metallogeny; Manitoba Economic Development, Investment and Trade, Manitoba Geological Survey, Open File OF2022-3, 119 p., URL <https://manitoba.ca/iem/info/libmin/OF2022-3.zip> [September 2023].

Yang, X.M. and Houlé, M.G. 2020: Geology of the Cat Creek–Euclid Lake area, Bird River greenstone belt, southeastern Manitoba (parts of NTS 52L11, 12); Manitoba Department of Agriculture and Resource Development, Manitoba Geological Survey, Geoscientific Report GR2020-1, 105 p., map at 1:20 000 scale, URL <https://manitoba.ca/iem/info/libmin/GR2020-1.zip> [September 2023].

Yang, X.M., Drayson, D. and Polat, A. 2019: S-type granites in the western Superior Province: a marker of Archean collision zones; Canadian Journal of Earth Sciences, v. 56, p. 1409–1436, URL <https://doi.org/10.1139/cjes-2018-0056>.

Yang, X.M., Gilbert, H.P. and Houlé, M.G. 2013: Cat Lake–Euclid Lake area in the Neoarchean Bird River greenstone belt, southeastern Manitoba (parts of NTS 52L11, 12): preliminary results of bedrock geological mapping and their implications for geodynamic evolution and metallogeny; *in* Report of Activities 2013, Manitoba Mineral Resources, Manitoba Geological Survey, p. 70–84, URL <https://manitoba.ca/iem/geo/field/roa13pdfs/GS-6.pdf> [September 2023].

GS2023-4

Preliminary examination of the Tappy, Eagle and F.D. No. 5 pegmatites in the Cat Lake–Winnipeg River pegmatite field, southeastern Manitoba (parts of NTS 52L5, 11)

by J. Roush[1], T. Martins, C.R.M. McFarlane[1], M.L. Rinne and L. Groat[2]

In Brief:

- A master's project was initiated focusing on selected Li-bearing pegmatites in the Cat Lake–Winnipeg River pegmatite field
- Observations and samples were taken at the Tappy, Eagle and F.D. No. 5 pegmatites
- Future work aims at accomplishing a robust time of emplacement and mineralogical report for these dikes

Citation:
Roush, J., Martins, T., McFarlane, C.R.M., Rinne, M.L. and Groat, L. 2023: Preliminary examination of the Tappy, Eagle and F.D. No. 5 pegmatites in the Cat Lake–Winnipeg River pegmatite field, southeastern Manitoba (parts of NTS 52L5, 11); *in* Report of Activities 2023, Manitoba Economic Development, Investment, Trade and Natural Resources, Manitoba Geological Survey, p. 20–26.

Summary

This study is part of an M.Sc. thesis based at the University of New Brunswick, initiated in 2023 in collaboration with the Manitoba Geological Survey. During this summer's fieldwork, the first author examined three pegmatite sites in the Cat Lake–Winnipeg River pegmatite field, located in southeastern Manitoba, from June through August. Fieldwork focused on the Tappy, Eagle and F.D. No. 5 pegmatites. Field observations on the mineralogy and structure of the three pegmatites were made in order to provide a preliminary description of the three lithium-bearing dikes. Samples were also collected from each locality for further investigation.

Introduction

Global demand for battery metals such as lithium (Li) is experiencing a sharp rise due to the implementation of new modes of energy production, distribution and storage. Electric vehicle technology, along with new and improved electronics for both small- and large-scale consumers, have helped increase this interest. As the attention to critical materials grows, so does the need to mine resources such as Li. Pegmatites are one of the earth's prominent carriers of rare and critical elements, acting to concentrate incompatible elements within them (Černý et al., 2012). Manitoba is well positioned in the critical minerals field, with a long and successful history of exploration and production of lithium from Li-bearing pegmatites (Tanco mine). The Cat Lake–Winnipeg River pegmatite field, located in the Bird River domain of the Archean Superior province, hosts various pegmatites, some highly evolved and some simple (Černý et al., 1981).

This project has several objectives concerning the Tappy, Eagle and F.D. No. 5 pegmatites:

- conduct fieldwork to assess the geological setting, macroscopic zonation and structure of the different pegmatites
- use whole-rock lithogeochemistry, mineral chemistry and geochronological analysis to better understand the petrogenesis and crystallization ages of the pegmatites
- determine if there is a petrogenetic relationship between the Eagle and F.D. No. 5 pegmatites
- compare genetic and geochemical relationships to other pegmatites in the Cat Lake–Winnipeg River pegmatite field

This information will help to build a better geological and mineralogical understanding of the pegmatite dikes' origin and aid exploration efforts in the area.

Regional geology

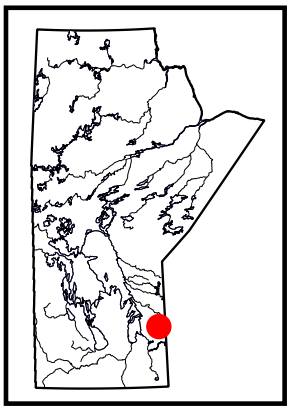

Compositionally, the Tappy, Eagle and F.D. No. 5 pegmatites can best be described as Li-bearing rare-element pegmatites that are broadly ascribed to the Li-Cs-Ta (LCT) family of pegmatites according to the classification by Černý and Ercit (2005). The Tappy pegmatite is located south of the Bird River along Provincial Road 315. The other two sites, the Eagle and F.D. No. 5 pegmatites, are located on the west and east sides, respectively, of Provincial Road 314 just north of Cat Lake. All three pegmatites are situated within the Cat Lake–Winnipeg River pegmatite field, approximately 200 km northeast of Winnipeg (Figure GS2023-4-1). Pegmatites in this region occur within the westernmost exposed portions of the Bird River domain, which is bounded to the north by the English River subprovince and to the south by the Winnipeg River terrane (Gilbert, 2008). The Cat Lake–Winnipeg River pegmatite field comprises two districts: the Winnipeg River district in the south and the Cat Lake district in the north (Černý et al., 1981).

The Tappy pegmatite occurs in the Winnipeg River pegmatite district, which extends east for approximately 50 km from Lac du Bonnet toward the Ontario border. It contains many pegmatites,

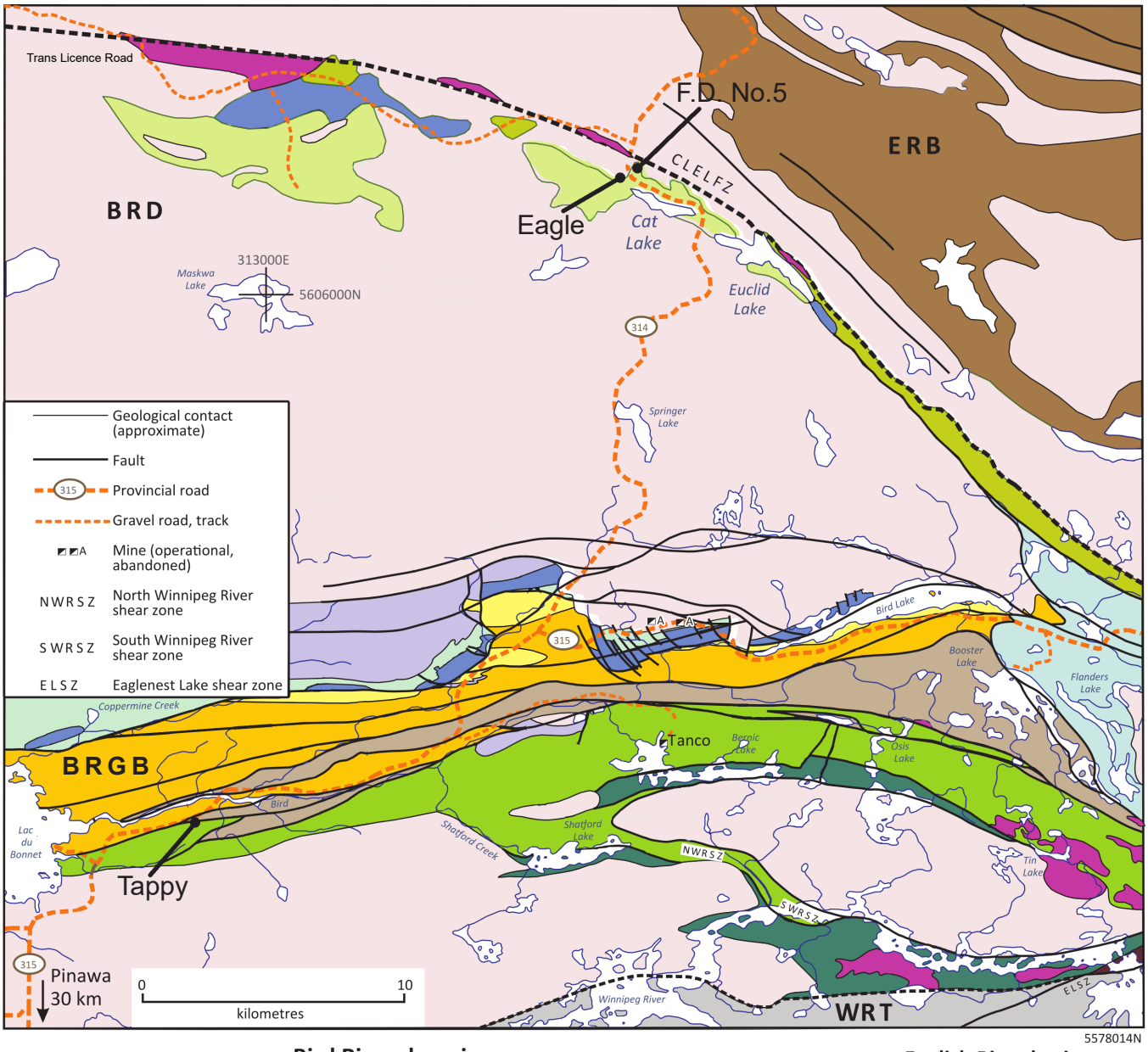

Bird River domain

Intrusive rocks

- S-type granite
- Granite, granodiorite, tonalite
- Gabbro, diorite, quartz diorite
- Pyroxenite, anorthosite, gabbro

Late sedimentary rocks

Flanders Lake formation

- Arenite, polymictic conglomerate

Booster Lake formation

- Greywacke, siltstone

Volcanic and sedimentary rocks

Bird River belt South Panel

Bernic Lake formation

- Heterolithic volcanic breccia, rhyolite, basalt, andesite

Eaglenest Lake formation

- Greywacke, siltstone

Southern MORB-type formation

- Basalt, aphyric; gabbro

Bird River belt North Panel

- Massive to fragmental, mafic to felsic volcanic and sedimentary rocks

Peterson Creek formation

- Massive to fragmental felsic volcanic rocks

Northern MORB-type formation

- Basalt, aphyric; gabbro

Cat Lake area

- Sedimentary and volcanic rocks, related gneiss
- Tholeiitic basalt

English River basin

- Paragneiss, granitoid intrusive rocks, migmatite, pegmatite

Winnipeg River terrane

- Tonalite, granodiorite, granitoid gneiss

- Domain or terrane boundary

Figure GS2023-4-1: *Tectonic assemblages of the Bird River greenstone belt (modified after Yang and Houlé, 2020). Locations of the studied pegmatites are shown with black arrows. Abbreviations: BRD, Bird River domain; BRGB, Bird River greenstone belt; CLELFZ, Cat Lake–Euclid Lake fault zone; ERB, English River basin; MORB, mid-ocean–ridge basalt; WRT, Winnipeg River terrane.*

both simple and Li-bearing, including the actively mined Tanco. The Tappy pegmatite is hosted within the Bird River greenstone belt (BRGB), a panel of supracrustal rocks described as a transitional oceanic-continental margin and composed of deformed and metamorphosed basalts, felsic volcanic to volcaniclastic rocks, and sedimentary rocks (Gilbert, 2008).

The other two pegmatites described in this study, the Eagle and F.D. No. 5 pegmatites, are located in the Cat Lake pegmatite district, which is located in the northern part of the Cat Lake–Winnipeg River pegmatite field. The Cat Lake pegmatite district lies to the north of the Maskwa Lake batholith within the northern part of the BRGB (Gilbert, 2008; Yang and Houlé, 2020). The northern part of the BRGB, which includes the Cat Lake pegmatite district, is separated from the ERB by the Cat Lake–Euclid Lake fault zone (see Figure GS2023-4-1; Yang and Houlé, 2020). This part of the BRGB is characterized by basalts, volcaniclastic and sedimentary sequences and other intrusive units overlying the older phases of the large Maskwa Lake batholith to the south (Yang and Houlé, 2020).

Geology of studied pegmatites

Tappy pegmatite

The Tappy pegmatite is a Li-rich spodumene-bearing pegmatite dike that is well exposed for more than 50 m (Bannatyne, 1985). It is narrowest at its southern end and broadens northward until eventually ending at a cliff (Figure GS2023-4-2). Another small outcrop with a composition similar to that of the Tappy pegmatite is visible roughly 100 m to the south; this is referred to as the Tappy South. The Tappy pegmatite is oriented north-south, with a strike ranging from 300° to 002°. At the widest extent of the pegmatite in the northern half of the exposure, the dike reaches almost 4 m in width, but the majority is less than 3 m in width, with the southern half having a maximum width of 1.5 m.

The Tappy pegmatite is hosted within foliated metamorphosed pillow basalt. The main foliation of the pillows strikes 243° and is subvertical. A pervasive, unevenly spaced cleavage through the metabasalt strikes 358° and is subvertical, which is similar to the strike of the pegmatite. The other structural feature is spaced fractures striking 300° and dipping 35° (Figure GS2023-4-3). Representative samples were taken from the Tappy pegmatite for geochemical analysis.

At the southernmost extent of the Tappy pegmatite, three distinct zones are visible. At this end, a light-coloured chilled margin less than 1 cm wide is present along much of the dike. Mineralogy is not easily discernible. Moving inward, the intermediate zone is present throughout the length of the pegmatite but has a variable thickness. It consists of quartz, feldspar and muscovite less than 0.5 cm in size. This area is partially hematized, with small veins of rust-coloured material running through it. The most distinct zone is the central zone, consisting of quartz, feld-

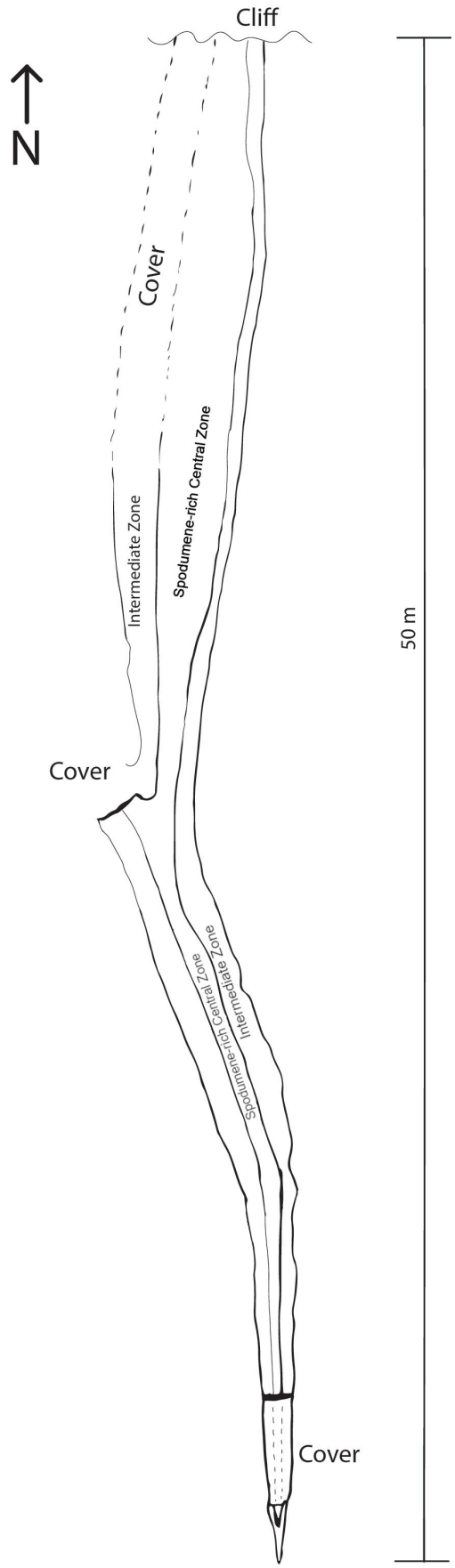

Figure GS2023-4-2: *Rough sketch of the Tappy pegmatite, showing its zonation, made during the 2023 field season. Proportions are not to scale so as to better show the approximate definition between the zones.*

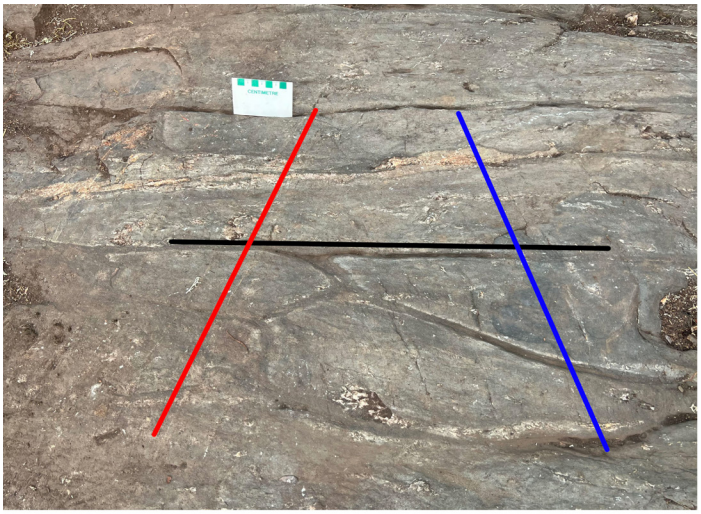

Figure GS2023-4-3: *Outcrop photograph of structures present in the pillow basalt around the Tappy pegmatite (facing northeast). The black line indicates the strike of the foliation in the pillowed metabasalts (063°, with subvertical dip). The red line indicates the spaced cleavages (striking 178° with subvertical dip) and the blue line indicates the other set of spaced cleavages (striking 300°).*

spar and muscovite but having a larger grain size (1–2 cm) than the intermediate zone. Hematization is also present in the central zone. Pervasive spodumene is readily visible, starting in the middle of the dike and extending northward. The size of the spodumene crystals increases northward, reaching 15 cm. It is unclear whether small grains of spodumene are present throughout the other zones of the pegmatite. Tantalite is observed as 1–3 mm crystals, which are most abundant in areas within the pegmatite that have larger sized crystals. Petrographic studies will provide more information on the distribution of minerals throughout the Tappy pegmatite.

Eagle pegmatite

The Eagle pegmatite outcrop consists of multiple, parallel dikes that trend east over an exposed area of bedrock (Bannatyne, 1985). Vegetation cover on the outcrop made it difficult to differentiate between the different dikes. However, it was sparse enough for thorough observation of the exposed areas. The dikes are hosted by a dominantly metagranitoid rock that is composed of variably deformed, mottled blue quartz and pink feldspar with minor biotite and hornblende. Moving to the south from the main exposure at Eagle, the metagranitoid grades into lighter-coloured rock composed of less biotite and more quartz. The southern part of the granitoid borders a weakly foliated and metamorphosed amphibolite (Bannatyne, 1985). The grains in this unit reach 1–3 mm. The amphibolite unit is weakly foliated, strikes 110° and borders the metagranitoid with a sheared boundary that also trends approximately 110°. The size of the grains within the metagranitoid unit is 0.5–1 cm. The granitoid extends from east to west for the majority of the exposure of the Eagle pegmatite. The pegmatite dikes of the Eagle range from approximately 10 cm to 9 m in width (Bannatyne, 1985). The composition of the pegmatites is relatively uniform, with variable modal percentages of feldspar, quartz, spodumene and white micas, and minor apatite, beryl and lepidolite.

The Eagle pegmatite exhibits crude zonation. In many parts, there is a visible chilled margin along the edge of the pegmatite, but it is never more than 1 cm thick. The nature of this zone made mineral identification impossible. Two main zones were observed: 1) an aplitic textured zone composed of white to pink aplitic quartz, feldspar, mica and minor garnet; and 2) a pegmatitic central zone composed of variably sized quartz, feldspar, mica and spodumene, with minor tourmaline, beryl and garnet (Figure GS2023-4-4). A third, less distinct zone within the Eagle dike is a mixture of both aplitic and pegmatitic textures.

In addition to field observations of the outcrops at the Eagle pegmatite, two drillcores were examined and logged (LT-21-09 and LT-21-11). The first drillhole (LT-21-09) is 89 m long and consists of granitic dikes crosscutting a dark, biotite-bearing granitoid rock. This hostrock is similar to that described for the Eagle pegmatite outcrop (Figure GS2023-4-4a). Core from this hole has multiple smaller pegmatites devoid of Li near the top of the hole and one larger spodumene-bearing pegmatite near the bottom. These smaller pegmatites are composed mainly of white feldspar, quartz and micas, and show varying degrees of hematization. The larger pegmatite near the end of drillhole LT-21-09 is 9 m in apparent width and consists of white feldspar, quartz that varies from clear to smoky, and spodumene. The foliated spodumene texture is abundant in this dike. Zones of this pegmatite are hematized to varying degrees.

The second drillhole (LT-21-11) is 119 m long and consists of granitic dikes crosscutting a very similar, granodiorite hostrock. This hole has a pattern similar to that in LT-21-09, with smaller pegmatites crosscutting the granodiorite near the top of the hole and one large, more mineralized pegmatite near the bottom. However, the core in drillhole LT-21-11 records more hostrock with some mafic volcanic xenoliths below the large pegmatite, due only to its greater length. The smaller pegmatites in the drillhole are composed mainly of white feldspar, quartz, and micas that show varying degrees of hematization (Figure GS2023-4-5a). The large pegmatite intersected in drillhole LT-21-11 is roughly 11 m in apparent width and consists of similar minerals to the pegmatite logged in drillhole LT-21-09. Various textures, such as a mixture of finer grained groundmass with comparatively large crystal sizes and foliated spodumene, are present in the pegmatites in both of the drillcores.

F.D. No. 5 pegmatite

The F.D. No. 5 pegmatite is composed of very coarse grained pegmatitic minerals in shades of pink to white. The pegmatite is hosted by a metagranodiorite similar to that observed at the Eagle and outcrops immediately northeast of it (Figure GS2023-4-6). Crystal size ranges from small (<1 cm) to large prismatic

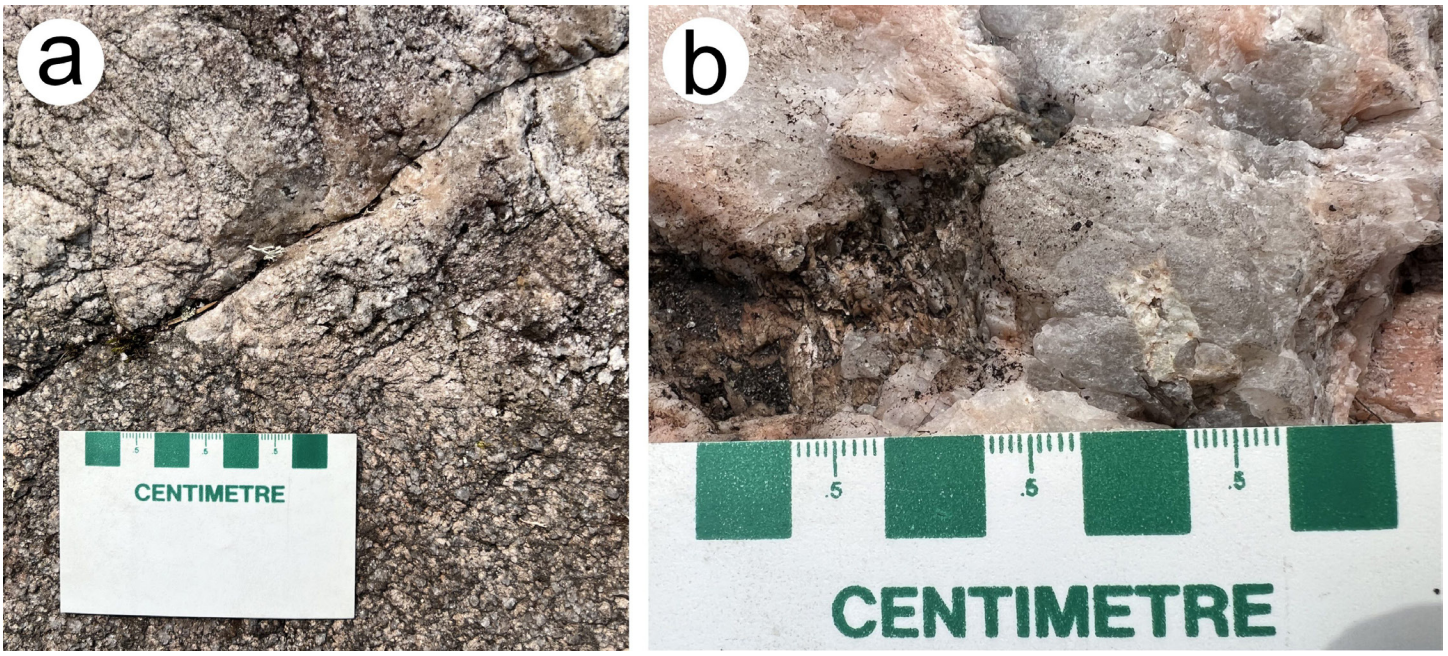

Figure GS2023-4-4: *Outcrop photographs of the Eagle pegmatite:* ***a)*** *border between the darker coloured metagranitoid country rock at the bottom and the lighter coloured aplitic section of pegmatite;* ***b)*** *detail of beryl in the eastern part of the pegmatite.*

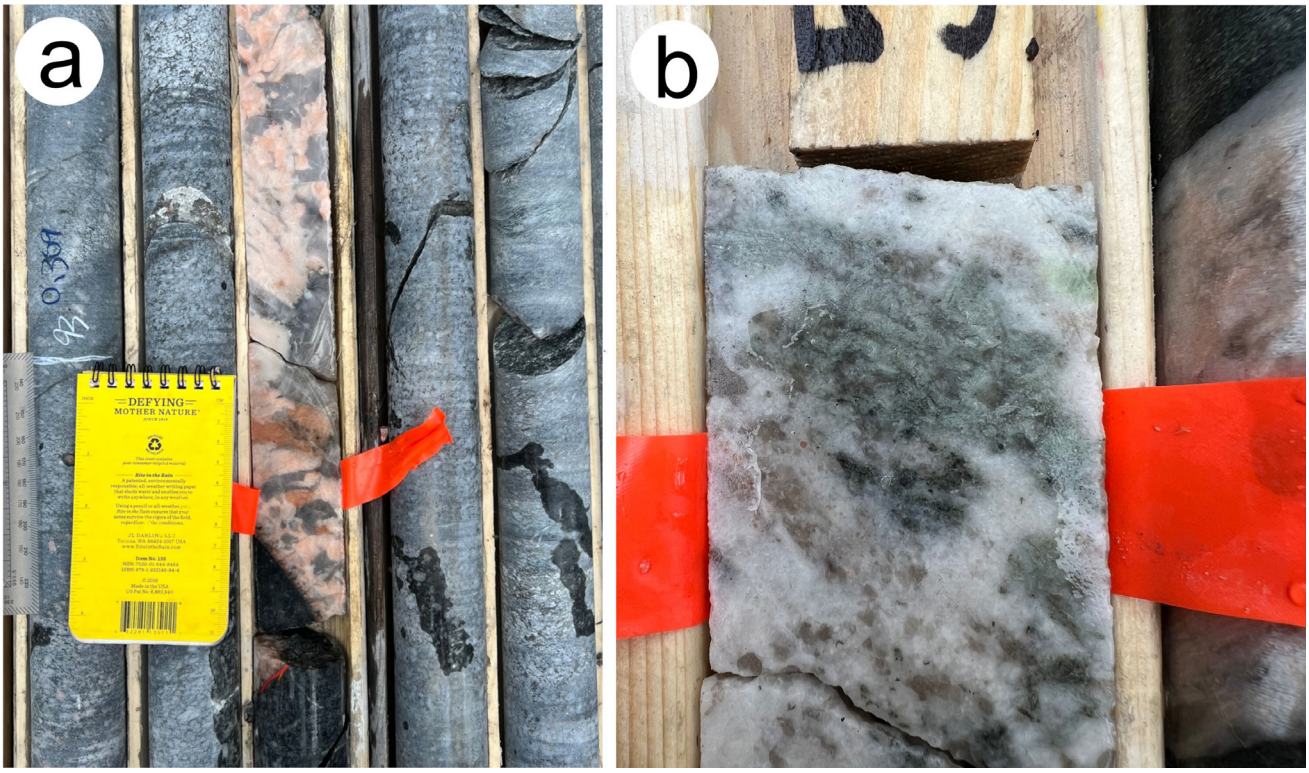

Figure GS2023-4-5: *Samples from drillhole LT-21-11:* ***a)*** *contact of a dike composed primarily of quartz and feldspar at 45 degrees to the core axis (95.8 m depth);* ***b)*** *green spodumene within a white dike (48.1 m depth). All core pictured is NQ (47.6 mm diameter).*

feldspars that reach over a metre in length but are sparsely distributed throughout the dike (Figure GS2023-4-7a). The exposure of the F.D. No. 5 pegmatite is composed primarily of quartz, feldspar and spodumene up to 4 cm and books of mica up to 7 cm wide. Spodumene is present in multiple areas throughout the pegmatite. Figure GS2023-4-7b shows a prominent exposure of one of these zones with large green spodumene crystals. Composition of this zone can locally be up to 80 modal percent spodumene, with other areas of high spodumene concentration being present elsewhere throughout the dike. Small veins

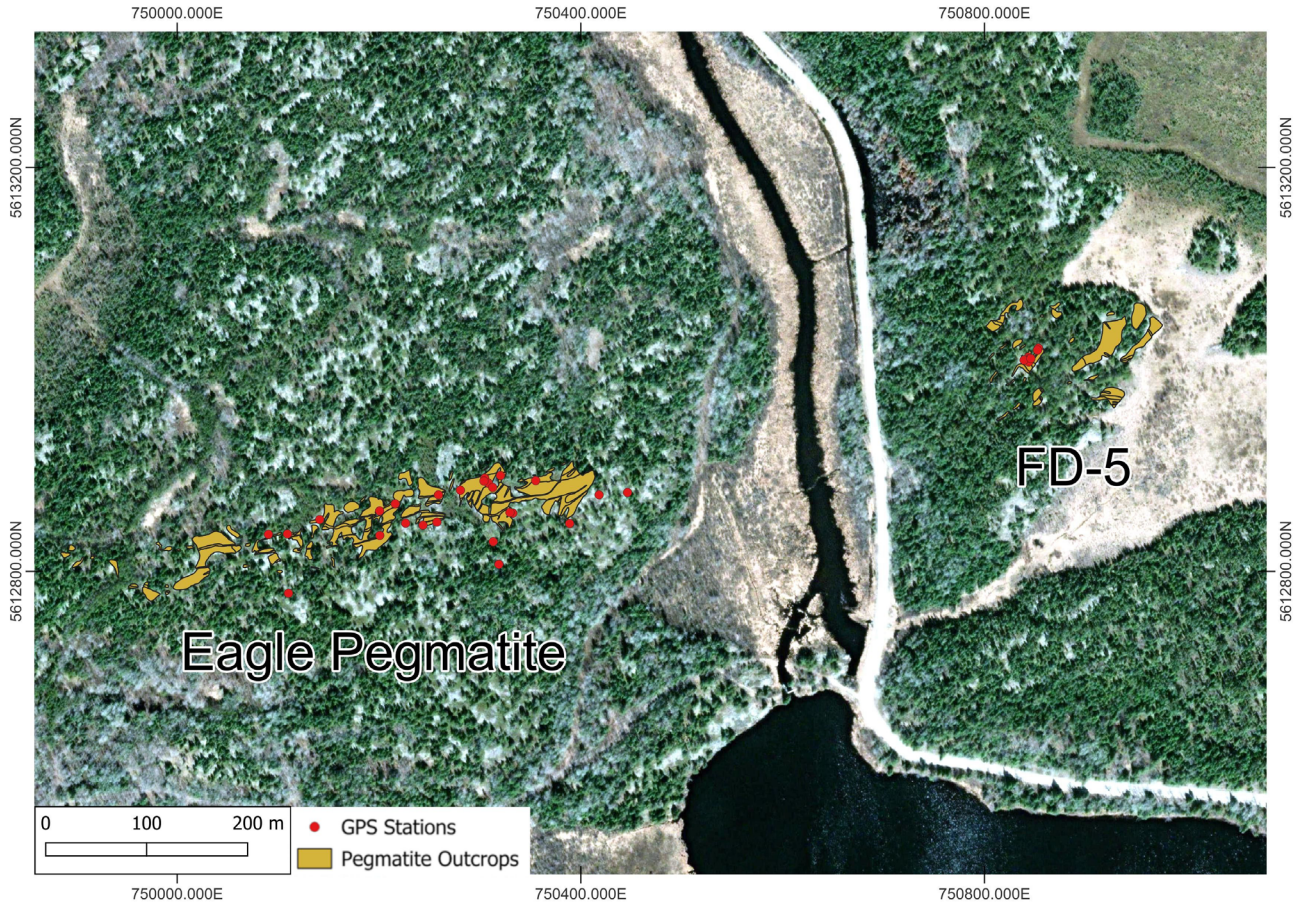

Figure GS2023-4-6: *Airphoto of the Eagle and F.D. No. 5 area with preliminary map of the pegmatite outcrops and larger bodies, showing the relationship between the Eagle and F.D. No. 5 dikes. Outcrop locations from D. Owens (unpublished data).*

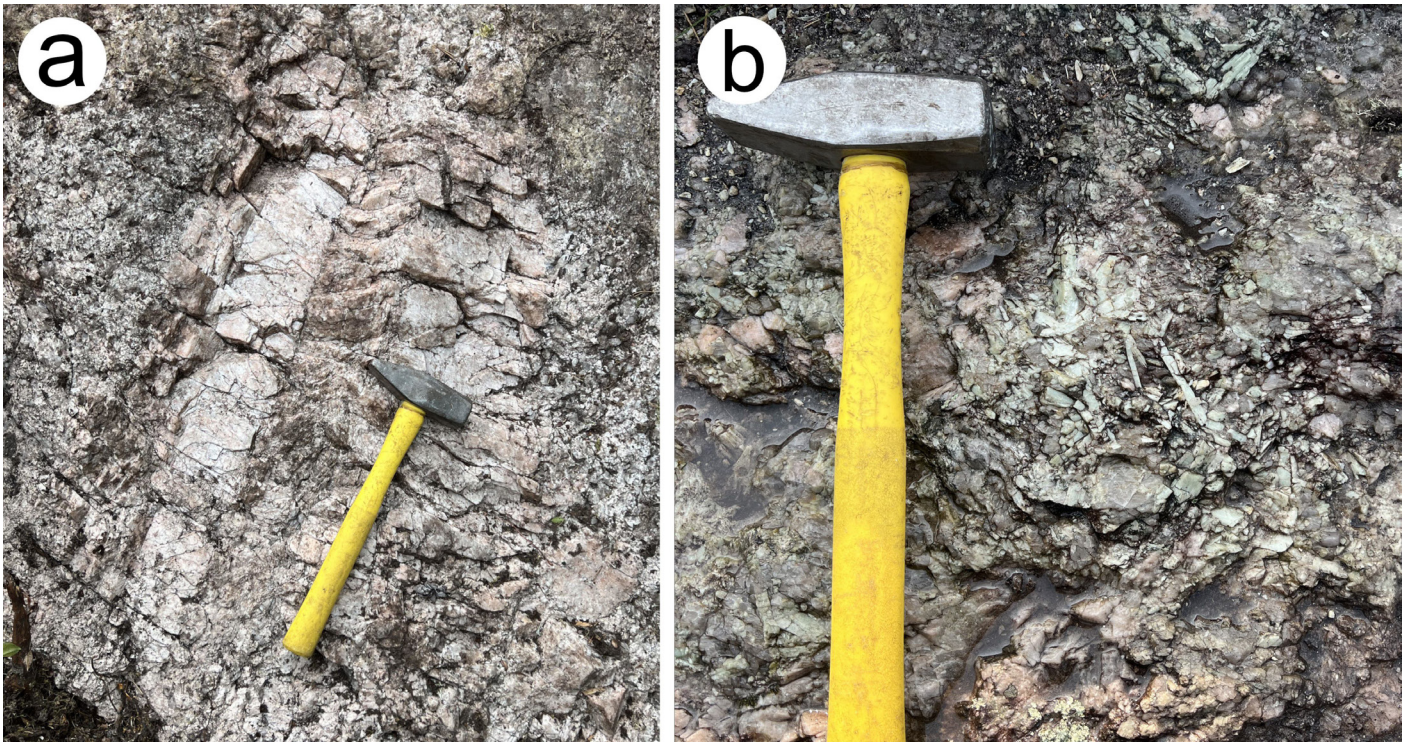

Figure GS2023-4-7: *Outcrop photographs of the F.D. No. 5 pegmatite:* ***a)*** *metre-scale feldspar crystal at the southeastern corner of the pegmatite;* ***b)*** *high concentrations of crystals of green spodumene (up to 10 cm in length).*

of black tourmaline (schorl) are also observed crosscutting the dike. Some areas of the F.D. No. 5 dike are composed of almost 15 modal percent beryl.

Economic considerations

The studied pegmatites are notable for their lithium enrichments and are easily accessible from existing provincial highways. This road accessibility is in contrast to other pegmatites in the region, which require longer, more challenging traverses or access by boat or helicopter. Regardless, the Cat Lake–Winnipeg River pegmatite field in southeastern Manitoba is prospective for Li-bearing pegmatites.

Lithium, primarily in the form of spodumene, is a prominent mineral present in all three pegmatites. The Tappy pegmatite stands out for its high spodumene concentration, often exceeding 60 modal percent in the central zone of the dike. Despite its smaller size, the Tappy pegmatite presents a simpler structural layout with well-defined zones, some of which are rich in spodumene. In contrast, the larger Eagle pegmatite, while still rich in spodumene, is characterized by a more complex textural assemblage, including aplite and mixed zonation. The F.D. No. 5 pegmatite contains significant spodumene, with a notable zone on its north side reaching a concentration of around 80 modal percent. Beryl, another mineral of interest, is less common, with only occasional occurrences, primarily in the F.D. No. 5 pegmatite.

Tantalite is most readily found in the Tappy pegmatite, forming small metallic crystals within spodumene- or quartz-rich zones. Although tantalite is present, it remains an accessory mineral and is therefore not in high concentrations. Further petrography, mineral chemistry and geochronological work will be conducted in the future at the University of New Brunswick to provide comprehensive mineralogical and petrogenetic information for these pegmatites in the Cat Lake–Winnipeg River pegmatite field of southeastern Manitoba.

Acknowledgments

Logistical and field support from the Manitoba Geological Survey and Axiom Group Consulting is truly appreciated. Thanks go to H. Chow for all of the assistance during the field season, as well as D. Owens for the map of the Eagle and F.D. No. 5 pegmatite area. Appreciation is given to New Age Metals Inc. for providing financial support through a Mitacs grant to C.R.M. McFarlane (University of New Brunswick) and L. Groat (The University of British Columbia). The authors thank D.R. Lentz for inputs to the project and suggestions on earlier versions of this communication, as well as X.M. Yang and K. Reid for further review of the report.

References

Bannatyne, B.B. 1985: Industrial minerals in rare-element pegmatites of Manitoba; Manitoba Energy and Mines, Geological Services, Economic Geology Report ER84-1, 96 p.

Černý, P. and Ercit, T.S. 2005: The classification of granitic pegmatites revisited; The Canadian Mineralogist, v. 43, p. 2005–2026.

Černý, P., London, D. and Novák, M. 2012: Granitic pegmatites as reflections of their sources; Elements, v. 8, p. 289–294.

Černý, P., Trueman, D.L., Zeihlke, D.V., Goad, B.E. and Paul, B.J. 1981: The Cat Lake–Winnipeg River and the Wekusko Lake pegmatite fields, Manitoba; Manitoba Department of Energy and Mines, Mineral Resources Division, Economic Geology Report ER80-1, 216 p.

Gilbert, H.P. 2008: Stratigraphic investigations in the Bird River greenstone belt, Manitoba (part of NTS 52L5, 6); *in* Report of Activities 2008, Manitoba Science, Technology, Energy and Mines, Manitoba Geological Survey, p. 121–138.

Yang, X.M. and Houlé, M.G. 2020: Geology of the Cat Creek–Euclid Lake area, Bird River greenstone belt, southeastern Manitoba (parts of NTS 52L11, 12); Manitoba Agriculture and Resource Development, Manitoba Geological Survey, Geoscientific Report GR2020-1, 105 p., 1 map at 1:20 000 scale.

GS2023-5

Logging of archived drillcore and re-interpretation of stratigraphy from the Halfway Lake area, Thompson nickel belt, central Manitoba (parts of NTS 63O1, 2)

by C.G. Couëslan

In Brief:

- Archived drillcore from industry and government core libraries was relogged to help constrain the extent and affinity of metasedimentary rocks at Halfway Lake
- A compiled lithologic section correlates well with Ospwagan group stratigraphy
- A working stratigraphic section has been created to aid exploration efforts in the Halfway Lake area

Citation:
Couëslan, C.G. 2023: Logging of archived drillcore and re-interpretation of stratigraphy from the Halfway Lake area, Thompson nickel belt, central Manitoba (parts of NTS 63O1, 2); *in* Report of Activities 2023, Manitoba Economic Development, Investment, Trade and Natural Resources, Manitoba Geological Survey, p. 27–39.

Summary

This report details the continuation of a bedrock mapping project at Halfway Lake in the Thompson nickel belt, which was initiated in 2022. During the winter and summer of 2023, archived drillcore from industry and government core libraries was relogged to help determine the extent and affinity of metasedimentary rocks in the area. A lithological section was compiled across four diamond-drill holes in the east-central Halfway Lake area. The section consists of orthogneiss, mylonite, calcareous and sulphidic metasedimentary rocks, and interbedded quartzite and metapelite. The lithological section correlates well with Ospwagan group stratigraphy. It implies Archean basement gneiss is in sheared contact with calcareous rocks of the Thompson formation, which is overlain by pelitic and sulphidic rocks of the P2 member of the Pipe formation, and interbedded quartzite and pelite with rare iron formation of the P3 member. Setting formation rocks likely overlie the last iron formation of the P3 member. Although not present in the lithological section, Bah Lake assemblage volcanic rocks occur along strike and are interpreted to overlie the Setting formation rocks.

Ultramafic rocks occur near the Thompson formation–Pipe formation transition and are locally in close spatial association with P2 member sulphidic rocks, which correlates with the ore horizon at the Thompson mine. Mineralized ultramafic rocks in this vicinity were the focus of previous exploration activity. A similar structural regime as that of the Thompson mine area implies that exploration efforts targeting F_3 fold structures for thickened zones of sulphide in hinge zones and mineralization hosted by metasedimentary rocks rather than by intrusions could be viable strategies in the Halfway Lake area.

Introduction

A mapping project at Halfway Lake was initiated in the summer of 2022 (Couëslan, 2022a). Mapping was conducted along the lakeshore at a scale of 1:20 000 utilizing the stratigraphic framework for the Thompson nickel belt (TNB). The goal of the project was to update the mapping with respect to the Ospwagan group stratigraphy and to characterize the mafic rocks of the southeastern Halfway Lake area, which are believed to be correlative with the Bah Lake assemblage. In addition, a search was made for possible Paint sequence rocks (Couëslan, 2016, 2022b) misidentified as Archean basement gneiss or as 'ghost successions' of the Ospwagan group (cf. Zwanzig et al., 2007).

Mapping revealed the extent of metasedimentary rock exposures on Halfway Lake to be significantly less than indicated by previous compilation work (Figure GS2023-5-1; Macek et al., 2006). Two metasedimentary rock packages were identified: a calcsilicate-semipelite assemblage, tentatively correlated with the Thompson formation of the Ospwagan group, and a quartzite-pelite assemblage of uncertain affinity. Archived drillcore from industry and government core libraries was relogged during the winter and summer of 2023 to help constrain the extent, and help determine the affinity of, the metasedimentary rocks at Halfway Lake. For a review of the regional and local geology, the reader is referred to Couëslan (2022a).

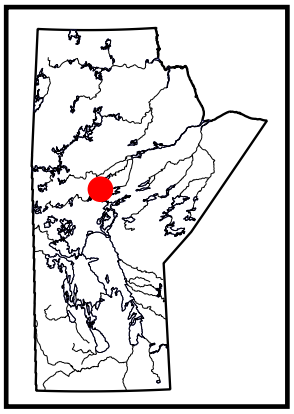

New results

Drillcore archived by the Manitoba Geological Survey, CaNickel Mining Ltd. and Vale Canada Ltd. was relogged in an effort to better constrain the geology of the Halfway Lake area. The drillcore was especially useful in determining the affinity of the sedimentary packages as well as the stratigraphic relationship between the calcsilicate-semipelite and quartzite-pelite assemblages. A lithological section believed to be representative for the Halfway Lake area was compiled using data from several drillholes located in the east-central Halfway Lake area. All rocks discussed in the text were metamor-

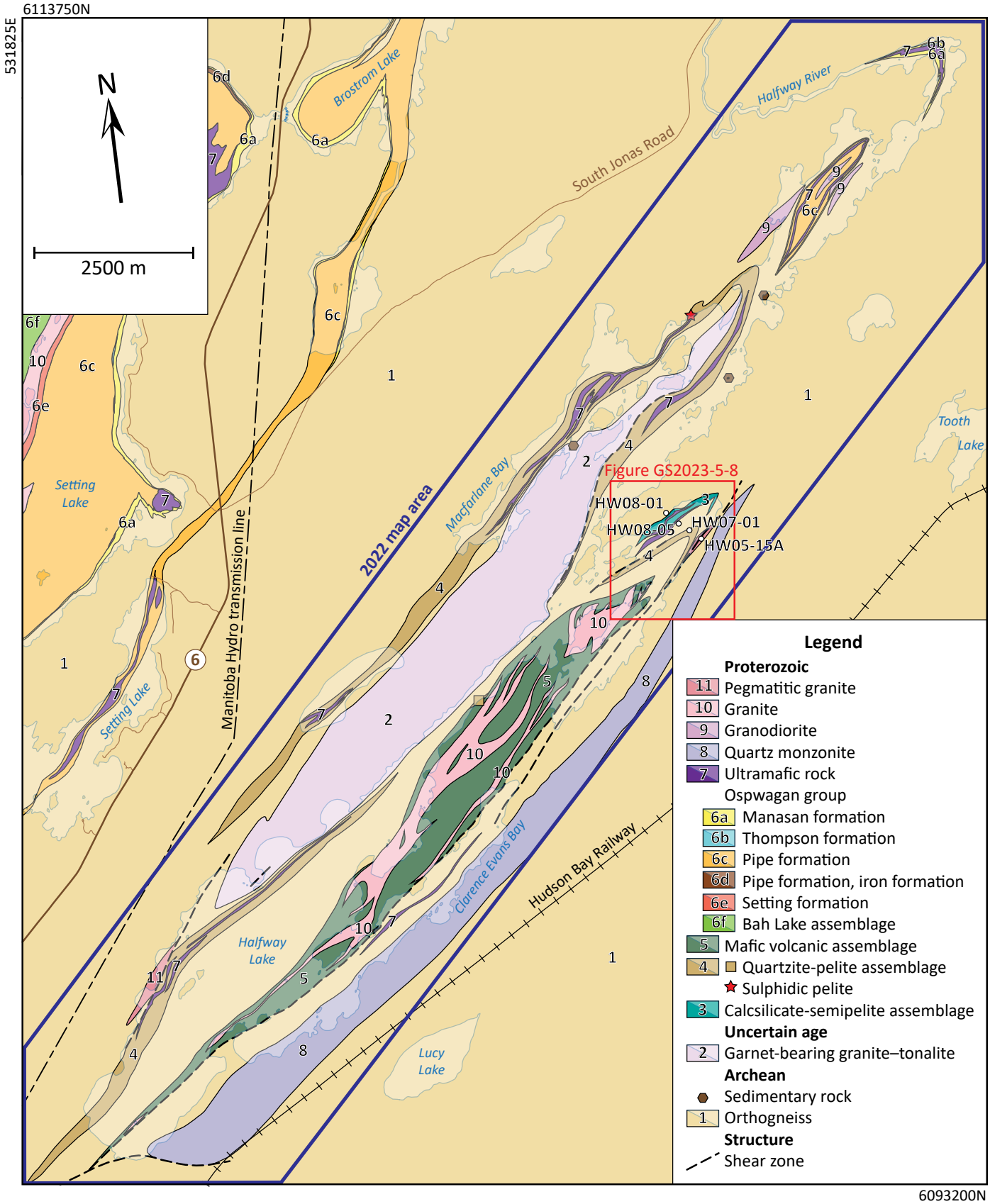

Figure GS2023-5-1: *Bedrock geology of the Halfway Lake area, central Manitoba (modified from Couëslan, 2022c). Lighter shade of colour indicates a body of water. White circles in the east-central Halfway Lake area indicate the location of drill collars used to construct the lithological section (Figure GS2023-5-2). Geology outside of the 2022 map area is from Macek et al. (2006). The red outline shows the location of Figure GS2023-5-8. All co-ordinates are in UTM Zone 14, NAD83.*

phosed to amphibolite-facies conditions; however, to improve the readability of the text, the 'meta-' prefix has been omitted from rock names.

Stratigraphic section from the east-central Halfway Lake area

A lithological section has been compiled across drillholes HW08-01, HW08-05, HW07-01 and HW05-15A (Figure GS2023-5-2; Assessment Files 74270, 74504, 74607; Manitoba Economic Development, Investment, Trade and Natural Resources, Winnipeg). These holes are arrayed across strike and define a northwest to southeast section through what is interpreted as a fold structure in the east-central Halfway Lake area. Drillhole HW08-01 is collared in Archean gneiss and directed southeast toward the calcsilicate-semipelite assemblage presented in Couëslan (2022a), whereas drillhole HW05-15A is collared in

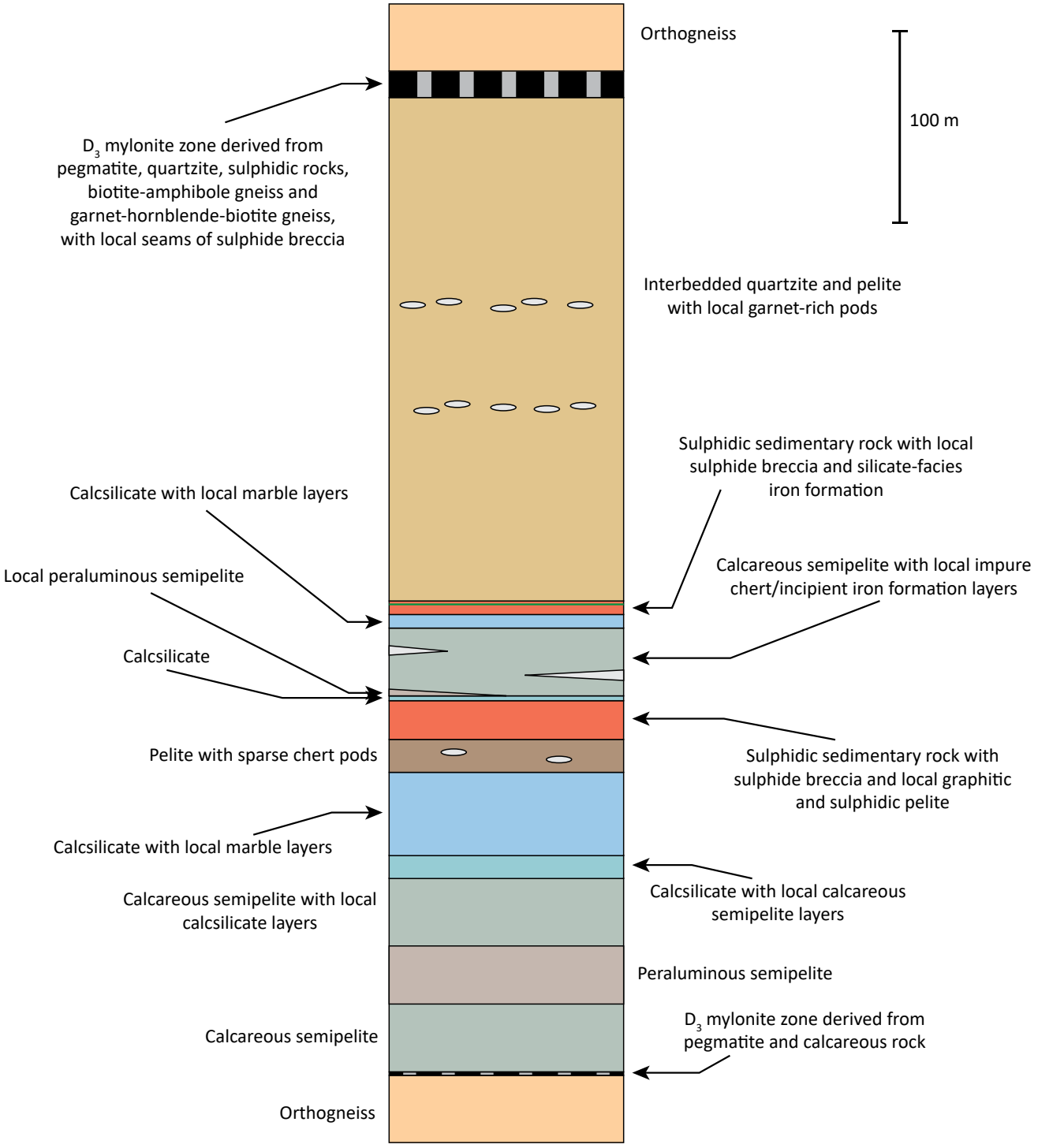

Figure GS2023-5-2: *Schematic lithological section compiled from drillcores HW08-01, HW08-05, HW07-01 and HW05-15A from the Halfway Lake area.*

Archean gneiss and directed northwest toward the quartzite-pelite assemblage. Drillholes HW08-05 and HW07-01 are collared between the previous two drillholes and are both directed toward the northeast.

Although the descriptions below are specific to this section, similar units and relationships were noted throughout the Halfway Lake area. The approximate true thickness is given for each lithological unit; however, the thickness of many units has been disrupted by granitic, mafic and ultramafic intrusions. Unit thicknesses are also expected to vary along strike because of isoclinal folding and attenuation and thickening along regional fold limbs and fold hinges, respectively. All units contain variable amounts of plagioclase amphibolite as metre- to centimetre-scale intersections. The plagioclase amphibolite is interpreted as mafic rock derived at least in part from the Molson dike swarm. Variable amounts of granitic pegmatite are present in all units with intrusions varying from centimetres to tens of metres in scale.

Orthogneiss

Drillhole HW08-01 is collared in grey orthogneiss (Figure GS2023-5-3a). The gneiss is tonalitic to granodioritic, with 7–10% biotite and trace to minor amounts of hornblende. The biotite content locally increases to 10–20%. The mafic minerals typically define gneissic laminations; however, the gneissosity is locally more diffuse. The gneiss shows signs of increasingly higher strain upsection, with local protomylonitic zones.

Shear zone

The Archean orthogneiss is in contact with a mylonitic zone 1.7 m wide. This zone appears to consist of sheared pegmatite and calcareous rocks (Figure GS2023-5-3b). Multiple seams of mylonitized carbonate rock <15 cm thick are present, along with one intersection of less deformed carbonate rock 5 cm thick.

Calcareous semipelite

Juxtaposed against the shear zone is a package of calcareous semipelite 100 m thick (Figure GS2023-5-3c). The calcareous semipelite is grey, medium- to coarse-grained, foliated to strongly foliated and nonmagnetic. It forms a poorly layered diatexite, with 10–20% biotite and a quartzofeldspathic groundmass. Calcic mineral content ranges from 3–5% hornblende in less calcareous zones to 10–12% diopside and/or tremolite in more calcareous compositions. The semipelite locally contains up to 5% pyrrhotite. It becomes increasingly calcareous upsection, where it becomes interlayered with local beds of calcsilicate <5 m thick.

Toward the middle of the calcareous semipelite package is an interval of peraluminous semipelite 30 m thick that is disrupted by abundant pegmatite, which makes up 60–70% of the core (Figure GS2023-5-3d). The semipelite forms a diatexite, with 10–30% biotite and trace amounts of sulphide and garnet in a quartzofeldspathic groundmass. It is locally more aluminous, with 5–7% garnet, or sulphidic, with 5–7% pyrrhotite.

Calcsilicate and marble

The calcareous semipelite grades over approximately 12 m into a sequence of calcsilicate and marble 35–50 m thick. This unit becomes increasingly calcareous upsection. Lower in the section, it consists of calcsilicate interlayered with minor calcareous semipelite beds <30 cm thick, whereas higher in the section, it consists of approximately equal proportions of calcsilicate and impure marble interlayered on a scale of <2 m.

The calcsilicate is green, coarse grained, foliated to massive and nonmagnetic (Figure GS2023-5-3e). It ranges from relatively quartzofeldspathic, with 10–20% biotite, 20–30% diopside and minor sulphide, to nearly solid diopside. Local layers contain minor amounts of a nonmagnetic, black, opaque mineral tentatively identified as spinel or possibly darkly coloured titanite. The calcsilicate ranges from well laminated to poorly layered on a scale of <1.5 m.

The marble is beige to greenish white, medium to coarse grained and foliated (Figure GS2023-5-3f). The composition varies from 20–30% phlogopite and carbonate, to 2–3% phlogopite, 3–5% diopside, 20–30% serpentinized olivine and carbonate. The marble ranges from relatively homogeneous to poorly layered on a scale of <10 cm.

Pelite

Upsection from the calcsilicate and marble package is a package of pelite 13–20 m thick (Figure GS2023-5-3g). The contact between the pelite and the previous calcareous metasedimentary rocks is obscured by pegmatite. The pelite is grey-brown, medium to coarse grained and strongly foliated. It forms a quartzofeldspathic diatexite, with 20–30% biotite, minor sillimanite and pink-violet garnet, and trace to minor amounts of sulphide. Sparse siliceous pods contain 10–20% fine-grained garnet and may represent nodules or discontinuous layers of chert. The pelite is intruded by pervasive pegmatite, which can be locally protomylonitic and brecciated. The brecciated zones locally contain veins and blebs of sulphide <1 cm thick.

Sulphidic sedimentary rock

Following the pelite is a unit of sulphidic sedimentary rock 12–27 m thick, with significant zones of sulphide breccia up to 3.3 m thick (Figure GS2023-5-3h). The sulphidic rocks are intruded by large volumes of pegmatite that make up 50–60% of the core. The sulphidic sedimentary rock is grey, medium grained, foliated to strongly foliated and magnetic. It is quartzofeldspathic, with 5–7% pyrrhotite and 10–20% biotite, and locally pelitic, with minor amounts of graphite, garnet and sillimanite.

The sulphide breccia is brown bronze, medium to coarse grained, foliated to brecciated and strongly magnetic. It consists

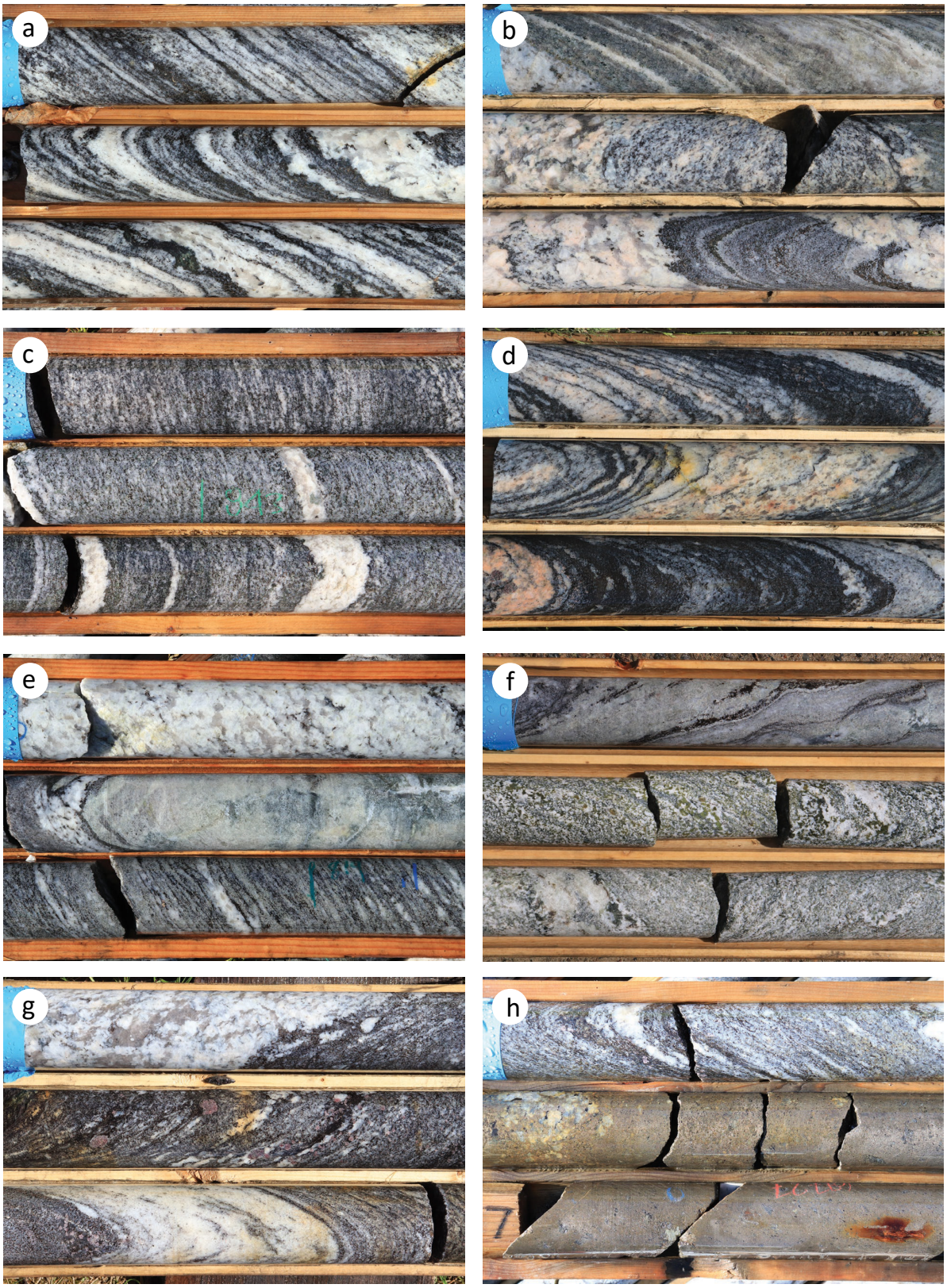

Figure GS2023-5-3: *Diamond-drill core images from the east-central Halfway Lake area:* ***a)*** *tonalitic orthogneiss (drillhole HW07-01, 571.6 m);* ***b)*** *mylonitic calcareous rock (top row) and pegmatite with semipelitic schlieren and xenoliths (bottom two rows; drillhole HW08-01, 94.2 m);* ***c)*** *calcareous semipelite with local pegmatitic injections and/or leucosome (drillhole HW05-15A, 816.0 m);* ***d)*** *peraluminous semipelite disrupted by pegmatitic injections (drillhole HW08-01, 163.4 m);* ***e)*** *pegmatite (top row) and calcsilicate (bottom two rows; drillhole HW05-15A, 816 m);* ***f)*** *calcsilicate (top row) and marble with serpentinized olivine (bottom two rows; drillhole HW08-05, 186.1 m);* ***g)*** *sillimanite- and garnet-bearing pelite with pegmatitic injections and/or leucosome (drillhole HW08-01, 403.1 m);* ***h)*** *sulphidic pelite (top row) and sulphide breccia (bottom two rows; drillhole HW05-15A, 674.0 m). The drillcore is NQ™ (diameter = 4.76 cm).*

of near solid pyrrhotite, with 10–20% biotite, 30–40% rounded to irregular fragments of quartzofeldspathic material <3 cm across, and minor graphite and garnet. Graphite is locally more abundant and can make up 10–12% of the breccia. Assay results reveal that the sulphidic rocks are not mineralized in Ni or Cu (Assessment Files 74270, 74504, 74607).

Calcareous semipelite

The sulphidic sedimentary rocks are followed respectively by a thin (2.5 m) layer of calcsilicate and an interval of calcareous semipelite 30–40 m thick. The semipelite is poorly layered on a scale of <1 m and is quartzofeldspathic, with 10–20% biotite and 3–5% hornblende or 5–7% diopside. It contains local siliceous layers <40 cm thick that contain abundant hornblende and red-burgundy garnet, which could be derived from impure chert or incipient iron formation (Figure GS2023-5-4a). The start of the semipelite interval is locally more aluminous, with 5–7% garnet and no hornblende or diopside.

Calcsilicate and marble

The calcareous semipelite grades into 5–10 m of calcsilicate, with minor marble layers <20 cm thick. The calcsilicate is light green and diopside rich, with minor biotite in a groundmass of quartz and feldspar. Sparse blebs of carbonate can be present. The calcsilicate ranges from poorly layered to well laminated and locally grades toward more biotite-rich compositions.

The marble varies from pinkish to greenish grey, and is coarse grained and foliated. It consists of white to pink carbonate, with abundant serpentinized olivine and minor to trace amounts of diopside, tremolite and phlogopite. The marble varies from poorly layered to well laminated.

Sulphidic sedimentary rock

The calcsilicate grades over 2 m into an interval of sulphidic sedimentary rock 7 m thick. The sulphidic sedimentary rock is locally more siliceous than previously described and can contain 20–30% biotite. It contains local seams of sulphide breccia <40 cm thick. In the upper part of the interval, a thin (20–35 cm) bed of silicate-facies iron formation grades upward into sulphide breccia (Figure GS2023-5-4b). The purplish grey-green iron formation is laminated, locally magnetic and contains 20–30% ferrosilite, 30–40% garnet and minor pyrrhotite in a siliceous groundmass. Assessment Files show this package to be barren of Ni and Cu mineralization.

Interbedded quartzite and pelite

Upsection from the sulphidic rocks is a package of quartzite and pelite 260 m thick. The quartzite and pelite are interlayered on a scale of <7 m. The quartzite is light grey to beige and contains minor to trace amounts of biotite, pink-violet garnet and pyrrhotite. The quartzite can grade toward protoquartzite, with 2–3% garnet, 7–10% biotite and an increased feldspar content (Figure GS2023-5-4c). The quartzite can be internally layered to laminated on a scale of <15 cm and beds of quartzite are commonly separated by thin pelitic laminations.

The pelite is brown grey, strongly foliated and weakly magnetic in places. It typically forms a quartzofeldspathic diatexite, with 20–30% biotite, minor sillimanite and pink-violet garnet, and trace amounts of pyrrhotite and graphite (Figure GS2023-5-4d). It can grade toward more semipelitic compositions, with no sillimanite and decreased biotite and garnet content, or toward more aluminous compositions, with 5–7% sillimanite and 30–40% biotite.

The interbedded quartzite-pelite sequence also contains at least two varieties of sparse, garnet-bearing pods <5 cm thick that vary from pink to green. The pink variety is garnet and quartz rich with subordinate feldspar. The green variety is quartz rich, with an abundant green mineral that could be either clinozoisite or amphibole and subordinate very pale pink garnet. Both varieties can be zoned with white, feldspar-bearing siliceous rims <2 cm thick (Figure GS2023-5-4e). These pods may represent impure chert nodules or layers and/or calcareous concretions.

Shear zone

The quartzite-pelite package terminates at a shear zone. The shear zone consists of an interval of protomylonitic to mylonitic rock 14 m thick that appears to be derived from pegmatite, quartzite, sulphidic gneiss, biotite-amphibole gneiss and garnet-hornblende-biotite gneiss, along with lenses of strongly foliated plagioclase amphibolite and local seams of sulphide breccia (Figure GS2023-5-4f).

Orthogneiss

Drillhole HW05-15A is collared in orthogneiss, which grades from foliated to protomylonitic with proximity to the above shear zone. The orthogneiss is grey, medium to coarse grained and nonmagnetic. It is tonalitic to granodioritic, with 10–20% biotite and trace amounts of red-burgundy garnet (Figure GS2023-5-4g). The orthogneiss locally contains minor hornblende.

Ultramafic rocks

Peridotite intrusions occur within the calcsilicate and marble package, and in contact with the sulphidic sedimentary rocks. The peridotite is serpentine-rich, with 10–20% anthophyllite and trace to minor amounts of sulphide and magnetite (Figure GS2023-5-4h). It locally grades in composition to dunite and pyroxenite. The peridotite contains local zones of ultramafic schist, typically in close spatial association with pegmatite intrusions. The ultramafic schist typically contains variable amounts of anthophyllite, chlorite and biotite. The schist can locally grade into monomineralic rocks consisting of any one of these three minerals. Although not part of this study, intersections of mineralized peridotite in the vicinity have yielded assays of 1.38%

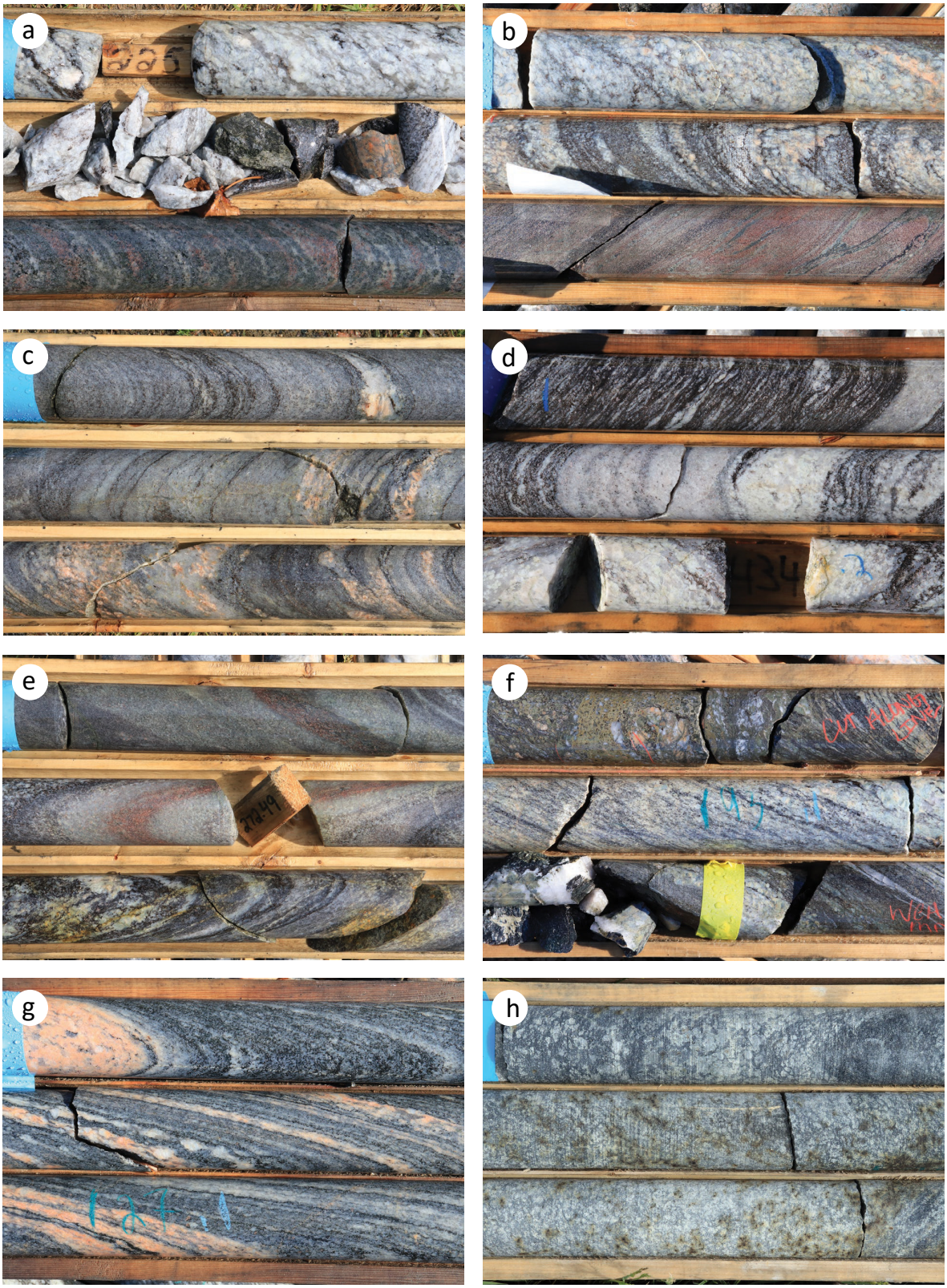

Figure GS2023-5-4: *Diamond-drill core images from the east-central Halfway Lake area:* ***a)*** *pegmatite (top two rows) and impure chert or incipient iron formation (bottom row; drillhole HW07-01, 224.9 m);* ***b)*** *pegmatite with schlieren and xenoliths of sulphidic sedimentary rock (top two rows) and silicate-facies iron formation (bottom row; drillhole HW05-15A, 575.5 m);* ***c)*** *protoquartzite with pelitic layers and laminations, and pegmatite injections (drillhole HW07-01, 91.7 m);* ***d)*** *pelite interlayered with quartzite and intruded by local pegmatite (drillhole HW05-15A, 431.0 m);* ***e)*** *zoned, garnet-rich concretions in quartzite (top two rows), and interlayered pelite and quartzite (bottom row; drillhole HW08-08, 271.0 m);* ***f)*** *protomylonite derived from biotite gneiss, pegmatite, and sulphidic and semipelitic rocks (drillhole HW05-15A, 91.5 m);* ***g)*** *garnet-bearing orthogneiss with sheared pegmatitic injections (drillhole HW05-15A, 24.2 m);* ***h)*** *peridotite (top row) grading into sulphide-bearing olivine pyroxenite (bottom two rows; drillhole HW05-15A, 751.4 m). Drillcore is NQ™ (diameter = 4.76 cm), except for (e), which is BQTK™ (diameter = 4.07 cm).*

Ni over 17.55 m (drillhole HW95-05; Assessment File 72905) and 1.58% Ni over 13.03 m (drillhole HW08-02; Assessment File 74607).

Correlations with 2022 mapping and regional stratigraphy

Two sedimentary rock assemblages were defined from geological mapping in 2022: the calcsilicate-semipelite assemblage and the quartzite-pelite assemblage (Couëslan, 2022a). Although the two assemblages were found in relatively close proximity in the east-central Halfway Lake area, it remained uncertain if they were part of a continuous stratigraphic sequence. From the lithological section described above, it appears that the calcareous semipelite and calcsilicate with marble packages correlate with the calcsilicate-semipelite assemblage of Couëslan (2022a), whereas the interlayered quartzite and pelite package correlates with the quartzite-pelite assemblage. The continuous, and locally gradational, nature of the units in the section implies that the two assemblages represent parts of a single continuous sedimentary rock succession. The sulphidic and graphitic pelite that was assigned to the quartzite-pelite assemblage in Couëslan (2022a) likely correlates to one of the two sulphidic sedimentary rock units observed in the drillcore section described above.

The wide variations in sedimentary lithologies observed in the Halfway Lake rocks do not match the relatively restricted range of compositions observed to date in the Paint sequence (Couëslan, 2016, 2022b). The drillcore section outlined above appears to be a better match for Ospwagan group stratigraphy (Figure GS2023-5-5).

Toward the base of the Ospwagan group is a substantial thickness of semipelite, which forms the M2 member of the Manasan formation (Figure GS2023-5-2). This could be correlative with

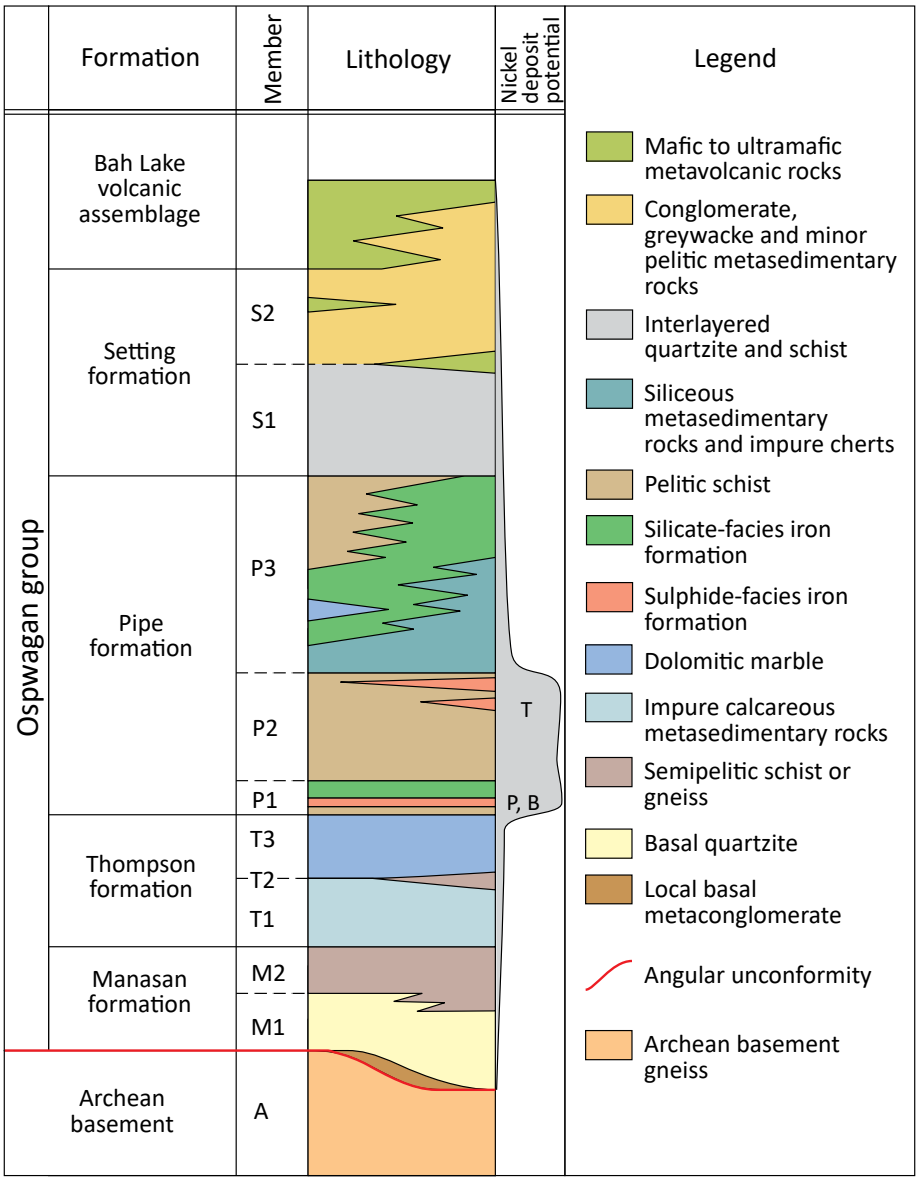

Figure GS2023-5-5: *Schematic lithostratigraphic section of the Ospwagan group (modified from Bleeker,1990). Abbreviations: B, stratigraphic location of the Birchtree orebody; P, stratigraphic location of the Pipe II orebody; T, stratigraphic location of the Thompson ore body.*

the calcareous semipelite near the base of the lithological section described above. However, this would require the input of a calcareous component not seen in the M2 member, which is typically peraluminous and muscovite or sillimanite bearing. In addition, the Ospwagan group stratigraphy as defined by Bleeker (1990) and updated by Zwanzig et al. (2007), assigned all calcareous rocks from the lower part of the Ospwagan group to the overlying Thompson formation. Therefore, by definition, both the calcareous semipelite and calcsilicate-marble units should be part of the Thompson formation. The calcareous semipelite likely represents a more clastic-rich portion of the T1 member or possibly a rather thick example of the semipelitic T2 member, which to date has only been documented as a thin (1–4 m), discontinuous layer at the Thompson mine (Bleeker, 1990; Zwanzig et al., 2007). The calcsilicate-marble unit is more typical of the Thompson formation, especially the T3 member.

The calcareous rocks of the Thompson formation are overlain by the Pipe formation of the Ospwagan group (Figure GS2023-5-5; Bleeker, 1990; Zwanzig et al., 2007). The P1 member at the base of the Pipe formation consists of graphitic and sulphidic schist or sulphide-facies iron formation. The P1 member sulphide-facies iron formation is overlain by silicate-facies iron formation 0.5–5 m thick, followed by cherts or siliceous schists, which become increasingly pelitic as they grade into the overlying P2 member pelite. This is in contrast with the Halfway Lake lithological section, where the calcareous rocks of the Thompson formation appear to be succeeded by pelitic schist, with sparse chert pods followed by sulphidic sedimentary rocks, which is analogous to the P2 member of the Pipe formation. Zwanzig et al. (2007) recognized that not all stratigraphic units are necessarily present at a given location, but could be attenuated or pinched out. It is therefore possible that the P1 member is missing from the section in the east-central Halfway Lake area.

The sulphidic rocks are followed by a return to calcareous sedimentation. The sulphidic rocks are overlain by 2.5 m of calcsilicate, followed by 30–40 m of calcareous semipelite and 5–10 m of calcsilicate, with minor marble. The calcsilicate and marble grade into an overlying unit of sulphidic sedimentary rock 7 m thick that is characterized by a thin silicate-facies iron formation near the top. There are at least three possibilities for this repeating sequence of sulphidic to calcareous and back to sulphidic rocks:

- There could be a cryptic, early D_2 thrust fault above the first sulphidic horizon. This would explain the repetition of broadly similar stratigraphy, where calcareous rocks appear to transition into sulphidic rocks twice within the same sequence (Figure GS2023-5-6a).
- Alternatively, the repeated sequence could represent an attenuated isoclinal fold. In this interpretation, the two sulphidic horizons are a repetition of the P2 member; however, attenuation has led to the pinching-out of the pelitic schist. Similarly, the Thompson formation rocks have been attenuated, such that the peraluminous semipelite pinches out, and the calcsilicate and marble unit after the first sulphidic horizon is attenuated to only 2.5 m (Figure GS2023-5-6b).
- A third alternative would require a sedimentary facies change from the classical Ospwagan group stratigraphy. In this scenario, the pelitic rocks and first sulphidic horizon would correlate to the P1 member of the Pipe formation. This would place the overlying calcareous rocks in the stratigraphic position of the upper P1 and/or P2 members, which consist of silicate-facies iron formation and pelitic schist in the classical Ospwagan group stratigraphy (Bleeker, 1990; Zwanzig et al., 2007). The second sulphidic horizon would then correlate with sulphide-facies iron formation at the top of the P2 member. The P2 member pelite at the Pipe II mine contains local, discontinuous calcsilicate layers, which indicates the deposition of some calcareous rocks at this time. Therefore, it is conceivable that the above discrepancy is the result of a facies change, where the typical P2 member pelite grades laterally into a package of more calcareous sedimentary rocks. This may be supported by the presence of local peraluminous semipelite near the base of the unit and the apparently gradational nature of the contact between the calcsilicate and marble, and the second sulphidic horizon. The local chert/incipient iron-formation layers within this calcareous semipelite unit in the Halfway Lake area is a shared feature with the P2 pelite at the Pipe II mine (Figure GS2023-5-6c; Bleeker, 1990).

The second scenario is tentatively the favoured interpretation as isoclinal folding is relatively common in the stratigraphy of the TNB; however, each of the three interpretations is potentially viable.

The P3 member of the Pipe formation at the Thompson mine consists largely of interbedded impure quartzite and pelite with subordinate iron formation (Bleeker, 1990). This correlates well with the interbedded quartzite-pelite package in the Halfway Lake area; however, iron formation is exceedingly rare. Although iron formation was not recognized in the four drillcores used to construct the lithological section, silicate-facies iron formations and chert layers were recognized in three nearby drillholes within the same fold structure (W118-23, Assessment File 93977; HW95-04, Assessment File 72905; HW96-10, Assessment File 73104). The iron formations can be up to 9 m thick, but rarely exceed 1 m. They vary from well laminated to almost massive and are typically garnet and quartz rich, with subordinate ferrosilite and minor biotite and sulphide. Hornblende and magnetite can be present in trace amounts.

The Setting formation is defined as all clastic rocks between the last iron formation of the Pipe formation and the mafic to ultramafic volcanic rocks of the overlying Bah Lake assemblage (Bleeker, 1990; Zwanzig et al., 2007). The clastic rocks of the S1 member commonly occur as interbedded quartzite and pelite similar to those described above. The relative scarcity of iron for-

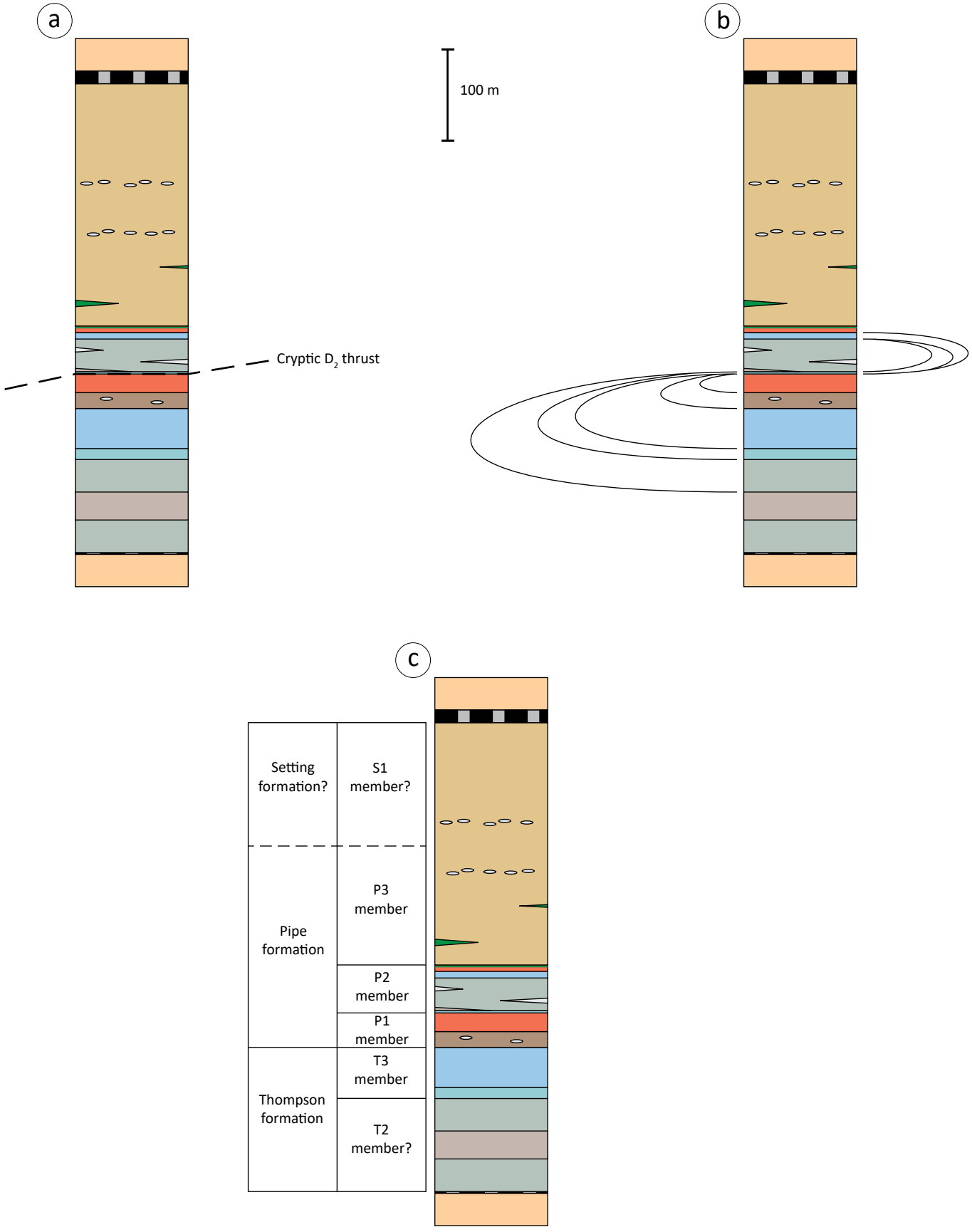

Figure GS2023-5-6: *Three possible interpretations for the lithological section of the east-central Halfway Lake area outlined in the text:* ***a)*** *cryptic D_2 thrust placing Thompson formation on P2 member rocks;* ***b)*** *isoclinal folding of Thompson and Pipe formation rocks;* ***c)*** *sedimentary facies change of the P2 member.*

mation within the interbedded quartzite-pelite package in the Halfway Lake area makes discriminating the boundary between the P3 member of the Pipe formation and the Setting formation difficult. Although Bah Lake assemblage rocks were not intersected along the lithological section, mafic volcanic rocks do occur toward the southwest in the core of the fold structure and are likely correlative.

The upper and lower contacts of the lithological section are truncated by D_3 mylonitic shear zones. The mylonite zones juxtapose the sedimentary rocks with orthogneiss and are interpreted as the sheared contact between the Ospwagan group and Archean basement. The lower shear zone appears to be derived from calcareous rocks and pegmatite, which implies that rocks below the Thompson formation (Manasan formation) are either tectonically removed, or mylonitized and attenuated, and can no longer be recognized. The upper shear zone is derived from a wider range of protolith including calcareous, sulphidic, semipelitic and siliceous sedimentary rocks. This could imply that the entire stratigraphic sequence below the P3 member is sheared and attenuated within the mylonite zone, which effectively represents a highly attenuated fold limb.

A stratigraphic column and new geological map of the east-central bay on Halfway Lake has been generated based on the above correlations (Figures GS2023-5-7, -8). The updated map was compiled using field observations from 2022, combined with the new drillcore observations from this summer. It indicates that, in many places, the lower part of the Ospwagan group sequence has either been tectonically removed or attenuated beyond the resolution of the map scale, such that only Pipe formation rocks are recognized. Additional data collected from archived drillcore will be used to update the geology for the remainder of the Halfway Lake area.

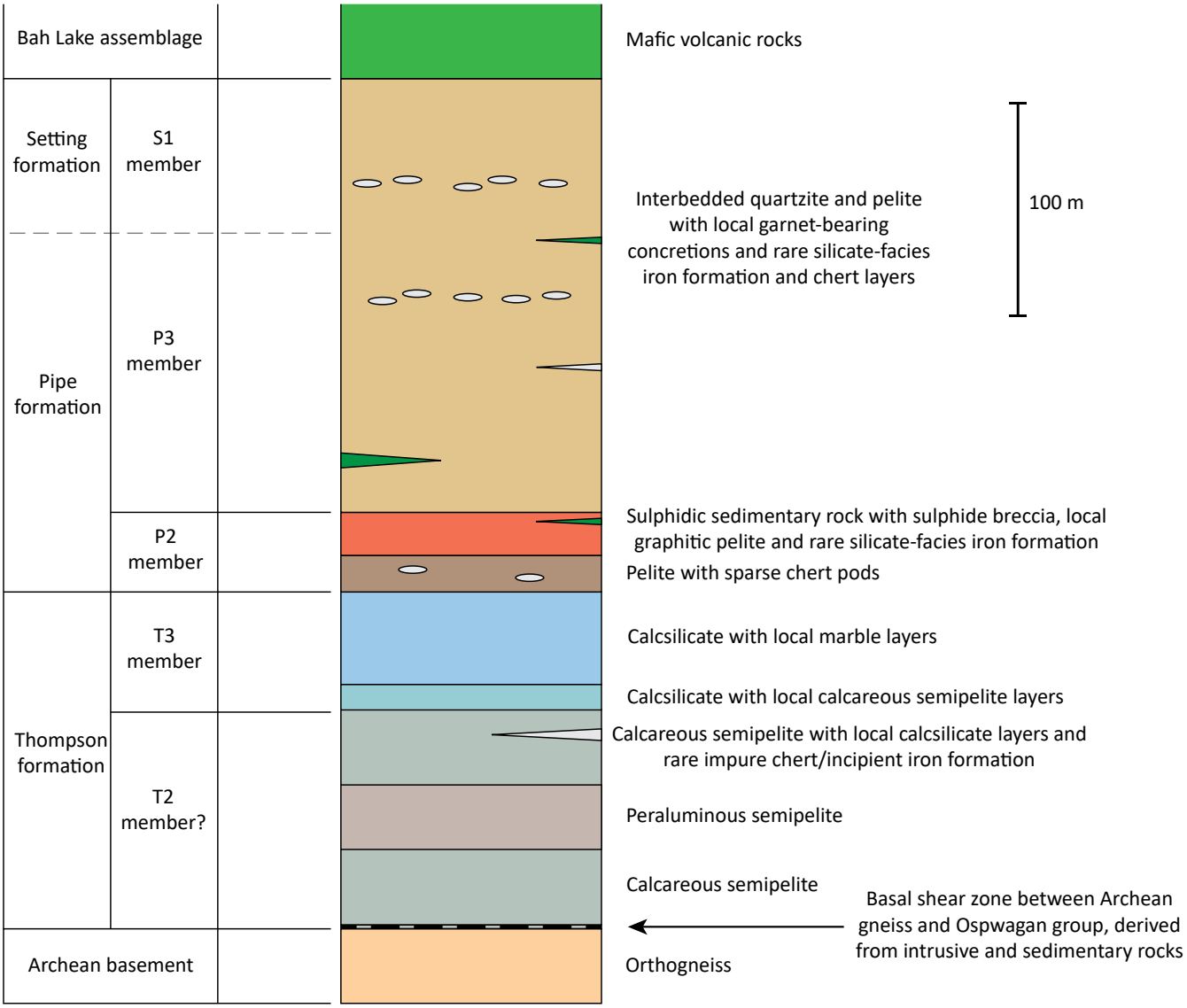

Figure GS2023-5-7: *Schematic stratigraphic section of the Ospwagan group rocks in the east-central Halfway Lake area.*

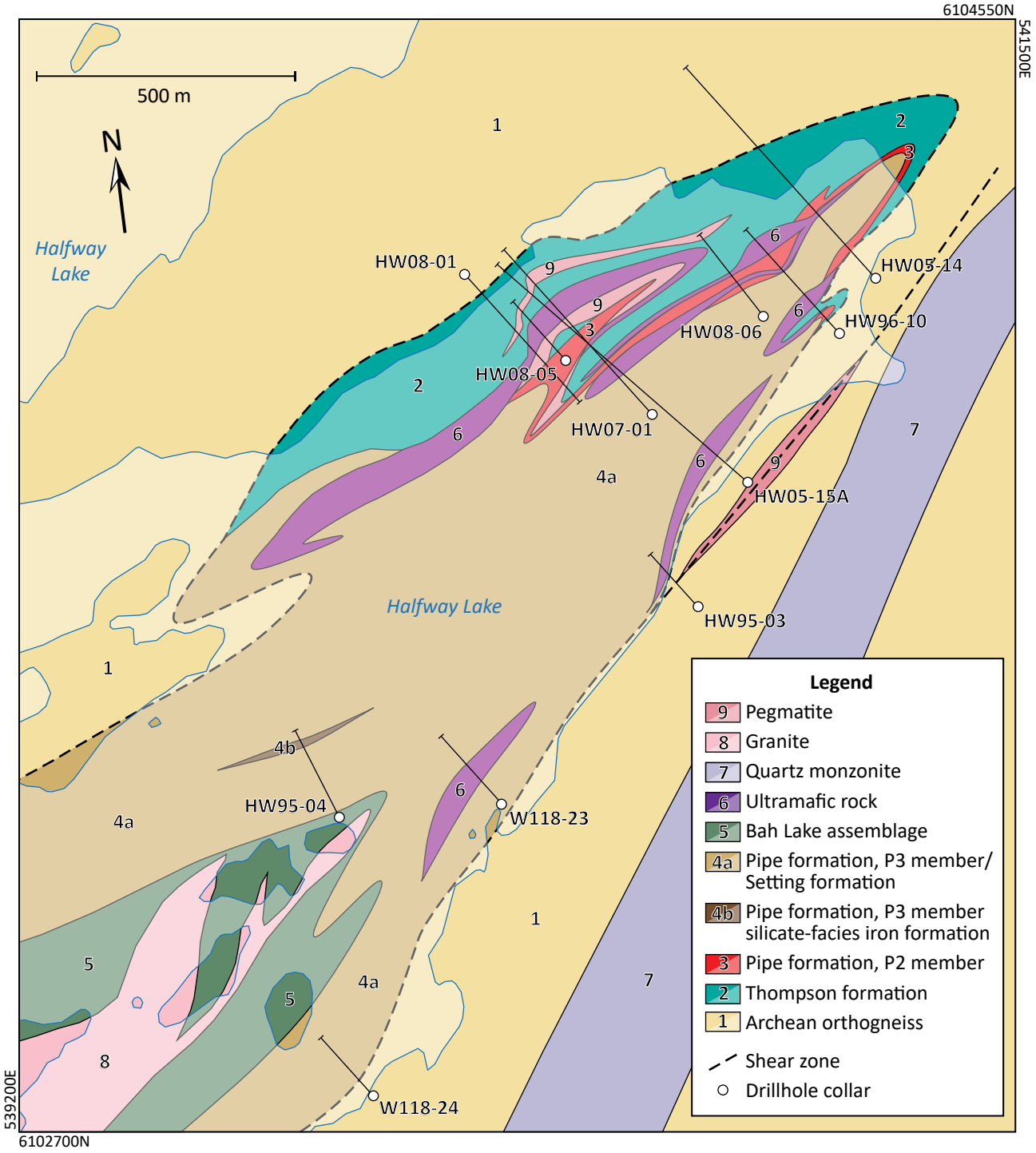

Figure GS2023-5-8: *Revised bedrock geology of the east-central Halfway Lake area. The plotted drillholes were those used for compilation of the geology. Lighter shade of colour indicates a body of water. All co-ordinates are in UTM Zone 14, NAD83.*

Economic considerations

The most widely accepted model for generating Ni-Cu deposits in the TNB invokes the intrusion of ultramafic magmas into sulphide-rich horizons of the Pipe formation of the Ospwagan group (Figure GS2022-3-5; Bleeker, 1990; Zwanzig et al., 2007). There the magmas scavenged sulphide from the host sedimentary rocks, leading to sulphur saturation of the melt and the precipitation and concentration of sulphides enriched in Ni and Cu. As a result, ultramafic bodies occurring in Pipe formation rocks are considered the most likely to host mineralization and are prime exploration targets in the TNB (Bleeker, 1990; Layton-Matthews et al., 2007; Zwanzig et al., 2007).

Relogging of archived drillcore has confirmed the presence of Ospwagan group rocks in the Halfway Lake area and has led

to the creation of a working stratigraphic section that can be used to guide exploration activities. This revised stratigraphy has identified sulphide-rich horizons, which likely correlate to the P2 member of the Pipe formation, in the east-central Halfway Lake area. This is the same stratigraphic level as the ore horizon at the Thompson mine (Bleeker, 1990; Lightfoot et al., 2017). A mineralized ultramafic body in this part of the lake was the focus of exploration for Falconbridge Ltd. (now Glencore Canada Corporation) and Crowflight Minerals Inc. (now CaNickel Mining Ltd.) between 1992 and 2008. The best mineralized intersections to date include 1.38% Ni over 17.55 m (drillhole HW95-05; Assessment File 72905) and 1.58% Ni over 13.03 m (drillhole HW08-02; Assessment File 74607). Additional sulphidic horizons are identified in outcrop and drillcore throughout the Halfway Lake area (Macek et al., 2006; Couëslan, 2022a).

Intersections of Ni mineralization in the Halfway Lake area include ultramafic-hosted disseminated and net-textured sulphide, similar to mineralization in much of the Thompson belt, as well as metasedimentary-hosted semisolid to solid sulphide, similar to mineralization at the Thompson mine (Assessment Files 74504, 74607). The metamorphic grade in the Halfway Lake area is comparable to that of the Thompson mine, which implies a similar ductile structural regime, with sulphides deforming in a plastic or viscous manner. A considerable portion of the Thompson orebody is contained within an F_3 hinge zone, with mineralization also associated with parasitic F_3 fold structures along one of the limbs (Lightfoot et al., 2017). Although it occurs at the same stratigraphic level as a train of ultramafic bodies, most of the Ni ore at the Thompson mine is hosted by Pipe formation rocks (Bleeker, 1990; Lightfoot et al., 2017).

Future exploration at Halfway Lake might consider targeting F_3 fold structures to look for thickened zones of sulphide plunging along hinge lines. The mineralized ultramafic body mentioned in the previous paragraph occurs along the western limb of an F_3 fold, not far from the hinge zone. Additional fold hinges and spatially associated sulphidic rocks are interpreted to occur throughout the Halfway Lake area. It should also be remembered that sulphide could have remobilized under high-grade metamorphic conditions and need not be directly associated with ultramafic bodies. Exploration at the same stratigraphic level as ultramafic bodies could reveal the presence of mineralization that is hosted by sedimentary rocks rather than by the intrusion.

Acknowledgments

The author thanks M. Friesen (University of Manitoba) and M. Kaan (University of Winnipeg) for providing excellent field assistance as well as C. Epp and P. Belanger for logistical support. Discussions with J. Macek helped formulate interpretations of the Halfway Lake stratigraphy; M. Nicolas and T. Martins reviewed earlier drafts of the report. Special thanks to K. Zhu, S. Anthony and C. Ducharme of CaNickel Mining Ltd.; and S. Kirby, S. Nicholson and D. Hanson of Vale Canada Ltd. (Manitoba Operations) for providing access to drillcore from Halfway Lake, which provided valuable insight into the geology of the Halfway Lake area.

References

Bleeker, W. 1990: Evolution of the Thompson Nickel Belt and its nickel deposits, Manitoba, Canada; Ph.D. thesis, University of New Brunswick, Fredericton, New Brunswick, 400 p.

Couëslan, C.G. 2016: Geology of the Paint and Phillips lakes area, Thompson nickel belt, central Manitoba (parts of NTS 63O1, 8, 9, 63P5, 12); Manitoba Growth, Enterprise and Trade, Manitoba Geological Survey, Geoscientific Report GR2016-1, 44 p., 1 map at 1:50 000 scale.

Couëslan, C.G. 2022a: Bedrock mapping in the Halfway Lake area, Thompson nickel belt, central Manitoba (parts of NTS 63O1, 2); *in* Report of Activities 2022, Manitoba Natural Resources and Northern Development, Manitoba Geological Survey, p. 12–24.

Couëslan, C.G. 2022b: Characterization of ultramafic-hosting metasedimentary rocks and implications for nickel exploration at Phillips Lake, Thompson nickel belt, central Manitoba (part of NTS 63O1); Manitoba Natural Resources and Northern Development, Manitoba Geological Survey, Geoscientific Paper GP2022-1, 33 p., 4 appendices.

Couëslan, C.G. 2022c: Bedrock geology of the Halfway Lake area, central Manitoba (parts of NTS 63O1, 2); Manitoba Natural Resources and Northern Development, Manitoba Geological Survey, Preliminary Map PMAP2022-1, scale 1:25 000.

Layton-Matthews, D., Lesher, C.M., Burnham, O.M., Liwanag, J., Halden, N.M., Hulbert, L. and Peck, D.C. 2007: Magmatic Ni-Cu-platinum-group element deposits of the Thompson Nickel Belt; *in* Mineral Deposits of Canada: a Synthesis of Major Deposit Types, District Metallogeny, the Evolution of Geological Provinces and Exploration Methods, W.D. Goodfellow (ed.), Geological Association of Canada, Mineral Deposits Division, Special Publication no. 5, p. 409–432.

Lightfoot, P.C., Stewart, R., Gribbin, G. and Mooney, S.J. 2017: Relative contribution of magmatic and post-magmatic processes in the genesis of the Thompson Mine Ni-Co sulfide ores, Manitoba, Canada; Ore Geology Reviews, v. 83, p. 258–286.

Macek, J.J., Zwanzig, H.V. and Pacey, J.M. 2006: Thompson Nickel Belt geological compilation map, Manitoba (parts of NTS 63G, J, O, P and 64A and B); Manitoba Science, Technology, Energy and Mines, Manitoba Geological Survey, Open File Report, OF2006-33, digital map on CD, URL <https://manitoba.ca/iem/info/libmin/OF2006-33.zip> [August 2023].

Zwanzig, H.V., Macek, J.J. and McGregor, C.R. 2007: Lithostratigraphy and geochemistry of the high-grade metasedimentary rocks in the Thompson Nickel Belt and adjacent Kisseynew Domain, Manitoba: implications for nickel exploration; Economic Geology, v. 102, p. 1197–1216.

GS2023-6

The Burntwood Lake syenite complex revisited: the site of voluminous carbonatite magmatism in the Kisseynew domain, west-central Manitoba (part of NTS 63N7)

by A.R. Chakhmouradian[1], C.G. Couëslan and T. Martins

In Brief:

- Improved exposure of the Burntwood Lake syenite complex suggest that it is a composite pluton that has been tilted and tightly folded
- Several carbonatite exposures were identified in the northern part of the complex
- Carbonatite is associated with at least three syenite complexes in the Trans-Hudson of Manitoba, which underlines the region's potential for rare-earth element exploration

Citation:
Chakhmouradian, A.R., Couëslan, C.G. and Martins, T. 2023: The Burntwood Lake syenite complex revisited: the site of voluminous carbonatite magmatism in the Kisseynew domain, west-central Manitoba (part of NTS 63N7); *in* Report of Activities 2023, Manitoba Economic Development, Investment, Trade and Natural Resources, Manitoba Geological Survey, p. 40–51.

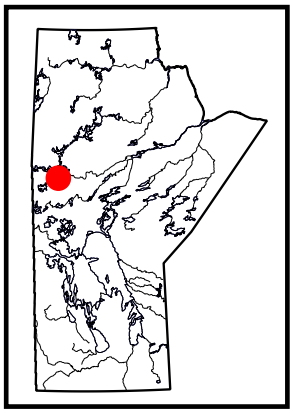

Summary

The Burntwood Lake syenite complex was revisited in 2023 to assess outcrop exposure after a recent forest fire. The complex is one of a series of alkaline igneous complexes in the Trans-Hudson orogen of Manitoba, two of which are known to host carbonatite dikes (the Eden and Brezden lakes complexes). The increased quality and extent of exposures at Burntwood Lake led to the discovery of numerous carbonatite dikes, both in situ and in locally derived boulders. The syenite body is interpreted as a composite pluton that was tilted toward the south and then folded around a southward-plunging isoclinal fold hinge. The current orientation places the more mafic floor of the composite body toward the north, overlain by the more-evolved upper portions of the complex to the south.

Carbonatite exposures were identified in the northern part of the complex over an area of approximately 0.3 km^2 and comprise diffuse, centimetre-scale veins and lenticular pods in the syenite, as well as discrete dikes and 'blows' up to 1 m wide. The carbonatite consists predominantly of calcite, clinopyroxene, apatite and xenocrysts of feldspar, along with accessory amphibole, biotite, titanite and allanite. Coarse-grained dolomite predating calcite was observed at one location. The carbonatite is typically inequigranular and ranges from granoblastic to foliated. Stable carbon and oxygen isotope analyses of carbonate minerals yield ^{13}C-depleted compositions consistent with a mantle source, possibly modified through subduction-related processes. Carbonatites from similar tectonic settings in California and China host several world-class deposits of rare-earth elements. The discovery of carbonatite associated with three syenite complexes in the Trans-Hudson orogen of Manitoba is an important step toward recognizing the Trans-Hudson alkaline-carbonatite igneous province and its potential value for rare-earth–element exploration.

Introduction

A scoping study of the Burntwood Lake syenite complex was undertaken during the summer of 2011 to investigate its potential for rare-earth–element (REE) mineralization (Martins et al., 2011). It was also recognized that the complex could host carbonatite, which had been previously reported from similar geological environments elsewhere (Mumin, 2002; Halama et al., 2005; Hou et al., 2009). During the 2011 field season, outcrops of igneous rock (predominantly, alkali-feldspar syenite) were found to be extensively moss- and lichen-covered and, although a sample of apatite-rich material with elevated concentrations of REEs (~4000 ppm Y + lanthanides) was collected, it was determined that further study of the complex was not feasible due to poor exposure. The discovery of carbonatite and lamprophyre in recently burnt areas at Brezden Lake (Hnatiuk et al., 2022) demonstrated the role of exposure in exploration and mapping, and signalled the importance of revisiting other known sites of alkaline magmatism in the Trans-Hudson orogen. A forest fire burned over the Burntwood Lake complex in the summer of 2022, which provided an impetus for conducting a new scoping study in June of 2023. The principal outcome of this recent work was the discovery of numerous carbonatite dikes, found both in situ and in displaced, locally derived material. The present report is a preliminary summary of these findings and follow-up analytical work conducted thus far.

Regional geology

The Burntwood Lake syenite complex is located in the central Kisseynew domain, approximately 70 km north-northwest of the town of Snow Lake. The Kisseynew domain forms part of the internal zone of the Trans-Hudson orogen in Manitoba, and is flanked by the Lynn Lake domain to the north, Flin Flon domain to the south, and Superior boundary zone to the east (Figure GS2023-6-1).

[1] Department of Earth Sciences, University of Manitoba, Winnipeg, Manitoba, anton.chakhmouradian@umanitoba.ca

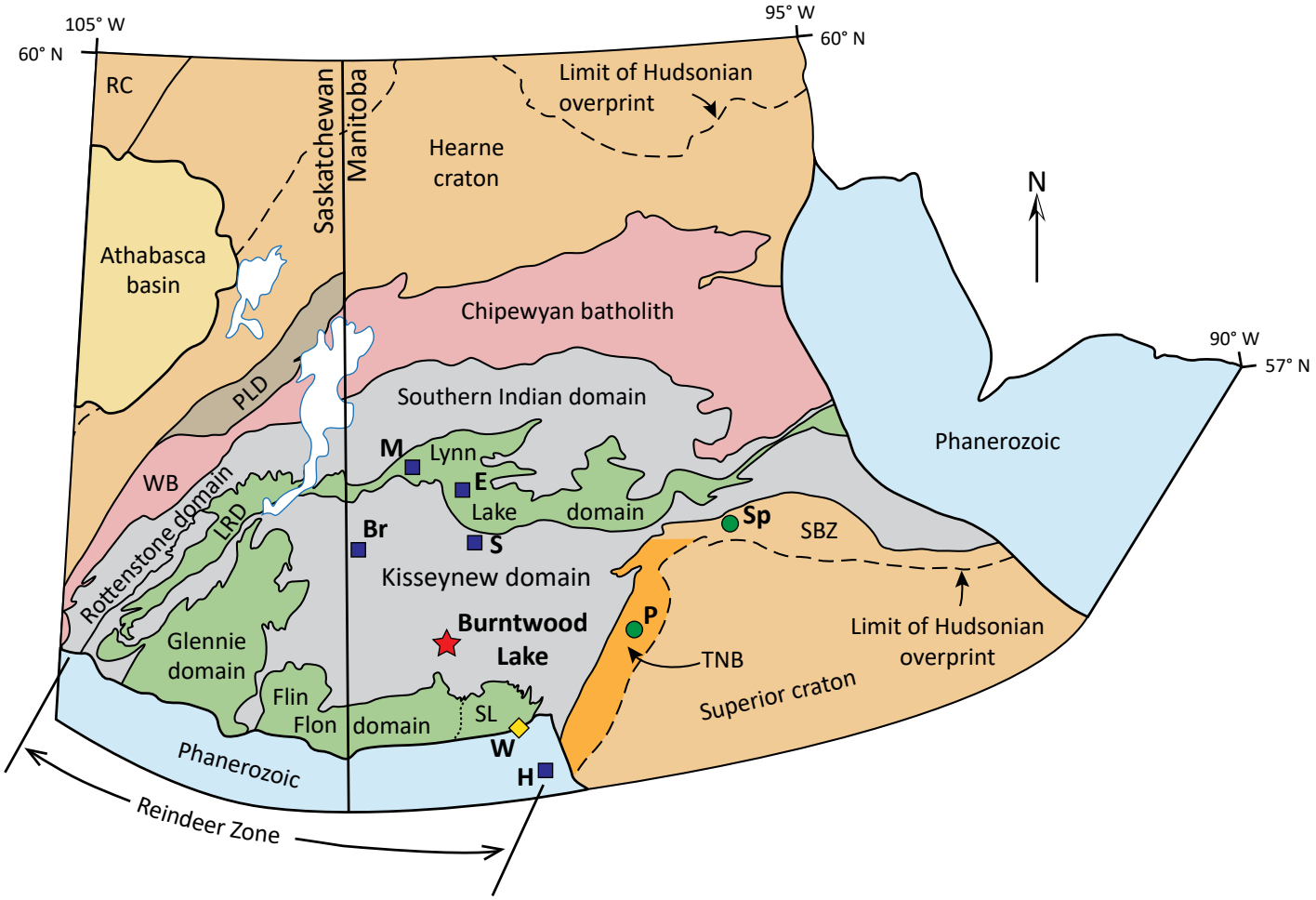

Figure GS2023-6-1: *A schematic map of major tectonic elements in the Manitoba–Saskatchewan segment of the Trans-Hudson orogen (modified from Lewry et al., 1990; Maxeiner et al., 2021; Manitoba Geological Survey, 2022). The location of the Burntwood Lake syenite complex is indicated with a red star. Blue squares indicate the locations of high-potassium to shoshonitic syenite complexes in the Trans-Hudson orogen. Green circles indicate the locations of Paleoproterozoic, late-orogenic carbonatite magmatism in the Superior boundary zone. The yellow diamond indicates the location of anorogenic carbonatite magmatism. Abbreviations: Br, Brezden Lake; E, Eden Lake; H, Huzyk Creek; LRD, La Ronge domain; M, McVeigh Lake; P, Paint Lake; PLD, Peter Lake domain; RC, Rae craton; S, Suwannee River; SBZ, Superior boundary zone; SL, Snow Lake subdomain; Sp, Split Lake; TNB, Thompson nickel belt; W, Wekusko Lake; WB, Wathaman batholith.*

The central Kisseynew domain is underlain by Burntwood group metagreywacke intruded by large plutons, sheets and lenses of felsic to ultramafic rocks (Zwanzig, 2008). The Burntwood group was deposited between 1860 and 1840 Ma (Machado et al., 1999; Murphy and Zwanzig, 2021) into what has been variously interpreted as a back-arc, inter-arc or fore-arc basin (Ansdell et al., 1995; Zwanzig, 1997; Zwanzig and Bailes, 2010). The detritus was largely derived from the adjacent, juvenile magmatic arcs, as indicated by prominent, overlapping detrital zircon age peaks of 1870–1850 Ma in probability plots (Zwanzig and Bailes, 2010; Murphy and Zwanzig, 2021).

Rocks of the central Kisseynew domain attained upper amphibolite– to granulite-facies metamorphic conditions. The migmatitic Burntwood group rocks contain zones of coarse, garnet- and cordierite-rich diatexite (Zwanzig, 2008). Gordon (1989) estimated peak metamorphic conditions of 750 ±50 °C and 5.5 ±1.0 kbar at ca. 1815 Ma for the central Kisseynew domain. However, estimated peak metamorphic conditions as high as 900 °C and 12 kbar at ca. 1800 Ma were reported by Growdon (2010). Large-scale, recumbent isoclinal folds predated peak metamorphism in this part of the domain, and were subsequently refolded during the regional metamorphism (Gordon, 1989; Zwanzig, 2008).

It is possible that the Burntwood intrusive suite was recognized as early as 1971 and interpreted as quartz monzonite–granite crosscut by aplite and pegmatite dikes and surrounded by amphibolitized metasedimentary rocks (unit 15 of McRitchie, 1971). However, the description provided in that report can also potentially refer to hornblende-biotite granite that is common in some parts of the intrusion. Syenitic rocks were decisively identified in McRitchie (1987, 1988), but were not revisited for more detailed work until 2011. Several other syenite complexes of shoshonitic affinity occur within the Trans-Hudson orogen of Manitoba (McRitchie, 1988; Chakhmouradian et al., 2008; Couëslan,

2023). The Burntwood Lake, Brezden Lake, Suwannee River and Huzyk Creek intrusions occur within the Kisseynew domain, whereas the Eden Lake and McVeigh Lake complexes occur within the Lynn Lake domain (Couëslan, 2005; Chakhmouradian et al., 2008; Martins et al., 2011, 2012; Hnatiuk et al., 2022; Martins and Couëslan, 2022; Couëslan, 2023). Granitoid rocks within these complexes typically range in composition from alkali-feldspar syenite (referred to as monzonite in some reports) to clinopyroxene melasyenite and leucocratic quartz syenite. Spatially associated lamprophyres have been reported at Brezden and McVeigh lakes, and carbonatite dikes crosscutting syenites have been reported at Brezden and Eden lakes (Mumin, 2002; Couëslan, 2005; Chakhmouradian et al., 2008; Hnatiuk et al., 2022). The latter intrusion hosts REE-rich apatite (up to 8 wt. % REE) and late, hydrothermal REE mineralization (Chakhmouradian et al., 2008; Mumin, 2010). The syenite complexes within the Trans-Hudson orogen have been the subject of exploration for Zr, REE, Th and U, with the majority of activity centred on Eden Lake (McRitchie, 1989; Mumin, 2010).

Results from 2023 scoping study: new data on the Burntwood Lake complex

Silicate rocks

The 2022 forest fire resulted in much better exposure in the Burntwood Lake area, with a significantly reduced cover of lichen and moss relative to 2011. The improved exposure enabled a better understanding of the structural relations among different rock types, particularly in recessed areas. In the text that follows, we provide a synthesis of the presently available field data combined with preliminary laboratory observations. The Burntwood Lake syenite complex is interpreted as a phacolithic syenite intrusion measuring approximately 1.4 by 2.4 km and hosted by Burntwood group diatexite and associated peraluminous granite (McRitchie, 1987). The intrusion is deformed, with two south-southeast-trending 'roots' partially wrapping around a shallow, north-plunging synformal fold hinge (Figure GS2023-6-2). A steep east-northeast-dipping, axial planar gneissosity is variably developed, but most pronounced along the flanks and within the hinge zone of the intrusion. Contacts between the syenite and the country rock are sharp, but locally metasomatized (McRitchie, 1987).

The syenite is a compositionally and texturally heterogeneous body that was broadly subdivided by Martins et al. (2011) into a pink-beige phase and a brick red phase. The readily apparent difference between the two phases is the colour of feldspar and relative abundance of albite and quartz, which are generally more common in the pink-beige variety. It is noteworthy, however, that some pink-beige syenite undoubtedly represents the brick red phase affected by bleaching at the contact with carbonatite (see 'Carbonate rocks', below). Clinopyroxene is the dominant mafic mineral in the syenite (Figure GS2023-6-3a), although amphibole is locally common and biotite was observed as an accessory phase (2–4 vol. %) in quartz syenite (Figure GS2023-6-3b, c). Where all three minerals are present, amphibole typically forms partial reaction rims on fractured and resorbed clinopyroxene, and is, in turn, replaced by biotite (Figure GS2023-6-3d).

In addition to discrete crystals distributed uniformly throughout the rock, clinopyroxene also occurs in mafic-rich zones within the syenite (melasyenite; Martins et al., 2011), including in relatively equant or irregularly shaped clots and discontinuous layers or lenses up to 15 cm in thickness (Figure GS2023-6-4a). These zones are dominated by dark green clinopyroxene and typically enriched in colourless, fine-grained apatite. Fine-grained rocks consisting of nearly massive apatite were also identified in narrow discontinuous zones up to 30 cm wide at two locations (Figure GS2023-6-4b). At one of these locations, the apatite-rich rock and host red syenite are crosscut by beige quartz syenite with abundant amphibole oikocrysts (Figure GS2023-6-3b). Outcrops containing abundant mafic- or apatite-rich rocks are typically recessed because of the susceptibility of clinopyroxene to fragmentation and erosion.

In many places across the northern part of the Burntwood Lake complex, mafic clots are so abundant as to give the host syenite a leopard-skin appearance. Orthogonal exposures of such areas suggest that clots are cross-sections of small lenticular pods defining a shear-induced lineation. Large fragments of mafic rock are commonly disaggregated and crosscut by pegmatite or syenite dikes, in which case the crosscutting felsic rock is typically enriched in clinopyroxene crystals (Figure GS2023-6-4a, c). Along the sublongitudinal shear zone in the northern part of the complex (Figure GS2023-6-2), mafic horizons are stretched into isolated or stacked lenticular bodies, whereas syenite is fragmented and locally boudinaged (Figure GS2023-6-4d). Assuming that clinopyroxene- and apatite-dominant lithologies represent early igneous products (cumulates), their folding, accompanied by a penetrative axial planar foliation, is in agreement with the overall structural interpretation of the syenite pluton by McRitchie (1987).

In the southern part of the Burntwood Lake pluton, pink-beige syenite is more common than farther north, and no evidence of bleaching was observed. In addition, the syenite is crosscut by numerous pegmatite dikes and, closer to the contact, contains rafts and xenoliths of biotite granite and randomly oriented metasedimentary rocks presumably derived from the Burntwood group. It is thus possible that 'unit 15' of McRitchie (1971) refers to the earlier granite phase predating the syenites. Fine-grained quartz syenite near the eastern contact with the Burntwood group contains fluorite and fluorite-quartz veinlets up to a few centimetres in width. The present authors concur with the earlier interpretation of Martins et al. (2011) that the fluorite-bearing syenite represents an evolved intrusive phase, which was probably emplaced near the roof of the Burntwood Lake pluton.

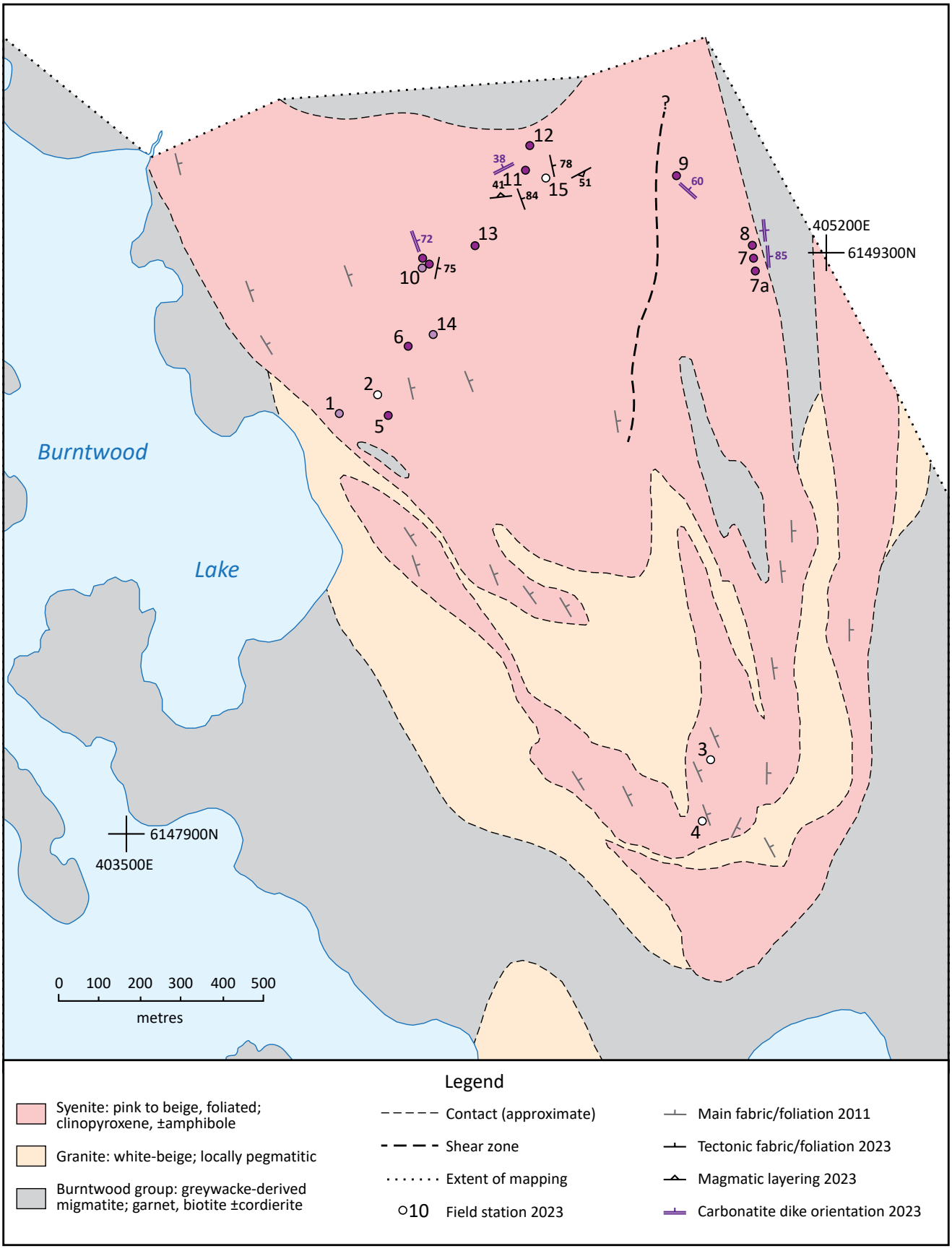

Figure GS2023-6-2: *Simplified geological map of the Burntwood Lake syenite, modified after McRitchie (1987) and Martins et al. (2011). Light purple stations indicate the occurrence of carbonatite in locally derived boulders, dark purple stations indicate carbonatite in outcrop. Stations without colour indicate no observed carbonatite. All co-ordinates are in UTM Zone 14, NAD83.*

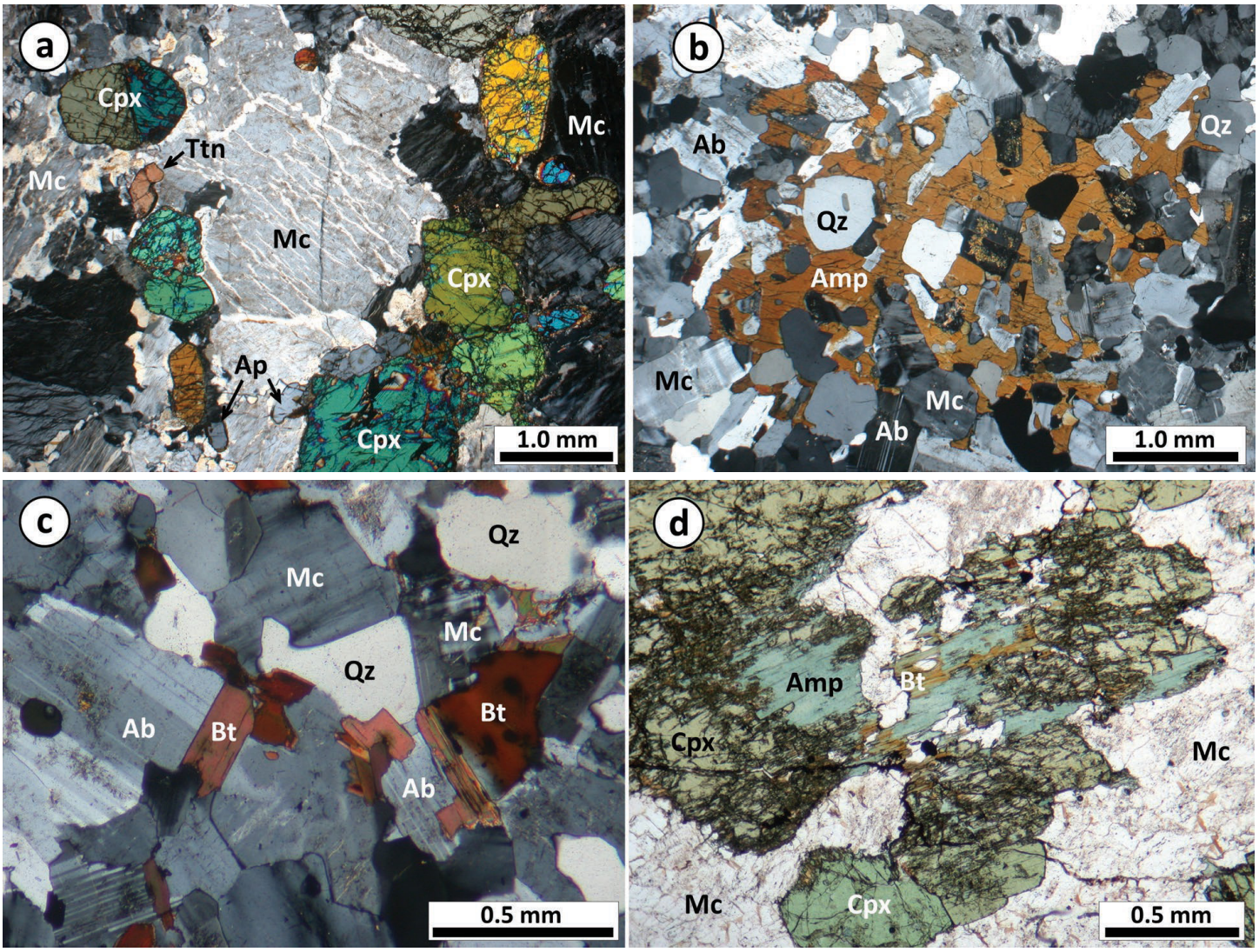

Figure GS2023-6-3: *Selected textural characteristics of the Burntwood Lake syenites:* ***a)*** *euhedral clinopyroxene, accessory apatite and titanite associated with microcline-perthite in mesocratic alkali-feldspar syenite, cross-polarized light (XPL);* ***b)*** *amphibole oikocryst containing inclusions of microcline, albite and quartz in leucocratic quartz syenite, XPL;* ***c)*** *accessory interstitial biotite in quartz syenite, XPL;* ***d)*** *resorption and replacement of clinopyroxene by amphibole and biotite in mesocratic alkali-feldspar syenite, plane-polarized light (PPL). Abbreviations: Ab, albite; Amp, amphibole; Ap, apatite; Bt, biotite; Cpx, clinopyroxene; Mc, microcline-perthite; Qz, quartz; Ttn, titanite.*

Carbonate rocks

Many occurrences of carbonate-rich rock and carbonate-bearing syenite were discovered in outcrop and as float in the northern part of the syenite complex, over a total area of 0.3 km^2 (Figure GS2023-6-2). Discrete trends of these rocks could, in some cases, be traced in outcrop over a distance of 70–80 m. Carbonate-bearing rocks were not observed south of stations 5 and 7 (Figure GS2023-6-2), although less time was spent exploring that part of the Burntwood Lake pluton. The newly discovered rocks range from vuggy, weathered red syenite with diffuse pods and veins of carbonate a few centimetres in width, to discrete dike-like bodies and 'blows' (cf. Wilson and Head, 2007) of predominantly carbonate rock up to 1 m across (Figure GS2023-6-5). In most cases, their emplacement was clearly structurally controlled, and confined to either contacts between different silicate units or steeply dipping linear features generally aligned with the fabric in the host syenite (Figure GS2023-6-5a, b). Wide 'blows', comprising predominantly coarse-grained calcite and albitized microcline, were observed at six locations and appear to be restricted to coarse-grained syenite (Figure GS2023-6-5c). Contacts between the veins and (mela)syenites are diffuse, owing to the presence of interstitial carbonate in the hostrocks and of numerous felsic xenoliths and xenocrysts of feldspar, clinopyroxene and quartz in the veins. The exocontact zone of fine-grained carbonate veins is typically bleached, presumably due to conversion of microcline-perthite to albite (see below).

Several varieties of carbonate-rich rock were identified based on their modal composition and textural characteristics. Their colour ranges from light pink to white and grey; most varieties are extremely inequigranular, but some of the veins (e.g., at stations 1 and 7) comprise more-or-less uniform saccharoidal material with abundant syenite xenoliths. Mineralogically, all of

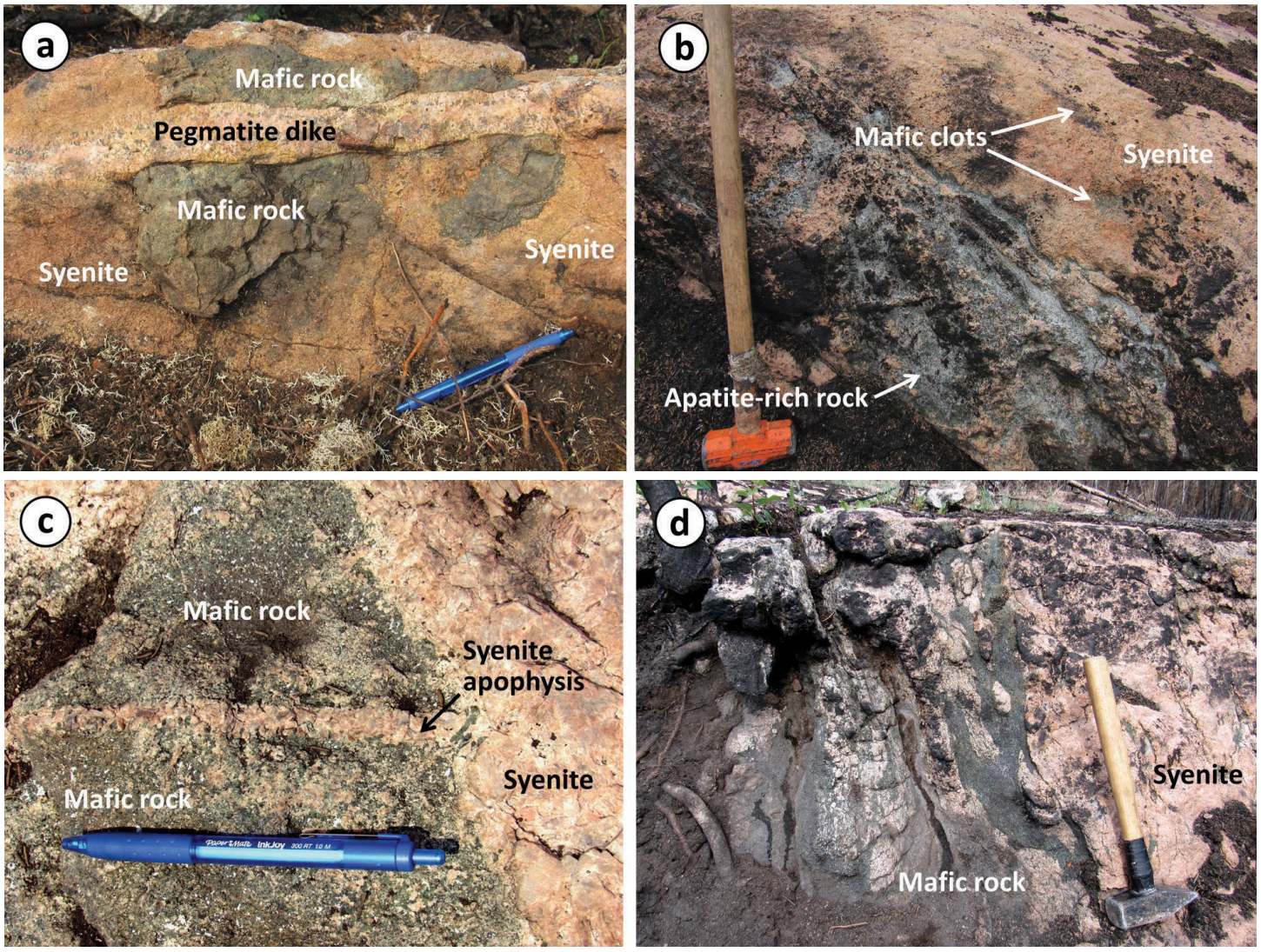

Figure GS2023-6-4: *Field relations of mafic silicate rocks in the Burntwood Lake complex:* ***a)*** *partially disaggregated xenolith of mafic rock (melasyenite) in coarse-grained leucocratic alkali-feldspar syenite, both rocks are crosscut by pegmatite;* ***b)*** *apatite-rich rock and mafic clots hosted by leucocratic syenite;* ***c)*** *mafic xenolith in alkali-feldspar syenite, note syenite apophysis crosscutting the mafic rock, and comb-like structure of clinopyroxene crystals within the apophysis;* ***d)*** *sheared mafic rock comprising stacked and attenuated lenses.*

the samples examined using polarizing microscopy comprise calcite, apatite and xenocrysts of microcline-perthite. Dolomite was observed only at station 10 as coarse porphyroclasts in a finer-grained mesostasis. Calcium clinopyroxene (diopside to aegirine-augite) occurs in the majority of veins and is represented both by sub- to euhedral crystals and by fragmented, resorbed xenocrysts derived from the host (mela)syenite (Figure GS2023-6-6a, b). In several localities, clinopyroxene xenocrysts are partially overgrown by acicular bluish-green amphibole, whereas their unaltered sub- to euhedral counterparts show no evidence of resorption or replacement and typically have a darker colour arising from a greater Na+Fe (aegirine) content. Microcline-perthite xenocrysts are very common in all veins and exhibit partial mesh-like and peripheral replacement by clear albite (Figure GS2023-6-6c). This type of texture, accompanied by clinopyroxene alteration to amphibole is well known in sodic fenites (e.g., Figure GS2023-6-6d).

Typical accessory minerals in the veins include subhedral, zoned crystals of allanite and titanite measuring up to 2.5 and 1.0 mm, respectively (Figure GS2023-6-6a, b). Allanite is most common in endocontact zones, where it forms partial overgrowths on silicate xenocrysts and is associated with fibrous amphibole and albite. Titanite is comparatively less abundant and occurs as discrete grains in clinopyroxene-rich rocks. Accessory biotite is scarce, but makes up 3–4 vol. % of the grey carbonate rock at station 13. The mineral occurs as deformed platy crystals showing strong normal pleochroism in shades of brown, which implies an elevated Fe^{2+} (annite) content.

Microscopically, the examined samples range from nearly equigranular granoblastic rocks with a mosaic texture (Figure GS2023-6-6e) to strongly foliated varieties with coarse calcite or, less commonly, dolomite porphyroclasts enveloped in dynamically recrystallized fine-grained material (Figure GS2023-6-6f). Such 'core-and-mantle' structures are invariably accompa-

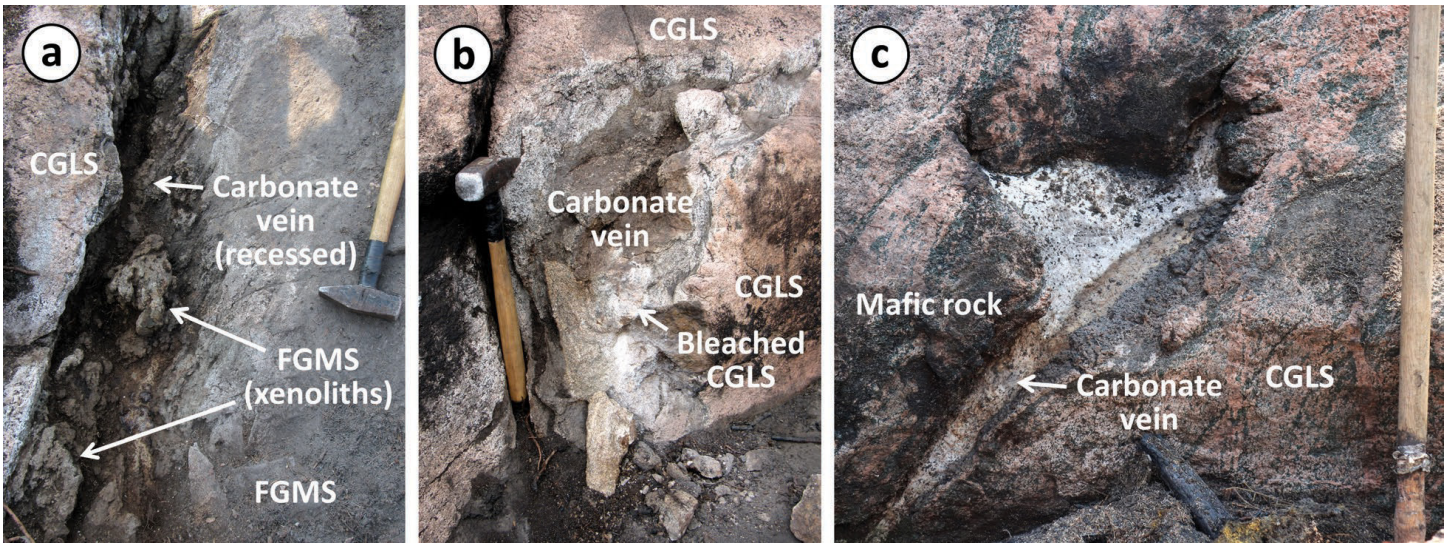

Figure GS2023-6-5: *Field relations of carbonate rocks in the Burntwood Lake complex:* ***a)*** *recessively weathered carbonate vein emplaced at the contact between fine-grained mesocratic syenite and younger coarse-grained leucocratic syenite;* ***b)*** *carbonate vein crosscutting coarse-grained leucocratic syenite, note bleaching of the syenite along the vein contacts;* ***c)*** *carbonate vein with a 'blow' 45 centimetres wide emplaced into coarse-grained leucocratic syenite with numerous mafic clots, sledgehammer handle at right for scale. Abbreviations: CGLS, coarse-grained leucocratic syenite; FGMS, fine-grained mesocratic syenite.*

nied by other evidence of deformation, including undulatory and curtain-like extinction, interrupted and bent polysynthetic twin lamellae in porphyroclasts, foliation-aligned biotite 'fish' and lenticular syenite xenoliths with 'wings' of recrystallized fine-grained calcite. This textural evidence is interpreted to indicate postemplacement ductile flow of the vein material in response to shear stress (Chakhmouradian et al., 2016).

Whole-rock powder samples were prepared from five petrographically distinct carbonate lithologies, including a coarse-grained pink variety with abundant feldspar xenocrysts, fine-grained equigranular white rocks with and without dolomite, and grey varieties with and without biotite. The samples were analyzed at Bureau Veritas Commodities Canada Ltd. (Vancouver, British Columbia) for major and trace elements using X-ray fluorescence and inductively coupled plasma–mass spectrometry, respectively. As can be expected from the available petrographic data (see above in this section), the chemical composition of all five samples is dominated by CaO and CO_2 (35.5–48.1 and 22.5–34.1 wt. %, respectively), whereas SiO_2 and Al_2O_3 concentrations fluctuate significantly (6.1–24.4 and 1.3–5.0 wt. %, respectively) owing to variations in the proportion of silicate xenocrysts in different carbonate veins. The P_2O_5 content is consistently high and reaches 6.1 wt. % (equivalent to 15 wt. % apatite) in the coarse-grained pink rock. Of note are elevated levels of Sr, Ba and REE in all samples; their maximum recorded concentrations are 12 200, 3150 and 4580 ppm, respectively.

Fifteen monomineralic concentrates of calcite and one sample of dolomite (from station 10) were hand-picked under a binocular microscope for stable-isotope analysis. Both fine- and coarse-grained varieties of calcite were extracted from five conspicuously inequigranular rocks. In addition, four mixed samples were prepared for competent fine-grained rocks, where feldspar xenocrysts could not be mechanically separated from calcite. All samples were powdered in an agate mortar, dried at 60 °C for four days and then analyzed by isotope-ratio mass spectrometry. The mass spectrometer was calibrated using calcite standards NBS-18 and IAEA-603 at the beginning, middle and end of each run. To monitor analytical quality, internal standards CHI (calcite) and SIL-MD (dolomite) were analyzed concurrently with 'unknowns', yielding $\delta^{13}C_{VPDB}$ (i.e., carbon isotope ratios with respect to the Vienna Pee Dee Belemnite standard) and $\delta^{18}O_{VSMOW}$ (i.e., oxygen isotope ratios with respect to the Vienna Standard Mean Ocean Water) well within 0.1 per mil (‰) of the accepted values. The results, expressed using the conventional delta notation, are summarized in Figure GS2023-6-7.

All C-O isotope data plot below the 'igneous carbonate box' of Taylor et al. (1967), which has been previously observed in calcite carbonatite from Eden Lake (Chakhmouradian et al., 2008) and Brezden Lake (A.R. Chakhmouradian, unpublished data, 2023). The foliated dolomite-calcite vein from station 10 is characterized by somewhat lower $\delta^{18}O_{VSMOW}$ ratios (7.1–7.6‰) in comparison with calcitic rocks (9.0–10.9‰), but their $\delta^{13}C_{VPDB}$ values overlap (–10.2 to –11.2‰ and –8.3 to –12.8‰, respectively).

Discussion

Preliminary petrogenetic interpretation

Clinopyroxene-rich silicate lithologies observed throughout the northern part of the Burntwood Lake complex during this scoping study can now be confidently interpreted as detached and transported fragments of unexposed cumulate units, ranging from clinopyroxenite to melasyenite in modal composition.

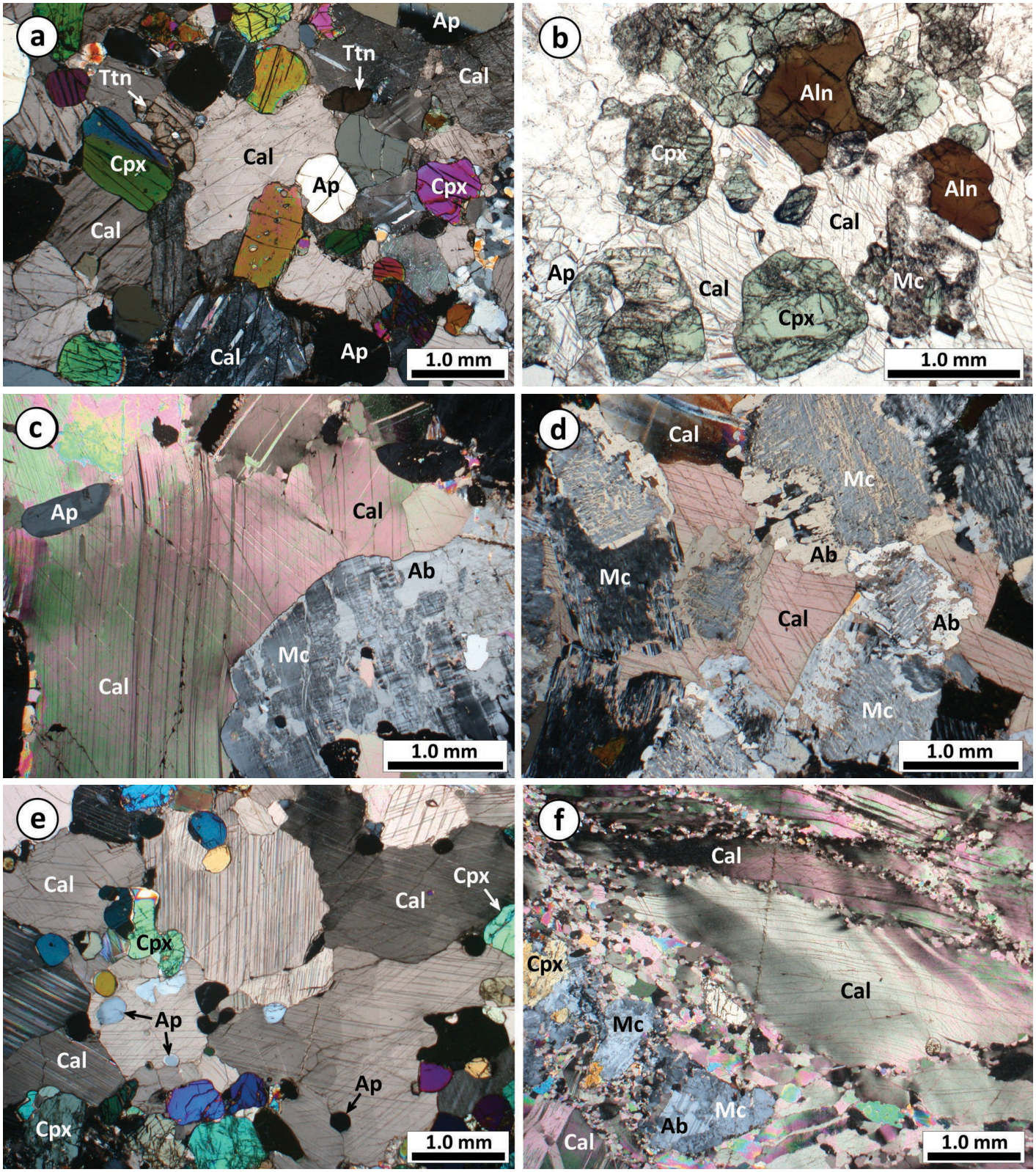

Figure GS2023-6-6: *Photomicrographs of carbonate rocks from the Burntwood Lake complex (a–c, e, f) and Fen complex, Norway (d):* ***a)*** *typical massive carbonate rock composed of calcite, clinopyroxene, apatite and accessory titanite, cross-polarized light (XPL);* ***b)*** *resorbed and altered xenocrysts of clinopyroxene and microcline in a massive carbonate rock; note allanite overgrowths on some xenocrysts, plane-polarized light (PPL);* ***c)*** *microcline xenocryst partially replaced by albite, note undulatory extinction and bent twin lamellae in calcite, XPL;* ***d)*** *typical sodic fenite developed at the contact with calcite carbonatite, from the Fen complex in Norway, XPL (S. Dahlgren and A.R. Chakhmouradian, work in progress) – compare with (c);* ***e)*** *granoblastic texture of nearly equigranular fine-grained carbonate rock, XPL;* ***f)*** *strongly foliated carbonate rock with syenite xenoliths comprising microcline, albite and clinopyroxene (XPL), note 'core-and-mantle' structures and deformation microtextures in calcite porphyroclasts. Abbreviations: Ab, albite; Aln, allanite; Ap, apatite; Cal, calcite; Cpx, clinopyroxene; Mc, microcline; Ttn, titanite.*

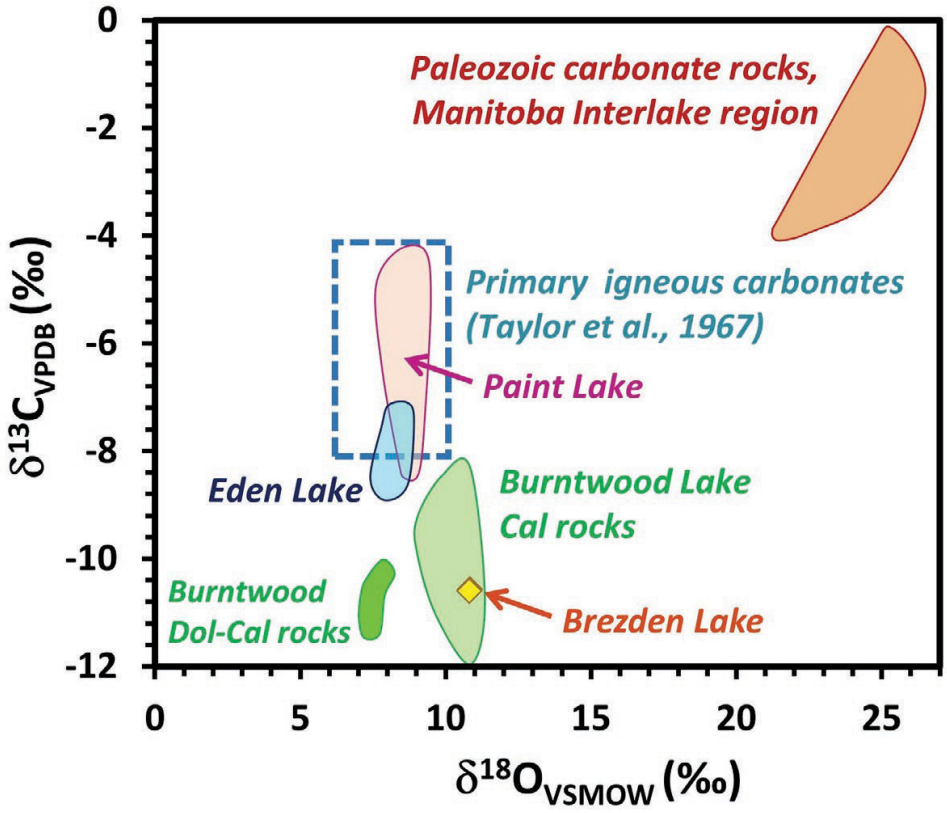

Figure GS2023-6-7: *Variations in carbon (C) and oxygen (O) stable-isotope composition in carbonatites from the Trans-Hudson orogen. The typical compositional range of Paleozoic sedimentary carbonate from the Manitoba Interlake Region and for primary igneous carbonate are plotted for comparison. Abbreviations: Cal, calcitic; Dol-Cal, dolomitic-calcitic. The label for the y-axis is $\delta^{13}C$ Vienna Pee Dee Belemnite ($\delta^{13}C_{VPDB}$), and the label for the x-axis is $\delta^{18}O$ Vienna Standard Mean Ocean Water ($\delta^{18}O_{VSMOW}$); both are expressed in per mil (‰). Source data: Brezden Lake, Paint Lake, Paleozoic sedimentary carbonate, A.R. Chakhmouradian (unpublished data, 2010, 2023); Eden Lake, Chakhmouradian et al. (2008); igneous carbonate, Taylor et al. (1967).*

Their distribution within the more voluminous alkali-feldspar syenite was clearly affected by postemplacement deformation, particularly along the wide shear zone shown in Figures GS2023-6-2 and -4d. The lesser abundance of mafic rocks in the southern portion of the complex, as well as much greater abundance of amphibole- and biotite-bearing quartz syenites, pegmatite dikes and metasedimentary rafts, imply that it represents the upper part of a composite pluton. The complex was tilted toward the south, and folded around a south-plunging isoclinal fold hinge. As a result, the floor of this composite pluton is dipping in an overall southward direction and, hence, more evolved rocks emplaced near the roof are exposed here over a larger area relative to the deeper, more mafic northern part of the complex. This is in contrast to the structural interpretation of a shallow, north-plunging synform by McRitchie (1987). The structural relations among the examined silicate rocks, and their petrographic characteristics, suggest the following emplacement sequence: clinopyroxenite (±apatite cumulate) ⇒ melasyenite ⇒ red alkali-feldspar syenite ⇒ amphibole-bearing quartz syenite (±accessory biotite) ⇒ fluorite-bearing quartz syenite and pegmatite.

The newly discovered carbonate-bearing rocks can be confidently identified as carbonatites based on the currently available evidence. With one exception (station 10), most of these rocks correspond to calcite carbonatite variably contaminated with wallrock silicate material and affected by shearing. The rock at station 10 is also rich in xenoliths and strongly deformed, but comprises similar proportions of dolomite and calcite. The available microtextural evidence (Figure GS2023-6-6c, d) is consistent with metasomatic reworking of syenite xenoliths by carbonatite-derived alkali-rich fluids. Similar metasomatic processes, collectively described as fenitization (Elliott et al., 2018), have been previously documented at Eden and Brezden lakes, which are also in the Trans-Hudson orogen (Chakhmouradian et al., 2008; Hnatiuk et al., 2022). Metasomatic reworking of carbonate rocks by silicate magmas, on the contrary, has not been observed at Burntwood Lake or the other two localities, and, hence, the possibility that the newly discovered carbonate rocks represent rafts of crustal calc-silicate material can be ruled out.

The stable-isotopic signature of the examined samples does not appear to have been modified by wallrock contamination or reaction with metamorphic fluids and is similar to those of calcite carbonatites at Eden and Brezden lakes (Figures GS2023-6-1, -7). The observed depletion in ^{13}C, typical of these rocks, may be related to their derivation from subducted crustal materials or to carbon isotope fractionation in the mantle (Chakhmouradian et al., 2008). The mineralogy, as well as structural relationships

with the host syenite, of the Burntwood Lake carbonatites are also similar to their counterparts at Brezden and Eden lakes. At all three localities, large carbonatite bodies (~1 m across) consist predominantly of calcite, clinopyroxene and apatite, and are found in coarse-grained syenite, which is affected by sodic fenitization (Mumin, 2002; Chakhmouradian et al., 2008; Hnatiuk et al., 2022). At all three localities, apatite, titanite and allanite are the principal REE-bearing phases, and the latter is paragenetically linked to wallrock silicate contamination. Allanite is therefore interpreted as the product of reaction between Si-Al–rich, largely feldspathic xenoliths and REE-bearing carbonatitic magma.

The whole-rock trace-element compositions of selected Burntwood Lake syenites reported by Martins et al. (2011) show enrichment in light REE (La–Eu), Ba and other large-ion-lithophile elements, coupled with relative depletion in high-field-strength elements (Ti, Zr, Hf, Nb and Ta). These characteristics are also shared by alkaline igneous rocks at Eden Lake (Couëslan, 2005; Chakhmouradian et al., 2008), Brezden Lake (Martins et al., 2012), Mountain Pass in California (Castor, 2008), Weishan and the Mianning–Dechang metallogenic belt of China (Hou et al., 2009; Zeng et al., 2022). At all these localities, carbonatites are predominantly calcitic in composition and occur in intimate spatial association with silica-saturated syenites. In some cases (e.g., Mountain Pass; Castor, 2008), the petrographic spectrum of associated silicate rocks is wide and ranges from very primitive compositions (e.g., olivine shonkinite) to miaskitic amphibole-quartz syenite. In other cases (Weishan and Mianning–Dechang: Hou et al., 2009; Zeng et al., 2022), the principal silicate constituent is evolved peralkaline quartz syenite. In terms of its diverse petrography, the Burntwood Lake pluton is similar to the Mountain Pass complex, which had a prolonged and complex evolutionary history spanning 60 Ma (Poletti et al., 2016).

The syenite-carbonatite associations in the Trans-Hudson orogen, California and China also share many geochemical characteristics (e.g., enrichment in trace lithophile elements and depletion in high-field-strength elements) and were emplaced in zones of continental plate collision. A large body of trace-element and isotopic evidence has been presented to demonstrate links between this type of magmatism, ocean closure, crust recycling, mantle refertilization and plate-collision processes (e.g., Chakhmouradian et al., 2008; Wang et al., 2019; Çimen et al., 2022; Hou et al., 2023). Well-studied examples elsewhere in the world range in age from ca. 2.0 Ga to 12 Ma (Liu et al., 2015; Djeddi et al., 2021). It is feasible that the composite syenite (±carbonatite±lamprophyre) intrusions in the Paleoproterozoic Trans-Hudson orogen (Figure GS2023-6-1) are broadly coeval and manifest the final stages of plate collision at ca. 1.8 Ga (Corrigan et al., 2009; Salnikova et al., 2019). If so, these complexes represent one of the oldest known and most extensive (~8700 km^2) expressions of collision-related alkaline-carbonatitic magmatism in the world, for which the authors propose the designation 'Trans-Hudson alkaline-carbonatite igneous province'. From a practical standpoint, it is noteworthy here that the Mountain Pass and Chinese carbonatites host economic rare-earth–element mineralization, mostly in the form of bastnäsite ($REECO_3F$).

Recommendations for future work

The wide variety of carbonatite discovered during this scoping study, and its spatial extent, suggest good potential for additional occurrences of these rocks both within the syenite pluton and in its exocontact zone. The collection of additional structural data will be key to reconciling the current geometry of the complex. A thorough characterization of the carbonate rocks, and their relationship to the syenite, would best be accomplished by one or more graduate-level projects. The abundance of these rocks suggests that future investigations should not be restricted to the syenite complex, but should include shoreline mapping in the northwestern Burntwood Lake area. Careful mapping and radiometric dating of discrete intrusive units will be essential to deciphering their temporal relations and ultimately the evolutionary history of the entire complex. The excellent exposures offered by the relatively fresh burn make future field studies time-sensitive, and ideally they should be conducted within the next few years.

Economic considerations

Carbonatites are the most economically important source of light lanthanides (La–Eu) and host the largest known REE deposits, including Bayan Obo in northern China and the aforementioned Mianning–Dechang, Weishan and Mountain Pass mines. China is currently the largest producer of REEs worldwide, supplying some 70% of the global demand (210 000 Mt REE oxide in 2022; Cordier, 2023). The Mountain Pass mine is the second-largest producer, with an annual output of 43 000 Mt REE oxide in the form of bastnäsite and monazite concentrate. However, all of China's current production is exported overseas, whereas the United States currently imports some $200 million worth of REE compounds and metals (Cordier, 2023). Increased demand for REEs, spurred on by the proliferation of low-carbon-footprint transportation, energy and communication technologies, has created a need for new economically viable REE deposits to sustain a reliable REE supply chain outside of the current producers, which are largely dependent on China. This has prompted the Government of Canada to include REEs on the list of critical minerals (Natural Resources Canada, 2022) and support exploration and research efforts focused on REEs under the Targeted Geoscience Initiative and other programs. In addition to revisiting well-known localities of alkaline and carbonatitic magmatism, these programs should be aimed at identifying new targets for critical-metal exploration and new potential metallotects. The discovery of REE-bearing carbonatites at Brezden Lake (Hnatiuk et al., 2022) and Burntwood Lake (this report) is an important step toward recognizing the Trans-Hudson alkaline-carbonatite igneous province and its potential value for rare-metal exploration.

Acknowledgments

Thanks to C. Epp and P. Belanger at the Manitoba Geological Survey Midland Sample and Core Library (Winnipeg, Manitoba) for logistical support, and C. English for GIS support. M. Friesen (University of Manitoba, Winnipeg) provided tireless assistance in the field and was always willing to carry another sample. Thanks to T. McCracken and Gogal Air Services of Snow Lake, Manitoba for float plane support, M. Yun for assistance with stable-isotope work, and Precision Petrographics for masterfully executed thin sections. Financial support for this project was provided, in part, by Natural Resources Canada's Targeted Geoscience Initiative program.

References

Ansdell, K.M., Lucas, S.B., Connors, K. and Stern, R.A. 1995: Kisseynew metasedimentary gneiss belt, Trans-Hudson orogen (Canada): back-arc origin and collisional inversion; Geology, v. 23, p. 1039–1043.

Castor, S.B. 2008: The Mountain Pass rare-earth carbonatite and associated ultrapotassic rocks, California; The Canadian Mineralogist, v. 46, p. 779–806.

Chakhmouradian, A.R., Mumin, A.H., Demény, A. and Elliott, B. 2008: Postorogenic carbonatites at Eden Lake, Trans-Hudson Orogen (northern Manitoba, Canada): geological setting, mineralogy and geochemistry; Lithos, v. 103, p. 503–526.

Chakhmouradian, A.R., Reguir, E.P. and Zaitsev, A.N. 2016: Calcite and dolomite in intrusive carbonatites. I. Textural variations; Mineralogy and Petrology, v. 110, p. 333–360.

Çimen, O., Ağrılı, H., Kuebler, C., Simonetti, A., Corcoran, L., Simonetti, S., Çolak, T., İnal, S. and Dönmez, C. 2022: Geochemical, isotopic and U-Pb geochronological investigation of the late Cretaceous Karaçayır carbonatite (Sivas, Turkey): insights into mantle sources within a post-collisional tectonic setting; Ore Geology Reviews, v. 141, art. 104650.

Cordier, D.J. 2023: Rare-earths; Mineral Commodity Summaries, January 2023, U.S. Geological Survey, URL <https://pubs.usgs.gov/periodicals/mcs2023/mcs2023-rare-earths.pdf> [September 2023].

Corrigan, D., Pehrsson, S., Wodicka, N. and de Kemp, E. 2009: The Paleoproterozoic Trans-Hudson Orogen: a prototype of modern accretionary processes; *in* Ancient Orogens and Modern Analogues, J.B. Murphy, J.D. Keppie and A.J. Hynes (ed.), Geological Society, Special Publication 327, p. 457–479.

Couëslan, C.G. 2005: Geochemistry and petrology of the Eden Lake carbonatite and associated silicate rocks; M.Sc. thesis, University of Western Ontario, London, Ontario, 201 p.

Couëslan, C.G. 2023: Age and petrology of zirconium- and light rare-earth element–enriched quartz monzonite in drillcore from the Huzyk Creek property, sub-Phanerozoic Kisseynew domain, central Manitoba (NTS 63J6); Manitoba Economic Development, Investment and Trade, Manitoba Geological Survey, Open File OF2023-2, 28 p.

Djeddi, A., Parat, F., Bodinier, J.-L., Ouzegane, K. and Dautria, J.-M. 2021: The syenite–carbonatite complex of Ihouhaouene (Western Hoggar, Algeria): interplay between alkaline magma differentiation and hybridization of cumulus crystal mushes; Frontiers in Earth Science, v. 8, art. 605116.

Elliott, H.A.L., Wall, F., Chakhmouradian, A.R., Siegfried, P.R., Dahlgren, S., Weatherley, S., Finch, A.A., Marks, M.A.W., Dowman, E. and Deady, E. 2018: Fenites associated with carbonatite complexes: a review; Ore Geology Reviews, v. 93, p. 38–59.

Gordon, T.M. 1989: Thermal evolution of the Kisseynew sedimentary gneiss belt, Manitoba: metamorphism at an early Proterozoic accretionary margin; *in* Evolution of Metamorphic Belts, J.S. Daly, R.A. Cliff and B.W.D. Yardley (ed.), Geological Society, Special Publication 43, p. 233–243.

Growdon, M.L. 2010: Crustal development and deformation of Laurentia during the Trans-Hudson and Alleghenian orogenies; Ph.D. thesis, Indiana University, Bloomington, Indiana, 221 p.

Halama, R., Vennemann, T., Siebel, W. and Markl, G. 2005: The Grønnedal-Ika carbonatite–syenite complex, South Greenland: carbonatite formation by liquid immiscibility; Journal of Petrology, v. 46, p. 191–217.

Hnatiuk, T., Couëslan, C.G., Chakhmouradian, A.R. and Martins, T. 2022: Preliminary results from targeted sampling of the Brezden Lake intrusive complex, west-central Manitoba (parts of NTS 64C4); *in* Report of Activities 2022, Manitoba Natural Resources and Northern Development, Manitoba Geological Survey, p. 42–48.

Hou, Z., Tian, S., Xie, Y., Yang, Z., Yuan, Z., Yin, S., Yi, L., Fei, H., Zou, T., Bai, G. and Li, X. 2009: The Himalayan Mianning–Dechang REE belt associated with carbonatite–alkaline complexes, eastern Indo-Asian collision zone, SW China; Ore Geology Reviews, v. 36, p. 65–89.

Hou, Z.-Q., Xu, B., Zhang, H., Zheng, Y.-C., Wang, R., Liu, Y., Miao, Z., Gao, L., Zhao, Z., Griffin, W.L. and O'Reilly, S.Y. 2023: Refertilized continental root controls the formation of the Mianning–Dechange carbonatite-associated rare-earth-element ore system; Nature: Communications Earth & Environment, v. 4, art. 293 (2023), 10 p., URL <https://doi.org/10.1038/s43247-023-00956-6>.

Lewry, J.F., Thomas, D.J., Macdonald, R. and Chiarenzelli, J. 1990: Structural relations in accreted terranes of the Trans-Hudson Orogen, Saskatchewan: telescoping in a collisional regime?; *in* The Early Proterozoic Trans-Hudson Orogen of North America, J.F. Lewry and M.R. Stauffer (ed.), Geological Association of Canada, Special Paper 37, p. 75–94.

Liu, Y., Hou, Z., Tian, S., Zhang, Q., Zhu, Z. and Liu, J. 2015: Zircon U–Pb ages of the Mianning–Dechang syenites, Sichuan Province, southwestern China: constraints on the giant REE mineralization belt and its regional geological setting; Ore Geology Reviews, v. 64, p. 554–568.

Machado, N., Zwanzig, H. and Parent, M. 1999: U-Pb ages of plutons, sedimentation, and metamorphism of the Paleoproterozoic Kisseynew metasedimentary belt, Trans-Hudson Orogen (Manitoba, Canada); Canadian Journal of Earth Sciences, v. 36, p. 1829–1842.

Manitoba Geological Survey 2022: Bedrock geology of Manitoba; Manitoba Natural Resources and Northern Development, Manitoba Geological Survey, Open File OF2022-2, scale 1:1 000 000.

Martins, T. and Couëslan, C.G. 2022: Critical minerals scoping study of the Suwannee River syenite intrusion, west-central Manitoba (part of NTS 64B4); *in* Report of Activities 2022, Manitoba Natural Resources and Northern Development, Manitoba Geological Survey, p. 36–41.

Martins, T., Couëslan, C.G. and Böhm, C.O. 2011: The Burntwood Lake alkali-feldspar syenite revisited, west-central Manitoba (part of NTS 63N8); *in* Report of Activities 2011, Manitoba Innovation, Energy and Mines, Manitoba Geological Survey, p. 79–85.

Martins, T., Couëslan, C.G. and Böhm, C.O. 2012: Rare metals scoping study of the Brezden Lake intrusive complex, western Manitoba (part of NTS 64C4); *in* Report of Activities 2012, Manitoba Innovation, Energy and Mines, Manitoba Geological Survey, p. 115–123.

Maxeiner, R., Ashton, K., Bosman, S., Card, C., Kohlruss, D., Marsh, A., Morelli, R. and Slimmon, W. 2021: Notes to accompany the new 2021 edition of the 1:1 000 000-scale geological map of Saskatchewan; Saskatchewan Geological Survey, Miscellaneous Report 2021-2, 20 p.

McRitchie, W.D. 1971: Burntwood Lake area (63N-7E, -8 and part of 10E); *in* Summary of Geological Field Work 1971, Manitoba Department of Mines, Resources and Environmental Management, Mines Branch, Geological Paper GP6/71, p. 30–33.

McRitchie, W.D. 1987: Burntwood Lake syenite; *in* Report of Field Activities 1987, Manitoba Energy and Mines, Minerals Division, p. 65–69.

McRitchie, W.D. 1988: Alkaline intrusions of the Churchill Province Eden Lake (64C/9) and Brezden Lake (64C/4); *in* Report of Field Activities 1988, Manitoba Energy and Mines, Minerals Division, p. 5–11.

McRitchie, W.D. 1989: Ground scintillometer reconnaissance of the Eden Lake aegerine-augite monzonite; *in* Report of Field Activities 1989, Manitoba Energy and Mines, Minerals Division, p. 7–12.

Mumin, A.H. 2002: Discovery of a carbonatite complex at Eden Lake (NTS 64C9); *in* Report of Activities 2002, Manitoba Industry, Trade and Mines, Geological Services, p. 187–197.

Mumin, H. 2010: The Eden Lake rare metal (REE, Y, U, Th, phosphate) carbonatite complex Manitoba – updated report; *in* NI 43-101 technical report prepared for Medallion Resources Ltd., p. 87–94.

Murphy, L.A. and Zwanzig, H.V. 2021: Geology of the Wuskwatim–Granville lakes corridor, Kisseynew domain, Manitoba (parts of NTS 63O, P, 64A–C); Manitoba Agriculture and Resource Development, Manitoba Geological Survey, Geoscientific Report GR2021-2, 94 p.

Natural Resources Canada 2022: Critical minerals: an opportunity for Canada; Natural Resources Canada, URL <https://www.canada.ca/en/campaign/critical-minerals-in-canada/critical-minerals-an-opportunity-for-canada.html> [September 2023].

Poletti, J.E., Cottle, J.M., Hagen-Peter, G.A. and Lackey, J.S. 2016: Petrochronological constraints on the origin of the Mountain Pass ultrapotassic and carbonatite intrusive suite, California; Journal of Petrology, v. 57, p. 1555–1598.

Salnikova, E.B., Chakhmouradian, A.R., Stifeeva, M.V., Reguir, E.P., Kotov, A.B., Gritsenko, Y.D. and Nikiforov, A.V. 2019: Calcic garnets as a geochronological and petrogenetic tool applicable to a wide variety of rocks; Lithos, v. 338-339, p. 141–154.

Taylor, H.P., Jr., Frechen, J. and Degens, E.T. 1967: Oxygen and carbon isotope studies of carbonatites from the Laacher See District, West Germany and the Alnö District, Sweden; Geochimica et Cosmochimica Acta, v. 31, p. 407–430.

Wang, C., Liu, J., Zhang, H., Zhang, X., Zhang, D., Xi, Z. and Wang, Z. 2019: Geochronology and mineralogy of the Weishan carbonatite in Shandong province, eastern China; Geoscience Frontiers, v. 10, p. 769–785.

Wilson, L. and Head, J.W., III 2007: An integrated model of kimberlite ascent and eruption; Nature, v. 447, p. 53–57.

Zeng, X., Li, X., Fan, H., Lan, T., Lan, J., Su, J., Zhang, P., Yang, K. and Zhao, X. 2022: Generation of REE-rich syenite-(carbonatite) complex through lithosphere-asthenosphere interaction: an *in-situ* Sr–Nd–O isotopic study of the Mesozoic Weishan pluton, Northern China; Journal of Asian Earth Sciences, v. 230, art. 105191.

Zwanzig, H.V. 1997: Comments on "Kisseynew metasedimentary gneiss belt, Trans-Hudson orogen (Canada): back-arc origin and collisional inversion" by Ansdell et al., 1995 (Geology, v. 23, p. 1039–1043); Geology, v. 25, p. 90–91.

Zwanzig, H.V. 2008: Correlation of lithological assemblages flanking the Kisseynew Domain, Manitoba (parts of NTS 63N, 63O, 64B, 64C): proposal for tectonic/metallogenic subdomains; *in* Report of Activities 2008, Manitoba Science, Technology, Energy and Mines, Manitoba Geological Survey, p. 38–52.

Zwanzig, H.V. and Bailes, A.H. 2010: Geology and geochemical evolution of the northern Flin Flon and southern Kisseynew domains, Kississing–File lakes area, Manitoba (parts of NTS 63K, N); Manitoba Innovation, Energy and Mines, Manitoba Geological Survey, Geoscientific Report GR2010-1, 135 p.

December 4, 2023

ERRATA NOTICE

In the “Whole-rock geochemical trends of the Wekusko Lake pegmatite dikes” section found on page 58 of GS2023-7 from the *Report of Activities 2023*, the following sentence was added to the first paragraph:

> However, due to the extremely coarse grain size and variable local distribution of minerals in the studied pegmatites bodies, the selected samples used for whole-rock geochemistry analysis might not represent the total extent of the pegmatite bodies chemistry.

Figures GS2023-7-6 and GS2023-7-7 have also been updated.

GS2023-7

Regional pegmatite mapping and geochemical fractionation trends from the Wekusko Lake pegmatite field, west-central Manitoba (parts of NTS 63J13, 14, 63O4)

by D. Silva[1], T. Martins, L. Groat[2] and R. Linnen[3]

In Brief:

- The Wekusko Lake pegmatite field contains multiple types of Li-pegmatites including spodumene- and lepidolite-bearing dikes
- Pegmatite dike occurrences were explored and mapped, mainly adjacent to the Berry Creek fault in the Bur zone
- Pegmatite whole-rock geochemical fractionation trends are discussed for the region

Citation:
Silva, D., Martins, T., Groat, L. and Linnen, R. 2023: Regional pegmatite mapping and geochemical fractionation trends from the Wekusko Lake pegmatite field, west-central Manitoba (parts of NTS 63J13, 14, 63O4); *in* Report of Activities 2023, Manitoba Economic Development, Investment, Trade and Natural Resources, Manitoba Geological Survey, p. 52–63.

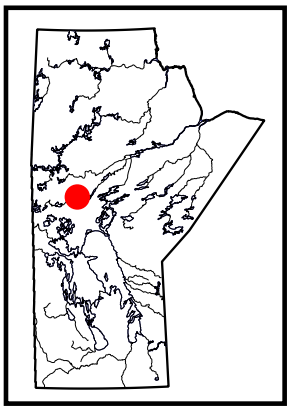

Summary

This report describes field observations gathered during the 2023 geological mapping campaign of lithium-bearing pegmatite dikes in the Wekusko Lake pegmatite field in west-central Manitoba, along with the regional geochemical fractionation trends of major and minor elements from pegmatite samples collected in the summer of 2022. Fourteen occurrences of pegmatite dikes were explored, primarily in the areas of north to northeast Wekusko Lake (Crowduck Bay, Sherritt-Gordon and Violet-Thompson pegmatite groups) and adjacent to the regional southwest-oriented Berry Creek fault in the Bur zone (Berry Creek pegmatite group). No new lithium-mineralized pegmatite dikes were discovered during the 2023 geological mapping; however, a new occurrence of spodumene- and lepidolite-bearing pegmatite in the Bur zone was recently discovered at depth, opening the potential for further discoveries of different types of lithium mineralization within the Wekusko Lake pegmatite field.

Whole-rock K/Rb, K/Cs and Nb/Ta ratios show a strong spatial geochemical trend, indicated by the evolution toward low elemental ratios in non-lithium–mineralized pegmatite groups located in the northern- and easternmost parts of the Wekusko Lake pegmatite field compared to those in lithium-enriched pegmatites near the Crowduck Bay shear zone. A decrease in the K/Rb ratio and an increase in P_2O_5 with increase in pegmatite peraluminosity is also observed in non-lithium–mineralized pegmatites compared to lithium-enriched pegmatites.

Introduction

As a result of electric-powered mobility and the transition to more sustainable electrical storage and energy production, the demand for lithium, nickel, cobalt, tantalum and rare-earth elements has increased. Because of the risk of supply to the manufacturing industry, as well as their economic and/or military significance, Canada classifies certain elements as 'critical minerals' (Natural Resources Canada, 2021). Rare-element pegmatites play an important role in the green revolution, because they contain large amounts of essential minerals, particularly lithium-bearing, making them targets for mineral exploration.

Manitoba is a well-established jurisdiction for lithium-bearing pegmatite exploration and mining due to the large scale of some deposits (e.g., the world-class Tanco deposit in southeast Manitoba; Černý, 2005). This report focuses on the Wekusko Lake pegmatite field in west-central Manitoba, which is known to contain spodumene- and lepidolite-bearing pegmatites. The Wekusko Lake pegmatite field is located about 25 km east of the town of Snow Lake. Numerous exploration programs targeting spodumene pegmatites are currently underway in the area due to the region's significant lithium potential (Lithium Foremost Resource & Technology Ltd., 2022; Snow Lake Lithium Ltd., 2022; Lodestar Battery Metals Corp., 2023). This study summarizes mineralogical and structural observations of the Wekusko Lake pegmatite field made during the summer of 2023, as well as results of lithogeochemical analyses on both barren and lithium-bearing pegmatite dikes.

Regional geology

The Wekusko Lake pegmatite field is part of the Snow Lake subdomain of the Flin Flon domain (Černý et al., 1981; Gordon et al., 1990; Lucas et al., 1996; Ansdell, 2005). The Snow Lake subdomain is located in the Reindeer zone of the Trans-Hudson orogen (Lewry and Collerson, 1990; David et al.,

[1] Department of Earth, Ocean and Atmospheric Sciences, The University of British Columbia, Vancouver, British Columbia, davidbsilva237@gmail.com
[2] Department of Earth, Ocean and Atmospheric Sciences, The University of British Columbia, Vancouver, British Columbia
[3] Department of Earth Sciences, Western University, London, Ontario

1996). The Kisseynew domain is part of the northeasternmost section of the Trans-Hudson orogen (Figure GS2023-7-1; David et al., 1996; Connors et al., 1999). The Snow Lake subdomain is underlain by three major 1.88–1.83 Ga Paleoproterozoic tectonostratigraphic packages: 1) the accreted Flin Flon arc and ocean-floor assemblages that formed the Flin Flon–Glennie complex (Gordon et al., 1990; Stern et al., 1993; Stern and Lucas, 1994; David et al., 1996; Ansdell et al., 1999; Machado et al., 2000; Reid, 2021a, b); 2) turbidite deposits of the Burntwood group (Bailes, 1980; Zwanzig, 1990); and 3) alluvial-fluvial sandstones of the Missi group (Figure GS2023-7-1; Ansdell, 1993; Ansdell and Connors, 1995; Ansdell and Norman, 1995; Reid, 2021a, b). In the Snow Lake region, 1.84–1.83 Ga late successor-arc plutons intruded all of these units (Gordon et al., 1990; David et al., 1996; Whalen et al., 1999). The Flin Flon domain is unconformably overlain in the south by a Paleozoic dolomitic limestone (NATMAP Shield Margin Project Working Group, 1998). The Flin Flon domain features a metamorphic field gradient that ranges from lower greenschist facies in the south to upper amphibolite facies in the north, near the boundary with the Kisseynew domain (Černý et al., 1981; Lewry et al., 1994; Kraus and Menard, 1997). The metamorphic field gradient in the Snow Lake area ranges from upper green-

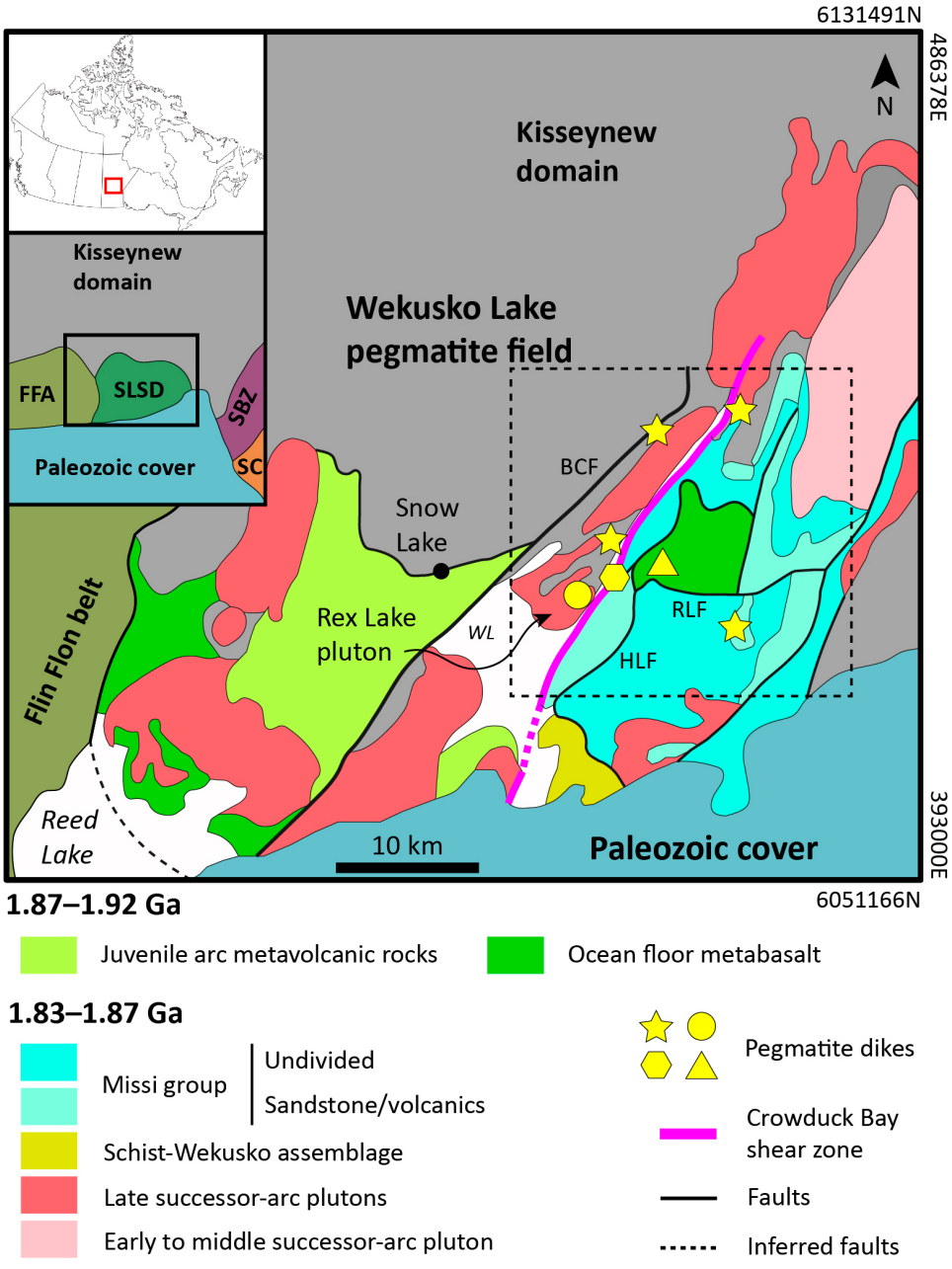

Figure GS2023-7-1: *Simplified regional geology of the Snow Lake subdomain (following Galley et al., 2007) and the location of pegmatite groups in the Wekusko Lake pegmatite field. Inset tectonic elements map of the Trans-Hudson orogen of central Manitoba is modified after Manitoba Geological Survey (2022). Symbols for pegmatite dikes: triangle, Green Bay group; circle, Sherritt-Gordon group; hexagon, Violet-Thompson group; star, unsubdivided. Abbreviations: BCF, Berry Creek fault; FFA, Flin Flon arc assemblage; HLF, Herb Lake fault; RLF, Robert Lake fault; SBZ, Superior boundary zone; SC, Superior craton; SLSD, Snow Lake subdomain; WL, Wekusko Lake. All co-ordinates are in UTM Zone 14, NAD83.*

schist–lower amphibolite facies to upper amphibolite facies, with migmatitic zones to the north, northeast and east of Wekusko Lake (Bailes, 1985; Lazzarotto, 2020).

Before craton stabilization at 1.70–1.65 Ga, the Snow Lake region underwent four deformational events (D_1–D_4). At 1.88–1.87 Ga, the Flin Flon–Glennie arc accreted, which is related to deformation event D_1 (Lucas et al., 1996; Connors et al., 1999; Schneider et al., 2007; Stewart et al., 2018). The Kisseynew domain and the Flin Flon–Glennie arc collided with the Sask craton, resulting in south to southwest compression at 1.84–1.81 Ga (Zwanzig, 1990; Connors, 1996; Connors et al., 1999). Peak metamorphism occurred around 1.81 Ga, coinciding with the transition from D_2 to D_3 in the east Snow Lake area (Connors et al., 2002). During the D_3 event, the main tectonic stress direction shifted from northeast-southwest compression to northwest-southeast compression, which is associated with the formation of the Crowduck Bay shear zone, and the Herb Lake and Roberts Lake regional transpressional faults (Connors and Ansdell, 1994; Kraus and Williams, 1994; Connors et al., 2002). The D_4 phase, which manifested as primarily brittle deformation, could be a continuation of the D_3 phase (Lucas et al., 1994; Fedorowich et al., 1995).

Dikes of the Wekusko Lake pegmatite field intruded a variety of lithologies, including conglomerate to quartzofeldspathic gneiss from the Missi group, and basalt to basaltic andesite of N-MORB (normal mid-ocean–ridge basalt) affinity from the Snow Lake arc assemblage (Syme et al., 2000; Benn et al., 2018). The pegmatite dikes vary in composition from barren to lithium bearing, with spodumene as the major lithium ore mineral (Černý et al., 1981; Martins et al., 2017). Lepidolite-bearing pegmatite dikes were recently discovered at depth in the northwest region of the Wekusko Lake pegmatite field, more specifically, in the Bur zone (Rockcliff Metals Corp., 2022). The Wekusko Lake pegmatite field was divided into three spodumene-mineralized groups by Černý et al. (1981): Sherritt-Gordon, Green Bay, and Violet-Thompson. Columbite from one Green Bay group pegmatite returned a U-Pb age of 1780 ±8.1 Ma, interpreted as the crystallization age (Martins et al., 2019). This pegmatite emplacement was considered by Benn et al. (2019) to be late D_3 to D_4, which predates the ca. 1.81 Ga peak metamorphism. The spodumene-bearing pegmatite dikes were considered by Černý et al. (1981) to be the result of fractional crystallization of nearby successor-arc granite suites; however, this leaves a roughly 50 m.y. time gap between the crystallization of the granite suites and the emplacement of the pegmatite dikes. Benn et al. (2019) associated the petrogenesis of the pegmatite dikes with the partial melting of metasedimentary rocks. Three emplacement mechanisms for spodumene-bearing pegmatites are proposed for the central Wekusko Lake pegmatite field: 1) oriented subparallel to the strike of shear zones in pull-apart openings (Violet-Thompson group of pegmatite dikes); 2) oriented subparallel to the main tectonic stress direction in tension-gash openings (Sherritt-Gordon group of pegmatite dikes); and 3) aligned in en échelon formation [Green Bay group of pegmatite dikes] (Černý et al., 1981; Silva et al., 2022, in press).

Regional pegmatite coverage and field description of pegmatite dikes

For this study, 14 occurrences of pegmatite dikes were explored, primarily in the areas of north to northeast Wekusko Lake (Crowduck Bay, Sherritt-Gordon and Violet-Thompson pegmatite groups), and adjacent to the Berry Creek fault (Highway 393) in the Bur zone. The subdivisions of Černý et al. (1981) are used herein to simplify the general description of the pegmatite occurrences. All the locations shown in Figure GS2023-7-2 were sampled for future geochemical and microstructural research.

Crowduck Bay pegmatite dikes

The pegmatite dikes of Crowduck Bay appear as a series of dikes 1 to 2 m thick, up to ~50 m in length and trending 030–050° along both sides of the northeast arm of Wekusko Lake, but occur mostly on the eastern shoreline of the lake and on islands in Crowduck Bay (Figure GS2023-7-3a). The pegmatites emplaced along the shoreline of Crowduck Bay occur as dikes physically spaced and segmented into elongated bodies 1 to 10 m in length (Figure GS2023-7-3a). Pegmatite dikes similar in width, length and strike are observed up to 120 m east of the Crowduck Bay shoreline. The majority of the islands in Crowduck Bay have pegmatite dikes, and their overall elongated shapes, parallel to the regional shear zone, are most likely a result of the competency contrast between the pegmatite dikes and the surrounding metasedimentary rock during deformation.

These pegmatite dikes consist of albite, quartz, K-feldspar and muscovite, with minor to trace tourmaline and garnet present in patches within the dikes (Figure GS2023-7-3b). The muscovite content of the pegmatite dikes varies, with higher concentrations found near contacts with the country rock. Tourmaline is usually observed in association with increased quartz content, and garnet is commonly found near mafic xenoliths or contacts with hostrocks. Lithium mineralization was not observed in this group of pegmatites. According to their mineralogy, these pegmatite dikes belong to the muscovite class of Černý and Ercit (2005). The dikes are most commonly found in the metasedimentary rocks of the Missi group and, less commonly, in the Burntwood group. The few pegmatite dikes observed to have intruded the Burntwood group were found along the western shoreline of Crowduck Bay. Postemplacement hematization was observed along fractures. This feature is common in pegmatite dikes of the Wekusko Lake pegmatite field (Benn et al., 2018), and the pink to red colouration associated with the metasomatic process can make feldspar identification difficult (e.g., Gysi et al., 2016; Benn et al., 2018). Tourmalinization of the hostrock is a typical occurrence around pegmatite contacts.

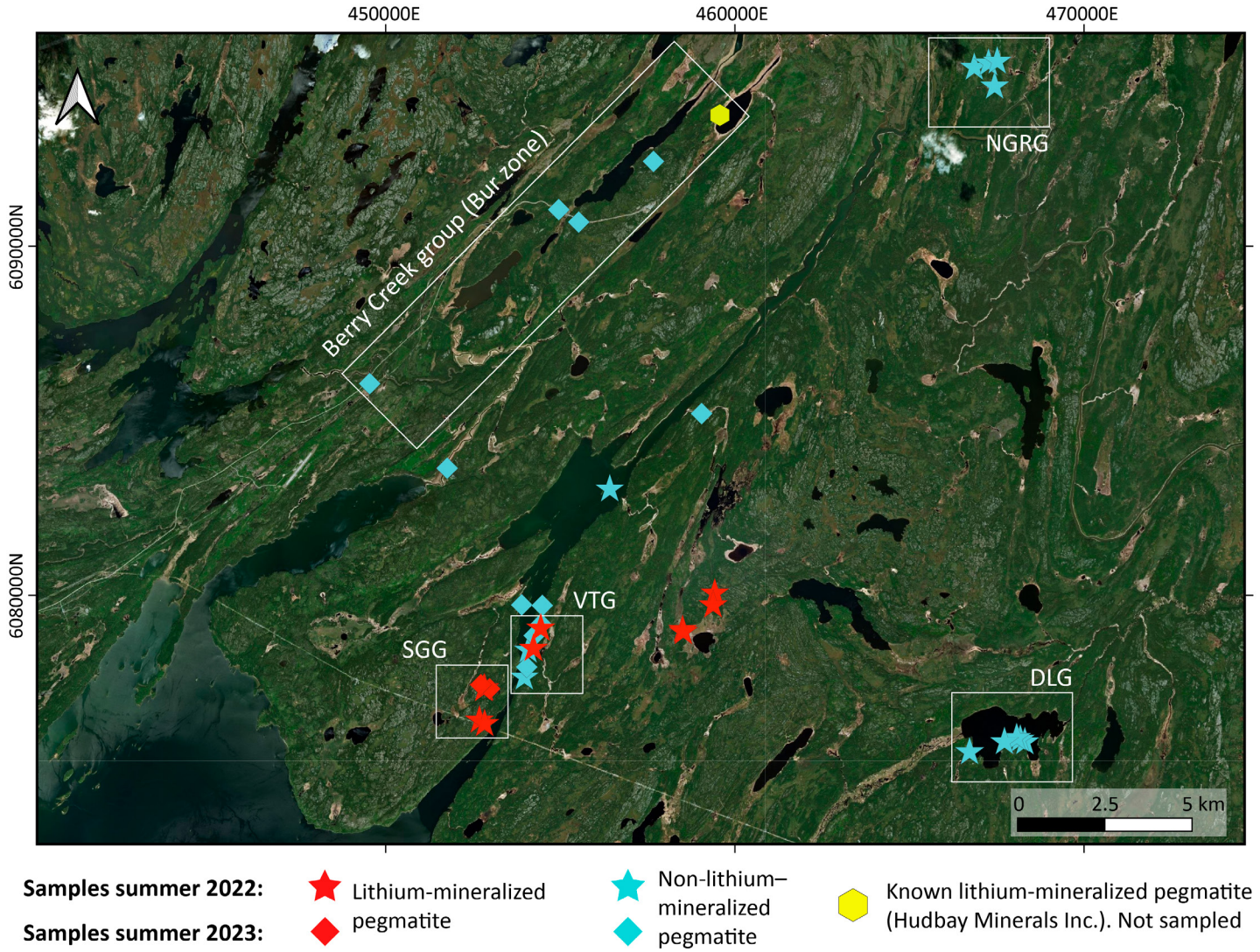

Figure GS2023-7-2: *Satellite imagery showing the locations of the pegmatite dikes visited and sampled during the summers of 2022 and 2023. Symbols for pegmatite dikes: red diamond and star, lithium-mineralized pegmatite dikes; blue diamond and star, non-lithium–mineralized or simple pegmatite dikes; hexagon, documented lithium-mineralized pegmatite dike. Abbreviations: DLG, Dion Lake pegmatite group; NGRG, North Grass River pegmatite group; SGG, Sherritt-Gordon pegmatite group; VTG, Violet-Thompson pegmatite group. All co-ordinates are in UTM Zone 14, NAD83.*

Sherritt-Gordon group (Grass River dikes)

This collection of metre-scale pegmatite dikes lies east-northeast of the Rex Lake pluton and intrudes masses of porphyritic gabbro west of the Crowduck Bay shear zone (Figures GS2023-7-1 and -2). The majority of pegmatite dikes from the Sherritt-Gordon group contain lithium mineralization in the form of green spodumene, classifying them as lithium-cesium-tantalum (LCT) rare-element pegmatites according to the pegmatite categorization of Černý and Ercit (2005). The main orientation of the pegmatite dikes is between 290 and 320°, with dips to the southwest of 60 to 70°. Lithium Foremost Resource & Technology Ltd. and Snow Lake Lithium Ltd. are presently exploring pegmatite dikes from this group. The pegmatites in this group are all exceedingly coarse grained (crystal size is >10 cm), with variable amounts of albite, K-feldspar, quartz, muscovite, garnet, tourmaline and spodumene inside a single pegmatite body. Spodumene can be found in the form of elongate prisms up to 50 cm long and 8 cm wide, or as equant basal sections 0.5–2.0 cm across. Spodumene prisms in the Grass River dikes are mainly oriented 045° and suborthogonal to the orientation of the pegmatite dikes. There is no clear mineral zonation within the dikes, based on observation of outcrops and drillcore; however, zones within pegmatite dikes with higher concentrations of spodumene (up to 40%) are usually associated with higher concentrations of quartz, muscovite and, in some cases, garnet. Tourmaline, apatite and garnet are present as accessory phases. Tourmaline concentrations are higher near dike margins, locally as parallel bands or as tourmaline crystals perpendicular to the contact of the dikes, and within zones of higher quartz concentration. The contacts of the pegmatite dikes appear to be gently folded perpendicular to the strike of the dikes (Figure GS2023-7-3c), indicating that southwest-directed compressional stress that resulted in the formation of

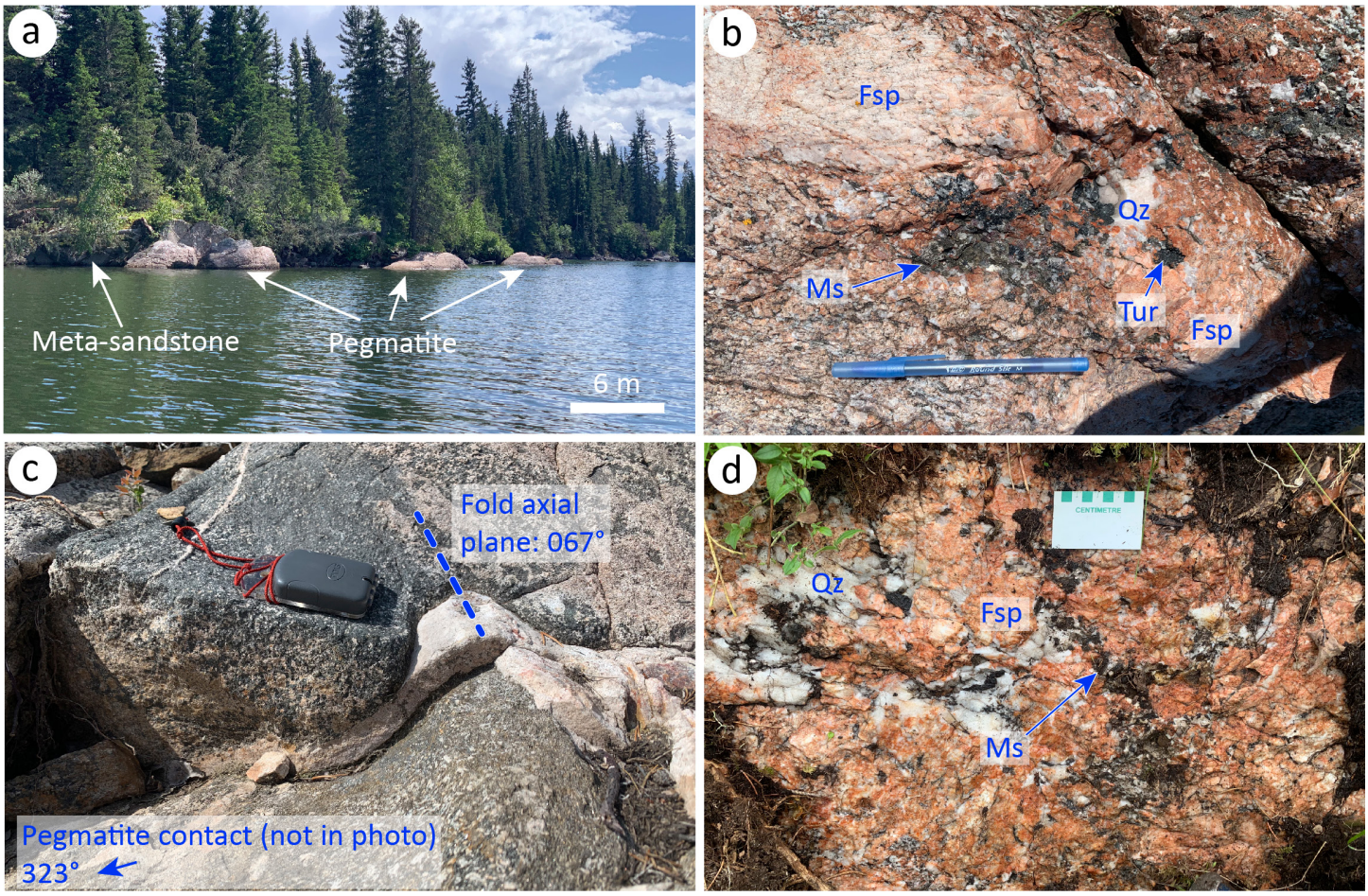

Figure GS2023-7-3: *Outcrop photographs showing pegmatite dikes from the Wekusko Lake pegmatite field:* ***a)*** *subvertical, hematized pegmatite dike segmented and interspersed with Missi group meta-sandstone, from the eastern shoreline of Crowduck Bay;* ***b)*** *example of simple mineralogical composition (albite-quartz-muscovite-tourmaline) of the Crowduck Bay pegmatite dike group;* ***c)*** *folded, centimetre-size offshoot of main pegmatite body of spodumene pegmatite from the Sherritt-Gordon pegmatite group. Fold axial plane is subperpendicular to the trend of the main pegmatite;* ***d)*** *example of simple mineralogical composition (albite-quartz-muscovite) and postemplacement hematization of a pegmatite dike located in the Bur zone. Pen for scale in panel (b) is 15 cm long, and the Silva compass in panel (c) is 10 cm long. Abbreviations: Fsp, feldspar; Ms, muscovite; Qz, quartz; Tur, tourmaline.*

extensional jogs used for emplacement of this pegmatite group melt (Silva et al., 2022, in press) persisted, or was reactivated, after crystallization of the pegmatites.

Berry Creek group (Bur zone)

The Berry Creek group within the Bur zone is located northeast of the town of Snow Lake, close to Highway 393 and the regional Berry Creek fault, which trends approximately northeast. The Bur zone is known for its high-grade copper-zinc potential within the Flin Flon–Snow Lake greenstone belt (Loveday, 2021) and, recently, lithium mineralization in the form of lepidolite-bearing pegmatites was found at depth (Rockcliff Metals Corp., 2022). The pegmatite dikes observed in outcrop in this area appear mostly as 1 to 3 m thick dikes that dip steeply, are up to ~30 m in length, and trend between 330° and 035–060° (Figure GS2023-7-4). From field observation, these pegmatite dikes do not appear to host lithium mineralization. Previous mapping of pegmatite dikes from these zones by the Manitoba Geological Survey (NATMAP Shield Margin Project Working Group, 1998) showed that multiple pegmatite dikes appear as large bodies of regional scale, with thicknesses of tens of metres and lengths of hundreds of metres. The trend of the pegmatite dikes varies, but it generally follows the northeast orientation of the deformation fabric observed in the bedrock. The pegmatite dikes are most commonly found intruding or adjacent to felsic gneiss within late successor-arc plutons (Figure GS2023-7-4). The pegmatites outlined in region A of Figure GS2023-7-4 form noticeable convex massive dikes tens of metres in both width and length, probably due to the difference in lithological competence compared to the surrounding felsic volcaniclastic rocks. Region B in Figure GS2023-7-4 has a 1.5–2 m wide elongated pegmatite dike that trends roughly northeast. The pegmatite dike in region C of Figure GS2023-7-4 differs from the others because of its approximate northwest trend and its intrusion into mafic igneous rocks.

The major mineral phases of these pegmatite dikes are albite, quartz, K-feldspar and muscovite, with minor to trace amounts

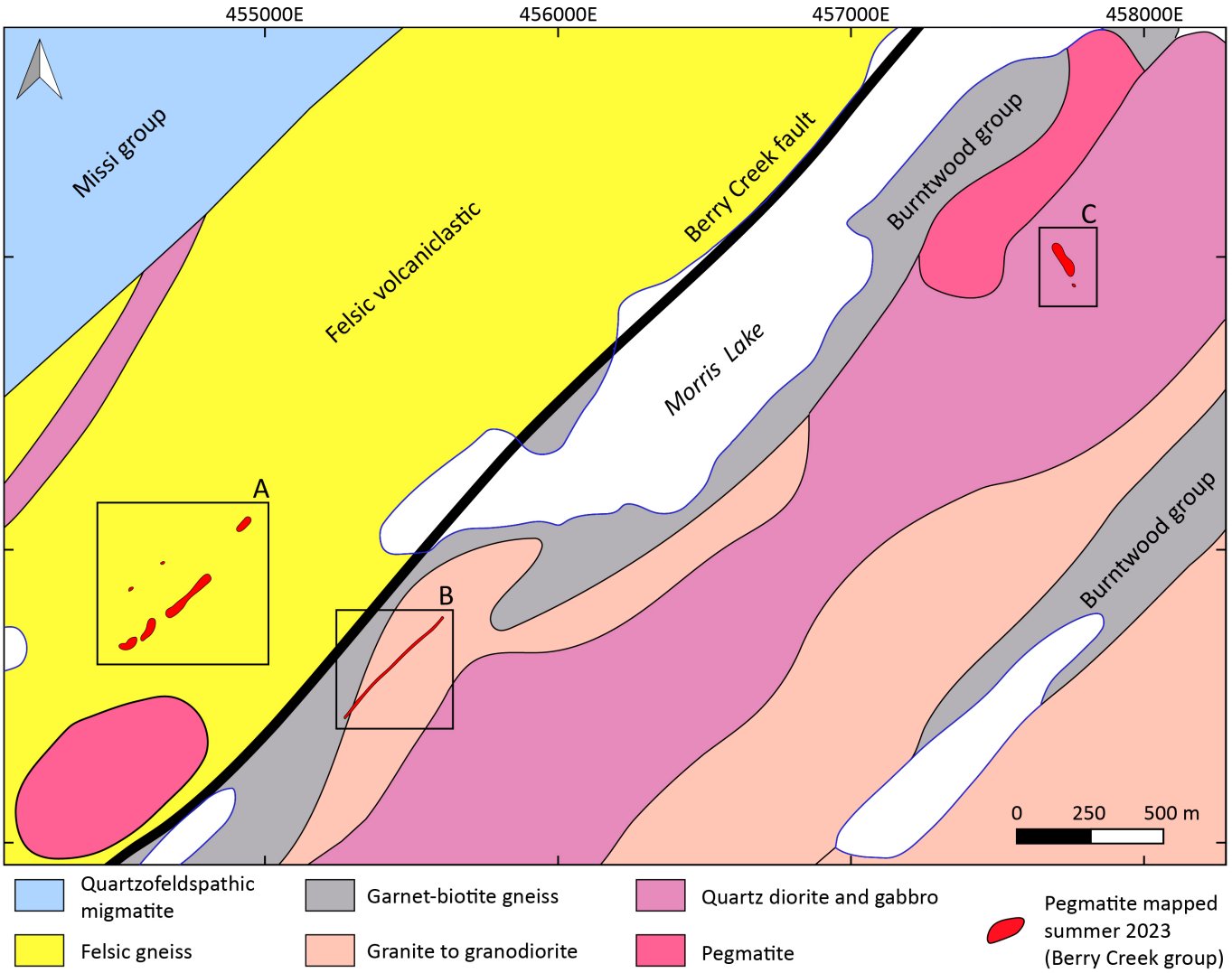

Figure GS2023-7-4: *Location of pegmatite dikes mapped during summer 2023 fieldwork in the Berry Creek group (Bur zone). The locations of the pegmatite dikes are superimposed on the Geological Survey of Canada's regional geology of the Flin Flon belt (NATMAP Shield Margin Project Working Group, 1998). Co-ordinates are in UTM Zone 14, NAD83.*

of tourmaline. The mineral grains range in size from medium to coarse. Similar to most non-lithium–mineralized pegmatite dikes in the Wekusko Lake pegmatite field, no internal zonation was observed in the pegmatite dikes mapped in the Berry Creek group dikes; however, some centimetre-size globular zones of higher concentrations of quartz, tourmaline and muscovite were observed (Figure GS2023-7-3d). Postemplacement hematization was observed in most of the pegmatite dikes in this region. Lithium mineralization was not observed in outcrop in this group of pegmatites, but spodumene- and lepidolite-bearing pegmatite dikes have recently been observed in drillcore from the Bur zone (Rockcliff Metals Corp., 2022).

Violet-Thompson group (Thompson Brothers dike)

The Violet-Thompson pegmatite group intruded a sequence of Missi group sandstone and pebble to cobble conglomerate. The Thompson Brothers pegmatite is located northeast of the Rex Lake pluton, proximal to the east side of the Crowduck Bay shear zone (Figures GS2023-7-1 and -2). Based on its mineral composition, this dike is classified as an LCT rare-element pegmatite, and contains spodumene, albite, quartz, K-feldspar, muscovite and black tourmaline. The pegmatite outcrop is up to 10 m wide, dips steeply, and is exposed for approximately 140 m along a strike of 035°. Drilling has revealed that the dike continues along strike for approximately 900 m (Snow Lake Lithium Ltd., 2022). This pegmatite dike shows a preferred alignment of spodumene crystals of 160°, which is oblique to the orientation of the dike and perpendicular to the orientation of the Crowduck Bay shear zone (Figure GS2023-7-5a). This preferred alignment is disrupted by local shear zones oriented subparallel to the pegmatite contact. These shear zones reoriented the spodumene crystals within the shear bands to an orientation closer to parallel with the trend of the dike (Figure GS2023-7-5a). Oriented samples collected from the Thompson Brothers pegmatite dike (Figure GS2023-7-5b) will

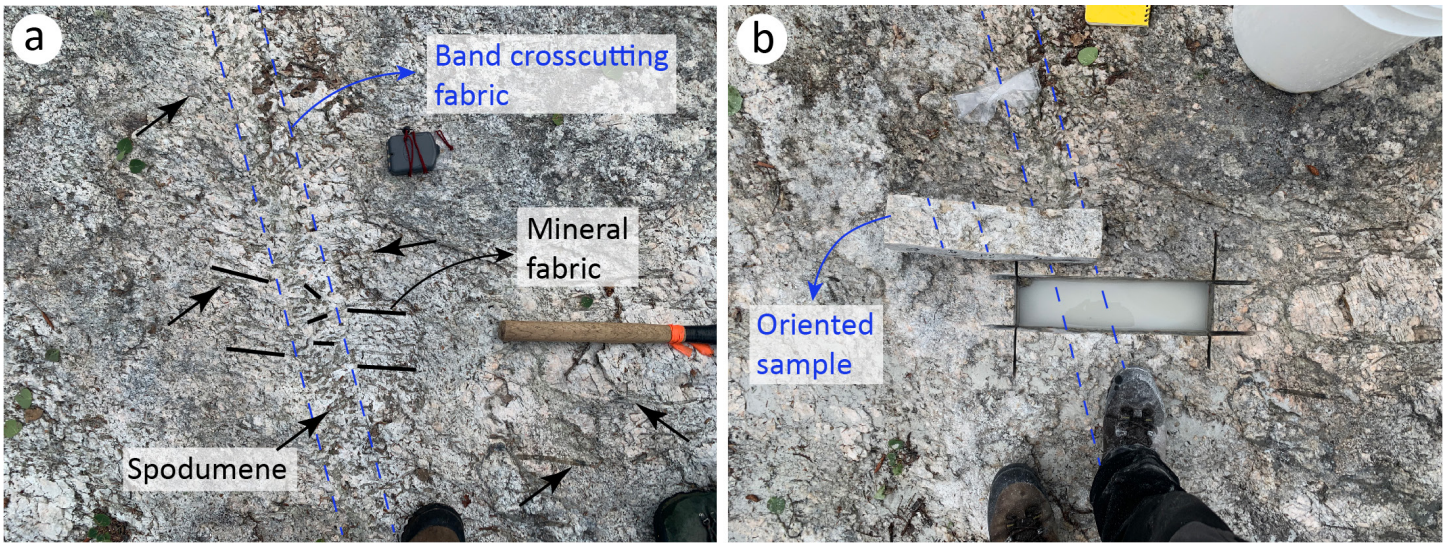

Figure GS2023-7-5: *Example of an oriented sample collected from the Thompson Brothers (Violet-Thompson pegmatite group) spodumene-bearing pegmatite dike from Snow Lake Lithium Ltd.:* ***a)*** *pegmatite outcrop before sample collection, showing a shear band crosscutting the mineral fabric;* ***b)*** *pegmatite outcrop after sample collection. Silva compass for scale in panel (a) is 10 cm long.*

be used for microchemical and microstructural analysis of the various minerals in the dike. These studies will help resolve the mode of crystallization, and the overall question of whether the fabric is the result of an igneous process or deformation.

Whole-rock geochemical trends of the Wekusko Lake pegmatite dikes

In the summer of 2022, twelve samples of pegmatite dikes from the Wekusko Lake pegmatite field (Dion Lake, North Grass River and Crowduck Bay islands groups) were gathered for whole-rock geochemical investigation (Figure GS2023-7-6a; Silva et al., 2022). All samples collected, usually pegmatite blocks between 20 to 50 cm in diameter, were selected to best represent the overall mineral composition of the pegmatite dike. However, due to the extremely coarse grain size and variable local distribution of minerals in the studied pegmatites bodies, the selected samples used for whole-rock geochemistry analysis might not represent the total extent of the pegmatite bodies chemistry. All samples were trimmed to eliminate weathered surfaces. Analyses were conducted by SRC Geoanalytical Laboratories (Saskatoon, Saskatchewan) using inductively coupled plasma–emission spectrometry (ICP-ES) to analyze major and minor elements, and inductively coupled plasma–mass spectrometry (ICP-MS) to analyze trace elements.

Ratios of K/Rb, K/Cs and Nb/Ta are well-documented bulk-rock or mineral indices for pegmatite fractionation systems (e.g., Černý and Burt, 1984; Černý, 2005; Selway et al., 2005). Using ratios of these elements derived from results of whole-rock geochemical analysis of samples from the Wekusko Lake pegmatite field, it is possible to see fractionation trends across the pegmatite field (Figure GS2023-7-6). Specifically, Rb and Cs are primarily partitioned into feldspar and muscovite, and Ta is enriched where there is a minor component of tantalite in the pegmatite dikes. Feldspar and muscovite minerals form a significant component of almost all of the dikes sampled, with muscovite content increasing in spodumene-bearing pegmatite dikes. The Wekusko Lake pegmatite dikes exhibit a strong fractionation trend, from simple pegmatites to lithium-enriched pegmatites, as shown in Figure GS2023-7-6. The non-lithium–mineralized pegmatite dikes of the Dion Lake group, and the barren North Grass River and Crowduck Bay islands groups all have high K/Rb, K/Cs and Nb/Ta ratios. The Dion Lake pegmatites are also enriched in uranium compared to the other pegmatites in the Wekusko Lake pegmatite field. The lowest values for K/Rb, K/Cs and Nb/Ta, which occur in the Sherritt-Gordon, Violet-Thompson and Green Bay pegmatite dikes, define a zone of highly differentiated pegmatites that are enriched in Be, Cs, Rb and Ta. In sum, the K/Rb, K/Cs and Nb/Ta values show fractionation trends toward highly differentiated lithium-enriched pegmatites, with an evolution from non-lithium–mineralized pegmatite dikes in the northern- and easternmost regions of the pegmatite field, to pegmatite dike groups with spodumene mineralization more centrally located in the Wekusko Lake pegmatite field (Figure GS2023-7-6), adjacent to the Crowduck Bay shear zone. Similar to the fractionation trend observed for spodumene-bearing pegmatite dikes, some barren pegmatites within the Sherritt-Gordon and Violet-Thompson groups show low K/Rb, K/Cs and Nb/Ta values. These low ratios, especially in the spodumene-bearing pegmatite dikes, are probably due to several factors, including the higher muscovite content and known enrichment of cesium-muscovite in the spodumene-bearing Zoro pegmatite dikes from the Green Bay group (Benn et al., 2022), Rb substitution in feldspars, and Ta enrichment from tantalite crystallization in comparison to the other pegmatite groups in the Wekusko Lake pegmatite field.

The increase in the alumina saturation index of the pegmatite dikes in the Sherritt-Gordon and Violet-Thompson groups fol-

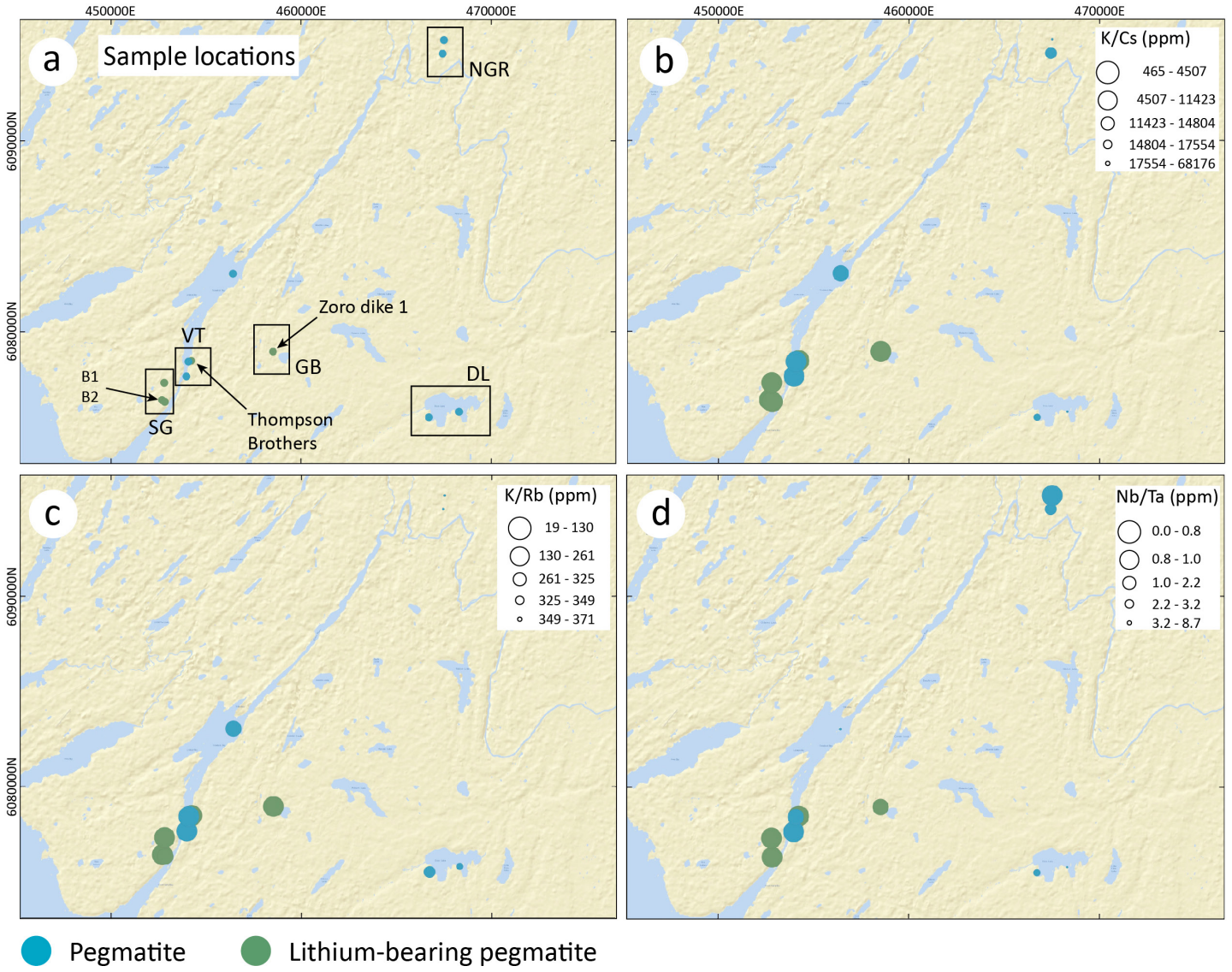

Figure GS2023-7-6: a) *Locations of pegmatite dikes sampled during the summer of 2022, and* ***(b–d)*** *spatial trends in elemental enrichment across the Wekusko Lake pegmatite field, superimposed on the same satellite imagery as in Figure GS2023-7-2:* ***b)*** *K/Cs;* ***c)*** *K/Rb; and* ***d)*** *Nb/Ta. Larger symbols represent lower values, to facilitate map interpretation. The main lithium-bearing pegmatite dikes are highlighted in panel (a). Co-ordinates are in UTM Zone 14, NAD83. Abbreviations: DL, Dion Lake pegmatite group; GB, Green Bay pegmatite group; NGR, North Grass River pegmatite group; SG, Sherritt-Gordon pegmatite group; VT, Violet-Thompson pegmatite group.*

lows the spatial trend of decreasing K/Rb, K/Cs and Nb/Ta ratios observed for the Wekusko Lake pegmatite field (Figure GS2023-7-7), reflecting the higher muscovite content of these dikes.

Figure GS2023-7-7 depicts the inverse relationship between increased peraluminosity (A/NK) and decreased K/Rb ratio from barren pegmatites to spodumene-bearing pegmatites, while also showing a positive relationship between peraluminosity and phosphorus content (P_2O_5). One clear outlier in P_2O_5 composition from a barren pegmatite is observed in Figure GS2023-7-7b. The anomalously high P_2O_5 composition could be explained as possible local enrichment of phosphate minerals in the analyzed sample (e.g., apatite, amblygonite or lithiophilite) that were not previously described for this sample. These element relationships have been observed in many other pegmatite fields (e.g., Selway et al., 2005; Roda-Robles et al., 2023), describing increased fractionation of incompatible elements and spatial pegmatite dike evolution. These element ratios can also vary, and imply a variability in the melt source for either fractionation from melt or direct anatexis models of pegmatite formation. According to the data shown in Figures GS2023-7-6 and -7, there may be a regional geochemical fractionation trend that extends from the eastern and northern boundaries of the Wekusko Lake pegmatite field to the spodumene pegmatite groups near the Crowduck Bay shear zone. This pattern also shows an evolution within the Wekusko Lake pegmatite field, from areas closer to high-grade metamorphism—up to migmatite—toward areas of lower metamorphic grade, of staurolite-first appearance (Lazzarotto, 2020).

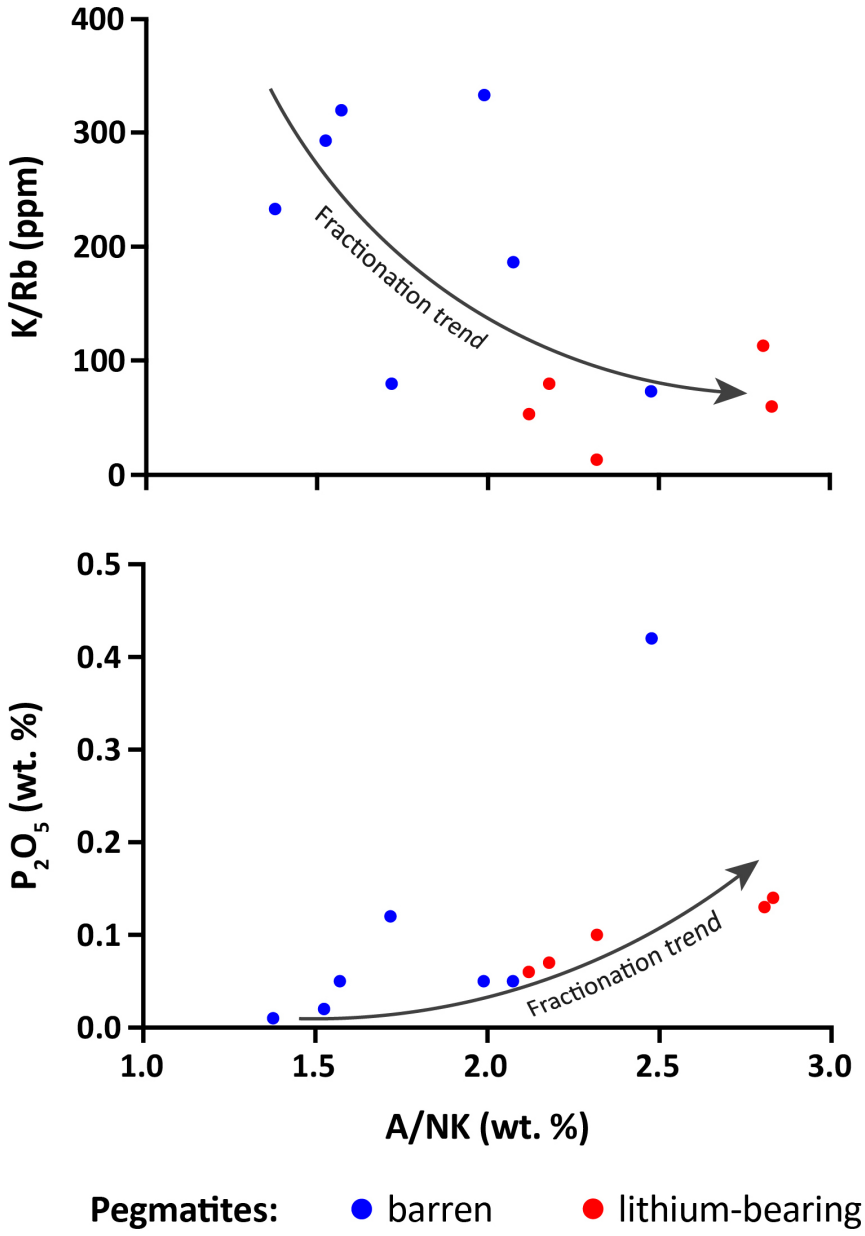

Figure GS2023-7-7: *Whole-rock geochemistry plots showing peraluminosity (A/NK) versus* ***(a)*** *K/Rb and* ***(b)*** *phosphorus content (P_2O_5), differentiating between barren pegmatites and spodumene-bearing pegmatites. The curved arrow demonstrates the fractionation trend.*

Economic considerations

Canada, and particularly Manitoba, is a key player in the green revolution due to the prevalence of lithium-bearing pegmatite occurrences like the Tanco pegmatite and pegmatites in the Wekusko Lake region. Because of its high concentration of lithium-mineralized dikes, ideal mineralogy for lithium extraction, and central location within Canada, the Wekusko Lake pegmatite field offers significant economic potential. The growing need for critical minerals, as well as the growing need to lessen our reliance on fossil fuels, emphasizes the economic relevance of identifying new rare-element pegmatite deposits and expanding our knowledge of existing ones. To accomplish these objectives, it is necessary to evaluate emplacement mechanisms and understand chemical fractionation models within the pegmatite fields. This is important, as it can contribute to a higher probability of discovering new lithium-bearing pegmatite bodies. The Wekusko Lake pegmatite field in west-central Manitoba is located in an active mining area, with established access and infrastructure, and well-studied regional geology. Several companies are actively exploring for lithium in the area. With the recent discovery of lepidolite-bearing pegmatites, the Wekusko Lake pegmatite field is now open for further discoveries of different types of lithium mineralization.

Acknowledgments

The authors thank Snow Lake Lithium Ltd. for access to their pegmatite properties and drillcore, and the Manitoba Geologi-

cal Survey for providing fieldwork and logistical support in Snow Lake. The project benefited from discussions with B. Young, R. Scott and K. Reid. This study is supported by a Mitacs Accelerate Industrial Postdoc grant with Lithium Foremost Resource & Technology Ltd. as financial and logistical partner, and Natural Sciences and Engineering Research Council of Canada Discovery grants to L. Groat and R. Linnen. Edits from reviewers M. Rinne and K. Reid from the Manitoba Geological Survey are truly appreciated.

References

Ansdell, K.M. 1993: U-Pb constraints on the timing and provenance of fluvial sedimentary rocks in the Flin Flon and Athapapuskow basins, Flin Flon domain, Trans-Hudson orogen, Manitoba and Saskatchewan; *in* Radiogenic Age and Isotopic Studies, Report 7, Geological Survey of Canada, Current Research 93-2, p. 49–57.

Ansdell, K.M. 2005: Tectonic evolution of the Manitoba-Saskatchewan segment of the Paleoproterozoic Trans-Hudson orogen, Canada; Canadian Journal of Earth Sciences, v. 42, no. 4, p. 741–759.

Ansdell, K.M. and Connors, K.A. 1995: Geochemistry of mafic volcanic rocks, east Wekusko Lake, Manitoba; LITHOPROBE Trans-Hudson Orogen Transect, Report of Fifth Transect Meeting, April 3–4, 1995, Regina, Saskatchewan, LITHOPROBE Secretariat, University of British Columbia, Vancouver, British Columbia, Report 48, p. 198–205.

Ansdell, K.M. and Norman, A.R. 1995: U-Pb geochronology and tectonic development of the southern flank of the Kisseynew belt, Trans-Hudson orogen, Canada; Precambrian Research, v. 72, p. 147–167.

Ansdell, K.M., Connors, K.A., Stern, R.A. and Lucas, S.B. 1999: Coeval sedimentation, magmatism, and fold-thrust belt development in the Trans-Hudson orogen: geochronological evidence from the Wekusko Lake area, Manitoba, Canada; Canadian Journal of Earth Sciences, v. 36, no. 2, p. 293–312.

Bailes, A.H. 1980: Origin of early Proterozoic volcaniclastic turbidites, south margin of the Kisseynew sedimentary gneiss belt, File Lake, Manitoba; Precambrian Research, v. 12, no. 1–4, p. 197–225.

Bailes, A. 1985: Geology of the Saw Lake area; Manitoba Energy and Mines, Geological Services, Geological Report GR83-2, URL <https://manitoba.ca/iem/info/libmin/GR83-2.zip> [September 2022].

Benn, D., Linnen, R.L. and Martins, T. 2018: Geology and bedrock mapping of the Wekusko Lake pegmatite field (northeastern block), central Manitoba (part of NTS 63J13); *in* Report of Activities 2018, Manitoba Growth, Enterprise and Trade, Manitoba Geological Survey, p. 79–88, URL <https://manitoba.ca/iem/geo/field/roa18pdfs/GS2018-7.pdf> [September 2022].

Benn, D., Martins, T. and Linnen, R.L. 2019: Interpretation of U-Pb isotopic dates of columbite-group minerals in pegmatites, Wekusko Lake pegmatite field, central Manitoba (part of NTS 63J13); *in* Report of Activities 2019, Manitoba Agriculture and Resource Development, Manitoba Geological Survey, p. 52–59, URL <https://manitoba.ca/iem/geo/field/roa19pdfs/GS2019-5.pdf> [August 2023].

Benn, D., Martins, T. and Linnen, R. 2022: Fractionation and enrichment patterns in white mica from Li pegmatites of the Wekusko Lake pegmatite field, Manitoba, Canada; The Canadian Mineralogist, v. 60, p. 933–956.

Černý, P. 2005: The Tanco rare-element pegmatite deposit, Manitoba: regional context, internal anatomy, and global comparisons; *in* Rare-Element Geochemistry and Mineral Deposits, R.L. Linnen and I.M. Samson (ed.), Geological Association of Canada, Short Course Notes 17, p. 127–158.

Černý, P. and Burt, D.M. 1984: Paragenesis, crystallochemical characteristics and geochemical evolution of micas in granite pegmatites; *in* Micas, Reviews in Mineralogy, S.W. Bailey (ed.), Mineralogical Society of America, v. 13, p. 257–297.

Černý, P. and Ercit, T. 2005: The classification of granitic pegmatites revisited; The Canadian Mineralogist, v. 43, no. 6, p. 2005–2026.

Černý, P., Trueman, D.L., Zeihlke, D.V., Goad, B.E. and Paul, B.J. 1981: The Cat Lake–Winnipeg River and the Wekusko Lake pegmatite fields, Manitoba; Manitoba Department of Energy and Mines, Mineral Resources Division, Economic Geology Report ER80-1, 216 p., URL <https://manitoba.ca/iem/info/libmin/ER80-1> [August 2023].

Connors, K.A. 1996: Unraveling the boundary between turbidites of the Kisseynew belt and volcano-plutonic rocks of the Flin Flon belt, eastern Trans-Hudson orogen, Canada; Canadian Journal of Earth Sciences, v. 33, p. 811–829.

Connors, K.A. and Ansdell, K.M. 1994: Timing and significance of thrust faulting along the boundary between the Flin Flon–Kisseynew domains, eastern Trans-Hudson orogen; LITHOPROBE Trans-Hudson Orogen Transect, Report of Fourth Transect Meeting, April 11–12, 1994, Saskatoon, Saskatchewan, LITHOPROBE Secretariat, University of British Columbia, Vancouver, British Columbia, Report 38, p. 112–122.

Connors, K.A., Ansdell, K.M. and Lucas, S.B. 1999: Coeval sedimentation, magmatism, and fold-thrust development in the Trans-Hudson orogen: propagation of deformation into an active continental arc setting, Wekusko Lake area, Manitoba; Canadian Journal of Earth Sciences, v. 36, no. 2, p. 275–291.

Connors, K., Ansdell, K. and Lucas, S. 2002: Development of a transverse to orogen parallel extension lineation in a complex collisional setting, Trans-Hudson orogen, Manitoba, Canada; Journal of Structural Geology, v. 24, no. 1, p. 89–106.

David, J., Bailes, A.H. and Machado, N. 1996: Evolution of the Snow Lake portion of the Paleoproterozoic Flin Flon and Caisson belts, Trans-Hudson orogen, Manitoba, Canada; Precambrian Research, v. 80, p. 107–124.

Fedorowich, J.S., Kerrich, R. and Stauffer, M.R. 1995: Geodynamic evolution and thermal history of the central Flin Flon belt, Trans-Hudson Orogen: constraints from structural development, $^{40}Ar/^{39}Ar$, and stable isotope geothermometry; Tectonics, v. 14, p. 472–503.

Galley, A.G., Syme, E.C. and Bailes, A.H. 2007: Metallogeny of the Paleoproterozoic Flin Flon belt, Manitoba and Saskatchewan; *in* Mineral Deposits of Canada: A Synthesis of Major Deposit-Types, District Metallogeny, the Evolution of Geological Provinces, and Exploration Methods, W.D. Goodfellow (ed.), Geological Association of Canada, Mineral Deposits Division, Special Publication No. 5, p. 533509–552531.

Gordon, T., Hunt, P., Bailes, A. and Syme, E. 1990: U-Pb ages from the Flin Flon and Kisseynew belts, Manitoba: chronology of crust formation at an early Proterozoic accretionary margin; *in* The Early Proterozoic Trans-Hudson Orogen of North America, J.F. Lewry and M.R. Stauffer (ed.), Geological Association of Canada, Special Paper 37, p. 177–199.

Gysi, A.P., Williams-Jones, A.E. and Collins, P. 2016: Lithogeochemical vectors for hydrothermal processes in the Strange Lake peralkaline granitic REE-Zr-Nb deposit; Economic Geology, v. 111, no. 5, p. 1241–1276.

Kraus, J. and Menard, T. 1997: A thermal gradient at constant P: implications for low- to medium-P metamorphism in a compressional tectonic setting, Flin Flon and Kisseynew domains, Trans-Hudson orogen, central Canada; Canadian Mineralogist, v. 35, p. 1117–1136.

Kraus, J. and Williams, P.F. 1994: Cleavage development and timing of metamorphism in the Burntwood group across the Threehouse synform, Snow Lake, Manitoba: a new paradigm; LITHOPROBE Trans-Hudson Orogen Transect, Report of Fourth Transect Meeting, April 11–12, 1994, Saskatoon, Saskatchewan, LITHOPROBE Secretariat, University of British Columbia, Vancouver, British Columbia, Report 38, p. 230–238.

Lazzarotto, M.C. 2020: Metamorphism of the Flin Flon greenstone belt, Manitoba; Ph.D. thesis, University of Calgary, Calgary, Alberta, 217 p.

Lewry, J.F. and Collerson, K.D. 1990: Trans-Hudson orogen: extent, subdivisions, and problems; *in* The Early Proterozoic Trans-Hudson Orogen of North America, J.F. Lewry and M.R. Stauffer (ed.), Geological Association of Canada, Special Publication 37, p. 1–14.

Lewry, J., Hajnal, Z., Green, A., Lucas, S.B., White, D., Stauffer, M.R., Ashton, K.E., Weber, W. and Clowes, R. 1994: Structure of Paleoproterozoic continent-continent collision zone: a LITHOPROBE seismic reflection profile across the Trans-Hudson orogen, Canada; Tectonophysics, v. 232, no. 1–4, p. 143–160.

Lithium Foremost Resource & Technology Ltd. 2022: Properties; URL <https://foremostlithium.com/> [September 2021].

Lodestar Battery Metals Corp. 2023: Lodestar advances exploration at flagship Peny project; URL <https://lodestarbatterymetals.ca/news/lodestar-advances-exploration-at-flagship-peny-project/> [September 2023].

Loveday, D. 2021: Bur zone project Manitoba, Canada; NI 43-101 technical report prepared for Rockcliff Metals Corp.

Lucas, S.B., Stern, R.A., Syme, E.C., Reilly, B.A. and Thomas, D.J. 1996: Intra-oceanic tectonics and the development of continental crust: 1.92–1.84 Ga evolution of the Flin Flon belt, Canada; Geological Society of America Bulletin, v. 108, p. 602–629.

Lucas, S.B., White, D., Hajnal, Z., Lewry, J., Green, A., Clowes, R., Zwanzig, H., Ashton, K., Schledewitz, D., Stauffer, M., Norman, A., Williams, P.F. and Spence, G. 1994: Three-dimensional collisional structure of the Trans-Hudson orogen, Canada; Tectonophysics, v. 232, p. 161–178.

Machado, N., Zwanzig, H. and Parent, M. 2000: U-Pb ages of plutonism, sedimentation, and metamorphism of the Paleoproterozoic Kisseynew metasedimentary belt, Trans-Hudson orogen (Manitoba, Canada); Canadian Journal of Earth Sciences, v. 36, no. 11, p. 1829–1842

Manitoba Geological Survey 2022: Bedrock geology of Manitoba; Manitoba Natural Resources and Northern Development, Manitoba Geological Survey, Open File OF2022-2, scale 1:1 000 000.

Martins, T., Benn, D. and McFarlane, C. 2019: Laser-ablation inductively coupled plasma–mass spectrometry (LA-ICP-MS) analyses of columbite grains from Li-bearing pegmatites, Wekusko Lake pegmatite field (northeastern block), central Manitoba (part of NTS 63J13); Manitoba Agriculture and Resource Development, Manitoba Geological Survey, Data Repository Item DRI2019003, Microsoft® Excel® file, URL <https://manitoba.ca/iem/info/libmin/DRI2019003.xlsx> [August 2023].

Martins, T., Linnen, R., Fedikow, M. and Singh, J. 2017: Whole-rock and mineral geochemistry as exploration tools for rare-element pegmatite in Manitoba: examples from the Cat Lake–Winnipeg River and Wekusko Lake pegmatite fields (parts of NTS 52L6, 63J13); *in* Report of Activities 2017, Manitoba Growth, Enterprise and Trade, Manitoba Geological Survey, p. 42–51, URL <https://manitoba.ca/iem/geo/field/roa17pdfs/GS2017-5.pdf> [August 2023].

NATMAP Shield Margin Project Working Group 1998: Geology, NATMAP Shield Margin Project area, Flin Flon belt, Manitoba/Saskatchewan; Geological Survey of Canada, Map 1968A, scale 1:100 000.

Natural Resources Canada 2021: Critical minerals; URL <https://www.nrcan.gc.ca/our-natural-resources/minerals-mining/critical-minerals/23414/> [September 2023].

Reid, K.D. 2021a: Bedrock geology of the Stuart Bay–Chickadee Lake area (east of Wekusko Lake), north-central Manitoba (parts of NTS 63J12, 13); Manitoba Agriculture and Resource Development, Manitoba Geological Survey, Preliminary Map PMAP2021-1, scale 1:15 000, URL <https://manitoba.ca/iem/info/libmin/PMAP2021-1.pdf> [October 2022].

Reid, K.D. 2021b: Results of bedrock geological mapping in the Stuart Bay–Chickadee Lake area (east of Wekusko Lake), north-central Manitoba (parts of NTS 63J12, 13); *in* Report of Activities 2021, Manitoba Agriculture and Resource Development, Manitoba Geological Survey, p. 29–39, URL <https://manitoba.ca/iem/geo/field/roa21pdfs/GS2021-4.pdf> [October 2022].

Rockcliff Metals Corp. 2022: Rockcliff completes drilling at the Bur property. Discovers lithium bearing pegmatite dykes near high grade Bur VMS deposit; URL <https://rockcliffmetals.com/investors/news-releases/rockliff-completes-drilling-at-the-bur-property-discovers-lithium-bearing-pegmatite-dykes-near-high-grade-bur-vms-deposit//> [August 2023].

Roda-Robles, E., Vieira, R., Lima, A., Errandonea-Martin, J., Pesquera, A., Cardoso-Fernandes, J. and Garate-Olave, I. 2023: Li-rich pegmatites and related peraluminous granites of the Fregeneda-Almendra field (Spain-Portugal): a case study of magmatic signature for Li enrichment; Lithos, v. 452–453 (2023), art. 107195.

Schneider, D., Heizler, M., Bickford, M., Wortman, G., Condie, K. and Perilli, S. 2007: Timing constraints of orogeny to cratonization: thermochronology of the Paleoproterozoic Trans-Hudson orogen, Manitoba and Saskatchewan, Canada; Precambrian Research, v. 153, p. 65–95.

Selway, J.B., Breaks, F.W. and Tindle, A.G. 2005: A review of rare-element (Li-Cs-Ta) pegmatite exploration techniques for the Superior Province, Canada, and large worldwide tantalum deposits; Exploration and Mining Geology, v. 14, no. 1–4, p. 1–30.

Silva, D., Groat, L., Martins, T. and Linnen, R. in press: Structural controls on the origin and emplacement of lithium-bearing pegmatites; The Canadian Journal of Mineralogy and Petrology, v. 61.

Silva, D., Martins, T., Groat, L. and Linnen, R. 2022: Preliminary observations on emplacement controls of pegmatite dikes from the Wekusko Lake pegmatite field, north-central Manitoba (parts of NTS 63J13, 14, 63O4); *in* Report of Activities 2022, Manitoba Natural Resources and Northern Development, Manitoba Geological Survey, p. 49–60.

Snow Lake Lithium Ltd. 2022: Presentation; URL <https://snowlakelithium.com/presentation/> [September 2021].

Stern, R.A. and Lucas, S.B. 1994: U-Pb zircon age constraints on the early tectonic history of the Flin Flon accretionary collage, Saskatchewan; *in* Current Research 1994-F, Geological Survey of Canada, p. 75–86.

Stern, R.A., Lucas, S.B., Syme, E.C., Bailes, A.H., Thomas, D.J., Leclair, A.D. and Hulbert, L. 1993: Geochronological studies in the Flin Flon domain, Manitoba-Saskatchewan, NATMAP Shield Margin Project area: results for 1992–1993; *in* Radiogenic Age and Isotopic Studies, Report 7, Geological Survey of Canada, Current Research 93-2, p. 59–70.

Stewart, M.S., Lafrance, B. and Gibson, H.L. 2018: Early thrusting and folding in the Snow Lake camp, Manitoba: tectonic implications and effects on volcanogenic massive sulfide deposits; Canadian Journal of Earth Sciences, v. 55, no. 8, p. 935–957.

Syme, E.C., Lucas, S.B., Bailes, A.H. and Stern, R.A. 2000: Contrasting arc and MORB-like assemblages in the Paleoproterozoic Flin Flon belt, Manitoba, and the role of intra-arc extension in localizing volcanic-hosted massive sulphide deposits; Canadian Journal of Earth Sciences, v. 36, no. 11, p. 1767–1788.

Whalen, J.B., Syme, E.C. and Stern, R.A. 1999: Geochemical and Nd isotopic evolution of Paleoproterozoic arc-type granitoid magmatism in the Flin Flon belt, Trans-Hudson orogen, Canada; Canadian Journal of Earth Sciences, v. 36, no. 2, p. 227–250.

Zwanzig, H.V. 1990: Kisseynew gneiss belt in Manitoba: stratigraphy, structure, and tectonic evolution; *in* The Early Proterozoic Trans-Hudson Orogen of North America, J.F. Lewry and M.R. Stauffer (ed.), Geological Association of Canada, Special Paper 37, p. 95–120.

GS2023-8

Geological investigations in the areas of Niblock Lake and Crowduck Bay (Wekusko Lake), north-central Manitoba (parts of NTS 63J13, 14)

by K.D. Reid

Summary

Bedrock investigations during the 2023 field season focused on geology east of Wekusko Lake, in the Crowduck Bay and Niblock Lake areas. Mapping at Niblock Lake confirmed the presence of subaqueously deposited bimodal mafic and felsic volcanic rocks. A unique facies transition from cross-bedded feldspathic sandstone to mudstone to poorly sorted conglomerate is indicative of deposition in an environment that transitions from terrestrial to below wave base, possibly with considerable adjacent relief.

Historical occurrences of lithium-bearing pegmatite in the Crowduck Bay area have garnered significant exploration attention in recent years. The lithological and structural character of rocks in the Crowduck Bay area was investigated to determine controls on pegmatite emplacement. Pre-existing ductile fabrics appear to play a role as ground preparation for later dilatational structures that host the lithium-bearing pegmatite.

In Brief:

- Niblock Lake contains subaqueously deposited mafic-pillowed flows and associated felsic volcaniclastic rocks of probable arc volcanic affinity
- Missi group sediments at Niblock Lake record a transition from low energy fluvial meandering river to slightly deeper water basin
- Pre-existing structural fabrics and faults in the Crowduck Bay area play a role in controlling emplacement of both barren and Li-bearing pegmatite dikes

Citation:
Reid, K.D. 2023: Geological investigations in the areas of Niblock Lake and Crowduck Bay (Wekusko Lake), north-central Manitoba (parts of NTS 63J13, 14); *in* Report of Activities 2023, Manitoba Economic Development, Investment, Trade and Natural Resources, Manitoba Geological Survey, p. 64–72.

Introduction

The structure and stratigraphic context of rocks between Wekusko Lake and the Superior boundary zone (Figure GS2023-8-1) are poorly understood; this is partly a result of poor outcrop exposure and lack of recent geological mapping (Frarey, 1950; Bailes, 1985). However, the presence of critical minerals such as spodumene (lithium-bearing pyroxene) as well as base metals (e.g., volcanogenic copper-zinc) and precious metals (e.g., orogenic gold) has resulted in renewed exploration interest and research activity in the area.

In 2023, the Manitoba Geological Survey initiated geological compilation and targeted mapping projects to expand geoscience knowledge in the Niblock Lake and Crowduck Bay (Wekusko Lake) areas, the objectives of which were to

- investigate volcanic and sedimentary rocks in the Niblock Lake area, with emphasis on determining age, geochemical affinity and potential tectonic setting; and
- examine possible lithological and structural controls on the emplacement of pegmatite from the Wekusko pegmatite field in the Crowduck Bay area along the Crowduck Bay fault.

Regional geology

The Snow Lake domain is one of several Paleoproterozoic domains that form the internal Reindeer zone of the Trans-Hudson orogen in Manitoba (Lewry and Collerson, 1990). The Snow Lake domain is bounded to the east by the Superior boundary zone (Figure GS2023-8-1) and to the north, the Snow Lake domain gives way to turbiditic greywacke and mudstone of the Kisseynew domain. Volcanic rocks west of Reed Lake are considered part of the Amisk collage (Figure GS2023-8-1; Lucas et al., 1996). Stern et al. (1995) suggested that stratigraphic and geochemical differences between the Snow Lake arc assemblage and volcanic rocks of the Amisk collage were likely the result of their having formed in distinct tectonic settings. To the south, the Snow Lake domain continues under younger Phanerozoic platform carbonate rocks (Figure GS2023-8-1).

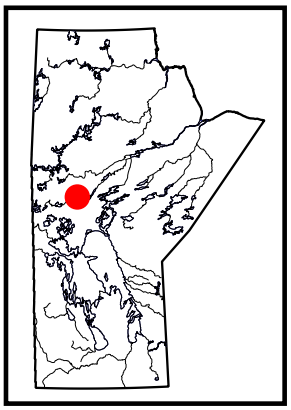

The eastern half of the Snow Lake domain is subdivided into three structural panels bounded by the northeast-trending Berry Creek shear zone and Crowduck Bay fault (Figure GS2023-8-1). The Berry Creek shear zone separates the Snow Lake arc assemblage (SLA) and the Herblet gneiss dome (HGD) from a northeast-trending panel of greywacke and mudstone 15–20 km wide that Ansdell et al. (1999) referred to as the Central Wekusko block (CWB; Figure GS2023-8-1). In the southwestern corner of the Wekusko Lake area, greywacke and mudstone are in structural contact with the Hayward Creek arc assemblage (HCA). Though no age determination is available for the Hayward Creek arc assemblage, it is thought to consist of ca. 1.89 Ga juvenile-arc rocks (Gilbert and Bailes, 2005).

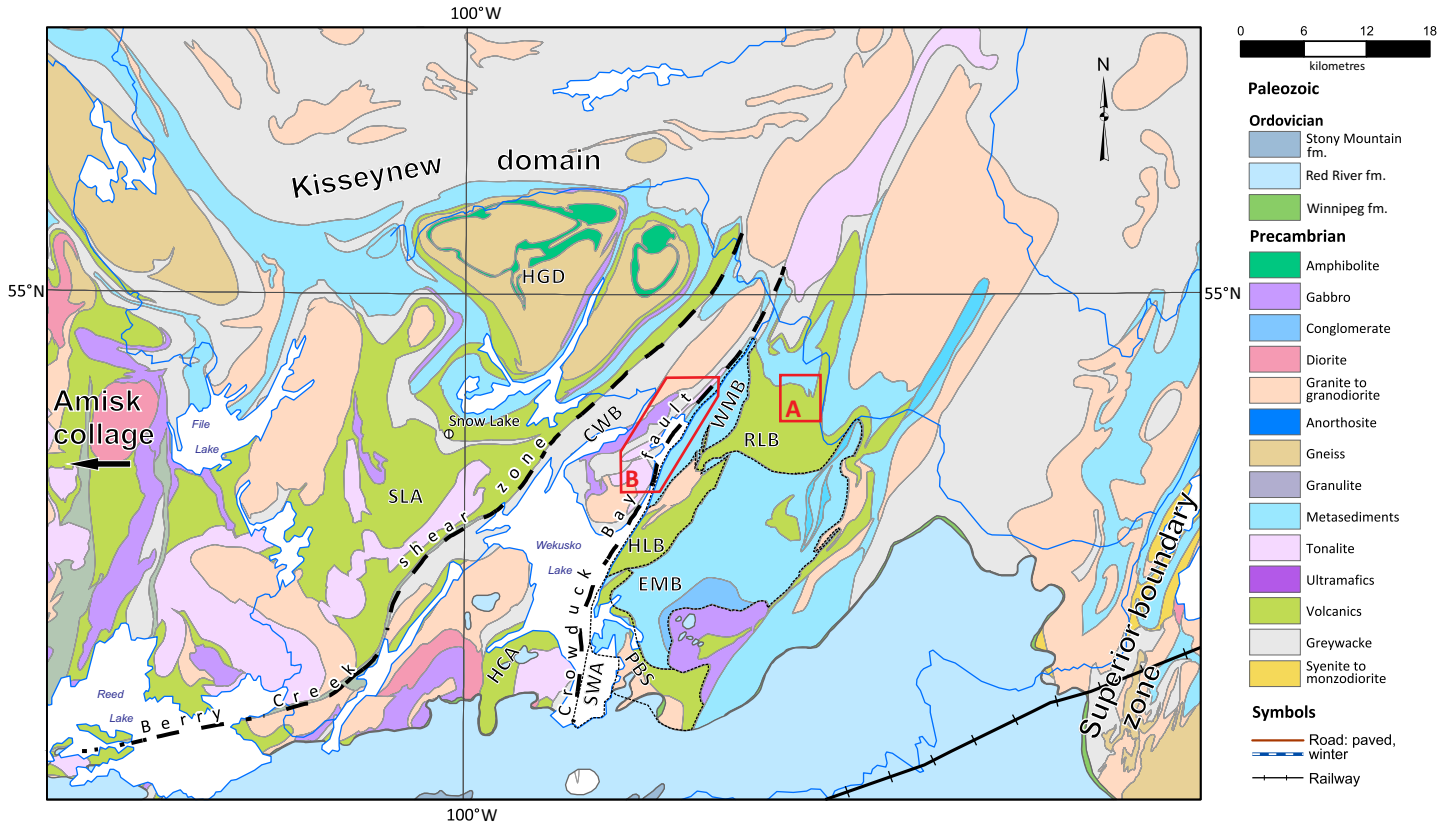

Figure GS2023-8-1: *Regional geology showing the Snow Lake domain, including the areas examined in 2023 (red polygons labelled A and B corresponding to Figure GS2023-8-2a, b) in north-central Manitoba (modified from Manitoba Geological Survey, 2022). Note the Kisseynew domain to the north, the Superior boundary zone to the east and Paleozoic cover rocks to the south. The Snow Lake arc assemblage (SLA), Herblet Gneiss dome (HGD), Hayward Creek arc assemblage (HCA), South Wekusko assemblage (SWA), Puella Bay suite (PBS), Eastern Missi fault block (EMB), Herb Lake fault block (HLB), Western Missi fault block (WMB), Roberts Lake block (RLB) and Central Wekusko fault block (CWB) are shown relative to the Berry Creek shear zone and Crowduck Bay fault. Small dashed lines show the approximate boundaries of assemblages and structural blocks on the eastern side of Wekusko Lake.*

The Crowduck Bay fault, a crustal-scale structure with a ductile and brittle-ductile history, separates the Central Wekusko block from rocks to the east (Connors et al., 1999). There is no formal designation for this panel to the east of the Crowduck Bay fault, but previous researchers have subdivided some rocks of similar lithotectonic character into fault-bounded blocks and/or related assemblages (e.g., Connors et al., 1999; Gilbert and Bailes, 2005; Reid, 2021). These include ocean-floor basalts of the South Wekusko assemblage (SWA) and Roberts Lake block (RLB); evolved-arc volcanic rocks of the Puella Bay suite (PBS) and Herb Lake fault block (HLB); and fluvial-alluvial sedimentary rocks of the Western Missi fault block (WMB) and Eastern Missi fault block (EMB; Figure GS2023-8-1; e.g., Ansdell et al., 1999; Connors et al., 1999; Gilbert and Bailes, 2005; Reid, 2021).

Bailes (1985), who mapped the eastern half of Niblock Lake as part of the Saw Lake mapping project, described the northern and eastern shore of Niblock Lake as consisting of metasiltstone, fluviatile metasandstone and polymictic pebble conglomerate, intercalated with massive and pillowed basalt. The fluvial-alluvial character of the siliclastic rocks and the massive character of the basalt led to the interpretation that these rocks are part of the younger Missi group. The southwestern shore contains pillow basalt, heterolithic felsic breccia and massive rhyolite that were believe to be part of the broader Amisk group rocks of the Flin Flon belt, but due to the Saw Lake map area only extending to the eastern half of Niblock Lake, the western extent of these rocks remained undetermined. More current maps (e.g., NATMAP Shield Margin Project Working Group, 1998) show the Niblock Lake area as a structural wedge of fluvial-alluvial sediments, basaltic flows and subordinate felsic volcanic rocks of uncertain geochemical affinity and age.

Highlights of fieldwork

Bedrock mapping in the Niblock Lake area documented several structural and stratigraphic features used to update the geology of the area (Figure GS2023-8-2a). A brief description of each map unit (oldest to youngest) and related features is provided below. All rocks in the Niblock Lake area have been metamorphosed to amphibolite facies, but for the sake of brevity the prefix 'meta'- has been omitted.

Samples of mafic and felsic rocks were collected for whole-rock lithogeochemistry, samarium-neodymium (Sm-Nd) isotopes

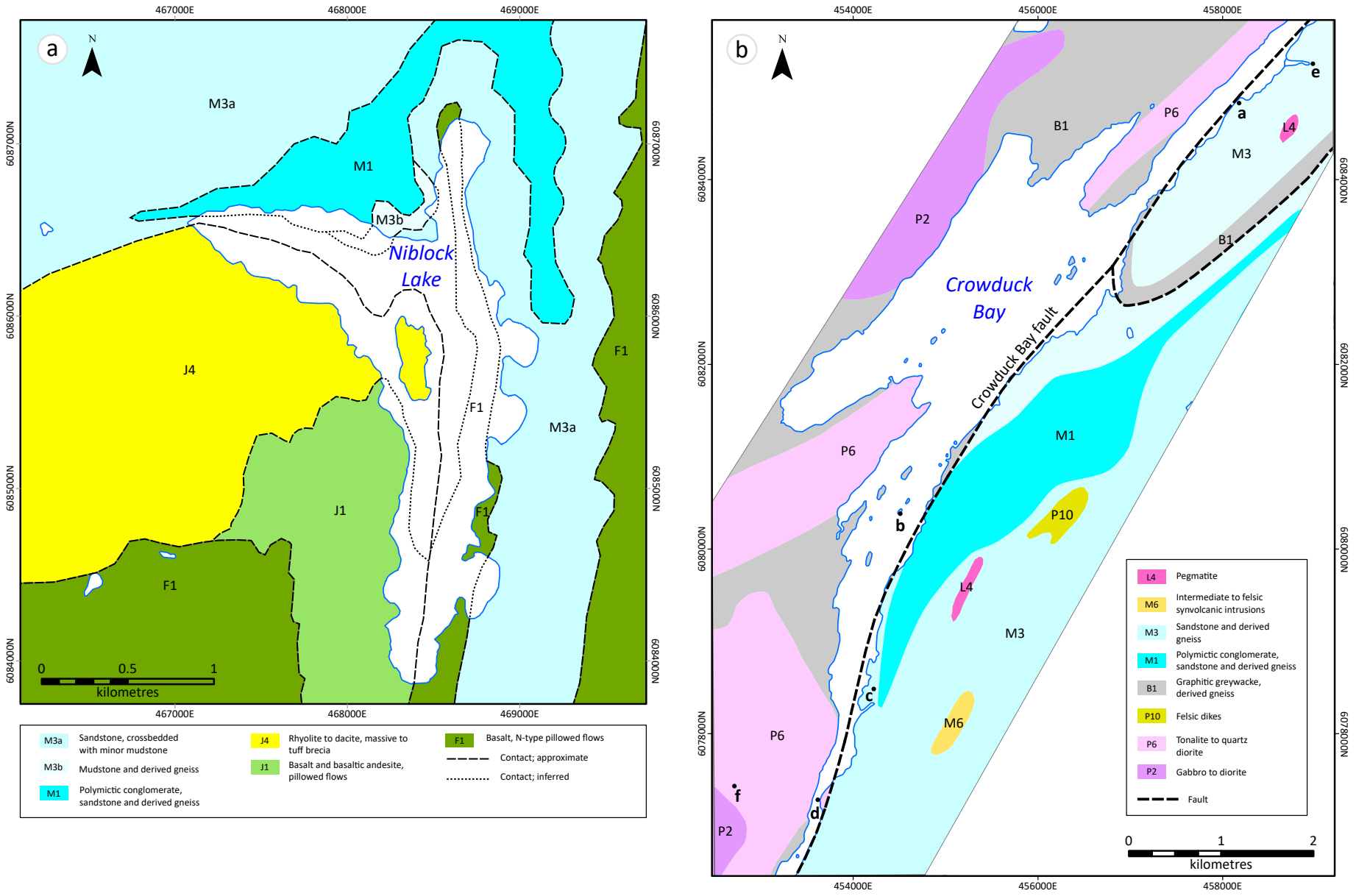

Figure GS2023-8-2: *Areas investigated during the 2023 field season (see Figure GS2023-8-1 for regional setting):* ***a)*** *updated geology of the Niblock Lake area;* ***b)*** *location of targeted outcrop visits in the Crowduck Bay area (geology from NATMAP Shield Margin Project Working Group, 1998) and location of outcrop photographs (points labelled with lower case letters) in Figure GS2023-8-4. All co-ordinates are in UTM Zone 14, NAD83.*

and uranium-lead (U-Pb) geochronology. Targeted outcrops in the Crowduck Bay area were visited to investigate the Burntwood (unit B1) and Missi (units M1, M3) groups, and their relationship to deformation along the Crowduck Bay fault (Figure GS2023-8-2b). Barren and spodumene-bearing pegmatite dikes were investigated to determine their level of deformation and relationship to the regional deformation history.

Niblock Lake

Mafic volcanic rocks (units F1 and J1)

Two variations of pillowed basalt flows are present in the Niblock Lake area. The first is observed along the southeastern shore and extends into a small bay at the northern end of the lake (unit F1; Figure GS2023-8-2a). The pillows are strongly attenuated (north trending) with dark green selvages, aphyric to weakly feldspar-pyroxene–phyric (Figure GS2023-8-3a), and commonly have concentric and radial cooling fractures. The pillowed flows are in sharp structural contact with feldspathic sandstone (unit M3a), possibly along a fault at a shallow angle to the sedimentary bedding. In the southeast corner of the lake, basalt and feldspathic sandstone alternate at the outcrop scale, which appears to be the result of very shallow-plunging, north-trending upright folds. Basalt of unit F1 is thought to be similar to basalt found in the Roberts Lake area and the South Wekusko assemblage, which has a normal (N-type) mid-ocean–ridge basalt chemical affinity (N-MORB; Gilbert and Bailes, 2005; Benn et al. 2018).

The second variation of pillowed basalt occurs along the southwestern shore of Niblock Lake (unit J1; Figure GS2023-8-2a). This feldspar-pyroxene–phyric basalt differs from the first in that it has pale grey-green selvages and contains abundant amygdules 1–3 mm in diameter (Figure GS2023-8-3b). Unit J1 is also characterized by an increased content of volcaniclastic rocks, with beds of mafic to intermediate lapilli tuff 1–2 m thick occurring between pillowed flows.

Felsic volcanic and volcaniclastic rocks (unit J4)

Angular rhyolite tuff breccia (unit J4) is the main rock type on the western side of Niblock Lake (Figure GS2023-8-3c). The contact between pillowed basalt (unit J1) and felsic volcaniclastic rocks (J4) is not directly observed, but is considered conformable given there is an increase in mafic matrix between clasts as well as the presence of intact pillow fragments with proximity to unit J1 (Figure GS2023-8-3d). The eastern part of the island in the centre of Niblock Lake contains feldspar-phyric dacite breccia and massive aphyric siliceous blue-grey rhyolite. Both the dacite and the rhyolite were sampled for whole-rock lithogeochemistry and U-Pb geochronology, and the results are pending.

Basalt dikes (unit J7)

Submetre, dark green, fine-grained basalt dikes (unit J7; not shown on Figure GS2023-8-2a) cut the mafic pillowed flows of unit J1 and the felsic volcaniclastic rocks of unit J4. The dikes have quartz-filled amygdules that define centimetre-scale zoning (Figure GS2023-8-3d). The dikes are tightly folded at the outcrop scale, with axial planes that strike between 345 and 360° and dip nearly vertically; the fold noses appear to plunge steeply to the north.

Sedimentary rock (units M1, M3a and M3b)

Examination of outcrops along the northern and eastern side of the lake confirms the presence of crossbedded feldspathic sandstone (unit M3a; Figure GS2023-8-2a), garnet- and staurolite-bearing mudstone (unit M3b), and poorly sorted heterolithic pebble and cobble conglomerate (unit M1; Figure GS2023-8-2a). Along the eastern shore, submetre beds of feldspathic sandstone alternate with garnet- and staurolite-bearing mudstone (Figure GS2023-8-3e). Heavy mineral laminations define tabular crossbeds in fine- to medium-grained feldspathic sandstone that are consistent with soft-sediment flame structures at the top of the mudstone. Locally, dark grey mudstone rip-up clasts as large as 10 cm are scattered within trough-crossbedded feldspathic sandstone. Stratigraphically above the feldspathic sandstone (unit M3a) is a garnet- and staurolite-bearing, millimetre- to centimetre-scale bedded mudstone (unit M3b; Figure GS2023-8-2a). Abundant parasitic (M) folds may result in the mudstone being fold thickened, but tracing this unit along shore suggests it is a minimum of 25 m thick. Stratigraphically above unit M3b is poorly sorted, clast-supported to matrix-supported conglomerate with a clast population that is dominated by mafic porphyritic and basaltic cobbles, and containing lesser amounts of yellow quartz, blue-grey dacite and dark grey mudstone (Figure GS2023-8-3f). The granule-rich matrix of the conglomerate contains a substantial dark grey wacke component.

Crowduck Bay

Early mapping in the Crowduck Bay area placed staurolite-garnet pelitic schist of the Burntwood group in sharp contact with sandstone and conglomerate of the Missi group (e.g., Stockwell, 1937; Frarey, 1950). Recent research indicates that this contact is a major structure, the Crowduck Bay fault, which juxtaposes these two lithologies for over 20 km along the Grass River and Crowduck Bay before trending southward along Wekusko Lake (e.g., Reid, 2019; Connors et al., 2002; Gilbert and Bailes, 2005). The fault is believed to be a deep-seated and long-lived structure (Connors et al, 2002) with links to observed mineralizing events, including orogenic gold (Stockwell, 1937; Reid, 2021), lithium-bearing pegmatites (Silva et al., 2022) and kimberlite-like intrusive rocks (Chakhmouradian and Reid, 2017). Presented here is a brief summary of lithological and structural observations in the Crowduck Bay area, including observed relationships with barren and spodumene-bearing pegmatite.

In the Crowduck Bay area, ductile fabrics that manifest as rod-shaped conglomerate clasts (axes ratio of 5:1:1) directly

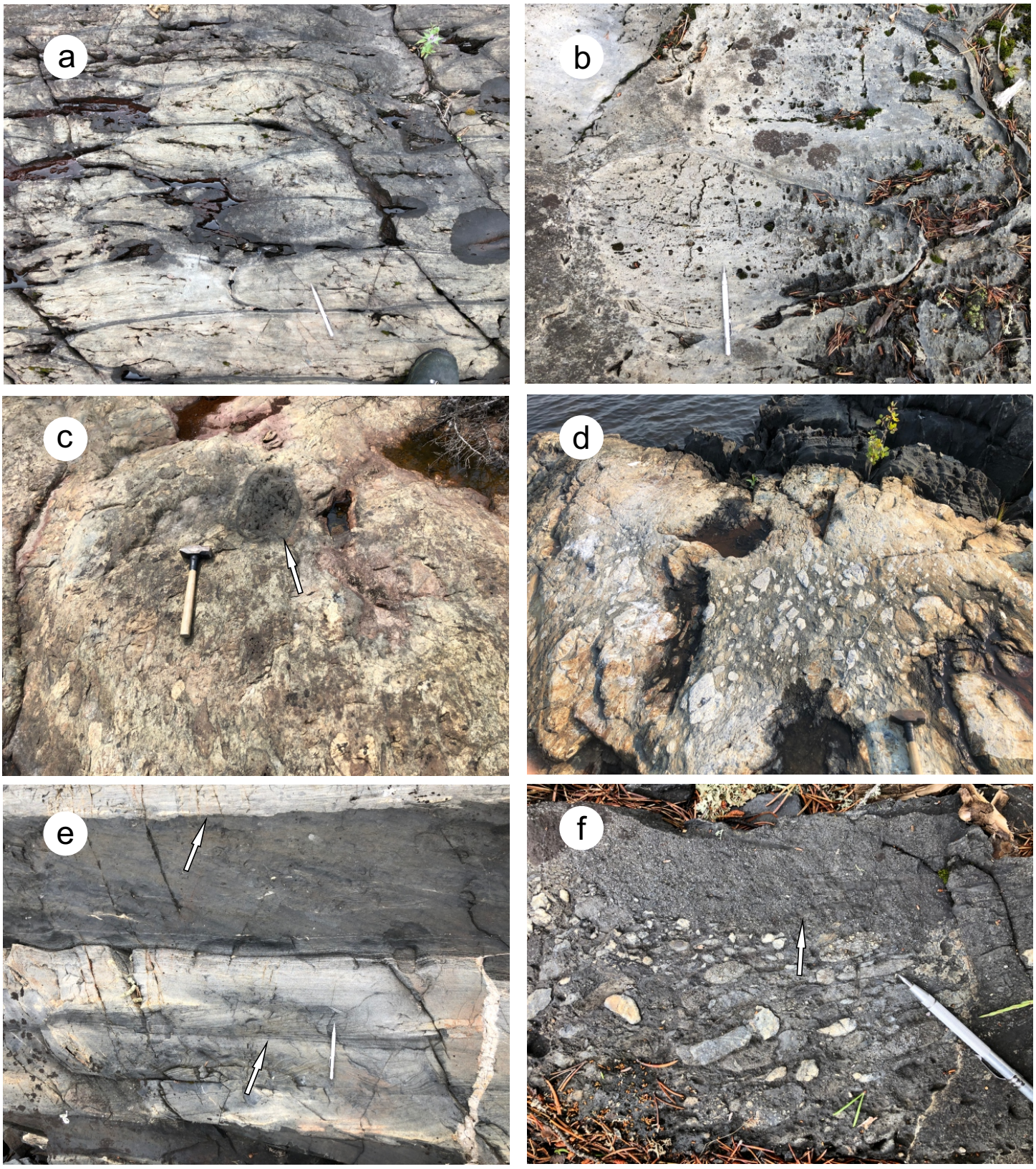

Figure GS2023-8-3: *Outcrop photographs from the Niblock Lake area:* ***a)*** *aphyric to weakly feldspar-pyroxene–phyric pillow basalt (unit F1; 468285E, 6084344N);* ***b)*** *feldspar-pyroxene–phyric pillow basalt with abundant quartz-filled amygdules (unit J1; 468169E, 6085542N);* ***c)*** *felsic tuff breccia with an intact pillow fragment indicated by the arrow (unit J4; 468111E, 6085766N);* ***d)*** *felsic tuff breccia cut by amygdule-rich mafic dike (units J4 and J7; 468002E, 6085913N);* ***e)*** *alternating <1 m planar beds of tabular to trough crossbedded feldspathic sandstone (lower arrow) and staurolite-bearing mudstone with flame structures at its upper contact (upper arrow; unit M3a; 468821E, 6086184N);* ***f)*** *poorly sorted heterolithic conglomerate with granule-rich dark grey wacke matrix and mudstone clasts indicated by the arrow (unit M1; 467234E, 6086609N) . All co-ordinates are in UTM Zone 14, NAD83.*

adjacent to the Crowduck Bay fault trend 043° and plunge 16° (Figure GS2023-8-4a). Staurolite porphyroblasts in biotite-staurolite-garnet schist in the Crowduck Bay area commonly have quartz-filled pressure shadows that show signs of sigma-type rotation indicative of dextral movement (Figure GS2023-8-4b). A unit of feldspathic wacke and conglomerate hostrock to the Thompson Brothers spodumene-bearing pegmatite dike has two fabrics: 1) a near-vertical penetrative cleavage in the feldspathic wacke that strikes 217° (S_2; 217°/87°), and 2) a weak clast-flattening/rodding in the conglomerate that trends 013° and plunges approximately 10 to 25°, likely related to D_4 overprinting (Figure GS2023-8-4c). In the narrows between Wekusko Lake and Crowduck Bay, a gabbro within several metres of the Crowduck Bay fault is cut by parallel shear bands that have associated S-C fabrics indicating sinistral movement (Figure GS2023-8-4d).

Silva et al. (2022) indicated that there are two varieties of pegmatite dikes in the Crowduck Bay area: barren pegmatites containing albite, quartz, K-feldspar and muscovite, with trace tourmaline and garnet; and spodumene-bearing pegmatite with albite, K-feldspar, quartz, tourmaline and muscovite. For a complete description of pegmatite dikes in the Wekusko Lake pegmatite field, the reader is referred to Černý et al. (1981) and Silva et al. (2022, 2023).

Barren pegmatite dikes form elongated, lobate, northeast-trending bodies at the metre- to decametre-scale in conglomerate and sandstone (units M1 and M3; Figure GS2023-8-2b) southeast of the Crowduck Bay fault, and in staurolite-garnet-biotite schist (unit B1; Figure GS2023-8-2b) northeast of the Crowduck Bay fault. These have irregular, but often sheared, contacts with folded keels (Figure GS2023-8-4e). Examination in cross-sectional view of a northeast-trending pegmatite ridge suggests that these are shallow, northeast-plunging, cigar-shaped bodies.

Spodumene-bearing dikes in Crowduck Bay (e.g., Sherritt-Gordon and Violet-Thompson groups; Silva et al., 2023) occur mainly as metre-scale, sheet-like features that trend 320 to 340°, with the exception of the Thompson Brothers dike, which trends ~040° and is slightly oblique to the Crowduck Bay fault. Intriguingly, the spodumene in the Thompson Brothers dike has a distinct lineation (~335°/10°) that appears to be the result of igneous crystallization during extension rather than later ductile deformation; this is broadly similar to the apparent strike of the Sherritt-Gordon group pegmatite dikes (320–340°). Work on microtextures from this dike should help provide additional constraints (Silva et al., 2023).

Exceptional exposures of the Sherritt-Gordon group pegmatite dikes show that contacts are sharp, straight and cut across all lithologies (Figure GS2023-8-4f) and earlier ductile fabrics, with minor extensional jogs and comb-structure mineral growth (feldspar, muscovite, tourmaline and spodumene) perpendicular to the wall margin of the dike. The pegmatite is very gently folded perpendicular to its strike length, with a wavelength of 2 m and a height of 0.2 m.

Discussion

Niblock Lake

Mapping conducted by Frarey (1950) indicated that the western side of Niblock Lake is composed of basaltic flows with an intrusive quartz-feldspar porphyry directly west of the lakeshore. Alternatively, field mapping by Bailes (1985) and the current study show that much of the western shoreline is composed of felsic volcanic rocks (unit J4; Figure GS2023-8-2a). At present, the geochemical affinity of volcanic rocks at Niblock Lake is unknown, but the presence of pillowed basalt flows (unit J1) suggests, at least in part, the subaqueous deposition of basalt. Mapping conducted by VMS Ventures Inc. identified felsic and mafic volcanic rocks to the west of Niblock Lake, at their Sails Lake project (between Sails Lake and Niblock Lake). Geochemical analyses indicate that both mafic and felsic rocks have an volcanic-arc signature (Bailes, unpublished report prepared for VMS Ventures Inc., 2010).

Bailes (1985) recognized that sedimentary rocks of the Missi group between Wekusko Lake and Saw Lake differed from their type localities at Flin Flon and Amisk Lake (Stauffer, 1990) in that they were more recrystallized and lithologically more diverse. Bailes (1985) considered two factors affecting this: a depositional environment that included marine as well as terrestrial conditions; and a modification of typical fluvial-alluvial sedimentation by localized volcanic activity, which provided volcanic flows and immature detritus.

The progression in sedimentary facies from <1 m interbedded, crossbedded feldspathic sandstone and mudstone (unit M3a) to mudstone (unit M3b) prior to deposition of poorly sorted, immature heterolithic conglomerate (unit M1) is considered to be part of a lateral and stratigraphic transition. Alternation of tabular crossbedded sandstone and mudstone likely reflects deposition in a meandering river system. The tabular crossbedded foreset beds probably reflect the lateral migration of the river channel, whereas the mudstone layers are likely the result of overbank deposition in meander cutoffs (e.g., Miall, 1996). The presence of fine centimetre-scale lamination and lack of fluvial sedimentary features in mudstone (unit M3b; Figure GS2023-8-2a) suggest that the fluvial system may transition into a slightly deeper water basin below extensive wave action or fluvial reworking. The presence of poorly sorted conglomerate overlying mudstone might indicate that the basin had considerable relief and that the conglomerate represents localized debris flows, which could explain the presence of mudstone clasts in granule-rich beds.

Crowduck Bay

Rocks along the Crowduck Bay fault have been affected by multiple deformation events and subsequent metamorphism (e.g., Connors et al., 1999; Connors et al., 2002; Reid, 2021). Connors et al. (1999) recognized two main periods of deformation

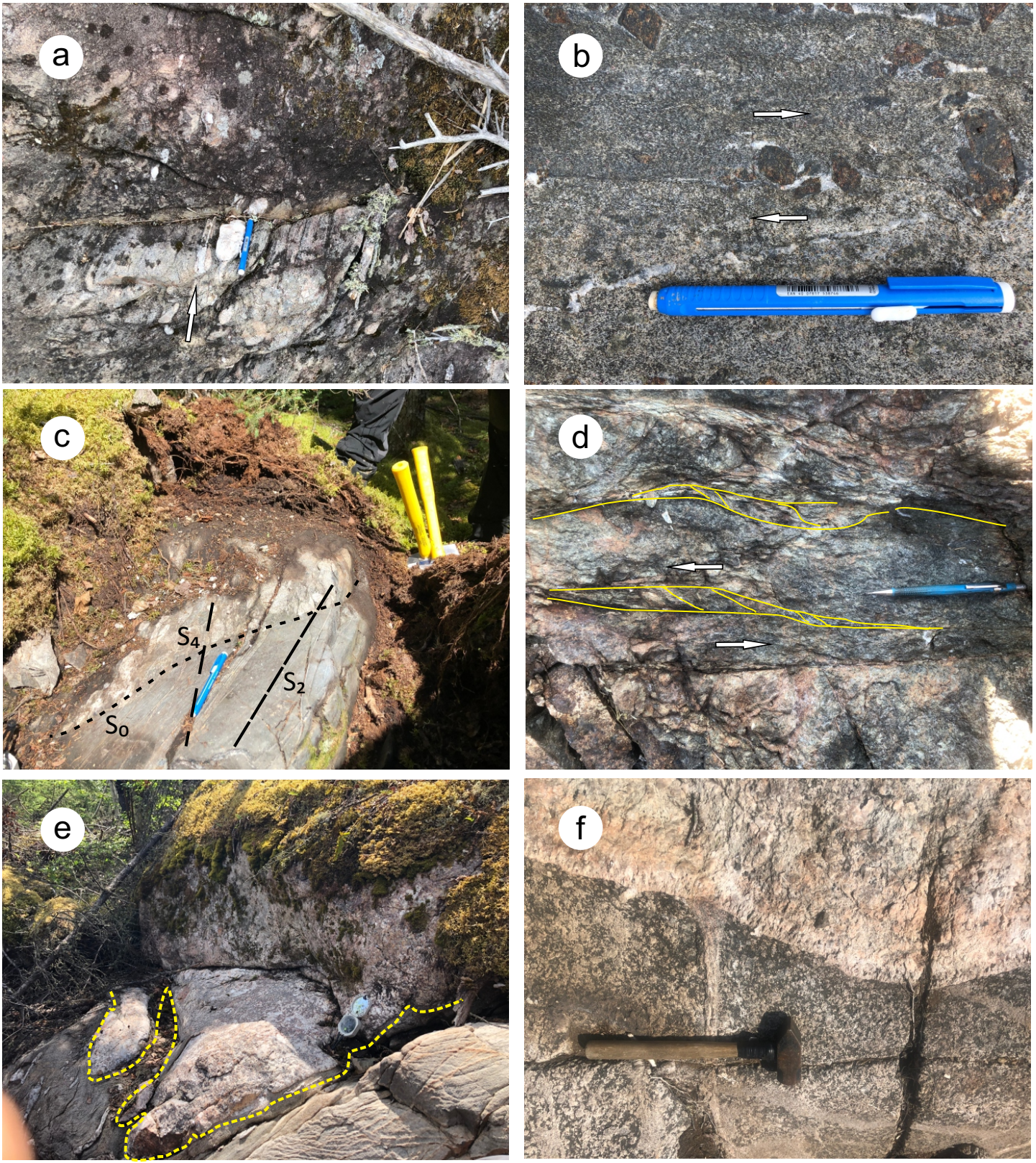

Figure GS2023-8-4: *Outcrop photographs from the Crowduck Bay area:* ***a)*** *rodded conglomerate clasts (arrow) with a 5:1:1 axes ratio (unit M3; 458177E, 6084830N);* ***b)*** *dextral sigma-type rotation of staurolite porphyroblasts (indicated by arrows; unit B1; 454509E, 6080384N);* ***c)*** *bedding S_0 overprinted by S_2 foliation and S_4 clast flattening/stretching (units M3 and M1; 454271E, 6078551N);* ***d)*** *S-C shear fabric (yellow lines and arrows) showing sinistral movement (453616E, 6077286N);* ***e)*** *barren pegmatite forming shallowly northeast-plunging body with tightly folded keel (yellow dashed line; 458976E, 6085256N);* ***f)*** *sharp contact between seriate gabbro and spodumene-bearing pegmatite (unit P2; 452713E, 6077434N). All co-ordinates are in UTM Zone 14, NAD83.*

affecting the rocks east of Wekusko Lake: 1) D_2, which involved thrust faulting and folding linked with southwest-directed transport between 1840 and 1830 Ma; and 2) D_3, characterized by north-northeast-trending, moderately to shallowly dipping stretching lineation and associated foliation that overprints D_2, and which resulted from northwest–southeast transpression between 1815 and 1805 Ma. Recent mapping by Reid (2021) summarized a similar history of fabrics, with a S_2 spaced cleavage linked to tight to isoclinal folding of Herb Lake volcanic rocks and adjacent sandstone and conglomerate. The axial planes of these folds strike from 045 to 060° and verge steeply to the northwest (equivalent to D_2; Connors et al., 1999). A less prominent near vertical S_3 spaced cleavage/jointing that strikes 330 to 340° overprints S_2 in the vicinity of Puella Bay (Wekusko Lake; D_3 of Reid, 2021). Closer to the Crowduck Bay fault, a strong penetrative foliation (S_4; 010–030°) related to D_4 (equivalent to D_3 of Connors et al., 2002) overprints all earlier fabrics.

It is important to note that deformation and peak metamorphism linked to D_3 folding and extension (D_3 of Connors et al., 2002; D_4 of Reid, 2021), between 1815 and 1805 Ma, have a strong control on emplacement and structural orientation of barren pegmatite dikes, which mimic clast elongation as seen in Figure GS2023-8-4a. The observed spodumene-bearing pegmatite dikes from the Sherritt-Gordon and Violet-Thompson groups, with the exception of the Thompson Brothers dike, intrude into brittle to brittle-ductile extensional structures trending 320 to 340° that cut the D_2 and D_3 fabrics of Connors et al. (1999) in the Crowduck Bay area. These mineralized dikes are younger than the barren pegmatite dikes, postdate peak metamorphism and are quite possibly linked to orogenic collapse or relaxation. This interpretation is supported by a recent 1780.0 ±8.1 Ma U-Pb radiometric age for dike 1 of the Green Bay group (Martins et al., 2019).

Interestingly, the S_3 spaced cleavage/jointing observed by Reid (2021) has a similar 320 to 340° orientation as the Sherritt-Gordon group spodumene-bearing pegmatite dikes. Arguably, this fabric potentially acts as ground preparation for later brittle-ductile extensional faults, especially in rocks with competent rheology such as gabbro. In addition to S_3 (320–340°) fabrics, it is likely the S_2 (045–060°) spaced cleavage and associated faults formed during D_2 deformation, which played a role in forming dilatational zones during postpeak metamorphic structural reactivation. The Thompson Brothers spodumene-bearing pegmatite has a trend of 040°, which is oblique to the adjacent 015° trending Crowduck Bay fault, likely formed along an early D_2 structure. As with many long-lived ductile structures, the Crowduck Bay fault likely did not have accommodation space for the emplacement of the mineralized pegmatite, but the secondary structures around it did.

Economic considerations

The presence of subaqueously deposited bimodal mafic and felsic volcanic rocks indicates that the rocks west of Niblock Lake have the potential to produce volcanogenic massive-sulphide deposits; rhyolite tuff breccia and conglomerate along the western shoreline have a strikingly similar appearance to rhyolite breccia observed in the Millrock member of the Flin Flon formation (e.g., Bailes and Syme, 1989). Structurally brecciated massive rhyolite and dacite in the Niblock Lake area is locally flooded with quartz and disseminated sulphide (gold-assay results are pending).

Understanding property-scale rheological differences, coupled with regional structural history and fabrics, is imperative to understanding potential emplacement sites for mineralized lithium-bearing pegmatite.

Acknowledgments

The author thanks J. Bautista and M. Michaw for providing enthusiastic field assistance, as well as C. Epp and P. Belanger for logistical support.

References

Ansdell, K.M., Connors, K.A., Stern, R.A. and Lucas, S.B. 1999: Coeval sedimentation, magmatism, and fold-thrust domain development in the Trans-Hudson orogen: geochronological evidence from the Wekusko Lake area, Manitoba, Canada; *in* NATMAP Shield Margin Project, S.B. Lucas (ed.), Canadian Journal of Earth Sciences, v. 36, p. 293–312, URL <https://doi.org/10.1139/e98-082>.

Bailes, A.H. 1985: Geology of the Saw Lake area; Manitoba Energy and Mines, Geological Services Branch, Geological Report GR83-2, 47 p.

Bailes, A.H. and Syme, E.C. 1989: Geology of Flin Flon–White Lake area; Manitoba Energy and Mines, Manitoba Geological Services Branch, Geological Report GR87-1, 313 p.

Benn, D., Linnen, R.L. and Martins, T. 2018: Geology and bedrock mapping of the Wekusko Lake pegmatite field (northeastern block), central Manitoba (part of NTS 63J13); *in* Report of Activities 2018, Manitoba Growth, Enterprise and Trade, Manitoba Geological Survey, p. 79–88.

Černý, P., Trueman, D.L., Zeihlke, D.V., Goad, B.E. and Paul, B.J. 1981: The Cat Lake–Winnipeg River and the Wekusko Lake pegmatite fields, Manitoba; Manitoba Department of Energy and Mines, Mineral Resources Division, Economic Geology Report ER80-1, 216 p., URL <https://manitoba.ca/iem/info/libmin/ER80-1.zip> [August 2023].

Chakhmouradian, A.R. and Reid, K.D. 2017: New occurrences of kimberlite-like intrusive rocks in drillcore from south of Wekusko Lake, eastern Flin Flon belt, north-central Manitoba (NTS 63J12); *in* Report of Activities 2017, Manitoba Growth, Enterprise and Trade, Manitoba Geological Survey, p. 78–90.

Connors, K.A., Ansdell, K.M. and Lucas, S.B. 1999: Coeval sedimentation, magmatism, and fold-thrust development in the Trans-Hudson orogen: propagation of deformation into an active continental arc setting, Wekusko Lake area, Manitoba; Canadian Journal of Earth Sciences, v. 36, p. 275–291.

Connors, K.A., Ansdell, K.M. and Lucas, S.B. 2002: Development of a transverse to orogeny parallel extension lineation in a complex collisional setting, Trans-Hudson orogen, Manitoba, Canada; Journal of Structural Geology, v. 24, p. 89–106.

Frarey, M.J. 1950: Crowduck Bay, Manitoba; Geological Survey of Canada, Map 987A, scale 1:63 360, URL <https://doi.org/10.4095/107132>.

Gilbert, H.P. and Bailes, A.H. 2005: Geology of the southern Wekusko Lake area, Manitoba (NTS 63J12NW); Manitoba Industry, Economic Development and Mines, Manitoba Geological Survey, Geoscientific Map MAP2005-2, scale 1:20 000.

Lewry, J.F. and Collerson, K.D. 1990: Trans-Hudson orogen: extent, subdivisions, and problems; *in* The Proterozoic Trans-Hudson Orogen of North America, J.F. Lewry and M.R. Stauffer (ed.), Geological Association of Canada, Special Publication, v. 37, p. 1–14.

Lucas, S.B., Stern, R.A., Syme, E.C., Reilly, B.A. and Thomas, D.J. 1996: Intraoceanic tectonics and the development of continental crust: 1.92–1.84 Ga evolution of the Flin Flon Belt, Canada; Geological Society of America, Bulletin, v. 108, p. 602–629.

Manitoba Geological Survey 2022: New edition of the 1:250 000 scale Precambrian bedrock geology compilation map of Manitoba; Manitoba Natural Resources and Northern Development, Manitoba Geological Survey, GeoFile 3-2022, URL <https://manitoba.ca/iem/info/libmin/geofile3-2022.zip> [October 2023].

Martins, T., Benn, D. and McFarlane, C. 2019: Laser-ablation inductively coupled plasma–mass spectrometry (LA-ICP-MS) analyses of columbite grains from Li-bearing pegmatites, Wekusko Lake pegmatite field (northeastern block), central Manitoba (part of NTS 63J13); Manitoba Agriculture and Resource Development, Manitoba Geological Survey, Data Repository Item DRI2019003, Microsoft® Excel® file, URL <https://manitoba.ca/iem/info/libmin/DRI2019003.xlsx> [October 2023].

Miall, A.D. 1996: The Geology of Fluvial Deposits; Springer-Verlag, New York, New York, 586 p.

NATMAP Shield Margin Project Working Group, 1998: Geology, NATMAP Shield Margin Project area, Flin Flon belt, Manitoba/Saskatchewan; Geological Survey of Canada, Map 1968A, 54 p., scale 1:100 000, URL <https://doi.org/10.4095/210073>.

Reid, K.D. 2019: Bedrock geological mapping of the Puella Bay area (Wekusko Lake), north-central Manitoba (part of NTS 63J12); *in* Report of Activities 2019, Manitoba Agriculture and Resource Development, Manitoba Geological Survey, p. 42–51.

Reid, K.D. 2021: Results of bedrock geological mapping in the Stuart Bay–Chickadee Lake area (east of Wekusko Lake), north-central Manitoba (parts of NTS 63J12, 13); *in* Report of Activities 2021, Manitoba Agriculture and Resource Development, Manitoba Geological Survey, p. 29–39.

Silva, D., Martins, T., Groat, L. and Linnen, R. 2022: Preliminary observations on emplacement controls of pegmatite dikes from the Wekusko Lake pegmatite field, north-central Manitoba (parts of NTS 63J13, 14, 63O4); *in* Report of Activities 2022, Manitoba Natural Resources and Northern Development, Manitoba Geological Survey, p. 49–60.

Silva, D., Martins, T., Groat, L. and Linnen, R. 2023: Regional pegmatite mapping and geochemical fractionation trends from the Wekusko Lake pegmatite field, west-central Manitoba (parts of NTS 63J13, 14, 63O4); *in* Report of Activities 2023, Manitoba Economic Development, Investment, Trade and Natural Resources, Manitoba Geological Survey, p. 52–63.

Stauffer, M.R. 1990. The Missi formation: an Aphebian molasses deposit in the Reindeer Lake Zone of the Trans-Hudson Orogen, Canada; *in* The Early Proterozoic Trans-Hudson Orogen of North America, J.F. Lewry and M.R. Stauffer (ed.), Geological Association of Canada, Special Paper, v. 37, p. 121–141.

Stern, R.A., Syme, E.C., Bailes, A.H. and Lucas, S.B. 1995: Paleoproterozoic (1.90–1.86 Ga) arc volcanism in the Flin Flon belt, Trans-Hudson orogen, Canada; Contributions to Mineralogy and Petrology, v. 119, p. 17–141.

Stockwell, C.H. 1937: Gold deposits of Herb Lake area, northern Manitoba; Geological Survey of Canada, Memoir 208, 46 p., URL <https://doi.org/10.4095/101640>.

GS2023-9

Field relationships, geochemical characteristics and metallogenic implications of gabbroic intrusions in the Paleoproterozoic Lynn Lake greenstone belt, northwestern Manitoba (parts of NTS 64C10–12, 14–16)

by X.M. Yang

In Brief:

- A number of gabbroic intrusions is evaluated for Ni-Cu fertility based on field relationships, geodynamic settings and geochemical characteristics
- Sulphide saturation in mafic magmas is largely caused by crustal contamination
- Low concentrations in platinum-group elements reflect fractionation of the mafic magma(s) formed by low-degree partial melting of the mantle

Citation:
Yang, X.M. 2023: Field relationships, geochemical characteristics and metallogenic implications of gabbroic intrusions in the Paleoproterozoic Lynn Lake greenstone belt, northwestern Manitoba (parts of NTS 64C10–12, 14–16); *in* Report of Activities 2023, Manitoba Economic Development, Investment, Trade and Natural Resources, Manitoba Geological Survey, p. 73–89.

Summary

In 2023, the Manitoba Geological Survey carried out a schematic study of gabbroic intrusions in the Paleoproterozoic Lynn Lake greenstone belt to address two essential questions: 1) why are some intrusions host to magmatic nickel-copper mineralization, whereas others are barren; and 2) what are the key controls on the mineralization. As a first step to tackling these questions, geochemical data on gabbroic rocks and related deposits published by the Manitoba Geological Survey were reviewed to extract valuable information on the metallogeny of the magmatic nickel-copper deposits in the belt. Several gabbro intrusions were then selected for further examination to investigate their relationships to the country rocks; their internal variation in mineralogy and grain size; their structural and magnetic susceptibility; and the presence and/or absence of sulphide minerals. Representative samples were also collected for further lithogeochemical, neodymium isotope and uranium-lead zircon geochronological studies.

Fertile gabbroic intrusions seem to occur mostly in the northern belt, whereas barren intrusions are present in the southern belt of the Lynn Lake greenstone belt. Geochemically, both the fertile and barren intrusions are dominantly metaluminous and tholeiitic (or calcic) to calcalkaline, showing typical volcanic-arc signatures. The geometry of the gabbro intrusions, ranging from vertical and tube-shaped (e.g., the Lynn Lake A and EL plugs) to tabular (Fraser Lake), appears to reflect the differences in the geological settings of magma emplacement and in the dynamics of mafic magmas. Geochemical proxies, such as highly siderophile elements including platinum-group elements, sulphur and oxygen stable isotopes, are therefore used to help assess the major controls on nickel-copper mineralization with respect to local geological settings, degree of fractionation and source heterogeneity or disparate degrees of partial melting of the mantle source. Relatively low-degree partial melting of the mantle source, early sulphide segregation of fractionating mafic magmas emplaced in an intra-oceanic–arc extensional setting and crustal contamination (particularly by volcanogenic massive-sulphide deposits) triggering sulphide saturation in the magmas are thought to be the key controls on nickel-copper mineralization in the Lynn Lake greenstone belt.

Introduction

Major to giant nickel–copper–platinum-group element (Ni-Cu-PGE) ore deposits are genetically associated with mafic-ultramafic mineral (magmatic) systems derived from the mantle and emplaced into extensional settings at continental margins (e.g., Lightfoot et al., 1990; Naldrett, 2004; Barnes and Lightfoot, 2005; Houlé et al., 2008; Begg et al., 2010; Lightfoot, 2017; Barnes et al., 2020). However, the nature of magmatic Ni-Cu-PGE deposits with relatively small tonnage and high grade in orogenic belts is less well understood. Although these deposits are enigmatic in origin, they have recently become more important and attractive exploration targets because of the high demand for critical metals and a foreseeable supply shortage (e.g., Maxeiner and Rayner, 2017; Yildirim et al., 2020; Deng et al., 2022; U.S. Geological Survey, 2023). The Lynn Lake magmatic Ni-Cu deposit (Pinsent, 1980) is hosted in the Lynn Lake intrusion. It occurs together with other mafic-ultramafic intrusions intruding the Wasekwan group supracrustal rocks of the Lynn Lake greenstone belt (Figure GS2023-9-1; Gilbert et al., 1980; Syme, 1985; Gilbert, 1993; Zwanzig et al., 1999; Yang and Beaumont-Smith, 2015; Hastie et al., 2018; Lawley et al., 2020, 2023; Yang, 2022). This provides an excellent opportunity to investigate the metallogeny of magmatic Ni-Cu mineral deposits in orogenic belts.

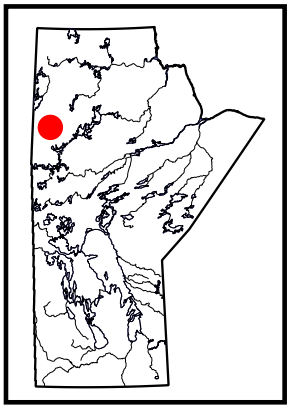

In 2023, the Manitoba Geological Survey (MGS) continued its multiyear bedrock geological mapping project in the Paleoproterozoic Lynn Lake greenstone belt (LLGB) in northwestern Manitoba (Figure GS2023-9-1), focusing on a schematic study of gabbroic intrusions in the belt. The objective of this

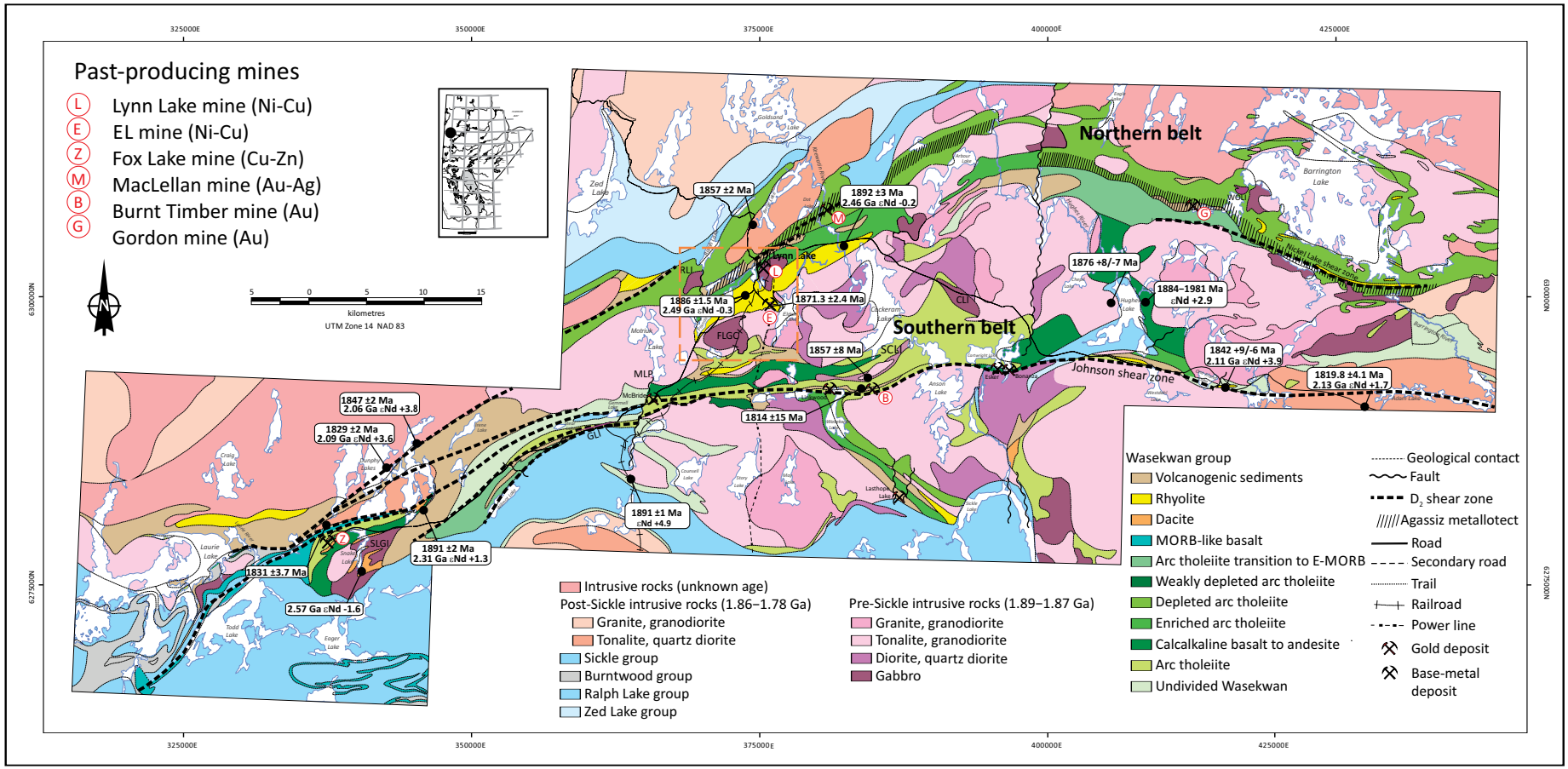

Figure GS2023-9-1: *Regional geology with uranium-lead zircon ages and neodymium isotopic compositions of the Lynn Lake greenstone belt (modified and compiled from Gilbert et al., 1980; Manitoba Energy and Mines, 1986; Gilbert, 1993; Zwanzig et al., 1999; Turek et al., 2000; Beaumont-Smith and Böhm, 2002, 2003, 2004; Beaumont-Smith et al., 2006; Jones et al., 2006; Beaumont-Smith, 2008; Yang and Beaumont-Smith, 2015, 2016, 2017; Lawley et al., 2020; Yang, 2022). Localities of gabbroic intrusions sampled in this study are shown. The location of Figure GS2023-9-2 is indicated by the orange box. Abbreviations: CLI, Cartwright Lake intrusion; FLGC, Fraser Lake gabbro complex; GLI, Gemmell Lake intrusion; MLP, Motriuk Lake plug; MORB, mid-ocean–ridge basalt; RLI, Ralph Lake intrusion; SCLI, Southern Cockeram Lake intrusion; SLGI, Snake Lake gabbro intrusion; WOLI, White Owl Lake intrusion.*

study was to evaluate the critical controls on magmatic Ni-Cu-PGE mineralization via a review of the MGS published data followed by field observations and investigations; structural and magnetic susceptibility (MS) measurements of outcrops; and geochemical sampling of representative bulk-rock samples. Results from this study indicate that metaluminous, tholeiitic to calcalkaline mantle-derived mafic magmas may have been largely contaminated by crustal materials, which may have triggered their sulphide saturation and segregation in the magmas as well as Ni-Cu mineralization, mostly at the base of the mafic-ultramafic intrusions. Structural analysis of the deformed gabbroic intrusions can help target Ni-Cu mineralization through reconstruction of their original configuration.

During the course of fieldwork this summer, forty-two whole-rock samples (including five gabbro samples from Corazon Mining Limited drillcore) were collected for geochemical analysis, including five for Sm-Nd isotopes and two for U-Pb zircon age determination. The geochronology work is to be carried out in collaboration with the Geological Survey of Canada through phase 6 of its Targeted Geoscience Initiative program (TGI-6). The results of the lab analyses are pending and will be reported in subsequent MGS publications.

Regional geology

The LLGB, an important element of the Paleoproterozoic Trans-Hudson orogen (Hoffman, 1988; Lewry and Collerson, 1990; Ansdell, 2005; Corrigan et al., 2007, 2009; Corrigan, 2012), is endowed with several styles of mineralization, such as volcanogenic massive sulphide (VMS) zinc-copper (Zn-Cu), magmatic nickel-copper-cobalt (Ni-Cu-Co) and orogenic gold (Au; Figure GS2023-9-1). This belt is bounded to the north by the Southern Indian domain and flanked to the south by the Kisseynew domain (Gilbert et al., 1980; Zwanzig and Bailes, 2010; Martins et al., 2022). It is composed of two east- to northeast-trending, steeply dipping belts (Figure GS2023-9-1) consisting of various supracrustal rocks of the Wasekwan group that were intruded by granitoid plutons of the 1.89–1.87 Ga Pool Lake intrusive suite (Baldwin et al., 1987). Younger, molasse-type sedimentary rocks of the Sickle group (≥1.836 Ga; see Lawley et al., 2020) unconformably overlie the Wasekwan group and the Pool Lake intrusive suite. Based on their crosscutting relationships with the Sickle group, the granitoid intrusions in the LLGB are divided into pre- and post-Sickle intrusions. The supracrustal rocks and the granitoid rocks experienced peak amphibolite-facies metamorphism at ca. 1.81–1.80 Ga (Lawley et al., 2020, 2023). Gabbros in the LLGB were metamorphosed to amphibolites or metagabbros in terms of their mineral assemblage; however, this report omits the prefix 'meta' in the rock names for brevity.

Significant differences in the geology and geochemistry of the northern and southern belts of the LLGB may reflect regional differences in tectonic settings obscured by structural transposition of multiple deformation events (D_1 to D_6; Zwanzig, 2000; Beaumont-Smith and Böhm, 2002, 2003, 2004; Jones et al., 2006). The northern and southern belts contain disparate volcanic assemblages that were later structurally juxtaposed, likely representing a tectonic collage (Zwanzig et al., 1999) formed by northward subduction, followed by contraction and underthrusting of the Kisseynew domain beneath the LLGB during terminal collision (White et al., 2000). Field observations and historical drilling records indicate the presence of disseminated to massive sulphides (e.g., sphalerite, chalcopyrite, pyrrhotite) in the Wasekwan supracrustal rocks, including the Fox VMS Zn-Cu ore deposit (Gilbert et al., 1980; Fedikow and Gale, 1982; Baldwin, 1989; Ferreira, 1993; Yang and Beaumont-Smith, 2015; Yang, 2022).

Geological settings

Recent bedrock geological mapping demonstrates that various gabbroic intrusions occur in both the northern and southern belts of the LLGB, including the Lynn Lake (A plug, EL plug), Fraser Lake, Ralph Lake, Cartwright Lake, Motriuk Lake, White Owl Lake, Gemmell Lake, Southern Cockeram Lake and Snake Lake areas (Figure GS2023-9-1). It should be noted that the Motriuk Lake plug comprises very coarse grained pyroxenite (Yang, 2019), which displays cumulative texture and contains abnormally high Cr values (1540 ppm; see Yang, 2023, Table 1_2), and that the Cartwright Lake intrusion has the highest MS values (80×10^{-3} to 150×10^{-3} SI; this study) registered in the gabbroic rocks of the LLGB, although no notable Ni-Cu mineralization is evident in its exposures. These gabbroic intrusions are all ascribed to the pre-Sickle intrusive suite and detailed descriptions of the gabbroic rocks can be found in the MGS publications by Yang and Beaumont-Smith (2015, 2016, 2017), Yang and Lawley (2018), and Yang (2019, 2021, 2022). Bulk-rock geochemical data of representative samples for these intrusions are tabulated in DRI2023013[1] (Yang, 2023); acquisition of these data began in 2015, when the current mapping project started.

The Lynn Lake and Fraser Lake gabbroic intrusions are the focus of the following sections as they host magmatic Ni-Cu ore deposits. The other intrusions are barren, although some of their outcrops show evidence of trace sulphide dissemination.

Lynn Lake gabbroic intrusion

The Lynn Lake gabbroic intrusion (Childs, 1950; Gilbert et al., 1980; Yang and Beaumont-Smith, 2015) comprises two separate plugs; A plug (~4 km^2) and EL plug (~0.12 km^2; Figure GS2023-9-2). The A plug contains approximately 28.4 Mt of ore grading 0.91% Ni and 0.49% Cu, with an average Ni/Cu ratio of 1.86,

[1] MGS Data Repository Item DRI2023013, containing the data or other information sources used to compile this report, is available online to download free of charge at https://manitoba.ca/iem/info/library/downloads/index.html, or on request from minesinfo@gov.mb.ca, or by contacting the Resource Centre, Manitoba Economic Development, Investment, Trade and Natural Resources, 360-1395 Ellice Avenue, Winnipeg, Manitoba R3G 3P2, Canada.

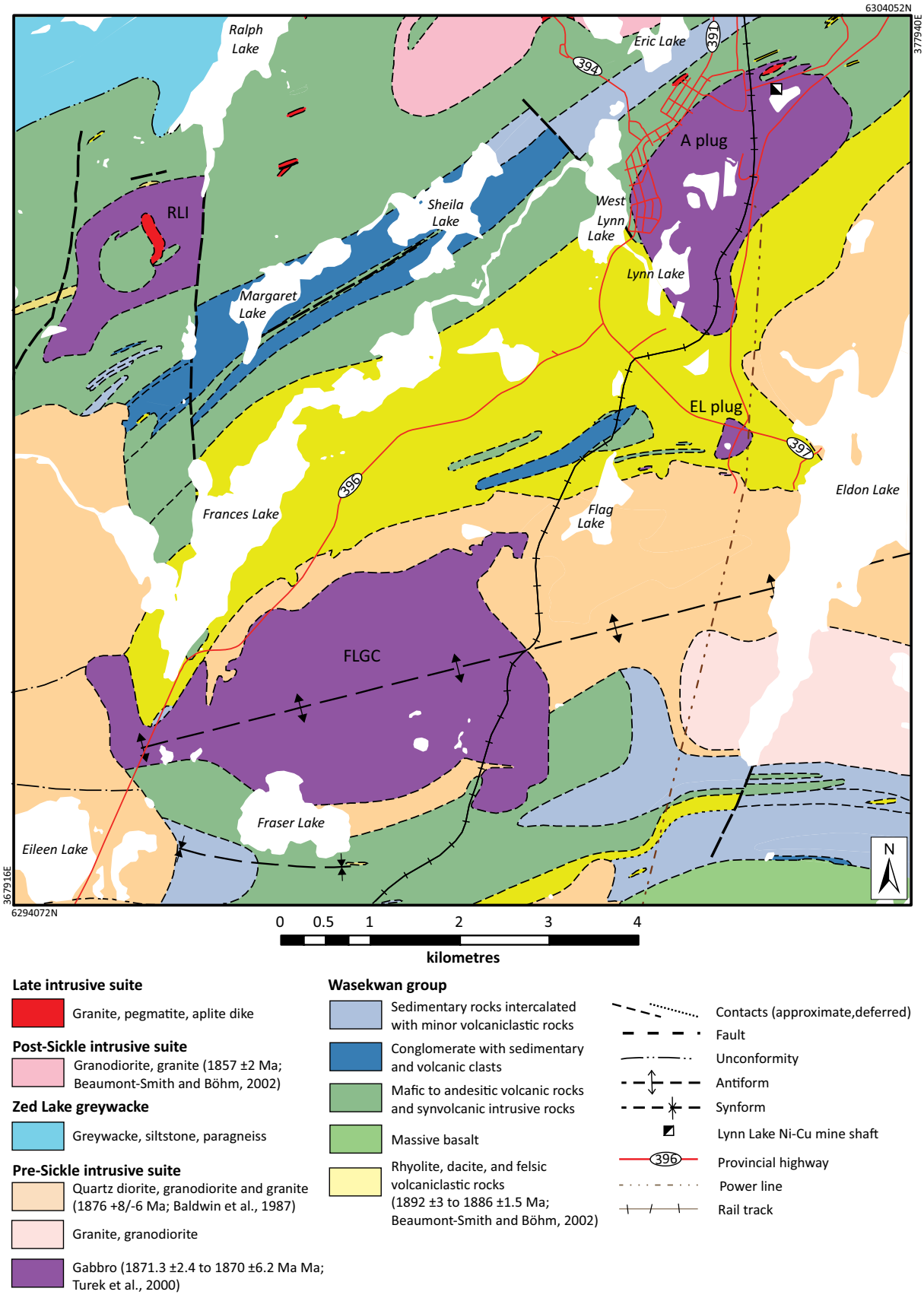

Figure GS2023-9-2: *Geology of gabbroic intrusions in the Lynn Lake area (modified from Gilbert et al., 1980; Yang and Beaumont-Smith, 2015; Manitoba Agriculture and Resource Development, 2021; Yang, 2021), showing geological relationships between the Lynn Lake A plug and EL plug, and the Fraser Lake gabbro complex associated with magmatic nickel-copper mineralization. Abbreviations: FLGC, Fraser Lake gabbro complex; RLI, Ralph Lake intrusion.*

and the EL plug has 1.9 Mt of ore grading 2.07% Ni and 0.76% Cu, with a Ni/Cu ratio of 2.72 (Pinsent, 1980). Some 16.3 Mt of ore grading 0.77% Ni and 0.33% Cu was produced from 1953 to 1976; a significant amount of Ni-Cu ore remains unmined below ground (https://corazon.com.au), where high concentrations of Co are also to be found (see below).

A plug

The A plug is emplaced into the Wasekwan group volcanic to volcaniclastic rocks and appears to be a vertical intrusion, with fabrics generally parallel to the regional structural trend (Pinsent, 1980; Dunsmore, 1986; Yang and Beaumont-Smith, 2015). Inclusions of the country rocks are variable in composition, size and shape; some of the xenoliths display diffusive edges, indicative of assimilation by intruding mafic magmas (Figure GS2023-9-3a). Contact-metamorphism aureoles are not well developed, likely due to a relatively smaller difference in temperature between the supracrustal succession and the intrusion. The A plug is composed primarily of medium-grained gabbro (and/or amphibolite) associated with minor peridotite, norite, mottled gabbro and diorite to quartz diorite. Magmatic fractionation led to the formation of very coarse grained to pegmatitic leucogabbro to anorthositic gabbro as in situ patches and/or pods in the intrusion (Figure GS2023-9-3b). More ultramafic phases are noted to occur mostly in the western section of the A plug, where they are associated with most of the Ni-Cu sulphide mineralization (Pinsent, 1980; Dunsmore, 1986).

Late diabase dikes of about 10 to 50 cm in width, trending north-northeast and west-northwest, cut the A plug gabbro intrusion in places. The diabase dikes have higher MS values (1.38×10^{-3} to 1.808×10^{-3} SI) than the A plug gabbros (0.23×10^{-3} to 0.954×10^{-3} SI). This confirms that both the magnetic high and low domains are present in the A plug, as demonstrated by detailed magnetic survey data collected by Corazon Mining Limited (https://corazon.com.au).

EL plug

The EL plug, dated at 1871.3 ±2.4 Ma (Turek et al., 2000), was emplaced into the ca. 1892–1886 Ma Lynn Lake rhyolite of the Waskewan group (Gilbert et al., 1980; Pinsent, 1980; Dunsmore, 1986; Beaumont-Smith and Böhm, 2002). There is no sign of a chilled margin on the contact of the EL plug with the Wasekwan rhyolitic volcanic to volcaniclastic rocks, although xenoliths of felsic to mafic volcanic rocks are evident. This plug shows a cored pipe structure narrowing from a surface diameter of about 500 m to a diameter of 200 m at depth (Pinsent, 1980).

The EL plug consists dominantly of medium-grained gabbro with minor diorite and peridotite, with an outer margin of contact-diorite and gabbro, and an inner core of gabbro (and/or amphibolite) and peridotite (Pinsent, 1980; Dunsmore, 1986). Locally, primary layering is well preserved, manifested by alternating plagioclase- and amphibole-rich layering (Figure GS2023-9-3c). As with the A plug, late mafic, west-northwest-trending (diabase) dikes cut the EL plug (Figure GS2023-9-3d); these are likely postmineralization dikes (Pinsent, 1980). Notably, there is no remarkable difference in the MS values between the dikes (0.613×10^{-3} to 0.725×10^{-3} SI) and EL gabbros (0.418×10^{-3} to 0.704×10^{-3} SI).

High-grade mineralization consists mainly of sulphide breccia-type ore in the core of the EL plug from the surface to about 300 m in depth; however, low-grade disseminated ore extends from the surface to about 925 m in depth (Pinsent, 1980). Primary sulphide minerals are pyrrhotite, pentlandite and chalcopyrite, with lesser to trace amounts of pyrite and sphalerite.

Fraser Lake gabbro complex

The Fraser Lake gabbro complex (FLGC; Hulbert, 1978), dated at 1870 ±6.2 Ma (Turek et al., 2000), is a tabular intrusion about 9.2 km^2 in area (Childs, 1950; Gilbert et al., 1980). The FLGC intrudes the Wasekwan group supracrustal rocks and has been cut by large granitoid plutons (Figure GS2023-9-2). Field observations revealed the presence of diverse volcaniclastic to basaltic xenoliths in the FLGC (Figure GS2023-9-3e), which is cut by granite dikes (Figure GS2023-9-3f). At contact zones, both volcanic and gabbroic inclusions are evident in the granitoid plutons southeast of Frances Lake and southwest of Flag Lake.

The FLGC is composed mostly of medium-grained gabbro with minor peridotite and amphibole (pseudomorphs of pyroxene)-phyric fine-grained gabbro. The gabbro appears homogeneous in mineralogy (~55 to 70% amphibole and ~30 to 45% plagioclase) and texture in most outcrops. It is metamorphosed to amphibolite facies, resulting in amphibole replacing primary pyroxene despite preservation of the magmatic texture. Green fibrous amphibole (actinolite-tremolite) occurs mostly along foliation planes and is likely attributed to retrograde metamorphism at greenschist-facies conditions. Minor amounts of finely disseminated sulphide minerals (e.g., pyrrhotite, chalcopyrite) and magnetite occur in gabbroic outcrops, but no major accumulation of sulphide is evident in most exposures (e.g., Childs, 1950; Hulbert, 1978; Dunsmore, 1986; this study). In 2023, Corazon Mining Limited reported an intersection of 55.4 m of sulphide (pyrrhotite-pentlandite-chalcopyrite) mineralization, including metre-scale intervals of massive sulphide intermixed with semimassive to disseminated sulphides, within the FLGC.

Magnetic susceptibility values of the FLGC gabbros range from 0.547×10^{-3} to 8.22×10^{-3} SI despite the presence of magnetic low and high domains within the intrusion, which are higher than most of the surrounding granitoid rocks (mostly $<0.5 \times 10^{-3}$ SI), as shown in an aeromagnetic survey image from Corazon Mining Limited (https://corazon.com.au).

Geochemical characteristics

Geochemical data including sulphur (S) and oxygen (O) stable isotope data of mafic-ultramafic rocks in the LLGB (Zwanzig et

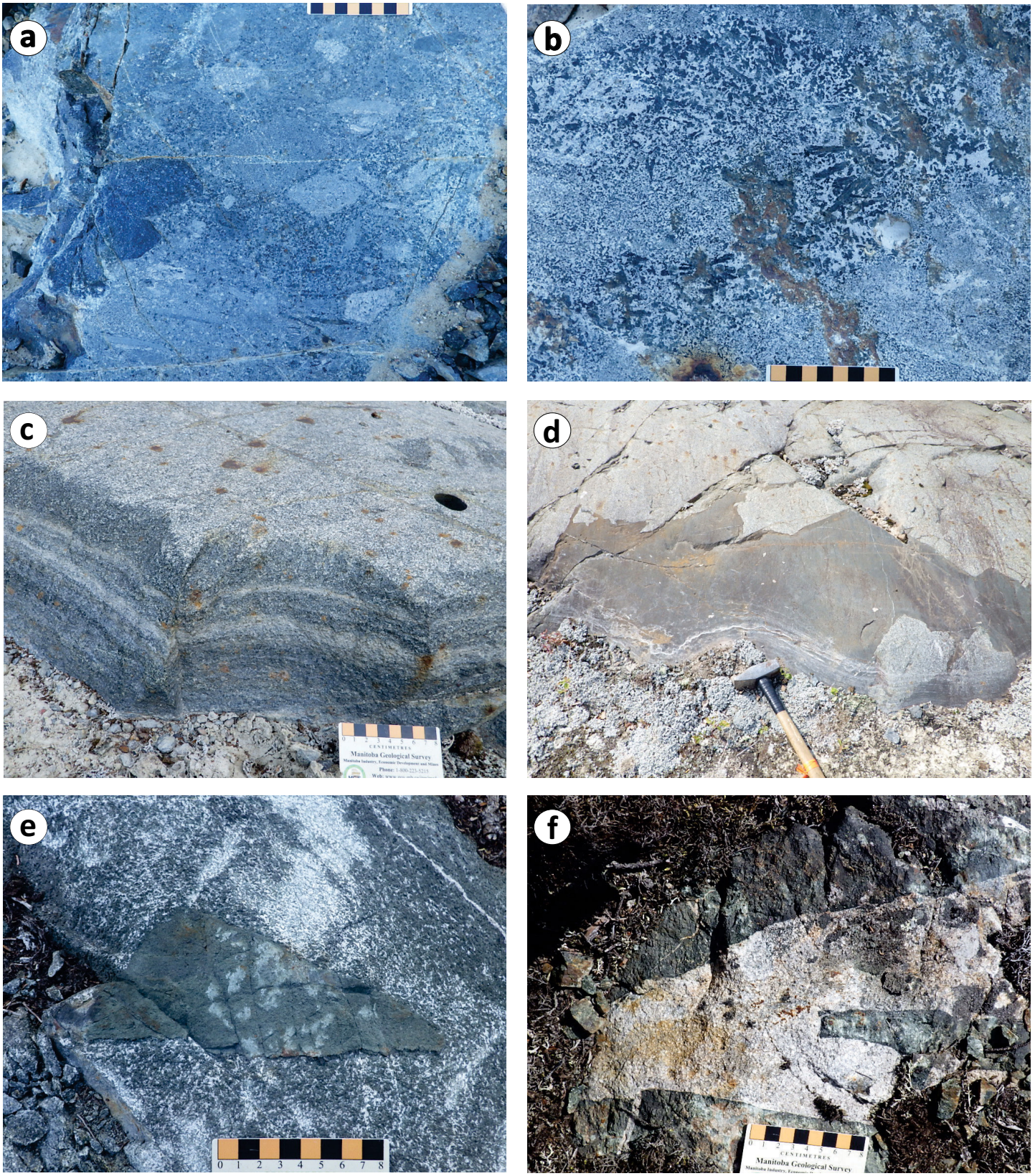

Figure GS2023-9-3: *Field photographs of gabbroic rocks in the Lynn Lake area, showing* ***a****) subrounded to angular xenoliths of basaltic to felsic and sedimentary rocks trapped in the A plug (375972E, 6302850N), with some xenoliths showing diffusive edges that is evidence for assimilation by intruding mafic magmas;* ***b****) very coarse grained to pegmatitic leucogabbro to anorthositic gabbro pod and/or patch in the A plug (375959E, 6302859N);* ***c****) primary layering in the EL plug (375836E, 6299203N);* ***d****) fine-grained mafic (diabase) dike cutting the EL plug gabbro (375836E, 6299203N);* ***e****) angular aphanitic basalt xenolith in the Fraser Lake gabbro complex (372429E, 6297114N);* ***f****) medium-grained granite dike cutting the Fraser Lake gabbro complex (372461E, 6297269N). All co-ordinates are in UTM Zone 14, NAD83.*

al., 1999; Hulbert and Scoates, 2000; Peck et al., 2000; Beaumont Smith, 2008), together with recently acquired data presented in DRI2023013 (Yang, 2023), are reviewed to extract some critical information about the metallogeny of the gabbroic intrusions. As the datasets contain different suites of elements analyzed using diverse techniques[2], these data are plotted separately in a set of diagrams in the following subsections to illustrate discernable features that can be used for fingerprinting magmatic sources and processes as well as recognizing Ni-Cu mineralization in the mafic-ultramafic mineral systems.

Geochemically, the gabbroic samples from both the fertile and barren intrusions are dominantly metaluminous and tholeiitic (or calcic) to calcalkaline based on the Shand index (Maniar and Piccoli, 1989) as well as the Rittmann Serial Index (σ) and Nb/Y ratios (Yang, 2007; X.M. Yang and C.J.M. Lawley, work in progress). These samples also show typical volcanic-arc signatures, as manifested by enrichment in large-ion lithophile elements relative to high-field-strength elements (Yang and Lawley, 2018; Yang, 2023). They are coeval with the Farley Lake A-type granites that were interpreted to have been emplaced in an intra-oceanic–arc setting (X.M. Yang and C.J.M. Lawley, work in progress), although part of the Wasekwan volcanic rocks is suggested to have formed at a rifted continental margin (e.g., Glendenning et al., 2015).

The niobium/thorium (Nb/Th) ratios of mafic-ultramafic rocks are sensitive to crustal contamination and copper/zirconium (Cu/Zr) ratios are sensitive to the state of sulphur saturation in the mafic melts (Lightfoot et al., 1990). Figure GS2023-9-4

[2] For details concerning detection limits, precision and accuracy of the analyses, please refer to Zwanzig et al. (1999), Hulbert and Scoates (2000), Peck et al. (2000), Beaumont Smith (2008) and Yang (2023).

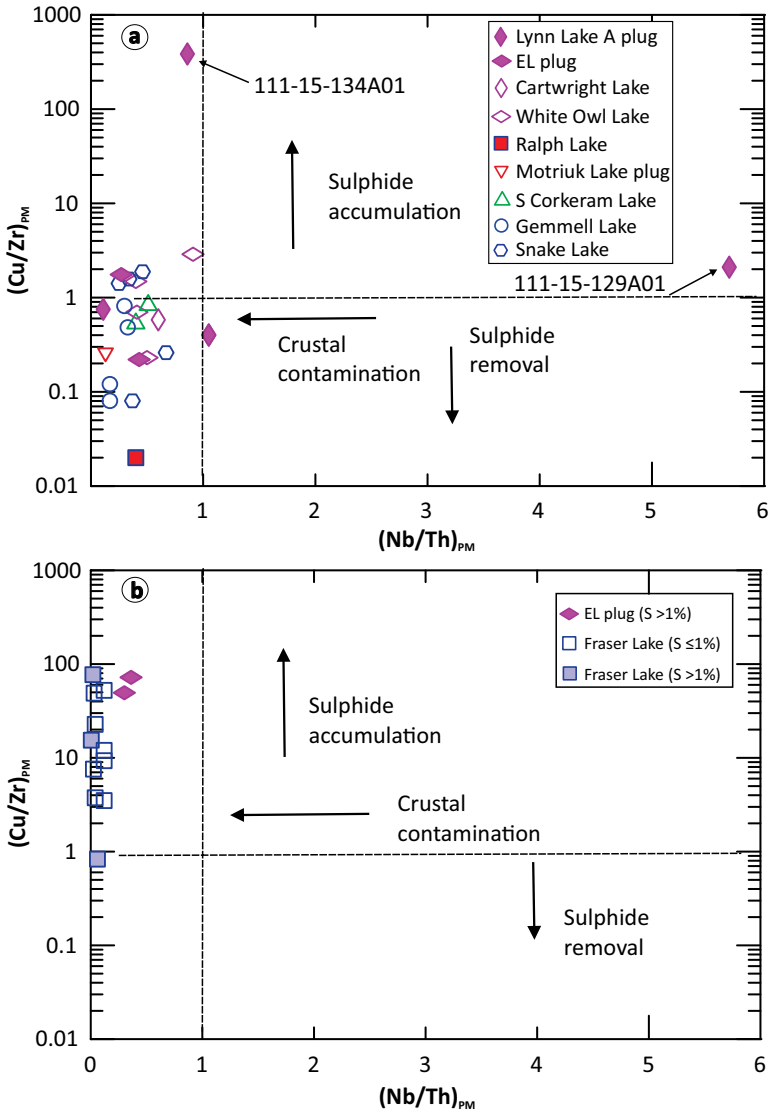

***Figure GS2023-9-4**: Plots of $(Cu/Zr)_{PM}$ versus $(Nb/Th)_{PM}$ in: **a)** unmineralized gabbroic rocks; and **b)** sulphide-bearing gabbros in the Lynn Lake greenstone belt. Data plotted in (a) from Yang (2023) and in (b) from Hulbert and Scoates (2000). Primitive mantle-normalized ($_{PM}$) values from McDonough and Sun (1995).*

shows variation in the primitive mantle-normalized $(Cu/Zr)_{PM}$ and $(Nb/Th)_{PM}$ ratios of selected gabbroic intrusions, which suggests that crustal contamination plays an important role in triggering sulphide saturation in mafic melts, regardless if it is mineralized or barren (Figure GS2023-9-4a, b). Sample 111-15-129A01 has an unusually high $(Nb/Th)_{PM}$ of 5.7, most likely reflecting the accumulation of Nb-bearing phases such as ilmenite or magnetite (Figure GS2023-9-4a). A mineralized gabbro (sample 111-15-134A01) has a $(Cu/Zr)_{PM}$ ratio >437 and a $(Nb/Th)_{PM}$ ratio of 0.75 (Yang, 2023) as Cu content is higher than 10 000 ppm (Yang, 2023, Table 2), and is plotted on the diagram using the analytical maximum value to illustrate the remarkable effect of sulphide accumulation (Figure GS2023-9-4a). Furthermore, the presence of high Zn contents in the Lynn Lake Ni-Cu deposits (Hulbert and Scoates, 2000; Peck et al., 2000) suggests that VMS deposits associated with the Wasekwan volcanic and sedimentary succession assimilated by intruding mafic-ultramafic magmas may have played an important role in providing external sulphur required for their sulphide saturation, segregation and mineralization (e.g., Lightfoot et al., 1990; Barnes and Lightfoot, 2005).

The Lynn Lake intrusion and the FLGC samples (n = 78; Hulbert and Scoates, 2000) display high sulphur/selenium (S/Se) ratios (the plot of S/Se versus aluminium oxide [Al_2O_3] is not shown), mostly higher than the mantle value (3000 ±200; see Lorand et al., 2021). This further confirms the effect of crustal contamination on these intrusions.

Metal tenors (i.e., metal contents in 100% sulphide) are calculated for 262 samples in the dataset of Peck et al. (2000), with the assumption that the metals are hosted in pyrrhotite, pentlandite and chalcopyrite (Barnes and Lightfoot, 2005). The calculated metal tenors display positive correlation between platinum, palladium and gold (Pt+Pd+Au) in ppb versus (Pt+Pd) in ppm/(Cu+Ni) in wt. % ratios, with a correlation coefficient (r) of 0.58 (n = 262). They show that barren gabbro intrusions (e.g., Cartwright Lake) appear to have higher (Pt+Pd)/(Cu+Ni) ratios and metal tenors (Figure GS2023-9-5). This indicates that the sulphide (melt) in the Cartwright Lake intrusion may have been in equilibrium with a larger volume of mafic melts (i.e., higher R-factor), possibly without extensive early sulphide segregation. In contrast, mineralized gabbro intrusions (e.g., the Lynn Lake A plug and EL plug) show relatively lower metal tenors and (Pt+Pd)/(Cu+Ni) ratios, likely reflecting either sulphide segregation from a smaller volume of mafic (silicate) melts (e.g., Naldrett, 2004) or earlier sulphide segregation in a dynamic magmatic system.

Most of the Lynn Lake intrusion samples display (Pt+Pd)/(Cu+Ni) ratios <0.1, whereas the FLGC complex and the Cartwright Lake intrusion samples have ratios >0.1 (Figure GS2023-9-5)

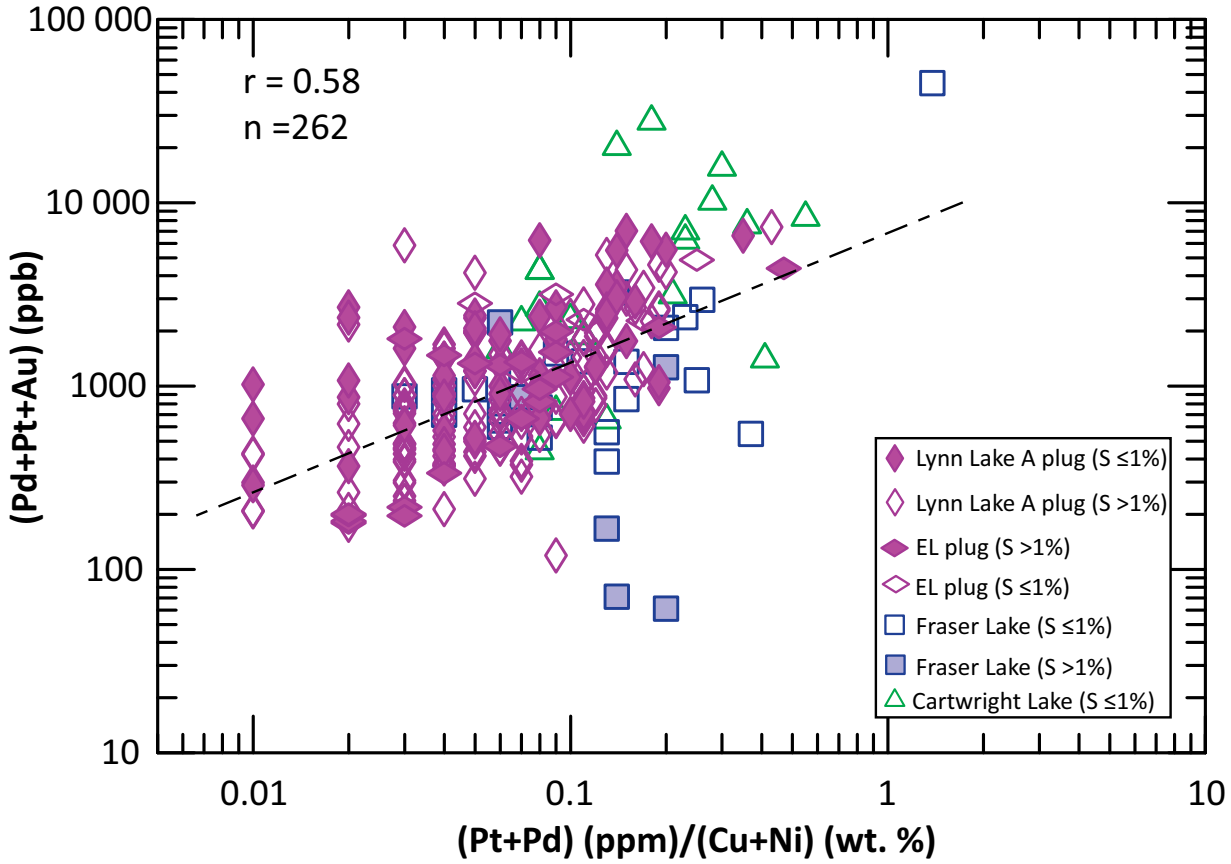

***Figure GS2023-9-5**: Diagram of metal tenors (Pt+Pd+Au) in ppb versus (Pt+Pd) in ppm/(Cu+Ni) in wt. % on the basis of 100% sulphide for gabbro intrusions in the Lynn Lake greenstone belt. Data from Peck et al. (2000). Calculation of metal tenors based on the formula in Barnes and Lightfoot (2005). Abbreviation: n, number.*

and higher metal tenors of (Pt+Pd), which suggests that there might not have been a significant segregation of sulphide melt from the mafic melts. On the other hand, a substantial amount of sulphides may have separated from the Lynn Lake mafic melts and concentrated at the base of the intrusion or the exit of the conduit/pathway connected to emplacement sites.

Highly siderophile elements (HSE)

Highly siderophile elements (HSE) include PGEs (osmium [Os], iridium [Ir], ruthenium [Ru], Pt, rhodium [Rh], Pd) as well as rhenium (Re) and Au (Lorand et al., 2021). The PGEs can be divided further into two subgroups: the iridium subgroup (IPGEs: Os, Ir, Ru) and the palladium subgroup (PPGEs: Pt, Rh, Pd). Not only do HSEs show strong affinity for a metallic iron phase but they are also strongly chalcophile and thus concentrate in a sulphide phase, when lacking the metallic iron phase in mafic-ultramafic systems (Rollinson and Pease, 2021). Therefore, HSEs together with chalcophile elements (Ni, Cu) whole-rock data are commonly used to investigate the fractionation and the state of sulphur saturation of mafic-ultramafic magmas and associated ore systems (Rollinson, 1993; Naldrett, 2004; Barnes and Lightfoot, 2005; Lorand et al., 2021; Rollinson and Pease, 2021; Orejana et al., 2023).

Seventy-eight bulk-rock and/or ore samples (Hulbert and Scoates, 2000) were analyzed for HSEs, which are evaluated and used to characterize PGE geochemistry of the Lynn Lake and Fraser Lake gabbroic intrusions. Based on S contents, these samples can be subdivided into two subgroups: unmineralized (S ≤1 wt. %) and mineralized (S >1 wt. %). Table GS2023-9-1 presents a summary of the data, revealing that the mineralized samples are relatively depleted in total (Σ) PGE concentrations (ranging from 27.2 to 222.1 ppb) and enriched in Co contents (i.e., averaging 855 ppm in the A plug and 410 ppm in the EL plug), when comparing with most major and giant magmatic Ni-Cu mineral deposits elsewhere (e.g., Naldrett, 2004). However, the unmineralized samples have abnormal ΣPGE contents of 9.4 to 53 ppb.

The HSEs with Ni and Cu data for the gabbroic rocks and associated ores (Hulbert and Scoates, 2000) in the LLGB are plotted in the order of their compatibility during partial melting of the mantle in Figure GS2023-9-6. It shows that the contents of less HSE-compatible elements (i.e., Au, Re, Pd) are higher and decrease in the direction of more compatible elements (i.e., Ru, Ir, Os), which suggests that the HSEs are controlled strongly by partial melting of the mantle. The most compatible element Ni and least compatible element Cu, both of which are attributed to chalcophile affinity, show much higher concentrations than the HSEs that had previously partitioned into the iron-nickel (Fe-Ni) core during differentiation from the mantle (Barnes and Lightfoot, 2005) and that were subsequently controlled by sulphide-silicate melts separation. The Ni-Cu deposits formed by the mantle-derived magmas tend to be depleted in PGEs relative to Ni and Cu, thus demonstrating a trough-shaped pattern in the primitive mantle-normalized profile, with typical positive steep HSE patterns of the gabbroic hosts (Figure GS2023-9-6).

According to Rollinson and Pease (2021), the primitive mantle-normalized (PM) ratio of $(Pd/Ir)_{PM}$ in mafic-ultramafic rock(s) can be used as a measure of the degree of fractionation during partial melting of the mantle, reflecting the fractionation between Pd (more incompatible) and Ir (more compatible) in PGEs. Most samples from the Lynn Lake intrusion and FLGC display enrichment of PPGEs over IPGEs indicated by $(Pd/Ir)_{PM}$ >1.0, which points to a lack of monosulphide solid solution in the residues during mantle partial melting. In this context, general positive correlation between Re/Os and $(Pd/Ir)_{PM}$ ratios (not shown), with a large range from 1 to 200 evident in the Lynn Lake intrusion (A and EL plugs), indicates that separation of monosulphide solid solution plays a key role (Lorand et al., 2021) in fractionating PPGEs from IPGEs in residual sulphide melts that formed Ni-Cu mineralization.

Platinum-group elements (PGEs)

Most of the samples with low S contents from the database (Hulbert and Scoates, 2000) were reanalyzed for a suite of elements (such as Pd, Pt, Au, S, Ni, Cu, Zn, Se, Te) by Peck et al. (2000). This review of the dataset confirms that the PGE content of the Lynn Lake samples is much lower than that of major to giant magmatic Ni-Cu-PGE deposits elsewhere (Naldrett, 2004; Barnes and Lightfoot, 2005). For instance, average ΣPGE content of 22 samples in the Lynn Lake A plug deposit is 222.1 ppb (Table GS2023-9-1), which is equivalent to 7.2 times the content of primitive mantle (Palme and O'Neill, 2014). As a comparison, average ΣPGE contents of those major to giant deposits (e.g., Naldrett, 2004) are 100 to 1000 times greater than that of primitive mantle.

Figure GS2023-9-7a shows that the Lynn Lake intrusion (A and EL plugs) is compositionally different from the FLGC based on Σ(PGE+Au) concentrations and (PPGE/IPGE) ratios. The Lynn Lake intrusion displays relatively high Σ(PGE+Au) values and less fractionation of PPGEs from IPGEs, which suggests that it may have been derived from a higher degree of partial melting of the mantle or formed by earlier phases of fractionating mantle-derived magmas. On the other hand, the FLGC contains lower Σ(PGE+Au) contents (<80 ppb; Figure GS2023-9-7b) with higher fractionation of PPGEs from IPGEs, likely reflecting an origin from a lower degree of partial melting of the mantle or derived from late phases of fractionating mantle-derived magmas. To determine which process was involved requires more precise age data because of the lack of field relationships for these two intrusions. Because their ages are identical within analytical uncertainties, the difference in timing between emplacement of the Lynn Lake intrusion (EL plug 1871 ±2.4 Ma) and that of the Fraser Lake (1870 ±6.2 Ma) intrusions could not be distinguished given the available age data (Turek et al., 2000).

Table GS2023-9-1: Average bulk-rock and ore sample geochemical compositions for the Lynn Lake and Fraser Lake gabbroic intrusions (data from Hulbert and Scoates, 2000).

Intrusion	Lynn Lake A plug				Lynn Lake EL plug		Fraser Lake gabbro complex			
Type	Unmineralized		Mineralized		Mineralized		Unmineralized		Mineralized	
	Average	SD	Average	SD	Average	SD	Average	SD	Average	SD
n	5		22		22		23		6	
SiO_2 (wt. %)	50.14	2.13	27.72	19.20	40.60	6.32	49.06	1.94	37.02	17.46
TiO_2	0.23	0.04	0.17	0.15	0.21	0.09	0.58	0.69	0.34	0.21
Al_2O_3	7.04	4.51	3.70	3.66	8.29	3.00	16.49	3.65	11.71	7.01
$Fe_2O_3^T$	11.03	2.87	39.44	23.41	22.80	7.96	11.91	2.79	na	
MnO	0.17	0.05	0.11	0.06	0.14	0.04	0.17	0.04	0.13	0.08
MgO	20.28	5.67	9.69	7.83	12.84	4.75	11.25	4.37	8.03	6.73
CaO	6.56	3.42	4.48	3.40	7.33	2.22	9.05	1.95	5.50	4.01
Na_2O	0.64	0.72	0.38	0.45	0.71	0.33	1.64	0.66	1.05	0.65
K_2O	0.46	0.62	0.23	0.32	0.18	0.12	0.28	0.18	0.58	0.32
P_2O_5	0.04	0.01	0.03	0.03	0.04	0.04	0.17	0.28	0.09	0.06
S	0.44	0.23	18.19	14.95	8.34	4.89	0.45	0.21	10.85	14.57
LOI	0.54	0.23	18.52	14.72	8.48	4.88	0.67	0.29	10.92	14.56
Total	97.13		100.55		101.62		101.27		75.35	
V (ppm)	112	9	87	43	99	30	209	176	248	161
Cr	1582	701	786	524	747	543	339	290	297	388
Co	73	22	855	695	410	265	65	19	98	37
Cu	520	369	8362	6562	4732	2949	226	105	652	318
Ni	1324	606	26805	22280	10005	6056	358	241	1037	664
Zn	110	28	210	87	150	47	100	22	1175	1840
Se	1.3	0.8	39.9	27.3	15.2	7.5	0.7	0.4	1.7	0.4
Te	na		2.6	1.3	1.4	1.4	0.3	0.0	0.3	0.0
La	7.8	0.8	6.4	2.2	5.6	2.8	8.1	7.7	6.8	6.2
Yb	0.6	0.2	0.3	0.4	0.3	0.5	0.6	0.4	2.2	1.7
Nb	3.8	1.1	4.0	1.2	3.8	1.4	1.0	1.0	0.8	1.0
Th	0.0	0.0	0.0	0.0	0.2	0.5	2.7	1.9	18.7	23.6
U	0.0	0.0	0.1	0.4	0.0	0.0	0.5	1.0	10.8	15.4
Y	3.6	2.3	2.4	3.5	3.2	3.9	2.7	3.6	4.7	5.1
Zr	22.6	6.5	11.0	10.1	23.8	21.3	6.4	8.1	17.8	19.8
Rb	7.6	15.9	2.7	7.7	0.6	1.2	5.3	5.0	17.3	13.5
Sr	100.8	138.5	47.5	73.2	146.3	101.6	399.6	128.8	214.0	185.1
Ba	96.0	141.0	81.0	80.8	56.8	30.5	80.4	40.5	106.7	51.6
Os (ppb)	1.0	0.0	2.7	1.8	1.6	1.5	0.5	0.0	0.5	0.0
Ir	0.8	0.3	3.9	3.3	1.0	1.5	0.1	0.0	0.2	0.1
Ru	8.0	5.0	16.1	11.4	8.8	14.0	0.5	0.0	0.5	0.0
Rh	0.6	0.2	5.2	4.6	1.8	2.2	0.6	0.2	0.8	0.6
Pt	32.0	15.4	104.0	93.1	87.5	80.0	3.7	4.8	12.7	18.1
Pd	10.6	5.1	90.2	48.8	70.0	45.2	4.0	3.6	12.5	10.4
Au	12.4	4.7	42.6	32.3	49.4	34.3	6.1	2.7	18.7	19.6
Re	2.0	0.0	3.6	2.6	15.2	16.7	0.5	0.0	18.2	27.9
ΣPGE	53.0		222.1		170.6		9.4		27.2	
PPGE	43.2		199.4		159.2		8.3		26.0	
IPGE	9.8		22.7		11.4		1.1		1.2	
PPGE/IPGE	4.4		8.8		13.9		7.6		22.1	
Σ(PGE+Au)	65.4		264.7		220.0		15.5		45.8	

Data from Hulbert and Scoates (2000).
PGE, platinum-group elements (Ru, Rh, Pa, Os, Ir, Pt); IPGE: Os, Ir, Ru; PPGE: Pt, Rh, Pd.
Abbreviations: LOI, loss-on-ignition; n, number of samples; na, not analyzed; SD, standard deviation.

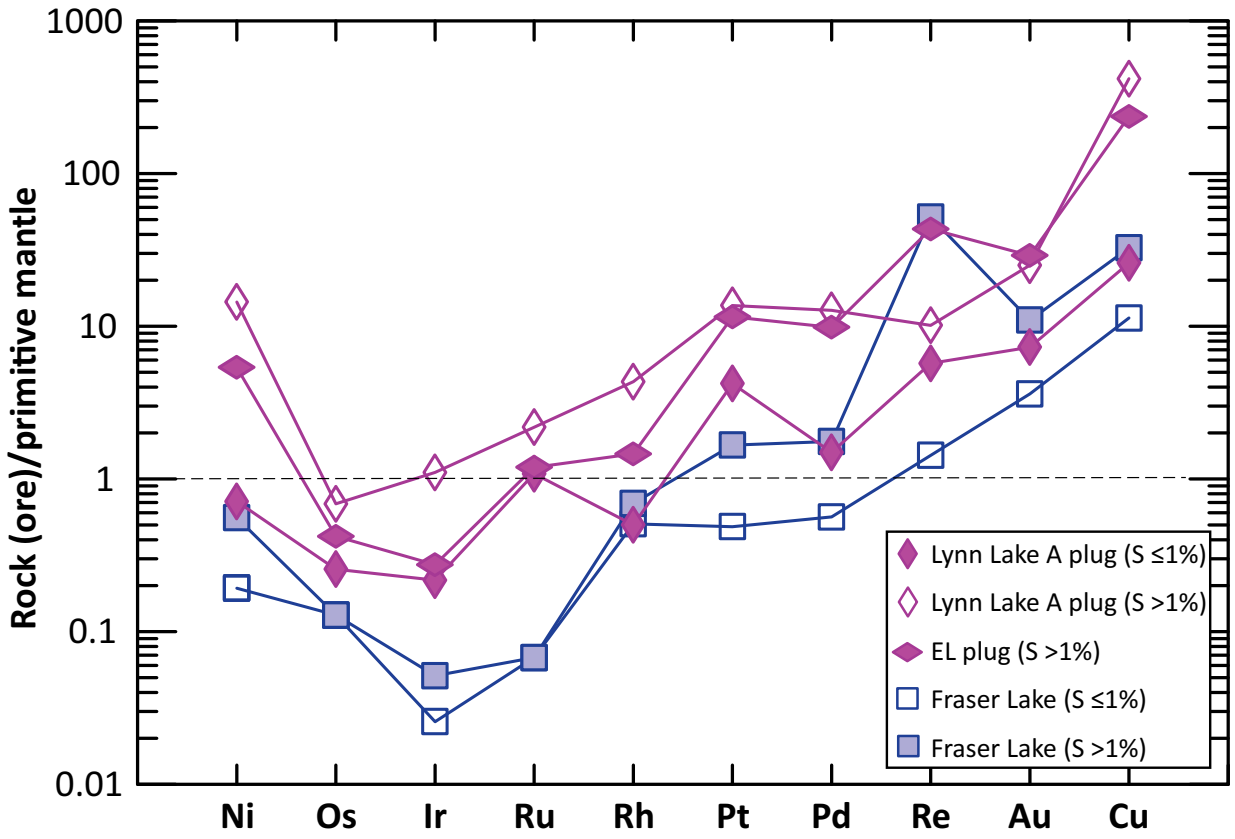

***Figure GS2023-9-6**: Diagram of primitive mantle-normalized highly siderophile elements together with contents of strongly chalcophile elements Ni, Re and Cu for mineralized and unmineralized gabbroic rocks in the Lynn Lake Ni-Cu deposit and the Fraser Lake gabbro complex. From left to right, the elements are arranged in order of decreasing mantle compatibility (after Rollinson and Pease, 2021). Data from Hulbert and Scoates (2000). Normalized values of primitive mantle from Palme and O'Neill (2014).*

Using MgO (wt. %) as a proxy for fractionation degrees of the mafic magmas versus the Σ(PGE+Au) values reveals that gabbroic samples of the Lynn Lake intrusion (A plug and EL plug) plot along a different trajectory from those of the FLGC, which are characterized by relatively lower concentrations of precious metals (<80 ppb) and lower MgO contents (Figure GS2023-9-7b). With an increasing degree of fractionation, Σ(PGE+Au) values appear to elevate in the Lynn Lake intrusion, whereas such values decline in the FLGC. This strongly suggests that different petrogenetic processes may have formed these two intrusions. Accumulative phases (e.g., olivine) are not likely involved before sulphide segregation from silicate melts in the Lynn Lake intrusion under dynamic environment conditions. In contrast, mafic-phase crystallization occurs simultaneously with sulphide separation from the magmas in the FLGC. Based on magnesium oxide (MgO) and Al_2O_3 contents, the FLGC is more evolved in chemical composition than the Lynn Lake intrusion (A and EL plugs; GS2023-9-7b). This observation is also supported by the fact that the FLGC contains relatively lower Ni and Co contents than the Lynn Lake intrusion (Table GS2023-9-1).

Sulphur- and oxygen-isotope compositions

Sulphur stable isotope composition of 53 bulk-sulphide samples reported in Hulbert and Scoates (2000) are plotted in Figure GS2023-9-8a to show the isotopic variation in three gabbroic intrusions of the LLGB (i.e., the Lynn Lake [A and EL plugs], Cartwright Lake and Fraser Lake). The distribution of $\delta^{34}S$ ratios in these intrusions are skewed to relatively lighter sulphur-isotope–composition values, with a mean value of 2.53 ±2.65‰. Most samples from the Lynn Lake intrusion (i.e., A and EL plugs) and the Cartwright Lake gabbro intrusion display a very narrow range of $\delta^{34}S$ ratios from 0.0 to 3.0‰, similar to typical mantle-derived mafic rocks (e.g., Rollinson and Pease, 2021). The FLGC shows a larger range of $\delta^{34}S$ values from 1.0 to 13.2‰, although mainly falling between 1.0 and 6.0‰. The $\delta^{34}S$ values indicate that the gabbros may have been affected by marine sedimentary rocks rich in heavy sulphur isotopes (up to 20‰) or contaminated by felsic rocks (e.g., Rollinson, 1993; Yang and Lentz, 2010; Rollinson and Pease, 2021). High Zn contents in mineralized gabbroic samples and massive sulphide ores (Table GS2023-9-1; Hulbert and Scoates, 2000; Peck et al., 2000) from the FLGC imply that the complex may have been contaminated (through assimilation) by VMS in the Wasekwan group.

Oxygen stable isotope composition of 41 bulk-rock samples (Hulbert and Scoates, 2000) also show a skewed distribution of the $\delta^{18}O$ values (Figure GS2023-9-8b), with a mean value of 6.9 ±1.2‰. Interestingly, the FLGC demonstrates a much smaller range in $\delta^{18}O$ ratios (5.5 to 7.0‰) than those of the Lynn Lake

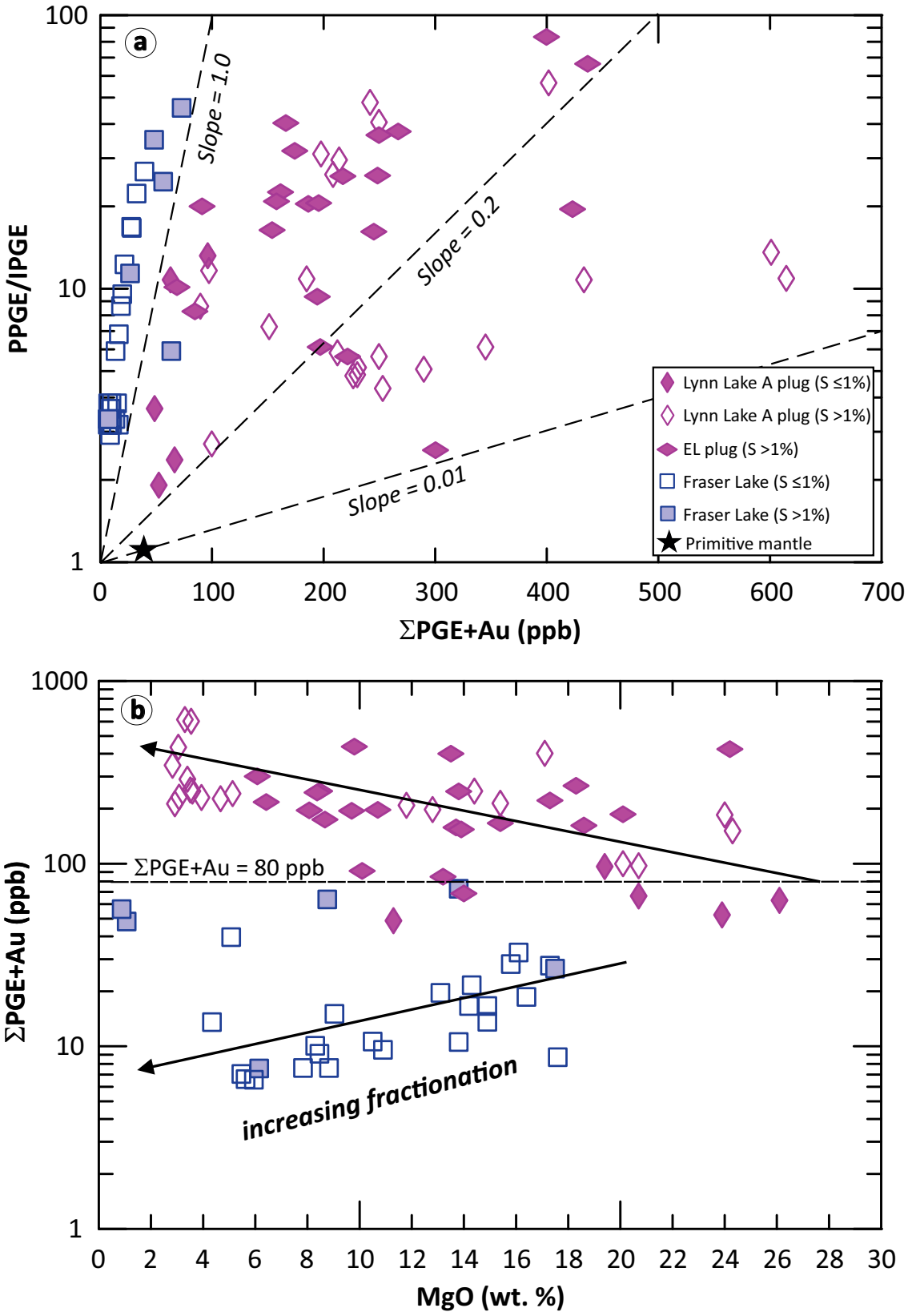

***Figure GS2023-9-7**: Discrimination diagram of geochemical data from the Lynn Lake and Fraser Lake gabbroic intrusions in the Lynn Lake greenstone belt, showing: **a)** Σ(PGE+Au) (ppb) contents versus (IPGE/PPGE) ratios and three dashed lines labelled slope equal to 1.0, 0.2 and 0.01, from left to right, indicating that fractionation between PPGE and IPGE decreases with increasing Σ(PGE+Au) concentrations; **b)** Σ(PGE+Au) (ppb) versus MgO (wt. %). Data from Hulbert and Scoates (2000). Values of primitive mantle from Palme and O'Neill (2014), with (IPGE/PPGE) ratio of 1.1, Σ(PGE+Au) content of 32.4 ppb and MgO of 36.77 wt. %. Abbreviations: PGE, platinum group element; IPGE, iridium platinum-group element subgroup (Os, Ir, Ru); PPGE, palladium platinum-group element subgroup (Pt, Rh, Pd).*

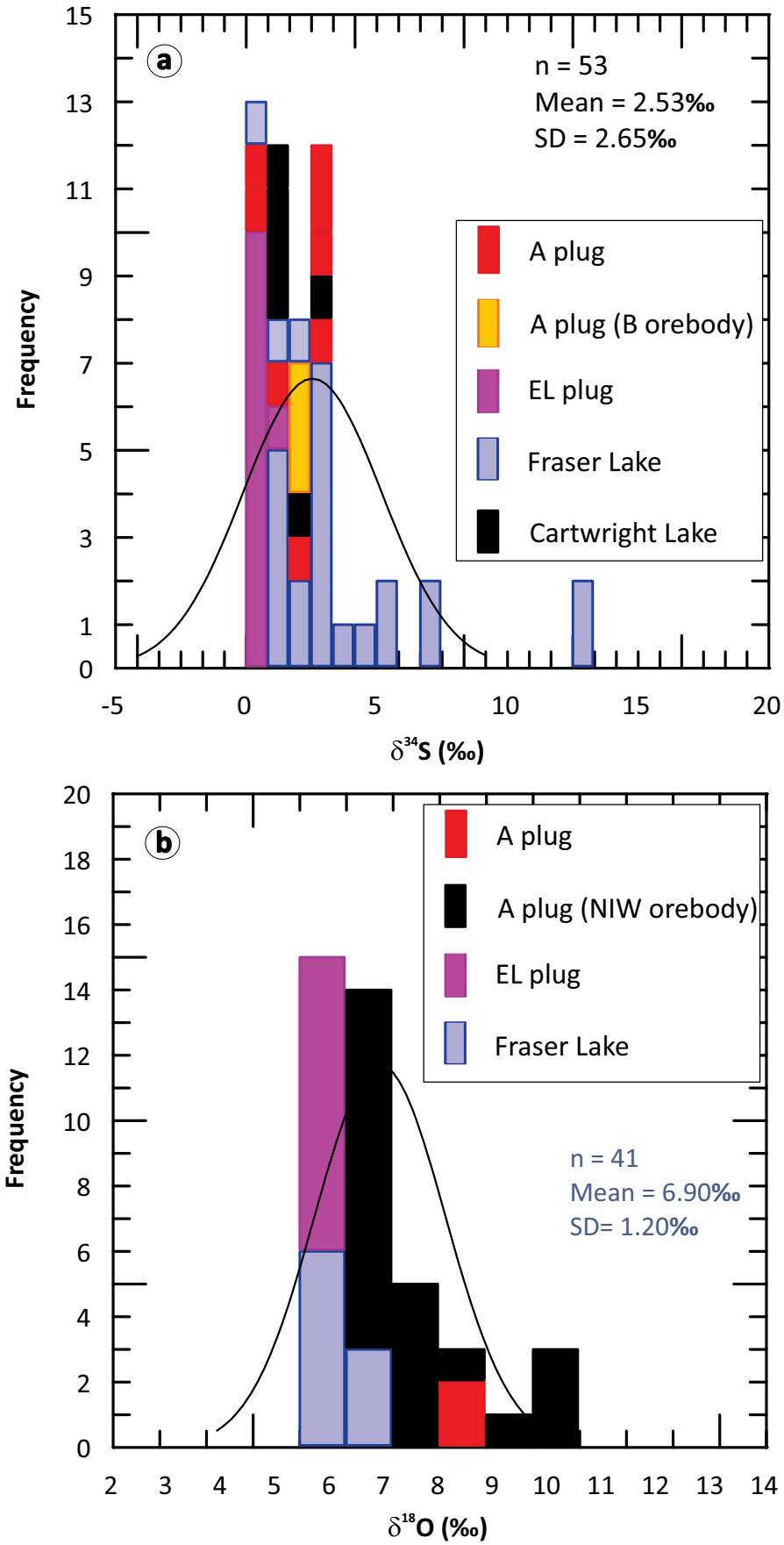

***Figure GS2023-9-8**: Histogram of **a)** sulfur-isotope composition (‰) and **b)** oxygen-isotope composition (‰) of bulk-sulphide samples from three gabbro intrusions in the Lynn Lake greenstone belt (data from Hulbert and Scoates, 2000). Abbreviations: n, number of samples; SD, standard deviation.*

intrusion (A plug and EL plug), mostly within the mantle value (5.7 ±0.2‰; Rollinson, 1993; Rollinson and Pease, 2021), which is consistent with a mantle-derived origin. In contrast, samples from the Lynn Lake A plug and EL plug show a large range of $\delta^{18}O$ values (5.5 to 10.0‰), which suggests that they may have interacted with low-temperature fluids, given that their $\delta^{34}S$ remains unaffected. These observations are consistent with the conclusion arrived at by Pinsent (1980), whereby hydrothermal activity may have locally remobilized sulphide ore and formed secondary sulphide veinlets in faults and/or fractures.

Economic considerations

Gabbroic rocks in the Lynn Lake intrusion host to Ni-Cu deposit and the FLGC are synchronous with the 1872.6 ±2.5 Ma A-type granites in the northern belt of the LLGB (Yang and Lawley, 2018), which suggests that these mafic and granite intrusions may have been emplaced into an intra-oceanic–arc extensional setting. Such an arc association at the Lynn Lake Ni-Cu deposit is underreported in the literature. There is likely a broader implication for how granitoid geochemistry (X.M. Yang and C.J.M. Lawley, work in progress) can track geodynamic transition(s) linked to the origin of VMS Cu-Zn, magmatic Ni-Cu and orogenic Au deposits in the Lynn Lake greenstone belt.

Gabbroic intrusions in the Lynn Lake greenstone belt are evaluated for fertility in terms of geological settings; field relationships; variation in lithologies and fabrics; and geochemical as well as S and O stable isotope features. Most gabbro intrusions display magmatic-arc signatures, but only some host magmatic Ni-Cu deposits. Crustal contamination of the mantle-derived mafic magmas appears to have triggered sulphide saturation and segregation in the magmas and mineralization systems. Sulphide-bearing Wasekwan sediments, and VMS deposits in particular, are potential candidates for providing external sulphur to the gabbroic intrusions. However, assimilation from the Wasekwan felsic volcanic to volcaniclastic rocks (e.g., Lynn Lake rhyolite) likely facilitates sulphide saturation in the intruding magmas. Cumulative mafic phases at contact zones seem to have higher potential to host Ni-Cu sulphide mineralization. A use of the PGE discrimination diagram (Figure GS2023X08-7) presented in this report demonstrates the difference between the Lynn Lake intrusion (A plug and EL plug) and the Fraser Lake gabbro complex, indicative of two distinct mineralizing systems.

Tube- and funnel-shaped orebodies evident in the Lynn Lake intrusion (i.e., A plug and EL plug) are probably the result of deformation (primarily D_2) from the original horizontal to a subvertical state. Therefore, structural analysis is a key to reconstructing the three-dimensional orientation of the intrusions and their hosted orebodies. However, it is likely that remobilization of the sulphide ores and redistribution may have taken place locally due to the deformation events(s) and metamorphism.

Acknowledgments

The author thanks W. Ezeana for providing enthusiastic field and laboratory assistance as well as for compiling some historical data; C. Epp and P. Belanger for thorough logistical support and processing of the samples; and H. Adediran and G. Keller for technical support. Thanks go to C.J.M. Lawley and M.G. Houlé of the Geological Survey of Canada for their collaboration and engaging discussions. The manuscript benefited greatly from constructive reviews by M. Rinne and T. Kennedy, technical editing by M.-F. Dufour and report layout by C. Steffano. Corazon Mining Limited is acknowledged for allowing field crew access to its property and drillcore; L. Hulbert and K. Wells are thanked in particular for guidance in core sampling; and Alamos Gold Inc. for providing their support.

References

Ansdell, K.M. 2005: Tectonic evolution of the Manitoba-Saskatchewan segment of the Paleoproterozoic Trans-Hudson Orogen, Canada; Canadian Journal of Earth Sciences, v. 42, p. 741–759.

Baldwin, D.A. 1989: Mineral deposits and occurrences in the Lynn Lake area, NTS 64C/14; Manitoba Energy and Mines, Geological Services, Mineral Deposit Series Report No. 6, 130 p., URL <https://manitoba.ca/iem/info/libmin/MDS6.zip> [September 2023].

Baldwin, D.A., Syme, E.C., Zwanzig, H.V., Gordon, T.M., Hunt, P.A. and Stevens, R.P. 1987: U-Pb zircon ages from the Lynn Lake and Rusty Lake metavolcanic belts, Manitoba: two ages of Proterozoic magmatism; Canadian Journal of Earth Sciences, v. 24, p. 1053–1063.

Barnes, S.-J. and Lightfoot, P.C. 2005: Formation of magmatic nickel-sulfide ore deposits and processes affecting their copper and platinum-group element contents; *in* Economic Geology 100th Anniversary Volume, J.W. Hedenquist, J.F.H. Thompson, R.J. Goldfarb and J.P. Richards (ed.), p. 179-213, URL <https://doi.org/10.5382/AV100.08>.

Barnes, S.J., Malitch, K.N. and Yudovskaya, M.A. 2020: Introduction to a Special Issue on the Norilsk-Talnakh Ni–Cu–platinum group element deposits: Economic Geology, v. 115, p. 1157–1172, URL <https://doi.org/10.5382/econgeo.4750>.

Beaumont-Smith, C.J. 2008: Geochemistry data for the Lynn Lake greenstone belt, Manitoba (NTS 64C11–16); Manitoba Science, Technology, Energy and Mines, Manitoba Geological Survey, Open File OF2007-1, 5 p., URL <https://manitoba.ca/iem/info/libmin/OF2007-1.zip> [October 2021].

Beaumont-Smith, C.J. and Böhm, C.O. 2002: Structural analysis and geochronological studies in the Lynn Lake greenstone belt and its gold-bearing shear zones (NTS 64C10, 11, 12, 14, 15 and 16), Manitoba; *in* Report of Activities 2002, Manitoba Industry, Trade and Mines, Manitoba Geological Survey, p. 159–170, URL <https://manitoba.ca/iem/geo/field/roa02pdfs/GS-19.pdf> [October 2021].

Beaumont-Smith, C.J. and Böhm, C.O. 2003: Tectonic evolution and gold metallogeny of the Lynn Lake greenstone belt, Manitoba (NTS 64C10, 11, 12, 14, 15 and 16), Manitoba; *in* Report of Activities 2003, Manitoba Industry, Economic Development and Mines, Manitoba Geological Survey, p. 39–49, URL <https://manitoba.ca/iem/geo/field/roa03pdfs/GS-06.pdf> [October 2021].

Beaumont-Smith, C.J. and Böhm, C.O. 2004: Structural analysis of the Lynn Lake greenstone belt, Manitoba (NTS 64C10, 11, 12, 14, 15 and 16); *in* Report of Activities 2004, Manitoba Industry, Economic Development and Mines, Manitoba Geological Survey, p. 55–68, URL <https://manitoba.ca/iem/geo/field/roa04pdfs/GS-06.pdf> [October 2021].

Beaumont-Smith, C.J., Machado, N. and Peck, D.C. 2006: New uranium-lead geochronology results from the Lynn Lake greenstone belt, Manitoba (NTS 64C11–16); Manitoba Science, Technology, Energy and Mines, Manitoba Geological Survey, Geoscientific Paper GP2006-1, 11 p., URL <https://manitoba.ca/iem/info/libmin/GP2006-1.pdf> [October 2021].

Begg, G.C., Hronsky, J.A.M., Arndt, N.T., Griffin, W.L., O'Reilly, S.Y. and Hayward, N. 2010: Lithospheric, cratonic, and geodynamic setting of Ni-Cu-PGE sulfide deposits; Economic Geology, v. 105, p. 1057–1070, URL <https://doi.org/10.2113/econgeo.105.6.1057>.

Childs, G.D. 1950: The petrology of the Myrna Lake and Fraser Lake basic intrusive bodies; M.Sc. thesis, University of Manitoba, Winnipeg, Manitoba, 102 p.

Corrigan, D. 2012: Paleoproterozoic crustal evolution and tectonic processes: insights from the LITHOPROBE program in the Trans-Hudson orogen, Canada; Chapter 4 *in* Tectonic Styles in Canada: The LITHOPROBE Perspective, J.A. Percival, F.A. Cook and R.M. Clowes (ed.), Geological Association of Canada, Special Paper 49, p. 237–284.

Corrigan, D., Galley, A.G. and Pehrsson, S. 2007: Tectonic evolution and metallogeny of the southwestern Trans-Hudson Orogen; *in* Mineral Deposits of Canada: A Synthesis of Major Deposit-Types, District Metallogeny, the Evolution of Geological Provinces, and Exploration Methods, W.D. Goodfellow (ed.), Geological Association of Canada, Mineral Deposits Division, Special Publication 5, p. 881–902.

Corrigan, D., Pehrsson, S., Wodicka, N. and de Kemp, E. 2009: The Palaeoproterozoic Trans-Hudson Orogen: a prototype of modern accretionary processes; *in* Ancient Orogens and Modern Analogues, J.B. Murphy, J.D. Keppie, and A.J. Hynes (ed.), Geological Society of London, Special Publications, v. 327, p. 457–479.

Deng, Y.-F., Song,, X.-Y., Xie, W., Chen, L.-M., Yu, S.-Y., Yuan, F., Hollings, P. and Wei, S. 2022: The role of external sulfur in triggering sulfide immiscibility at depth: evidence from the Huangshan–Jingerquan Ni-Cu metallogenic belt, NW China; Economic Geology, v. 117, p. 1867–1879, URL <https://doi.org/10.5382/econgeo.4928>.

Dunsmore, D.J. 1986: A paleomagnetic study of the Lynn Lake and Fraser Lake gabbros, Northern Manitoba; M.Sc. thesis, University of Windsor, 116 p., URL <https://scholar.uwindsor.ca/etd/6795> [June 2023].

Fedikow, M.A.F. and Gale, G.H. 1982: Mineral deposit studies in the Lynn Lake area; *in* Report of Field Activities 1982, Manitoba Department of Energy and Mines, Mineral Resources Division, p. 44–54, URL <https://manitoba.ca/iem/geo/field/rfa1982.pdf> [October 2022].

Ferreira, K.J. 1993: Mineral deposits and occurrences in the Laurie Lake area, NTS 64C/12; Manitoba Energy and Mines, Geological Services, Mineral Deposit Series Report No. 9, 101 p., URL <https://manitoba.ca/iem/info/libmin/MDS9.zip> [September 2022].

Gilbert, H.P. 1993: Geology of the Barrington Lake–Melvin Lake–Fraser Lake area; Manitoba Energy and Mines, Geological Services, Geological Report GR87-3, 97 p., URL <https://manitoba.ca/iem/info/libmin/GR87-3.zip> [October 2021].

Gilbert, H.P., Syme, E.C. and Zwanzig, H.V. 1980: Geology of the metavolcanic and volcaniclastic metasedimentary rocks in the Lynn Lake area; Manitoba Energy and Mines, Mineral Resources Division, Geological Paper GP80-1, 118 p., URL <https://manitoba.ca/iem/info/libmin/GP80-1.zip> [October 2021].

Glendenning, M.W.P., Gagnon, J.E. and Polat, A. 2015: Geochemistry of the metavolcanic rocks in the vicinity of the MacLellan Au-Ag deposit and an evaluation of the tectonic setting of the Lynn Lake greenstone belt, Canada: evidence for a Paleoproterozoic-aged rifted continental margin; Lithos, v. 233, p. 46–68.

Hastie, E.C.G., Gagnon, J.E. and Samson, I.M. 2018: The Paleoproterozoic MacLellan deposit and related Au-Ag occurrences, Lynn Lake greenstone belt, Manitoba: an emerging, structurally controlled gold camp; Ore Geology Reviews, v. 94, p. 24–45.

Hoffman, P.H. 1988: United plates of America, the birth of a craton: Early Proterozoic assembly and growth of Laurentia; Annual Reviews of Earth and Planetary Sciences, v. 16, p. 543–603.

Houlé, M.G., Gibson, H.L., Lesher, C.M., Davis, P.C., Cas, R.A.F., Beresford, S.W. and Arndt, N.T. 2008: Komatiitic sills and multigenerational peperite at Dundonald Beach, Abitibi greenstone belt, Ontario: volcanic architecture and nickel sulfide distribution; Economic Geology, v. 103, p. 1269–1284, URL <https://doi.org/10.2113/gsecongeo.103.6.1269>.

Hulbert, L.J. 1978: Geology of the Fraser Lake Gabbro Complex, Manitoba; M.Sc. thesis, University of Regina, Regina, Saskatchewan, 414 p.

Hulbert, L.J. and Scoates, R.F.J. 2000: A map of magmatic nickel, copper±platinum group element occurrences and mafic-ultramafic intrusions in Manitoba; Manitoba Industry, Trade and Mines, Economic Geology Report ER2000-1, CD-ROM, URL <https://manitoba.ca/iem/info/libmin/ER2000-1.zip> [May 2023].

Jones, L.R., Lafrance, B. and Beaumont-Smith, C.J. 2006: Structural controls on gold mineralization at the Burnt Timber Mine, Lynn Lake Greenstone Belt, Trans-Hudson Orogen, Manitoba; Exploration and Mining Geology, v. 15, p. 89–100.

Lawley, C.J.M., Yang, X.M., Selby, D., Davis, W., Zhang, S., Petts, D.C. and Jackson, S.E. 2020: Sedimentary basin controls on orogenic gold deposits: new constraints from U-Pb detrital zircon and Re-Os sulphide geochronology, Lynn Lake greenstone belt, Canada; Ore Geology Reviews, v. 126, art. 103790, URL <https://doi.org/10.1016/j.oregeorev.2020.103790>.

Lawley, C.J.M., Schneider, D.A., Camacho, A., McFarlane, C.R.M., Davis, W.J. and Yang, X.M. 2023: Post-orogenic exhumation triggers gold mobility in the Trans-Hudson orogen: new geochronology results from the Lynn Lake Greenstone Belt, Manitoba, Canada; Precambrian Research, v. 395, art. 107127, URL <https://doi.org/10.1016/j.precamres.2023.107127>.

Lewry, J.F. and Collerson, K.D. 1990: The Trans-Hudson Orogen: extent, subdivisions and problems; *in* The Early Proterozoic Trans-Hudson Orogen of North America, J.F. Lewry and M.R. Stauffer (ed.), Geological Association of Canada, Special Paper 37, p. 1–14.

Lightfoot, P.C. 2017: Nickel sulfide ores and impact melts: origin of the Sudbury igneous complex; Elsevier, Amsterdam, Netherlands, 662 p.

Lightfoot, P.C., Naldrett, A.J., Gorbachev, N.S., Doherty, W. and Fedorenko, V.A. 1990: Geochemistry of the Siberian Trap of the Noril'sk area, USSR, with implications for the relative contributions of crust and mantle to flood basalt magmatism; Contributions to Mineralogy and Petrology, v. 104, p. 631–644, URL <https://doi.org/10/1007/BF01167284>.

Lorand, J.-P., Pont, S., Guttierez-Narbona, R. and Gervilla, F. 2021: Chalcophile-siderophile element systematics and regional-scale magmatic percolation in the Ronda peridotite massif (Spain); Lithos v. 380–381, art. 105901, URL <https://doi.org/10.1016/j.lithos.2020.105901>.

Maniar, P.D. and Piccoli, P.M. 1989: Tectonic discrimination of granitoids; Geological Society of America, Bulletin, v. 101, p. 635–643, URL <https://doi.org/10.1130/0016-7606(1989)101%3C0635:TDOG%3E2.3.CO;2>.

Manitoba Agriculture and Resource Development 2021: Lynn Lake, Manitoba (NTS 64C14); Manitoba Agriculture and Resource Development, Manitoba Geological Survey, Lynn Lake Bedrock Compilation Map 64C14, scale 1:50 000, URL <https://manitoba.ca/iem/info/libmin/lynn_lake_compilation_2021.zip> [October 2021].

Manitoba Energy and Mines 1986: Granville Lake, NTS 64C; Manitoba Energy and Mines, Minerals Division, Bedrock Geology Compilation Map 64C, scale 1:250 000, URL <https://manitoba.ca/iem/info/libmin/bgcms/bgcms_granville_lake.pdf> [October 2022].

Martins, T., Rayner, N., Corrigan, D. and Kremer, P. 2022: Regional geology and tectonic framework of the Southern Indian domain, Trans-Hudson orogen, Manitoba; Canadian Journal of Earth Sciences, v. 59, p. 371–388, URL <https://doi.org/10.1139/cjes-2020-0142>.

Maxeiner, R.O. and Rayner, N.M. 2017: Geology, U–Pb zircon geochronology, and geochemistry of PGE-bearing Neoarchean and Paleoproterozoic gabbroic rocks of the Peter Lake domain, southern Hearne craton, Canada; Canadian Journal of Earth Sciences, v. 54, p. 587–608, URL <https://doi.org10.1139/cjes-2016-0104>.

McDonough, W.F. and Sun, S.-s. 1995: The composition of the Earth; Chemical Geology, v. 120, p. 223–253, URL <https://doi.org/10.1016/0009-2541(94)00140-4>.

Naldrett, A.J. 2004: Magmatic sulfide deposits: geology, geochemistry and exploration; Springer-Verlag, Berlin, Germany, 727 p., URL <https://doi.org/10.1007/978-3-662-08444-1>.

Orejana, D., García-Rodríguez, M., de Ignacio, C. and Ruiz-Molina, S. 2023: Noble and base metal geochemistry of late- to post-orogenic mafic dykes from central Spain; Mineralogy and Petrology, URL <https://doi.org/10.1007/s00710-023-00844-z>.

Palme, H. and O'Neill, H. 2014: Cosmochemical estimates of mantle composition; *in* Treatise on Geochemistry (2nd edition), H.D. Holland and K.K. Turekian (ed.), v. 3, Elsevier, Oxford, United Kingdom, p. 1–39, URL <https://doi.org/10.1016/B978-0-08-095975-7.00201-1>.

Peck, D.C., Theyer, P., Hulbert, L., Xiong, J., Fedikow, M.A.F. and Cameron, H.D.M. 2000: Preliminary exploration database for platinum-group elements in Manitoba; Manitoba Industry, Trade and Mines, Manitoba Geological Survey, Open File OF2000-5, CD-ROM, URL <https://manitoba.ca/iem/info/libmin/OF2000-5.zip> [May 2023].

Pinsent, R.H. 1980: Nickel-copper mineralization in the Lynn Lake gabbro; Manitoba Energy and Mines, Geological Services, Economic Geology Report ER79-3, 138 p., URL<https://manitoba.ca/iem/info/libmin/ER79-3.pdf > [May 2023].

Rollinson, H.R. 1993: Using geochemical data: evaluation, presentation, interpretation; Routledge, London, United Kingdom, 384 p., URL <https://doi.org/10.4324/9781315845548>.

Rollinson, H. and Pease, V. 2021: Using geochemical data to understand geological processes (2nd edition); Cambridge University Press, Cambridge, United Kingdom, 346 p., URL <https://doi.org/10.1017/9781108777834>.

Syme, E.C. 1985: Geochemistry of metavolcanic rocks in the Lynn Lake Belt; Manitoba Energy and Mines, Geological Services/Mines Branch, Geological Report GR84-1, 84 p.

Turek, A., Woodhead, J. and Zwanzig H.V. 2000: U-Pb age of the gabbro and other plutons at Lynn Lake (part of NTS 64C); *in* Report of Activities 2000, Manitoba Industry, Trade and Mines, Manitoba Geological Survey, p. 97–104, URL <https://manitoba.ca/iem/geo/field/roa00pdfs/00gs-18.pdf> [October 2021].

U.S. Geological Survey 2023: Nickel—Mineral Commodity Summaries 2023, URL <https://pubs.usgs.gov/periodicals/mcs2023/mcs2023-nickel.pdf> [September 2023].

White, D.J., Zwanzig, H.V. and Hajnal, Z. 2000: Crustal suture preserved in the Paleoproterozoic Trans-Hudson orogeny, Canada; Geology, v. 28, p. 527–530.

Yang, X.M. 2007: Using the Rittmann Serial Index to define the alkalinity of igneous rocks; Neues Jahrbuch für Mineralogie, v. 184, p. 95–103.

Yang, X.M. 2019: Preliminary results of bedrock mapping in the Gemmell Lake area, Lynn Lake greenstone belt, northwestern Manitoba (parts of NTS 64C11, 14); *in* Report of Activities 2019, Manitoba Agriculture and Resource Development, Manitoba Geological Survey, p. 10–29, URL <https://manitoba.ca/iem/geo/field/roa19pdfs/GS2019-2.pdf> [October 2021].

Yang, X.M. 2021: Bedrock mapping at Ralph Lake, Lynn Lake greenstone belt, northwestern Manitoba (part of NTS 64C14): preliminary results and geological implications; *in* Report of Activities 2021, Manitoba Agriculture and Resource Development, Manitoba Geological Survey, p. 40–58, URL <https://manitoba.ca/iem/geo/field/roa21pdfs/GS2021-5.pdf> [November 2021].

Yang, X.M. 2022: Preliminary results of bedrock geological mapping in the Fox mine−Snake Lake area, Lynn Lake greenstone belt, northwestern Manitoba (part of NTS 64C12); *in* Report of Activities 2022, Manitoba Natural Resources and Northern Development, Manitoba Geological Survey, p. 71–86, URL <https://manitoba.ca/iem/geo/field/roa22pdfs/GS2022-9.pdf> [November 2022].

Yang, X.M. 2023: Geochemical data of gabbroic rocks from the Lynn Lake greenstone belt, northwestern Manitoba (parts of NTS 64C10–12, 14–16); Manitoba Economic Development, Investment, Trade and Natural Resources, Manitoba Geological Survey, Data Repository Item DRI2023013, Microsoft® Excel® file.

Yang, X.M. and Beaumont-Smith, C.J. 2015: Granitoid rocks in the Lynn Lake region, northwestern Manitoba: preliminary results of reconnaissance mapping and sampling; *in* Report of Activities 2015, Manitoba Mineral Resources, Manitoba Geological Survey, p. 68–78, URL <https://manitoba.ca/iem/geo/field/roa15pdfs/GS-5.pdf> [October 2021].

Yang, X.M. and Beaumont-Smith, C.J. 2016: Geological investigations in the Farley Lake area, Lynn Lake greenstone belt, northwestern Manitoba (part of NTS 64C16); *in* Report of Activities 2016, Manitoba Growth, Enterprise and Trade, Manitoba Geological Survey, p. 99–114, URL <https://manitoba.ca/iem/geo/field/roa16pdfs/GS-9.pdf> [October 2021].

Yang, X.M. and Beaumont-Smith, C.J. 2017: Geological investigations of the Wasekwan Lake area, Lynn Lake greenstone belt, northwestern Manitoba (parts of NTS 64C10, 15); *in* Report of Activities 2017, Manitoba Growth, Enterprise and Trade, Manitoba Geological Survey, p. 117–132, URL <https://manitoba.ca/iem/geo/field/roa17pdfs/GS2017-11.pdf> [October 2021].

Yang, X.M. and Lawley, C.J.M. 2018: Tectonic setting of the Gordon gold deposit, Lynn Lake greenstone belt, northwestern Manitoba (parts of NTS 64C16): evidence from lithogeochemistry, Nd isotopes and U-Pb geochronology; *in* Report of Activities 2018, Manitoba Growth, Enterprise and Trade, Manitoba Geological Survey, p. 89–109, URL <https://manitoba.ca/iem/geo/field/roa18pdfs/GS2018-8.pdf> [October 2021].

Yang, X.M. and Lentz, D.R. 2010: Sulfur isotopic systematics of granitoids from southwestern New Brunswick, Canada: implications for magmatic-hydrothermal processes, redox conditions and gold mineralization; Mineralium Deposita, v. 45, p. 795–816, URL <https://doi.org/10.1007/s00126-010-0307-6>.

Yildirim, E., Yildirim, N., Dönmez, C., Günay, K., Korkmaz, T., Akyildiz, M. and Gören, B. 2020: Composition of Pancarli magmatic Ni-Cu±(PGE) sulfide deposit in the Cadomian–Avalonian Belt, eastern Turkey; Journal of Earth Science, v. 31, p. 536–550, URL <https://doi.org/10.1007/s12583-020-1299-5>.

Zwanzig, H.V. 2000: Geochemistry and tectonic framework of the Kisseynew Domain–Lynn Lake belt boundary (part of NTS 63P/13); *in* Report of Activities 2000, Manitoba Industry, Trade and Mines, Manitoba Geological Survey, p. 91–96, URL <https://manitoba.ca/iem/geo/field/roa00pdfs/00gs-17.pdf> [October 2021].

Zwanzig, H.V. and Bailes, A.H. 2010: Geology and geochemical evolution of the northern Flin Flon and southern Kisseynew domains, Kississing–File lakes area, Manitoba (parts of NTS 63K, N); Manitoba Innovation, Energy and Mines, Manitoba Geological Survey, Geoscientific Report GR2010-1, 135 p, URL <https://manitoba.ca/iem/info/libmin/GR2010-1.zip> [October 2021].

Zwanzig, H.V., Syme, E.C. and Gilbert, H.P. 1999: Updated trace element geochemistry of ca. 1.9 Ga metavolcanic rocks in the Paleoproterozoic Lynn Lake belt; Manitoba Industry, Trade and Mines, Geological Services, Open File Report OF99-13, 46 p., URL <https://manitoba.ca/iem/info/libmin/OF99-13.zip> [October 2021].

GS2023-10

Thompson Facility and Compound core recovery project, east-central Manitoba (parts of NTS 54C, 63P, 64A)

by C.G. Couëslan

Summary

A project was initiated in 2023 to salvage diamond-drillcore that has been stored outdoors at the Manitoba Geological Survey's Thompson Facility and Compound since the early 2000s. The drillcore boxes are in varying states of decay, with much of it in danger of becoming lost. Damaged boxes were either fixed or replaced, and missing, damaged or illegible box labels were replaced with metal DYMO® tags. The core was stacked back into new cross piles for greater stability, roofed with salvaged core boxes, and covered with tarps.

In Brief:

- A project was initiated to salvage archived drillcore stored outdoors at the Thompson Facility and Compound
- Damaged boxes were fixed or replaced, and relabelled if necessary
- Core boxes were re-stacked, roofed, and covered with tarps

Citation:
Couëslan, C.G. 2023: Thompson Facility and Compound core recovery project, east-central Manitoba (parts of NTS 54C, 63P, 64A); *in* Report of Activities 2023, Manitoba Economic Development, Investment, Trade and Natural Resources, Manitoba Geological Survey, p. 90–92.

Project introduction and progress

Diamond-drillcore has been stored in 70 outdoor cross piles at the Manitoba Geological Survey's Thompson Facility and Compound since the early 2000s and is in varying states of decay (Figure GS2023-10-1a). The aim of this project is to recover and/or document as much of the salvageable core as possible before it is lost. The majority of core was drilled during gold exploration programs in the Assean Lake area (Assessment Files 74035 and 74112, Manitoba Economic Development, Investment, Trade and Natural Resources, Winnipeg); however, core from north of the Fox River belt and north and southeast of Thompson are also present (Figure GS2023-10-2). It was decided to focus this summer's efforts on this latter core, which was drilled in remote and inaccessible parts of the province where our geological knowledge is limited. It is hoped that the recovered core can be moved to secure indoor storage where it will be available for future study by industry, academic and government geologists.

During July and August of 2023, the core was removed from the cross piles and laid out. Damaged boxes were either fixed or replaced, and missing, damaged or illegible box labels were replaced with metal DYMO® tags. The core was restacked in new cross piles. The cross piles were roofed with salvaged core boxes and covered with tarps (Figure GS2023-10-1b, c). Details of the recovered drillcore, including collar location, year drilled and name of exploration company that conducted the drilling, are listed in DRI2023006[1] (Couëslan, 2023).

Overall condition of the core was good; however, ultramafic rocks where generally found to be in poor condition from the many years of outdoor storage. Core recovery was close to 100%, with very few boxes being lost because of missing box tags, or core box collapse. Anywhere from 10 to 90% of core boxes were replaced in each cross pile. During recovery, it was found that some cross piles had become infested by carpenter ants. The debris created by the ants was washed out of the boxes whenever possible to reduce the likelihood of re-infestation, accumulation of moisture and promotion of rot.

In addition, drillcore that was salvaged in the fall of 2022 from the Thompson core shed, which collapsed in the winter of 2020, and was stacked in unsecured parallel piles were beginning to lean and collapse (Figure GS2023-10-1d). Tarps that were covering some of these piles had come loose and were only partially covering the core. An attempt was made to recover as much of the spilled core as possible, resulting in about 50% recovery. The piles were bound with steel strapping to prevent further loss of core, while ensuring that the tarps remain secure.

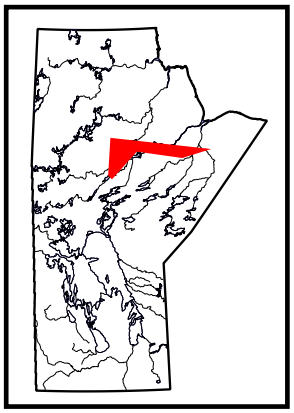

Economic considerations

Drillcore is a valuable resource that should be preserved, especially when it is drilled in inaccessible and remote areas. A conservative estimate of the cost to drill 181 holes would be in excess of $20

[1] MGS Data Repository Item DRI2023006, containing the data or other information sources used to compile this report, is available online to download free of charge at https://manitoba.ca/iem/info/library/downloads/index.html, or on request from minesinfo@gov.mb.ca, or by contacting the Resource Centre, Manitoba Economic Development, Investment, Trade and Natural Resources, 360-1395 Ellice Avenue, Winnipeg, Manitoba R3G 3P2, Canada.

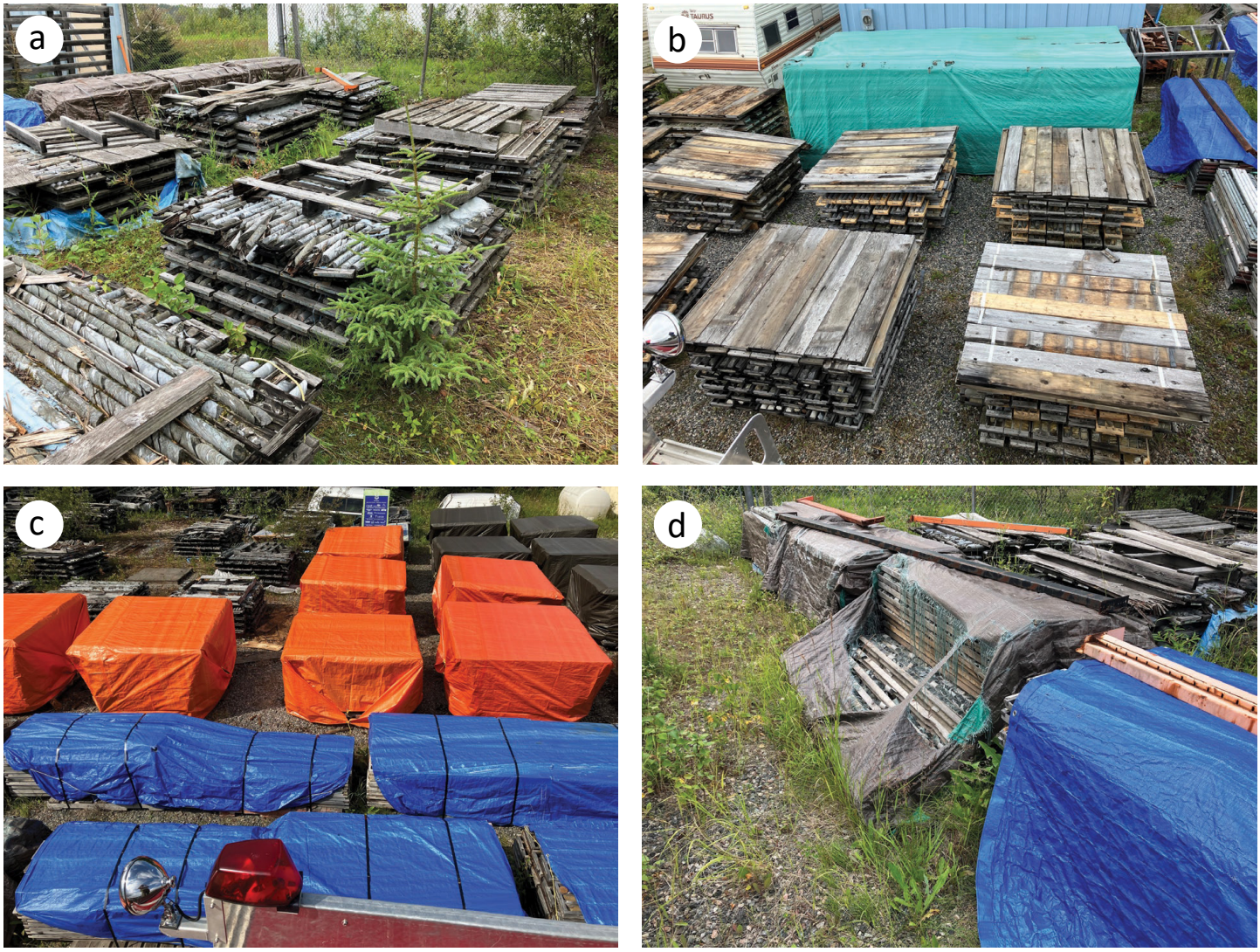

Figure GS2023-10-1: *Diamond-drillcore stored at the Manitoba Geological Survey's Thompson Facility and Compound:* ***a)*** *cross piles stored since the early 2000s;* ***b)*** *salvaged drillcore in new cross piles with recycled core boxes for roofs;* ***c)*** *stacked cross piles of salvaged drillcore with tarps;* ***d)*** *spilled core that was previously stored in the core shed and moved in 2022.*

million, and that would not include the additional cost of access to remote sites and the transportation of the core. Archived drillcore is often used by industry geologists to evaluate the mineral potential of an area, and can be a determining factor in whether or not investment dollars are spent in Manitoba. In addition, the core can be used by geologists from provincial and federal surveys and academia to further our understanding of the geology of Manitoba, which can, in turn, open up areas to new exploration activities and targets. It is hoped that the drillcore recovered during this project can be moved to a secure indoor storage facility where it can be made available to geologists wishing to learn more about the geology and mineral potential of the province.

Acknowledgments

Thanks to M. Friesen and M. Michaw (University of Manitoba) for their capable field assistance, and C. Epp and P. Belanger for logistical support. Vale Exploration in Thompson graciously lent use of their binding equipment to secure the parallel stacked core. T. Martins and M. Nicolas provided reviews for previous drafts of this report.

References

Couëslan, C.G. 2023: Salvaged diamond-drillcore at the Thompson Facility and Compound, from east-central Manitoba (parts of NTS 54C, 63P, 64A); Manitoba Economic Development, Investment, Trade and Natural Resources, Manitoba Geological Survey, Data Repository Item DRI2023006, Microsoft® Excel® file.

Manitoba Geological Survey 2022: Bedrock geology of Manitoba; Manitoba Natural Resources and Northern Development, Manitoba Geological Survey, Open File OF2022-2, scale 1:1 000 000.

McGregor, C.R. 2012: GIS compilation of exploration drillcore from all Manitoba Geological Survey drillcore libraries; Manitoba Innovation, Energy and Mines, Manitoba Geological Survey, Open File OF2012-1, 1 DVD, URL <https://manitoba.ca/iem/info/libmin/OF2012-1.zip> [June 2023].

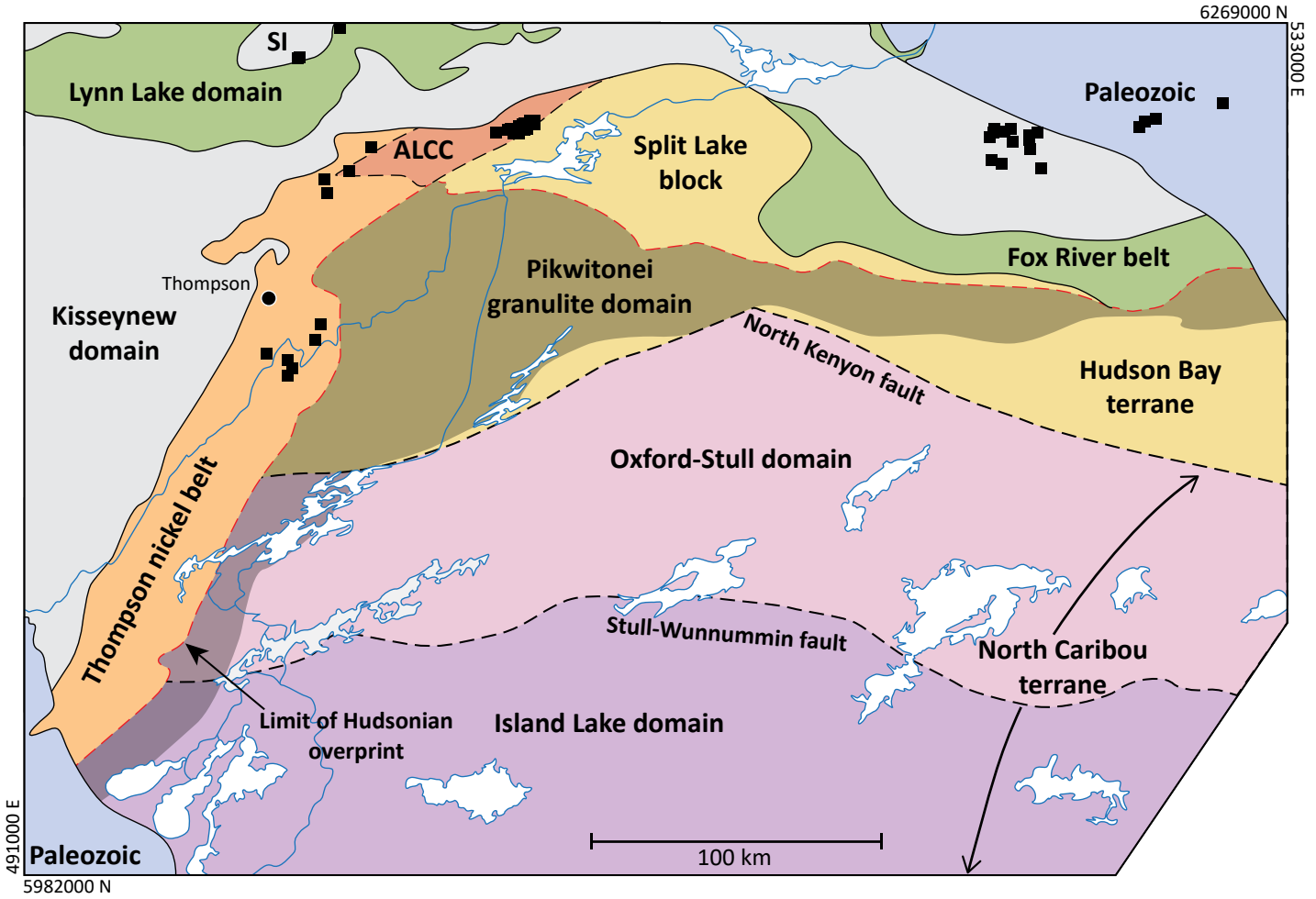

Figure GS2023-10-2: *Geological domain map of east-central Manitoba. The collar locations of the drillcore stacked in cross piles at the Thompson Facility and Compound are indicated by black squares. Abbreviations: ALCC, Assean Lake crustal complex; SI, Southern Indian domain. Drill collar locations are from McGregor (2012). Geological domains are modified from Manitoba Geological Survey (2022).*

GS2023-11

Volatiles analysis of drill cuttings to evaluate the helium prospectivity of southwestern Manitoba (parts of NTS 62F2, K3)

by M.P.B. Nicolas, C.M. Smith[1] and M.P. Smith[1]

Summary

The helium prospectivity of southwestern Manitoba was evaluated using the Rock Volatiles Stratigraphy (RVS) system. Drill cuttings from three legacy oil wells (L.S. 9, Sec. 6, Twp. 2, Rge. 26, W 1st Mer. [abbreviated 9-6-2-26W1], 13-24-12-27W1 and 16-29-12-29W1) were analyzed for a wide range of volatile compounds, including C1–C10 hydrocarbons, carbon dioxide, water and helium. The deepest portions of each well were sampled, from the Precambrian basement to the Dawson Bay Formation, at intervals defined by the drill cuttings recovered. All three wells show signs of helium accumulation with economic potential. Of particular note is the well at 9-6-2-26W1, it had the highest helium values ever measured by the RVS system to date in any legacy sample for which self-sourcing of the helium—formed by radioactive decay of in situ uranium- and thorium-bearing basement rocks or shale—was not possible. These values are higher than those measured in samples from Saskatchewan's producing helium plays. These high values indicate an active prolific helium system in southwestern Manitoba. Additionally, analysis of the RVS data indicates bypassed deep hydrocarbon system opportunities in Manitoba.

In Brief:

- Volatiles analysis of legacy drill cuttings was done on three oil wells
- High helium values indicate potential economic concentrations in the Red River and Deadwood formations
- Hydrocarbon indicators show hydrocarbon systems in the Dawson Bay and Red River formations

Citation:
Nicolas, M.P.B., Smith, C.M. and Smith, M.P. 2023: Volatiles analysis of drill cuttings to evaluate the helium prospectivity of southwestern Manitoba (parts of NTS 62F2, K3); *in* Report of Activities 2023, Manitoba Economic Development, Investment, Trade and Natural Resources, Manitoba Geological Survey, p. 93–104.

Introduction

A review of helium occurrences in southwestern Manitoba oil and gas wells by Nicolas (2018) indicated that 80% of oil and gas wells tested in Manitoba have helium gas occurrences, including six wells with economic helium concentrations, between 0.30 and 2.00 mol. % helium (Figure GS2023-11-1). This work points to deeper lower Paleozoic formations, particularly the Ordovician Winnipeg and Cambrian Deadwood formations, as the most prospective for helium. Since hydrocarbon accumulations have not been identified in these horizons yet in Manitoba, helium accumulations and production would be classified as green helium because of the low greenhouse gas emissions associated with production. This is in contrast to brown helium, where helium production is a byproduct of oil and gas operations with its associated greenhouse gas emissions.

In Manitoba, Williston Basin strata occur at relatively shallow depths, the maximum depth to the Precambrian basement is 2.7 km in the extreme southwestern corner of the province. This means Manitoba is a low-cost location to explore for hydrocarbons and helium, however, despite this shallow depth, deep exploration in Manitoba has been limited to historical hydrocarbon exploratory holes. Modern oil and gas exploration and production is currently focused in late Devonian, Mississippian and Jurassic strata, leaving a large portion of Manitoba's stratigraphic column, over a large geographic region, underexplored for pore-space resources. By studying and analyzing drill cuttings recovered from deep exploratory archival wells drilled over the last 70 years or more, a new appreciation for once hidden economic treasures may come to light using innovative analytical techniques.

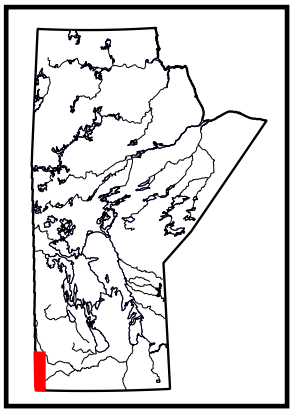

The geochemical analysis of core and drill cuttings is an important tool in understanding the mineralogy, diagenesis, depositional environment and fluid history of a unit. Common analysis methods include traditional core analyses (rock properties and water/oil saturations), X-ray diffraction (XRD), X-ray fluorescence (XRF), isotopic geochemistry and Rock-Eval pyrolysis. Detailed analysis of the geochemical signature of the residual volatile fraction of the fluids trapped within sample pore spaces using the Rock Volatiles Stratigraphy (RVS) system is an innovative new approach that provides valuable information and insights into the fluid history of a stratigraphic unit and its surrounding area. The RVS system directly measures the residual volatile fraction trapped in drill cuttings and core samples, including C1–C10 hydrocarbons, helium, water and other volatile compounds, as well as the mechanical rock strength. These data can then be used to provide proxy data for rock and reservoir properties, such as permeability, wettability, hydrocarbon and helium pay zones and gas and oil migration routes, and to determine the proximity to the oil-water contact. The advantage of this analytical method is

[1] Advance Hydrocarbon Stratigraphy, Inc., Tulsa, Oklahoma

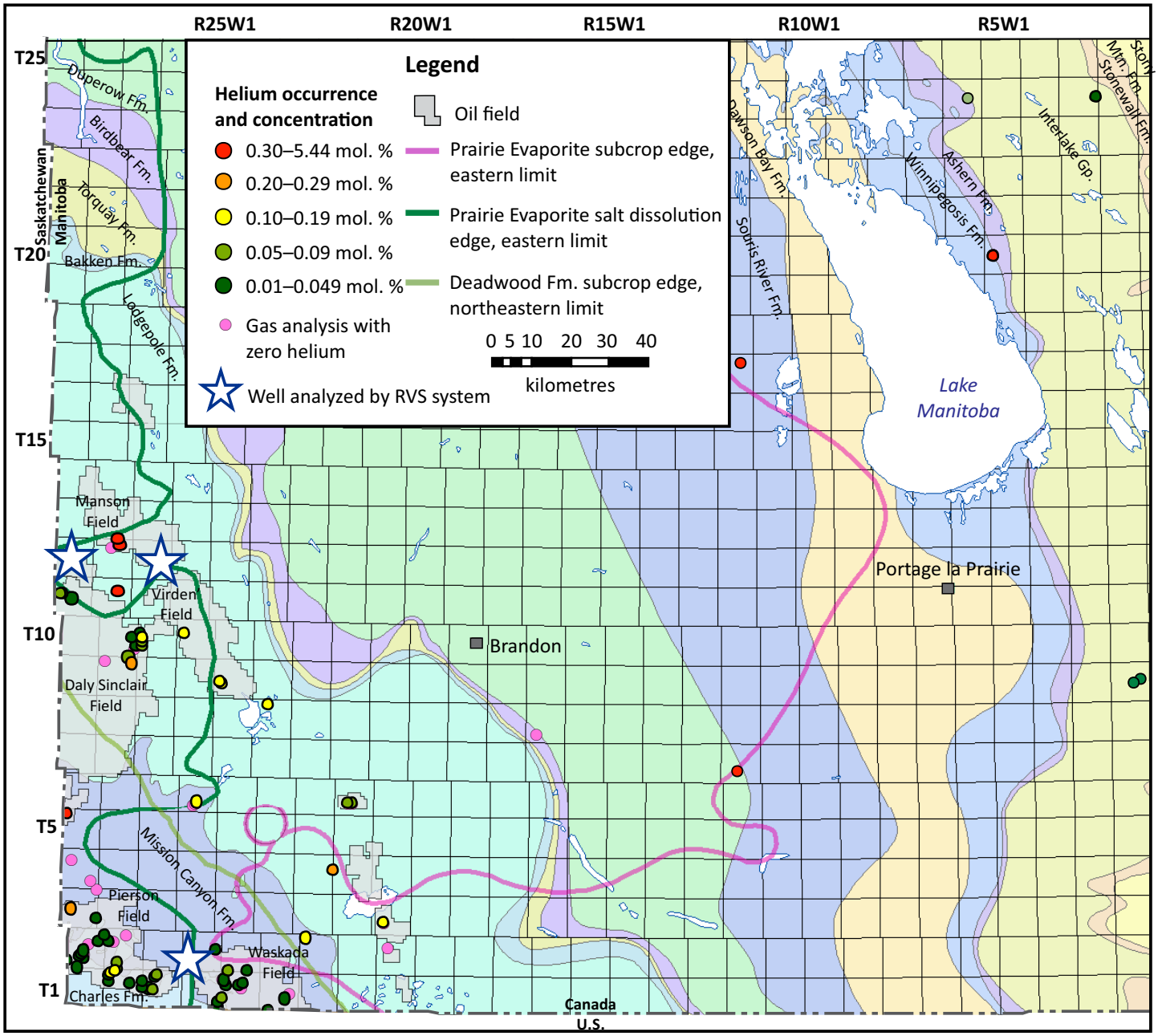

Figure GS2023-11-1: *Location map of sampled sites in southwestern Manitoba (modified from Nicolas, 2018). Abbreviation: RVS, Rock Volatiles Stratigraphy.*

that it does not require freshly drilled or wellsite-sealed samples for reliable and useful results—this method works equally well on old legacy samples collected more than 60 years ago (Smith and Smith, 2020). Additionally, the RVS system uses a small sample size (0.4 cm^3) making it suitable for the analysis of drill cuttings. Unlike short interval cores, the benefits of using drill cuttings are their regular sampling interval throughout the drilling of a well and the number of wells with drill cuttings. This allows for higher density sampling across multiple formations and vertical depths.

The Manitoba Geological Survey (MGS) in partnership with Advanced Hydrocarbon Stratigraphy, Inc. (AHS) studied the volatile fraction of fluids in drill cuttings from three oil wells (Table GS2023-11-1) drilled in the lower Paleozoic by measuring fluid, gas, hydrocarbon, rock and reservoir properties to evaluate for helium prospectivity in Manitoba, and provide additional insights into local hydrocarbon systems.

Rock Volatiles Stratigraphy

Applications of the RVS system and previous studies

Rock Volatiles Stratigraphy analyses have been conducted on legacy drill cuttings and core from various international locations to evaluate the potential for subsurface pore-space resources, as well as to conduct post-mortem analysis on underperforming wells. Resources evaluated using the RVS system include helium,

Table GS2023-11-1: List of wells sampled.

Unique well identifier (UWI)	Licence number	Easting (Zone 14, NAD83)	Northing (Zone 14, NAD83)	Year drilled	Total depth (m TVD)	Sample depth range (m TVD)	Sample interval	Stratigraphy	Comments
100/09-06-002-26W1/00	2610	358365.58	5440090.64	1979	1986.0	1485–1985	5 m	Dawson Bay Fm. to Precambrian	Salt-gel drilling mud used in deeper section; drilled with mill-tooth drill bit
100/13-24-012-27W1/00	10911	352879.84	5544135.85	2018	1496.0	1005–1496	5 m	Dawson Bay Fm. to Precambrian	Salt-saturated drilling mud used below 1039 m; drilled with PDC drill bit
100/16-29-012-29W1/00	2532	327790.04	5546621.49	1974	1664.2	1362–1664	~3 m (10 ft.)	Interlake Gp. to Precambrian	Salt-gel drilling mud used below 589 m; drilled with mill-tooth drill bit

Abbreviations: PDC, polycrystalline diamond compact; TVD, true vertical depth.

hydrocarbon, hydrogen and geothermal. It can also evaluate the potential of the rock for carbon storage.

Prior work in Saskatchewan included using the RVS system to analyze three cores where helium was confirmed in drillstem tests (DSTs; Smith et al., 2022a, 2023c). This work began in 2022 with the examination of the British American Saskatchewan Landing core from the Wilhelm area and is reported in Smith et al. (2022a). The Wilhelm helium play area was developed in the 1960s starting with the discovery well B.A. Wilhelm 101/03-10-017-14W3/00 (petroleum and gas well licence 62H013, Saskatchewan Ministry of Energy and Resources, Regina). The DST results of 1.8 to 2.0% helium were achieved from the Cambrian Deadwood Formation (Yurkowski, 2016; Smith et al., 2022a) and this well produced $3.036 \times 10^6 m^3$ (107,250 million standard cubic feet) of helium from 1963 to 1977 as 1.3% of the total produced gas volume. Data from the RVS study showed strong relationships with historical DST, core and wireline data providing confidence that zones with higher relative helium—identified as a median value of 0.7 and mean value of 1.1 ±0.85 nanomoles (nmol) of helium measured in the historical pay zone interval—could be identified in the core, as well as the identification of features relevant to the subsurface helium system (Smith et al., 2022a). Of particular note, using the RVS system, tight zones (low porosity and permeability) were found to contain more helium than high porosity and permeability zones. In addition, mathematical techniques that are weighted more toward determining a baseline value, like using a median or the centre of a Gaussian fit to a data histogram to identify an apparent baseline mode across the section, were found to produce helium values that were more representative than a mean value. An expansion of this study in 2023 included the analysis of two additional cores from Shell Prud'homme 6-36-38-28W2 (Shell Prud'homme; petroleum and gas well licence 67E067 Saskatchewan Ministry of Energy and Resources, Regina; Winnipegosis test) and CPEC Forget 11-16-007-07W2 (CPEC Foget; petroleum and gas well licence 97E213, Saskatchewan Ministry of Energy and Resources, Regina; Red River-Yeoman test). Both sections had reported concentrations of 0.44% helium by DST. Using the RVS system, core samples covering the Shell Prud'homme DST interval had a median of 0.218 and mean of 0.221 ±0.019 nmol of helium, and the similar CPEC Forget DST interval had a median of 0.203 and mean of 0.218 ±0.035 nmol of helium (Smith et al., 2023c). This RVS analysis demonstrated that both the mean and median of the measured nanomoles of helium from the tested core provided similar ratios of helium to the DST values, showing that RVS results can provide meaningful semiquantitative information from core that can be related back to subsurface helium content (Smith et al., 2022a, 2023a, c). The RVS technology has been used to evaluate other helium plays, such as those in the Four Corners region and Oklahoma panhandle in the United States (Smith et al., 2022b, 2023c).

Sample considerations and comparisons

The availability of samples, whether drill cuttings or core, that can be recovered from any given well will vary, as will the volatile data that can be extracted. The benefit of core samples is they allow for representative sampling of small stratigraphic intervals, as demonstrated by Smith et al. (2023a). Therefore core is the superior sample type due to the ability to select features, control sample intervals, better preserve the absolute quantities of volatiles and extract unique water data. However, core is limiting as it is more rarely collected and covers short specific (biased) intervals compared to drill cuttings.

Drill cuttings have the benefit of covering a wider stratigraphic section and of being collected from a higher density of wells. However, they do not afford detailed geological interpretation/description or core analyses, and they are small, have a predetermined sampling interval and may have been washed and dried at the wellsite prior to storage. Some tests have shown that unwashed but dried drill cuttings provide good quality RVS results, likely due to the drilling mud encapsulating the grains. For drill cuttings, the drill bit used and drilling mud composition can also affect the results, and these factors need to be considered during interpretation. For example, polycrystalline diamond compact (PDC) drill bits, commonly used to drill modern wells, shear and grind the rock to a much finer grain size, destroying much of the macro- and microporosity, compared to mill-tooth bits, such as tricone/rock/cable tool diamond-drill bits, typical of

older technologies. For RVS analysis, larger drill cuttings are preferred as rock morphology has not been overly compromised and sample handling has been minimal thus the escape of volatiles from pore spaces has been minimized.

The sample type will directly affect the range of compounds that can be analyzed. For example, core samples will allow for the measurement of a wider range of volatile compounds and can allow for unique water data collection, permeability measurements, and more accurate mechanical strength data collection. In comparison, cuttings may not retain volatiles as effectively as core given the higher degree of trauma and disaggregation of the rock samples.

When comparing between core and drill cuttings data, the data can only be used semiquantitatively. Broadly, the data from cuttings and core can only be compared at the microcrystalline level and care should be taken in comparing data from different sample types. However, learning from multiple datasets over the years, AHS has developed standards to carefully compare RVS results between wells and sample types, thus allowing a careful comparison of the data reported here with other RVS study results (Smith et al., 2022a, 2023a, c).

Using the RVS system for helium studies

The work by Smith et al. (2022a) in Saskatchewan prompted this study of drill cuttings to provide insights into the helium prospectivity of the stratigraphy of Manitoba. Smith et al. (2022a) described core samples in relation to existing well data to assist in understanding the RVS results, as they can be applied to helium-prospectivity and systems analysis.

Smith et al. (2022a) found that more than 40 volatile compounds can be measured from core samples, but that less compounds could be reliably analyzed from drill cuttings. Table GS2023-11-2 shows the list of compounds analyzed for this study. Despite the data compromise that comes from drill cuttings, the ability to measure a wider stratigraphic section and to have more well selection options was found to be beneficial for RVS analysis for helium-prospectivity mapping. Using drill cuttings is an effective way to evaluate a large area with limited data, as is found in Manitoba. It should also be noted that the data gathered also provide valuable insight into hydrocarbon- and water-rich zones, CO_2-rich intervals, oil-water contacts, depositional environments and mechanical rock strength.

Table GS2023-11-2: Generalized list of compounds and rock properties analyzed by the Rock Volatiles Stratigraphy system on drill cuttings in this study. Data Repository Item DRI2023014 (Nicolas et al., 2023) provides details on compounds, properties, proxies and calculations.

Compounds	Rock properties
Methane	Mechanical strength
Ethane	Permeability proxy
Propane	Hydrocarbon liquid volume
Butanes	Hydrocarbon gas volume
Pentanes	Total water
Benzene	Equivalent oil production
C6 naphthenes	Equivalent gas production
Hexanes	Gas-oil ratio (GOR)
Toluene	
C7 naphthenes	
Heptanes	
C8 aromatics	
C8 naphthenes	
Octanes	
C9 naphthenes	
Nonanes	
C10 naphthenes	
Decanes	
CO_2	
Helium	
Nitrogen	
Formic acid	
Acetic acid	
SO- (sulphate proxy)	

Methodology

Drill cuttings from three historical petroleum exploration wells in southwestern Manitoba were sampled for testing by the RVS system (Figure GS2023-11-1). The three wells sampled for this study are 1) Corex Coulter Prov. 100/09-06-002-26W1/00 (oil and gas well licence 2610, Manitoba Economic Development, Investment, Trade and Natural Resources, Winnipeg) in L.S. 9, Sec. 6, Twp. 2, Rge. 26, W 1st Mer. (abbreviated 9-6-2-26W1); 2) Surge North Hargrave COM SWD 100/13-24-012-27W1/00 (oil and gas well licence 10911) in 13-24-12-27W1; and 3) ASM-BTO et al Kirkella Prov. 100/16-29-012-29W1/00 (oil and gas well licence 2532) in 16-29-12-29W1. Sampling intervals were restricted to the cuttings vials in storage; the sampling interval was either ~3 m (10 ft.) or 5 m (Table GS2023-11-1).

Well selection was based on several criteria, including availability of Precambrian samples at depths of ≥1500 m, recovered samples of the Deadwood and/or Winnipeg formations, drill cuttings quality and quantity and regularity of the sampling interval. Geographic location was also considered, locations with known or suspected structural disturbances nearby, such as salt collapse or faulting, were selected. The rationale for this was that the areas with more disturbances may provide more opportunities for potential migration of helium and other volatile substances through the section. The wells at 9-6-2-26W1 and 16-29-12-29W1 have had the entire Prairie Evaporite salts section dissolved, whereas the well at 13-24-12-27W1 has the thick Prairie Evaporite section preserved but is in close proximity to known structural disturbances and possible faulting, which formed the southern extent of the Manson oil field.

The samples were sent to the Advance Hydrocarbon Stratigraphy, Inc. (AHS) laboratory in Tulsa, Oklahoma, for analysis by their proprietary cryotrap mass spectrometer (CT-MS) system specially designed to analyze for C1–C10 hydrocarbons, helium, formation water, CO_2, sulphur gases, organic acids and mechanical strength (Table GS2023-11-2). Each sample consisted of 3 g of drill cuttings from each vial, starting with the deepest cuttings vial, then sampling upsection for a total of 100 samples per well. Approximately 0.4 cm^3 of rock sample was crushed with a 1.8 tonne (2 ton) force applied by a piston press over a 6.35 mm (¼ in.) square area, while inside a plugged hollow brass cylinder. The cylinder was interfaced to the CT-MS system through a syringe inserted into a nitrile septum at the top of the brass cylinder; the crushing force was applied radially. After crushing, the volatiles were gently vacuum extracted and analyzed in two aliquots using the same rock sample. The first aliquot was analyzed at 20 mbar pressure (1/50th of an atmosphere pressure), and the second aliquot was analyzed 2 mbar pressure (1/500th of an atmosphere pressure). The benefit of analyzing the same suite of volatiles from the same rock sample, but under increasing vacuum extraction conditions, provides insights into where the volatiles resided in the fabric of the rock and how readily they were released from the rock sample. These measurements can be related to rock properties, such as permeability. Following the vacuum extraction, the volatiles were condensed in a liquid nitrogen cooled cryotrap—after extraction and condensation of a given aliquot was completed the cryotrap was slowly warmed and volatiles sublimated off sequentially providing a separation stage before they were passed to the mass spectrometer. Some volatiles, like helium and methane, do not condense under liquid nitrogen conditions, these are analyzed by effectively capturing headspace samples from the cryotrap, which are passed directly to the mass spectrometer. Under this workflow, helium was only measured for the 20 mbar vacuum extraction. Mechanical strength of the rock sample was measured as a byproduct of the crushing process. This was accomplished by measuring the thickness of the sample following the crushing process and is directly related to the competency of the rock. In the case of cuttings, this has been observed to potentially relate more to grain strength than unconfined compressive strength, due to the disaggregated nature of the cuttings. More details of the methods used and how they can be interpreted are described in Smith and Smith (2020) and Smith et al. (2021).

Rock Volatiles Stratigraphy results and interpretations

The entirety of the RVS data is available in Data Repository Item DRI202314 (Nicolas et al., 2023)[2]. There is a significant amount of interpretation that can be extracted from the RVS data. This report will focus on the data used to evaluate helium prospectivity, but also on select data on other fluids, such as hydrocarbons, water and CO_2, as they provide information about the overall fluid dynamics of the system.

Oil and gas well at 9-6-2-26W1 (licence 2610)

Drill cuttings collected from the well at 9-6-2-26W1 were sampled from 1985 m true vertical depth (TVD), in Precambrian rocks, to 1485 m TVD, in the lower Burr Member of the Dawson Bay Formation. Figure GS2023-11-2 shows the data logs for select analyses, including helium, as they relate to stratigraphy.

When comparing to similar work done in Saskatchewan (Smith et al., 2022a), a helium reading above 0.7 nmol helium on an RVS log indicates a potential economic accumulation of helium, however, correlation and interpretation with other RVS data must be done to narrow down the true potential pay zone. The helium data show three discrete very high helium intervals: 1585–1600 m TVD (lower Ashern Formation to upper Interlake Group), 1645–1675 m TVD (lower Interlake Group to upper Stonewall Formation), 1705–1725 m TVD (Stony Mountain Formation), however, most of the interval from 1645 to 1980 m TVD (lower Interlake Group to Precambrian) has nearly constant ≥0.7 nmol helium readings, with only a few short intervals with lower values. Helium and other gas volumes are expected to be underrepresented in the data due to degassing over time during storage, therefore, these values will serve as a minimum of the expected true amounts in the subsurface. In Figure GS2023-11-2, the ≥0.7 nmol helium concentrations are highlighted in yellow.

The interval of particular interest in this well is in the Red River Formation and uppermost bed of the Winnipeg Formation, where between 1785 and 1902 m TVD the logs have a distinctive blocky response. The gamma-ray log indicates a moderately clean carbonate—likely dolostone—with an increasing silty-sand content through the Hecla beds into the uppermost Winnipeg Formation sandstone, as is typical for this interval. When comparing the deep resistivity and total water logs, the results complement each other since the resistivity is consistently high on average, whereas the total water is on average the lowest in the section. This suggests this interval could contain either hydrocarbon fluids and/or other gases. To get a better reading on what fluids may be dominating the section, other logs provide valuable information. The CO_2 and hydrocarbon liquid and gas indicator logs all show no anomalous readings, and actually have slightly lower readings on average compared to many other parts of the section. In contrast, helium values are on average consistently high—above the 0.7 nmol cutoff—suggesting this may be a helium-prospective zone.

Within the Red River Formation, a spike in total water centred at 1825 m TVD is associated with a moderate increase in

[2] MGS Data Repository Item DRI2023014, containing the data or other information sources used to compile this report, is available online to download free of charge at https://manitoba.ca/iem/info/library/downloads/index.html, or on request from minesinfo@gov.mb.ca, or by contacting the Resource Centre, Manitoba Economic Development, Investment, Trade and Natural Resources, 360-1395 Ellice Avenue, Winnipeg, Manitoba R3G 3P2, Canada.

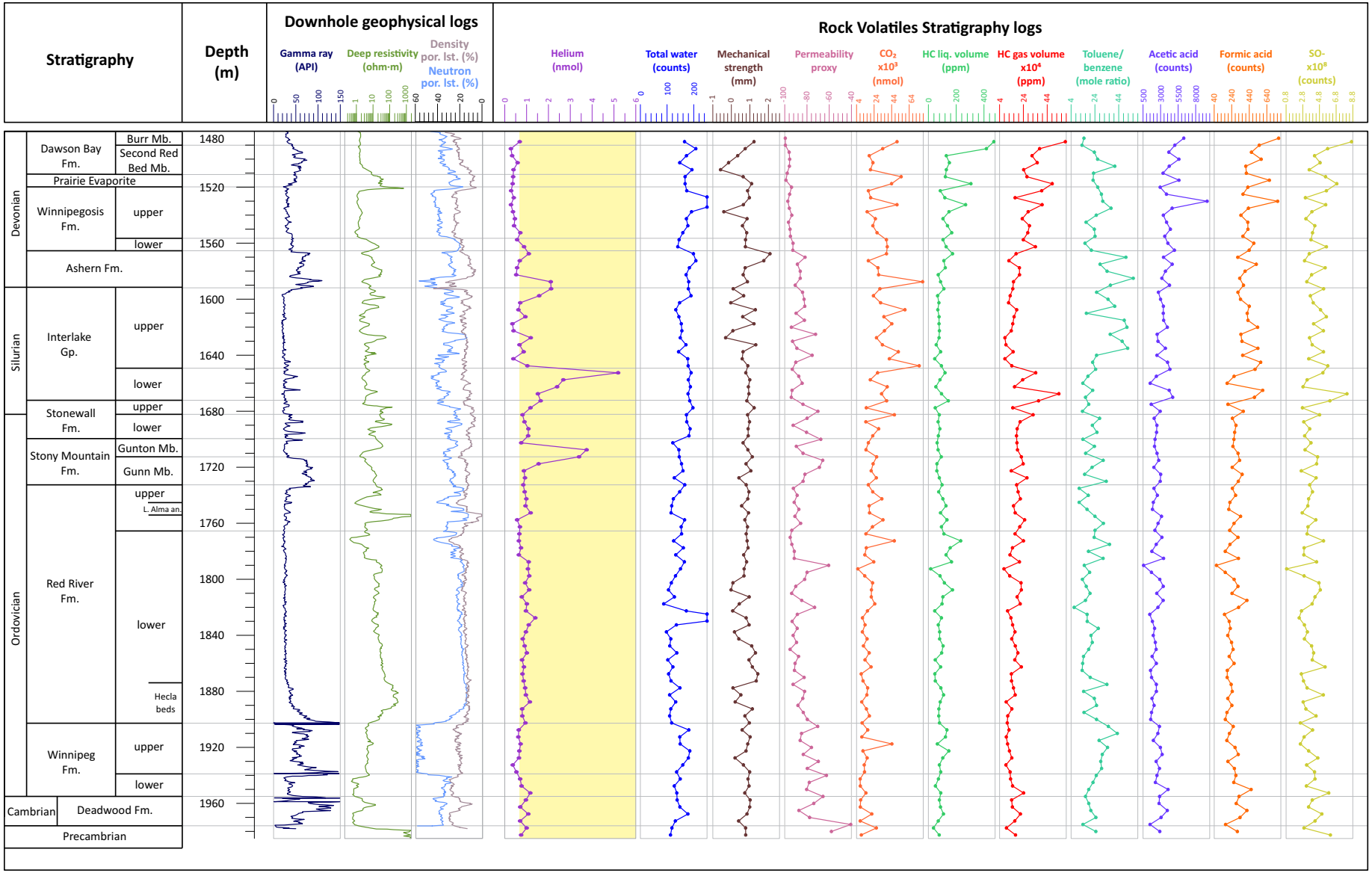

Figure GS2023-11-2: *Stratigraphy and Rock Volatiles Stratigraphy (RVS) data logs for the oil and gas well at L.S. 9, Sec. 6, Twp. 2, Rge. 26, W 1st Mer. (9-6-2-26W1), including select downhole geophysical logs; RVS sample intervals are every 5 m. Yellow highlighted area on the helium track shows values ≥0.7 nanomoles (nmol). Mechanical strength of the sample increases from left to right on the mechanical strength log; the permeability proxy log indicates increased permeability from left to right. Abbreviations: HC, hydrocarbon; L. Alma an., Lake Alma anhydrite; liq., liquid; por. lst., porosity of limestone.*

helium. On the mechanical strength log, the total water spike occurs in the middle of a zone of lower mechanical strength, between 1800 and 1845 m TVD. This decreased mechanical strength supports a potential zone of natural fractures within the Red River Formation, as has been identified in other deep wells at this same stratigraphic interval. Additionally, immediately above this water spike, the CO_2, hydrocarbon liquid and gas values increase, but still within the zone of high helium. This suggests that the composition of any fluid resource in this formation may be different above the spike than that below it.

The basal sand of the lower Winnipeg Formation and the upper half of the Deadwood Formation interval also have similar log responses to the Red River Formation, suggesting another thin helium-prospective zone, with the upper Winnipeg Formation middle shale unit acting as a partial barrier separating the upper zone from the lower zone, and with the Precambrian basement granite underlying these units as the source of helium.

Going upsection, in the interval that includes the Stony Mountain Formation, the higher helium values are concentrated in the Gunton Member, where the neutron log indicates a higher porosity. Additionally, the resistivity changes from low to high, forming a distinct 'shoulder' in the log response, with corresponding decreases in the total water, CO_2 and mechanical strength, all corresponding to the increase in helium. This combination of changes suggests the helium is diffusing upward abutting against a top seal (lower Stonewall Formation) in a zone of lower porosity, this interpretation would be consistent with core analysis done in Saskatchewan using the RVS system (Smith et al., 2022a). Given that the diameter of a helium atom is so small, it is able to diffuse into smaller pore spaces than larger molecules of water and CO_2, making the effective porosity for helium lower and the helium more mobile in seemingly tight spaces. This top seal did not prevent the helium from being present and/or migrating upward, but did act as a very strong sealing feature to other compounds or a baffle for the helium, requiring volatiles to move laterally to infiltrate past the feature. The gamma-ray log does not suggest a local in situ radioactive decay source in the sedimentary rock, and the high values are more likely the result of helium migration through a complex fracture network.

Further upsection, there are two helium anomalies within the Interlake Group. The upper Interlake Group anomaly shows higher than average CO_2 and total water values, and lower mechanical strength. This suggests that this interval, which is high in helium, is also high in other gases and is likely water-wet. Increased porosity and a decrease in mechanical strength in the upper Interlake Group anomaly interval may be related to the major erosional unconformity between the Silurian Interlake Group and Devonian Ashern Formation, which would have compromised these rock units through erosion, weathering, leaching and surface fractures. In the lower Interlake Group anomaly, the total water values and hydrocarbon gas volume responses are high, the CO_2 response is high immediately above the highest helium response, and the neutron log suggests possibly more porosity immediately below the high helium response. This may be due to a molecular sorting process whereby the relatively mobile hydrocarbon gases, which are better preserved in legacy samples, got trapped in porous rocks and were unable to move into the very tight rocks, which trapped and preserved the helium being observed here.

At the top of the sampled section, in the Dawson Bay Formation, immediately above the Second Red Bed Member, the hydrocarbon liquid and gas logs show a positive excursion. The logs indicate the presence of residual oil and gas within porous beds, although the low resistivity and higher total water values indicate that the beds may be water-wet. The acetic acid and formic acid responses increase as well, indicating the proximity to an oil-water contact. These oil and gas indicators mimic those shown in the well at 13-24-12-27W1 (licence 10911), discussed later in this report. Of interest, leading up to the Dawson Bay Formation, the Winnipegosis Formation shows marked increases in hydrocarbon gas and liquid volumes across the entire formation section.

When comparing data from the well at 9-6-2-26W1 to the data from the other two wells, the well at 9-6-2-26W1 has significantly higher values for helium, hydrocarbon oil and gas and CO_2. This points to a more active fluid system in the deeper parts of the basin in Manitoba, specifically in the Waskada and Pierson oil fields area (Twp. 1 to 3, Rge. 24 to 29W1). Reinforced by the core analyses done in Saskatchewan (Smith et al., 2022a, 2023b), the high helium responses in Manitoba require a significant helium source to be present and helium in sufficient quantities for it to accumulate to that degree. In the history of AHS doing these RVS tests and studies on legacy samples, this well returned the highest helium values measured to date using RVS analysis on samples for which uranium- and thorium-rich basement rocks or sedimentary rocks were not directly present to self-source the helium. These results are indicative of a high level of prospectivity and a significant amount of helium migrating through the system, with particular focus on the lower Red River Formation section.

Oil and gas well at 13-24-12-27W1 (licence 10911)

Drill cuttings collected from the well at 13-24-12-27W1 were sampled from 1496 m TVD, in the Precambrian rocks, up to 1005 m TVD, in the lower Burr Member of the Dawson Bay Formation. Figure GS2023-11-3 shows the data logs for select analyses, including helium, as they relate to stratigraphy.

The helium values for this well are considerably low, with all data points but one plotting below 0.7 nmol helium, with the sample at 1255 m TVD having a reading of 0.75 nmol. This one sample also has corresponding small peaks in hydrocarbon liquid and gas values. With a thickness of less than 10 m, this zone is too small for consideration as a helium target.

The lower Red River Formation section and Winnipeg Formation (from 1365 to 1480 m TVD) shows a consistently higher

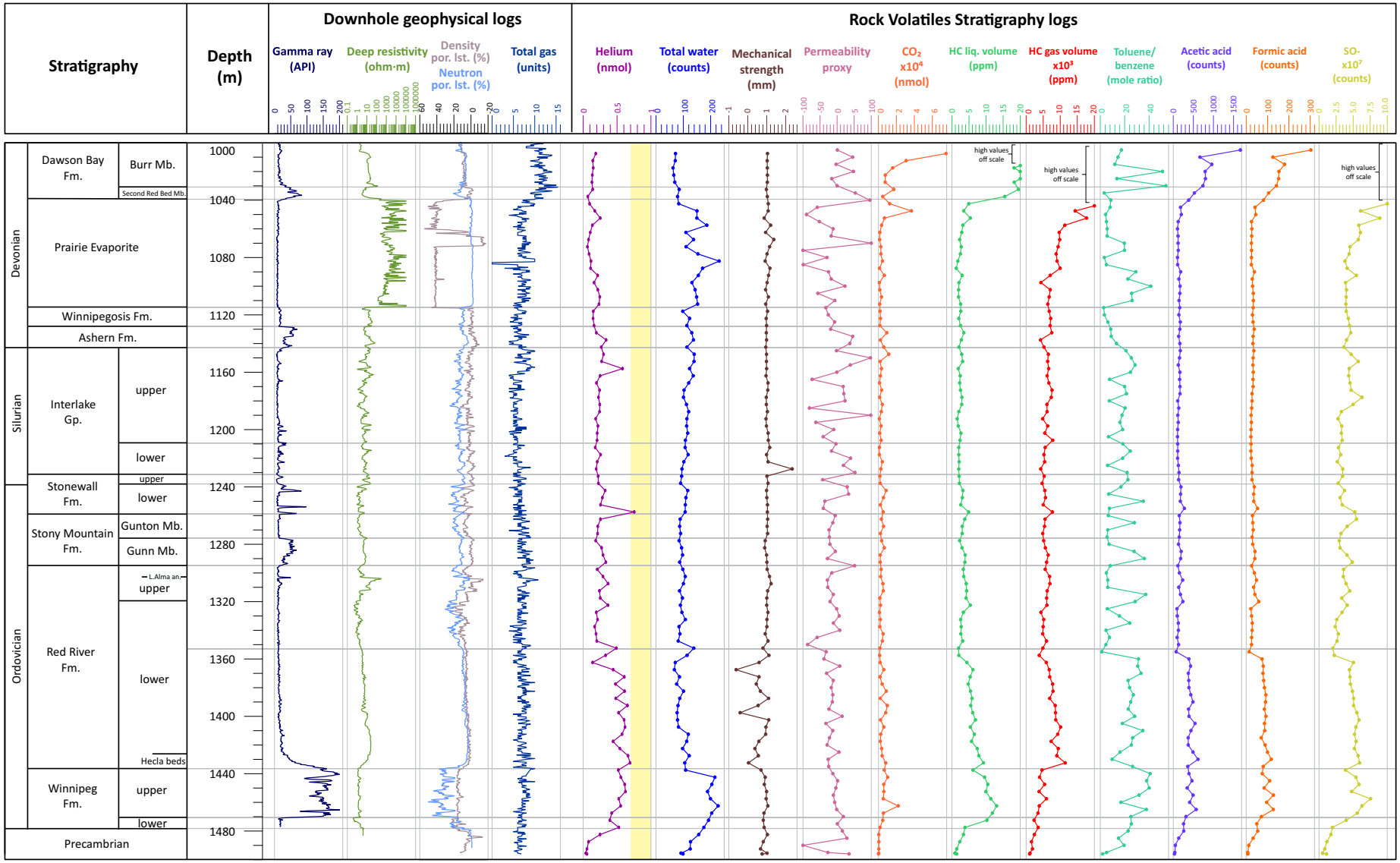

Figure GS2023-11-3: *Stratigraphy and Rock Volatiles Stratigraphy (RVS) data logs for the well at L.S. 13, Sec. 24, Twp. 12, Rge. 27, W 1st Mer. (13-24-12-27W1), including select downhole geophysical logs; RVS sample intervals are every 5 m. Yellow highlighted area on the helium track shows values ≥0.7 nanomoles (nmol). Mechanical strength of the sample increases from left to right on the mechanical strength log; the permeability proxy log indicates increased permeability from left to right. Abbreviations: HC, hydrocarbon; L. Alma an., Lake Alma anhydrite; liq., liquid; por. lst., porosity of limestone.*

helium content than the strata above, but still falls just below the 0.7 nmol helium cutoff. The lower Red River Formation section is marked by a decrease in porosity, as seen by the neutron log and low mechanical strength responses. The gamma-ray and resistivity logs do not show any significant changes, suggesting a subtle change in lithology, perhaps more diagenetic, has occurred between 1365 and 1480 m TVD. Changes in the SO- (sulphate proxy) data support this, as this measures the presence of sulphate compounds as they breakdown in the system, which can be tied to depositional environment and diagenesis. Sample descriptions in the technical well file (Fire Sky Energy Inc., 2018) indicate a change between 1350 and 1355 m TVD from dolostone above to limestone below. The decrease in mechanical strength may reflect this porosity increase, but may also be related to fracturing within this interval. A potential zone of natural fractures is also seen within this same stratigraphic interval on the logs for the well at 9-6-2-26W1 (Figure GS2023-11-2).

The section from 1365 to 1480 m TVD overall has high total water values, particularly in the Winnipeg Formation section, with an increase in hydrocarbon liquid values, and a corresponding increase in toluene/benzene ratio and acetic and formic acid counts. The Winnipeg Formation section has distinctly lower hydrocarbon gas values than the overlying section. This combination of trends suggests that significant volumes of hydrocarbons have likely migrated through the Winnipeg Formation to Red River Formation interval, and the Winnipeg Formation interval is now water-wet as most hydrocarbon liquids and gases have been flushed out. The Winnipeg Formation flushed zone corresponds to the Winnipeg Formation sandstone aquifer.

The Burr Member of the Dawson Bay Formation section, immediately above the Second Red Bed Member, also shows the presence of a good hydrocarbon system, with the hydrocarbon liquid and gas logs both showing very high (off the scale) values, and low total water values, which suggest the system is not fully flushed. The acetic and formic acids logs show positive inflections indicating the proximity to or location of an oil-water contact. Positive inflections in the toluene/benzene ratio indicate the migration of hydrocarbons through the strata (Smith, 1968). In support of the findings of the RVS data, a gas log collected while drilling shows an increase in total gas within the same Dawson Bay Formation interval, and sample descriptions in the technical well file indicate oil shows in the cuttings (Fire Sky Energy Inc., 2018).

Overall, the well at 13-24-12-27W1 has the lowest RVS values of all three wells. This is likely a function of the drill cuttings themselves, which were much finer grained than those from the other two wells, which is a direct reflection of the PDC drill bit used at this wellsite. The drill cuttings from this well were the size of coarse- to medium-grained sand, which is common in modern drilling, in comparison to the other wells that were more coarse-grained sand to pebble-sized cuttings. It is suspected that the size of the cuttings themselves impact the RVS results, with the coarser grained cuttings providing more reliable results since they have not been subjected to as much surface area exposure through grinding and 'washing' during standard sample preparation at the wellsite. The coarser grained cuttings would also maintain a more accurate representation of original macro- and microporosity and rock properties and would retain more pore-space fluids and volatiles. This reinforces the work of AHS, which suggests that the RVS values from finer grained cuttings, although still valuable, have more attenuated responses, which need to be considered when evaluating the fluid systems in these wells and when comparing them to other datasets.

Oil and gas well at 16-29-12-29W1 (licence 2532)

Drill cuttings collected from the well at 16-29-12-29W1 were sampled from 1664.2 m TVD, in the Precambrian rocks, up to 1362.5 m TVD, in the Interlake Group. Figure GS2023-11-4 shows the data logs for select analyses, including helium, as they relate to stratigraphy.

The helium values for this well show good results, above 0.7 nmol consistently between 1420.4 and 1572.8 m TVD, correlating to the lower Stonewall Formation to lower Red River Formation interval, but with particularly high values in the lower portion of the lower Red River Formation section (1511.8–1572.8 m TVD). Within this latter section, between 1536.2 and 1572.8 m TVD, the total water, CO_2 and hydrocarbon liquid values are lower than those above. These indicators suggest that the interval between 1536.2 and 1572.8 m TVD may be the best helium-prospective interval. Immediately above 1536.2 m TVD, which still has high helium values, the hydrocarbon liquid and gas and total water values all increase, suggesting that even though there is good helium accumulation here, hydrocarbons and water may dilute the helium. In addition, the interval between 1472.2 and 1536.2 m TVD shows more variable resistivity readings in the zone with higher helium values, with minor variations in the gamma-ray log and large responses in the SO- data, which may suggest a changing rock type. According to the sample descriptions in the technical well file (Asamara Oil Corporation Limited, 1975) for this well, this interval corresponds to a change from dolostone above ~1493 m TVD to limestone below. In addition to the lithology change, the SO- data may give insight into the brine composition of the formation waters, which ultimately affected the resistivity response. The depositional environment of the Red River Formation gradually changed from open marine to a more restricted environment upsection, resulting in the deposition of the Lake Alma anhydrite. The sulphate proxy (SO-) may be an indication of this change, as the SO- values drop off immediately after the deposition of the anhydrite bed.

The hydrocarbon liquid and gas logs between 1414.3 and 1533.1 m TVD suggest that this well is close to a hydrocarbon system. Similar to the situation with the Dawson Bay Formation section in the 13-24-12-27W1 well, the toluene/benzene ratios indicate the migration of hydrocarbon liquids (Smith, 1968). The positive inflection of acetic and formic acids at 1533.1 m TVD

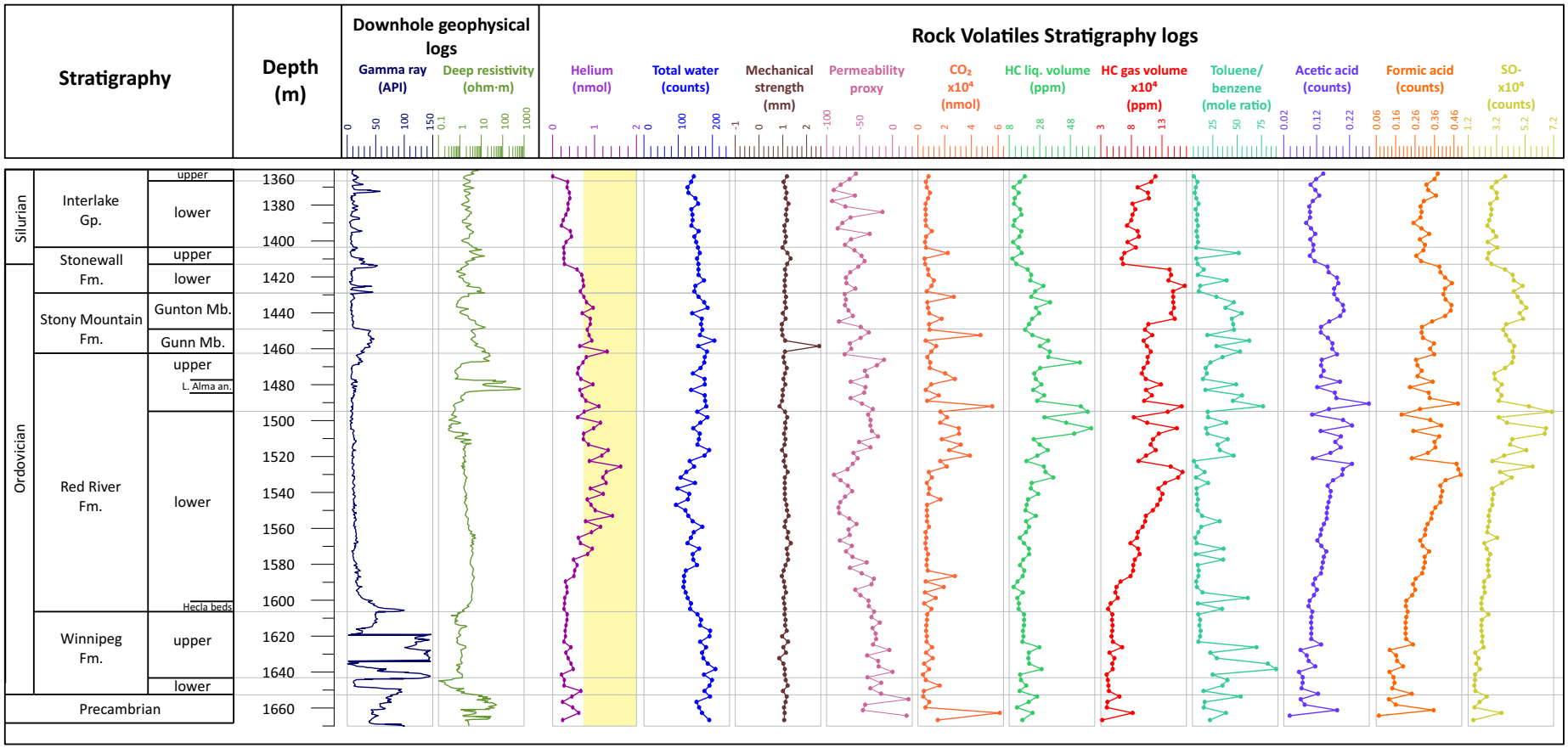

Figure GS2023-11-4: *Stratigraphy and Rock Volatiles Stratigraphy (RVS) data logs for the well at L.S. 16, Sec. 29, Twp. 12, Rge. 29, W 1st Mer. (16-29-12-29W1), including select downhole geophysical logs; RVS sample intervals are every ~3 m (10 ft.). Yellow highlighted area on the helium track shows values ≥0.7 nanomoles (nmol). Mechanical strength of the sample increases from left to right on the mechanical strength log; the permeability proxy log indicates increased permeability from left to right. Abbreviations: HC, hydrocarbon; L. Alma an., Lake Alma anhydrite; liq., liquid.*

indicate an oil-water contact nearby, with oil and water interactions occurring throughout the 1414.3–1533.1 m TVD section. Sample descriptions in the technical well file make note of oil staining and oil cut between 1493 and 1500 m TVD (Asamara Oil Corporation Limited, 1975).

Interestingly, the mechanical strength range for this well is fairly low, with only one large spike at 1457.0 m TVD, which correlates to a stratigraphic break suggesting possible diagenetic changes in the rocks in this area. This suggests the strata in this area have a fairly uniform rock strength competency, with no fracture zones.

Deeper down in the section, within the Winnipeg Formation, there are some indicators of a hydrocarbon system moving through, with slight increases in the values for hydrocarbon liquid and gas and high toluene/benzene ratio values. The total water values here are higher, suggesting a water-wet interval.

Tectonic effects, fracturing and basement features

As mentioned previously, the three wells selected for RVS analysis were chosen based on certain criteria. A focus on areas with known structural disturbance was key, in order to maximize the opportunity for fluid migration throughout the section and to verify sealing and trapping mechanisms, as well as potentially provide insight into helium sources. Multistage dissolution of the Prairie Evaporite and structural collapse of overlying strata has been well documented in Manitoba (e.g., Nicolas 2012; Nicolas and Yang, 2022); the dissolution front is shown in Figure GS2023-11-1 as a north-trending, westward-moving front, with a path of accelerated dissolution around Twp. 12. The dissolution of this thick salt section has been linked to fluid flow from deep Precambrian-derived fractures formed by movement related to the sub-Phanerozoic Superior boundary zone that underlies southwestern Manitoba. These structures and processes all play an important part in helium sourcing, migration and trapping. Additionally, the Precambrian paleotopography and composition and the presence of the Deadwood Formation, which is productive for helium in Saskatchewan (Yurkowski, 2016, 2021), all play an important role in deciphering the helium story.

The magnitude of the helium values and the wide stratigraphic distribution of those values seen in this dataset was unexpected, and suggests a more complex system of fractures and helium sources at play in Manitoba. There is a need for more detailed data collection and analysis from more wells, perhaps in areas with less obvious structural affects, including detailed lithological and mineralogical study and evaluation of seismic cross-sections in the vicinity of the three wells studied here.

Conclusions

All three wells in this study show signs of helium accumulation of varying degrees. The well at 9-6-2-26W1 has returned the highest helium values measured by the RVS system to date in legacy samples for which self-sourcing of the helium from in situ uranium- and thorium-bearing basement rocks or shale was not possible. This indicates an active prolific helium system and bypassed deep hydrocarbon system opportunities in Manitoba. Helium target zones in this well include the Red River Formation and the Winnipeg–Deadwood formations intervals. The well at 16-29-12-29W1 also shows good indications of potential helium target zones within the Red River Formation. At first glance, the data from the well at 13-24-12-27W1 suggests that there is no helium target zone, since most helium values fall below 0.7 nmol, however, if the affect of drill cutting size on the RVS analysis is taken into consideration, there is an expectation of an attenuation of results, thus the Red River Formation could be a zone of interest. Further testing for helium is recommended. Additionally, if the helium data from RVS analysis are considered as minimum values, all three wells have helium target zones in the Red River Formation. In the deeper basin, an additional target zone would be the porous strata of the Deadwood Formation immediately overlying the Precambrian basement.

Despite the lack of hydrocarbon production in Manitoba from below the Devonian Torquay Formation, the hydrocarbon indicators in the RVS data clearly show that significant amounts of hydrocarbons have migrated through these deep strata. No economical deep hydrocarbon accumulations have yet been discovered in Manitoba, and little exploration in these deeper horizons has occurred in more than three decades. Modern evaluation of these deep strata using modern economic analysis, combined with advanced drilling techniques and downhole geophysical logs, is required to accurately and meaningfully evaluate these horizons to unlock the pore-space resources, including helium and hydrocarbons, contained within them.

Economic considerations

The global demand for helium has resulted in a dramatic increase in helium exploration projects, with many of them located in Canada. With concerns about climate change, extracting helium from nonhydrocarbon reservoirs—known as green helium–is of particular interest. The RVS data from three Manitoba wells indicate a robust helium presence in the deeper parts of the southwestern subsurface of Manitoba. Since these helium shows are not associated with large producing oil and gas pools, this would classify most, if not all of Manitoba's helium, as green helium, automatically making it an attractive investment and exploration opportunity waiting to be unlocked.

Acknowledgments

The authors would like to thank M. Yurkowski from the Saskatchewan Geological Survey for her good discussions and insights into the helium systems, and for her technical peer review of this report. P. Fulton-Regula is also acknowledged for her critical review of this report.

References

Asamara Oil Corporation Limited 1975: Drilling - engineering geological report, ASM-BTO et al Kirkella Prov. Lsd. 16, Sec. 29, Twp. 12, Rge. 29, WPM, Province of Manitoba; Manitoba Mines, Resources and Environmental Management, Petroleum Technical Well File 2532, 61 p., URL <https://content.gov.mb.ca/iem/petroleum/documents/technical/002532.pdf> [September 2023].

Fire Sky Energy Inc. 2018: Geological report on Fire Sky North Hargrave 13-24-12-27 (WPM); Manitoba Growth, Enterprise and Trade, Petroleum Technical Well File 10911, 234 p., URL <https://content.gov.mb.ca/iem/petroleum/documents/technical/010911.pdf> [September 2023].

Nicolas, M.P.B. 2012: Stratigraphy and regional geology of the Late Devonian-Early Mississippian Three Forks Group, southwestern Manitoba (NTS 62F, part of 62G, K); Manitoba Innovation, Energy and Mines, Manitoba Geological Survey, Geoscientific Report GR2012-3, 92 p.

Nicolas, M.P.B. 2018: Summary of helium occurrences in southwestern Manitoba; *in* Report of Activities 2018, Manitoba Growth, Enterprise and Trade, Manitoba Geological Survey, p. 110–118.

Nicolas, M.P.B. and Yang, C. 2022: Stratigraphy and distribution of the potash-bearing members of the Devonian Prairie Evaporite, southwestern Manitoba (parts of NTS 62F, K); *in* Report of Activities 2022, Manitoba Natural Resources and Resource Development, Manitoba Geological Survey, p. 87–95.

Nicolas, M.P.B., Smith, C.M. and Smith, M.P. 2023: Rock Volatiles Stratigraphy data from drill cuttings from three oil wells in southwestern Manitoba (parts of NTS 62F2, K3); Manitoba Economic Development, Investment, Trade and Natural Resources, Manitoba Geological Survey, Data Repository Item DRI2023014, Microsoft® Excel® file.

Smith, C.M. and Smith, M.P. 2020: Evaluating failure: extracting relevant volatile geochemical information from legacy geological materials from dry holes and under performing wells; GeoGulf Transactions, v. 70, p. 297–309.

Smith, C., Cammack, J., Smith, T., Gordon, P. and Smith, M. 2023a: Helium and low-hydrocarbon reservoir in San Juan County, Utah: unconventional methods to detect reservoir zonations and gas-water contacts, part 2; *in* The Rocky Mountain Association of Geologists, North American Helium Conference, Program Book, March 22–23, 2023, Westminster, Colorado, p. 69–70.

Smith, C.M., Mercer, D., Smith, T.M., Liaw, V., Gordon, P.S. and Smith, M.P. 2021: A volatiles analysis case study evaluating the petroleum system, pay zones, seals, chemical compartments, and potential pay zones from a Gulf of Mexico well in Main Pass Field using legacy, oil based mud and PDC bit cuttings, with tie ins to wireline and seismic data; GeoGulf Transactions, v. 71, p. 265–279.

Smith, C.M., Smith, M.P., Gordon, P.S., Smith, T.M. and Duncan, E. 2023b: Advanced Hydrocarbon Stratigraphy (AHS) use of proprietary Rock Volatiles Stratigraphy (RVS) system to analyze cuttings samples of Great Bear Pantheon's exploration wells on the North Slope; Society of Petroleum Engineers, Western Regional Meeting, May 22–25, 2023, Anchorage, Alaska, paper presented, p. 1–19.

Smith, C.M., Smith, M., Gordon, P., Smith, T., Flynn, J., Priddell, T. and Yurkowski, M. 2022a: Rock volatiles analyses of the B.A. Saskatchewan Landing core — detailed fluid, reservoir, and cap rock insights from the C1-C10 hydrocarbons, organic acids, CO_2, formation water, helium, various sulfur gases, and mechanical strength: implications for helium system analysis; *in* Twenty-Ninth Williston Basin Petroleum Conference, Dr. Don Kent Core Workshop Volume, Saskatchewan Geological Society, Special Publication No. 27, p. 1–9.

Smith, C.M., Smith, T.M., Gordon, P.S. and Smith, M.P. 2022b: Rock Volatiles Stratigraphy analysis of helium in 60+ year old cores from the Keyes Dome Field in Oklahoma: implications for helium exploration and development; Society of Applied Geoscientists and Engineers, 2nd SAGE Applied Geoscience and Engineering Symposium, June 30, 2022, Lafayette, Louisiana, abstract volume.

Smith, C., Yurkowski, M., Flynn, J., Kohlruss, D., Smith, T., Gordon, P. and Smith, M. 2023c: Understanding the subsurface helium system of Saskatchewan with a focus on traps/seals via volatiles analysis of helium and other compounds in legacy cores; *in* The Rocky Mountain Association of Geologists, North American Helium Conference, Program Book, March 22–23, 2023, Westminster, Colorado, p. 50–51.

Smith, H.M. 1968: Qualitative and quantitative aspects of crude oil composition; U.S. Department of the Interior, Bureau of Mines, Bulletin 642, 136 p.

Yurkowski, M.M. 2016: Helium in southwestern Saskatchewan: accumulation and geological setting; Saskatchewan Ministry of the Economy, Saskatchewan Geological Survey, Open File Report 2016-1, 20 p.

Yurkowski, M.M. 2021: Helium in southern Saskatchewan: geological setting and prospectivity; Saskatchewan Ministry of Energy and Resources, Saskatchewan Geological Survey, Open File Report 2021-2, 77 p.

GS2023-12

Current Quaternary geology investigations in southeastern Manitoba and implications for mineral exploration (parts of NTS 52L, 62P, 63A)

by T.J. Hodder and T. Martins

Summary

Quaternary geology investigations were conducted in southeastern Manitoba, to map paleo–ice-flow indicators, collect till samples and assess the suitability of current surficial geology mapping to guide drift exploration. Additionally, this study aims to characterize the dispersal of detritus from known lithium-bearing pegmatites in the Bird River area to better inform how drift prospecting methods can be used for critical minerals. Initial results from a pilot study conducted indicate that spodumene can be recovered from till that was collected down-ice of a known occurrence. Surprisingly, one sample from the road connecting Manigotagan and Berens River (east-side road) recovered two spodumene grains. This was an unexpected occurrence since there is no known lithium-bearing pegmatites in the region; however, the till-matrix geochemistry in this region has elevated lithium and cesium concentrations indicating that there is potential for lithium-mineralized systems in this underexplored region of Manitoba. The recovery of the rare-earth-element (REE) minerals euxenite and parisite from till along the east-side road indicate that there is also potential for uranium-thorium-REE–mineralized systems in the region. Elevated gold grain counts in till collected near Cat Lake is a significant occurrence and the source of these gold grains is unknown. The surficial geology mapping available for the Bird River area overrepresents the proportion of glacial-derived sediments (diamicton) in the area and underrepresents the proportion of glaciolacustrine sediments (sand). This characteristic of these surficial maps needs to be considered when planning any drift exploration in the Bird River area.

In Brief:

- Investigating the glacial dispersal of detritus from known Li-bearing pegmatites in the Bird River area using multiple parameters
- Collection of ice-flow data to reconstruct the glacial history and aid drift exploration
- Release of 2022 pilot study indicator mineral results

Citation:
Hodder, T.J. and Martins, T. 2023: Current Quaternary geology investigations in southeastern Manitoba and implications for mineral exploration (parts of NTS 52L, 62P, 63A); *in* Report of Activities 2023, Manitoba Economic Development, Investment, Trade and Natural Resources, Manitoba Geological Survey, p. 105–119.

Introduction

The Manitoba Geological Survey (MGS) initiated a multidisciplinary Precambrian and Quaternary geology project focusing on the Bird River area of the Superior province of southeastern Manitoba (Figure GS2023-12-1). This report presents ongoing investigations regarding the Quaternary geology and the reader is referred to Martins et al. (2023) and Roush et al. (2023) for current bedrock mapping and compilation geology studies in the region. Quaternary geology fieldwork was conducted for one day in October 2022 and 14 days in June and August of 2023. A total of 139 field sites were visited to document the Quaternary sediments, collect till samples and measure the orientation of ice-flow indicators. As part of a pilot study, one till sample was analyzed over the winter of 2022 to assess if Li-bearing minerals could be recovered from till sampled down-ice of a known occurrence. Additionally, four samples were analyzed to assess if there is any potential for Li-mineralization along the road connecting Manigotagan and Berens River (east-side road).

The goals of this project are to

- map paleo–ice-flow indicators to assist reconstructions of the glacial history, which in turn guides drift exploration studies;
- assess the use of till-matrix geochemistry and indicator minerals to characterize the dispersal of detritus from Li-bearing pegmatites in the Bird River area; and
- assess the suitability of published surficial geology maps to guide drift exploration in this region of Manitoba.

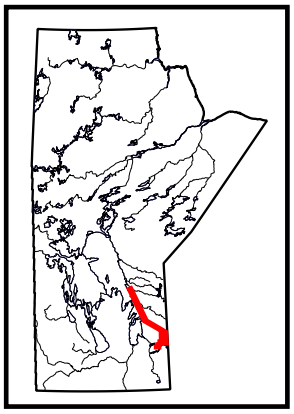

Previous work

Surficial geology mapping

Southeastern Manitoba was mapped at a 1:100 000 scale during the National Geoscience Mapping Program (NATMAP; Southern Prairies and Greater Winnipeg projects; Matile and Fulton, 1994; Matile et al., 1998). An inventory of published surficial geology maps from this program is available through the MGS website (Manitoba Geological Survey, 2023). However, these series of maps were

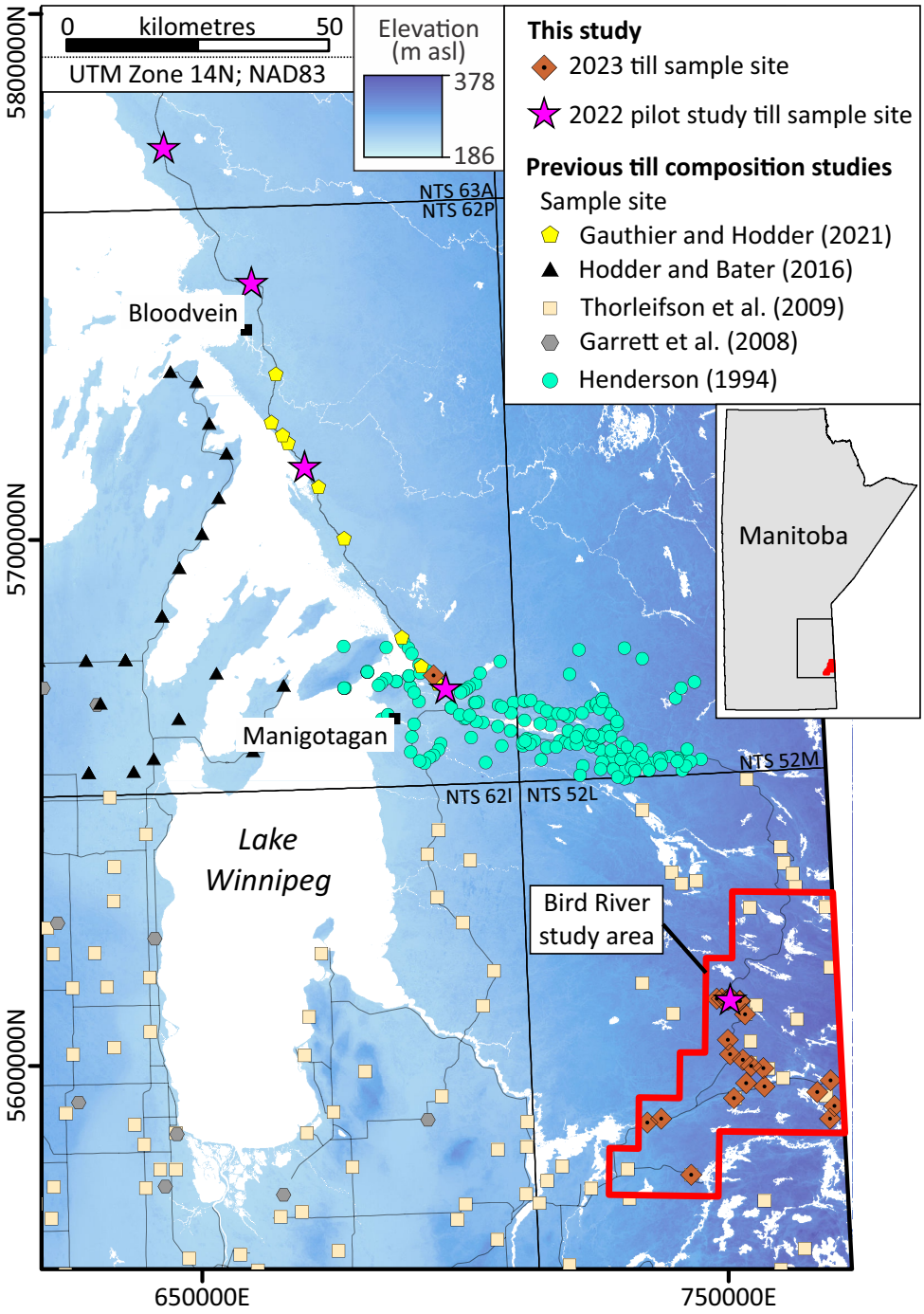

Figure GS2023-12-1: *Location of the Bird River study area (red polygon) in southeastern Manitoba. The locations of the five till samples analyzed as part of the 2022 pilot study are highlighted by pink stars. Sample locations from previous till-composition datasets for the region are plotted for reference. Background elevation data is provided by Earth Observation Research Center and Japanese Aerospace Exploration Agency (2022).*

published without any of the supporting field-based observations and station locations. This is useful information to understand where surficial geology mapping has been 'ground truthed', as a map is more accurate closest to those sites. Field-based data collected during the NATMAP projects were recovered from digital archives at the MGS and are published as Data Repository Items DRI2023009 (Matile et al., 2023b) and DRI2023010 (Matile et al., 2023c). Additionally, the published surficial geology maps from the NATMAP Greater Winnipeg project were missing collected field-based erosional ice-flow indicator measurements. This dataset was recovered from digital archives and also recently published (Matile et al., 2023a).

Till sampling

Till composition studies over the Precambrian shield of southeastern Manitoba were initially completed in the 1990s. These studies include an ultra-low density till sampling study

of the Canadian prairies (Thorleifson and Garrett, 1993; Garrett et al., 2008), a detailed regional-scale till sampling study of the Rice Lake belt (Henderson, 1994) and a reconnaissance-scale till-sampling study of southeastern Manitoba during the NATMAP projects (Thorleifson et al., 2009; Figure GS2023-12-1). A reconnaissance-scale till-sampling study of the newly established road between Manigotagan and Berens River was undertaken in 2020 (Gauthier and Hodder, 2020, 2021).

Methods

Field data

A total of 139 field sites were visited to ground-truth previous surficial geology mapping, collect till samples and map paleo–ice-flow indicators. The surficial materials at each field station were investigated by means of a hand-dug shovel hole, a Dutch auger (1.2 m long) hole, gravel pit or roadcut/trailcut exposures. Where encountered, till samples were collected from the hand-dug pits or cut exposures within the Bird River study area (e.g., Figure GS2023-12-2). At each site, a smaller ~2–3 kg sample and a larger ~14–16 kg sample were collected from C-horizon (n = 19 of 23) diamicton, interpreted as till, or in cases where C-horizon diamicton was in limited supply due to thin till cover, samples consisting of a mix of B- and C-horizon diamicton were collected (n = 4 of 23). The 2–3 kg till samples were split for archival purposes at the MGS Midland Sample and Core Library (Winnipeg, Manitoba) and will be analyzed for matrix grain size and geochemistry. This study will analyze the geochemistry of two different grain-size fractions and use similar digestion methods to work ongoing near the Brazil Lake pegmatite in Nova Scotia (McClenaghan et al., 2023). The 14–16 kg samples were submitted to Overburden Drilling Management Limited (ODM; Ottawa, Ontario) for indicator-mineral analyses and recovery of clasts for lithological classification.

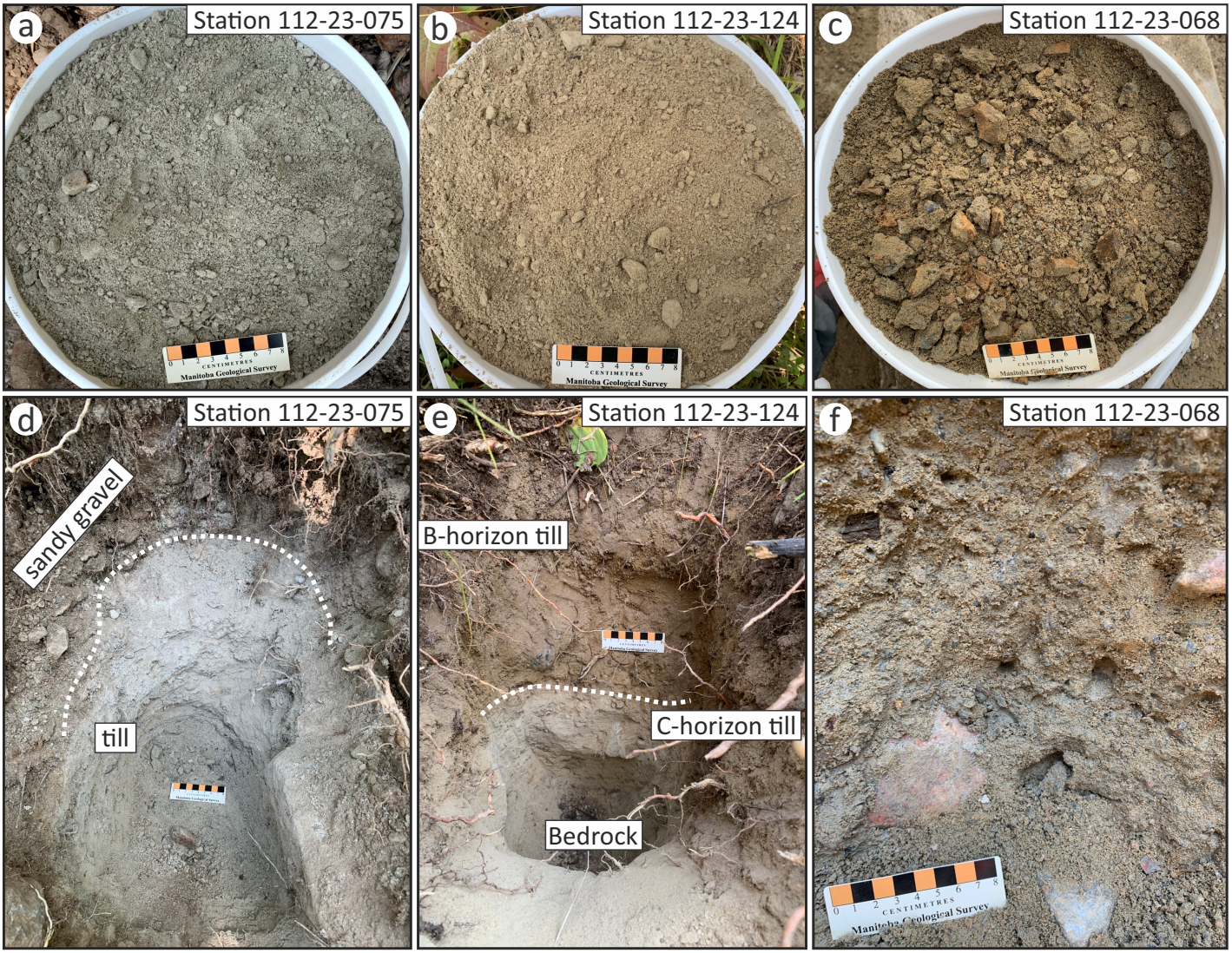

Figure GS2023-12-2: *Examples of till sampled and the hand-dug pits or exposures that they were obtained from:* ***a)*** *sandy-silt diamicton;* ***b)*** *sandy diamicton;* ***c)*** *sandy diamicton with a blocky appearance;* ***d)*** *overgrown trailcut exposure where till could be sampled underlying sandy gravel;* ***e)*** *hand-dug pit where C-horizon till could be sampled overlying bedrock;* ***f)*** *recently exposed site where till buried beneath postglacial sediments could be sampled, sediments which would not have been accessible in a hand-dug pit.*

Erosional paleo–ice-flow indicators, such as striae and grooves, were mapped at bedrock outcrops within the study area (e.g., Figure GS2023-12-3). The relative chronology at outcrops that exhibited multiple paleo–ice-flow indicators was deciphered using the crosscutting and outcrop relationships of facets and striae (McMartin and Paulen, 2009). Till-fabric measurements were completed at one site within the Bird River study area, where recently exposed sediments allowed access to a vertical face of till that was buried beneath postglacial sediments, and at one site near Manigotagan, which was initially visited in 2020 (Gauthier and Hodder, 2020). Each till-fabric measurement included the long-axes orientation of 30 elongated clasts, defined by a minimum 1.5:1.0 ratio of the a-axis (longest) to the b-axis (middle). These elongated clasts tend to rotate within the till matrix and orient parallel to the overlying glacier's shear stress direction (Holmes, 1941). Ice-flow data collected in 2023 is published in Data Repository Item DRI2023012 (Hodder and Gauthier, 2023)[1]. This ice-flow data will be combined with the forthcoming till-composition data to help interpret the till provenance and glacial history of the study area.

Indicator-mineral processing

The five till samples collected in 2022 were processed at ODM and results are presented in Data Repository Item DRI2023011 (Hodder, 2023)[2]. The <2 mm size fraction was passed across a shaker table to preconcentrate the mid- and heavy density mineral fractions. The preconcentrate was then micropanned to recover fine-grained gold, sulphide and other indicator minerals. The 0.25–2.0 mm concentrate was then processed using a heavy liquid separation to a specific gravity (SG) of 3.0 to produce a mid-density mineral concentrate (SG 2.8–3.0; MDMC) and at 3.2 to produce a heavy mineral concentrate (SG >3.2; HMC). Ferromagnetic minerals were removed from the MDMC and HMC fractions using a magnet. The nonferromagnetic MDMC and HMC fractions were then sieved into 0.25–0.5, 0.5–1.0 and 1.0–2.0 mm size fractions. The 0.25–0.5 HMC was then refined with a paramagnetic separation to assist counting of this fine fraction. These size fractions were then visually picked for metamorphic massive-sulphide–indicator minerals (MMSIMs®), lithium-indicator minerals (LIMs) and kimberlite-indicator minerals (KIMs). A select number of MMSIM, LIM and KIM grains were then verified using a scanning electron microscope (SEM) and these grains are noted in the remarks column for each table within Data Repository Item DRI2023011 (Hodder, 2023). Till samples collected in 2023 will be processed using the same methods.

Raman spectroscopy analyses

Picked spodumene grains from the 0.25–0.5 mm size fraction of the MDMC of two samples (n = 4 grains) were selected for Raman spectroscopy for additional mineral confirmation. Analytical techniques such as SEM are unable to detect Li, meaning that mineral phases containing this light element can sometimes be misidentified using this technique alone. Raman spectroscopy can easily identify Li-bearing mineral phases, is nondestructive and requires minimal sample preparation. The analytical work was carried out at the University of Manitoba (Winnipeg, Manitoba) using a HORIBA Scientific LabRAM ARAMIS instrument equipped with a 460 mm focal length spectrometer, multichannel electronically cooled charge-coupled device detector, motorized x–y–z stage and solid-state 532 nm laser (mpc6000 by Laser Quantum) with a nominal output power of 50 megawatts (mW). The instrument was operated in confocal mode; an Olympus microscope coupled to the spectrometer was used to focus the laser beam on the sample surface and collect the generated Raman signal. The spectra were collected with a diffraction grating of 1800 g/mm; other instrumental parameters (data-collection times, slit width, etc.) were optimized by performing multiple measurements on the same area. Raman spectrum from spodumene reference material from the University of Manitoba collection was collected for comparison.

Preliminary results

Ice-flow reconstruction

Erosional ice-flow indicators were mapped at 38 field stations during the 2022 and 2023 field season in the Bird River study area (Hodder and Gauthier, 2023; Figure GS2023-12-4a). Striations and grooves account for the majority of documented erosional paleo–ice-flow indicators. Most of the outcrops visited were not glacially polished, due to postglacial subaerial weathering, and these outcrops generally only preserved the most recent ice-flow direction. The exception to this is at the Irgon pegmatite where the Quaternary sediments covering the bedrock were recently removed and glacially polished bedrock is now exposed, which provides an excellent opportunity to document the preserved ice-flow indicators (e.g., Figure GS2023-12-3a–d).

Four phases of ice flow are interpreted based on relative-age relationships observed in the study area (Figure GS2023-12-4b). The oldest ice-flow events preserved in the erosional record are toward the west-southwest to west (255–270°) and south to south-southwest (185–208°). There were no age relationships observed between these two ice-flow events in the study area. Following these older ice-flow events, east-southeast to

[1] MGS Data Repository Item DRI2023012, containing the data or other information sources used to compile this report, is available online to download free of charge at https://manitoba.ca/iem/info/library/downloads/index.html, or on request from minesinfo@gov.mb.ca, or by contacting the Resource Centre, Manitoba Economic Development, Investment, Trade and Natural Resources, 360-1395 Ellice Avenue, Winnipeg, Manitoba R3G 3P2, Canada.

[2] MGS Data Repository Item DRI2023011, containing the data or other information sources used to compile this report, is available online to download free of charge at https://manitoba.ca/iem/info/library/downloads/index.html, or on request from minesinfo@gov.mb.ca, or by contacting the Resource Centre, Manitoba Economic Development, Investment, Trade and Natural Resources, 360-1395 Ellice Avenue, Winnipeg, Manitoba R3G 3P2, Canada.

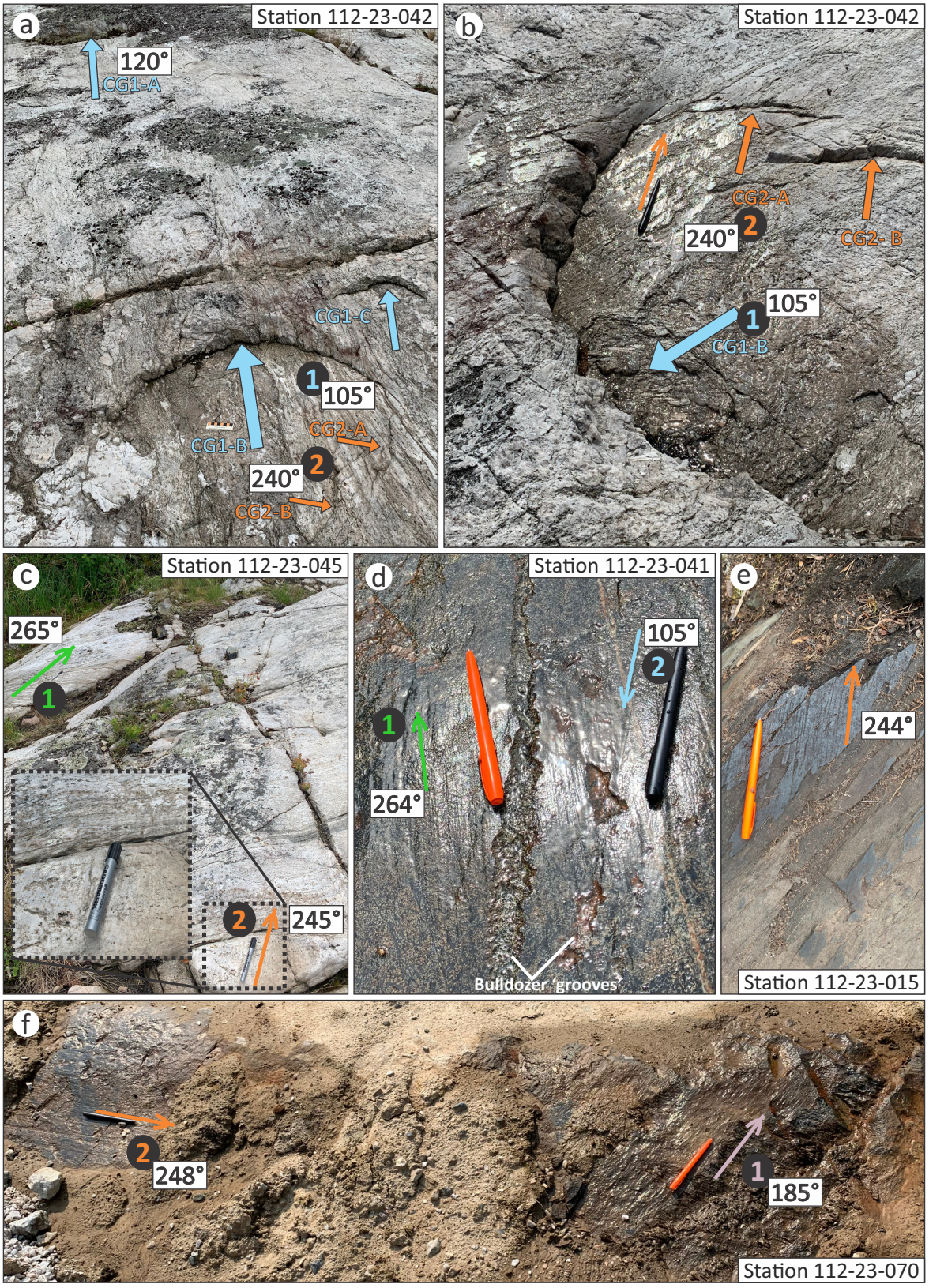

Figure GS2023-12-3: *Examples of field-based erosional ice-flow indicators observed:* ***a, b)*** *crescentic gouges and striations on the crest of the Irgon pegmatite. Note, specific crescentic gouges have been labelled (e.g., CG1-A, CG2-B) to help the reader orient themselves between photos. The right limb of the CG1-B crescentic gouge has been remoulded by the later 240° ice flow providing a relative age relationship at this site;* ***c)*** *striations oriented at 265° are situated on the down-ice side of the outcrop that was protected from the most recent 245° ice flow;* ***d)*** *striations oriented toward 264° are crosscut by a younger set of striations oriented at 105–285° on a surface of the Irgon pegmatite that is at a lower elevation than the crest of the pegmatite (protected);* ***e)*** *a more resistant part of the outcrop is striated at 244° on top;* ***f)*** *striations oriented at 185° are situated on a facet that was protected from a later 248° ice flow.*

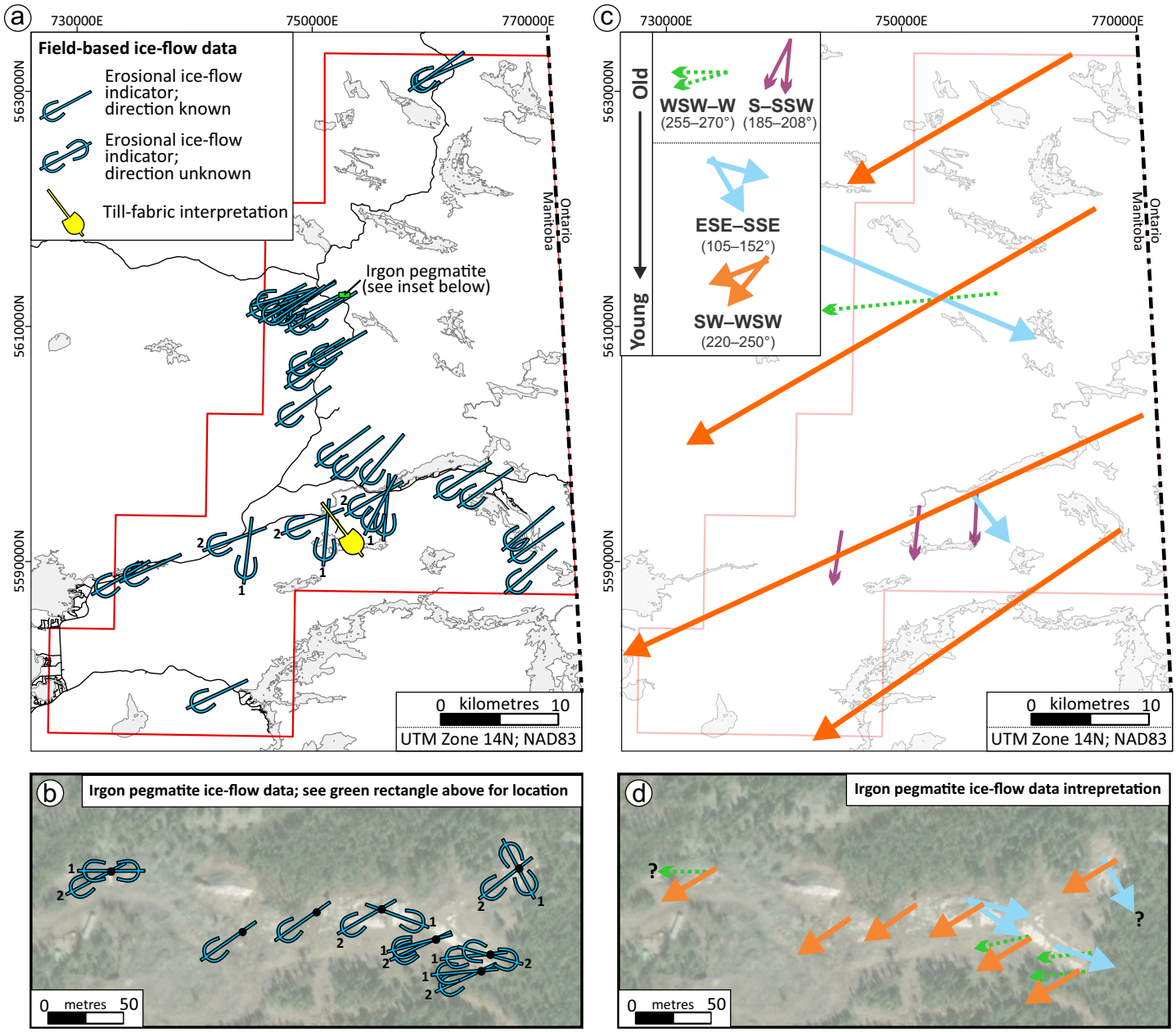

Figure GS2023-12-4: *Ice-flow indicator data and interpretation of the relative ice-flow history in the Bird River area:* ***a)*** *field-based ice-flow indicator data measured in the study area;* ***b)*** *aerial view of the area around the Irgon pegmatite and ice-flow indicators measured;* ***c)*** *an interpretation of the relative ice-flow history;* ***d)*** *aerial view of the area around the Irgon pegmatite and ice-flow data interpretation. Abbreviations: E, east; N, north; S, south; W, west. Basemap imagery in b) and c) was created using ArcGIS® software by Esri. ArcGIS® and ArcMap™ are the intellectual property of Esri and are used herein under license. Copyright © Esri. All rights reserved. For more information about Esri software please visit <https://esri.ca/>.*

southeast-trending (105–152°) ice overrode the study area. This ice-flow event is evidenced by large-scale crescentic gouges on the crest (Figure GS2023-12-3a, b) and as striations in relatively low-lying areas of the Irgon pegmatite (Figure GS2023-12-3d). A till fabric measured in a relatively denser till with a blocky soil structure (Figure GS2023-12-2c, f), which is qualitatively different than surficial till sampled in the study area, yielded a northwest-southeast (323-143°) fabric orientation and is tentatively correlated to this ice-flow event. This till is situated at 2.5 m below ground surface. The last ice-flow event that the region experienced trended southwest to west-southwest (220–250°). Erosional indicators associated with this ice-flow event are visible at most outcrops visited in the study area.

Indicator-mineral pilot study

Five till samples were submitted as part of a pilot study to determine if Li-bearing minerals could be recovered from till samples (Figure GS2023-12-1). This sampling consisted of a single sample collected ~150 m southwest of the spodumene-bearing F.D. No. 5 pegmatite in the Bird River study area (see Martins et

al., 2023; Roush et al., 2023), which is down-ice of the dominant ice-flow direction in the region, and four samples extracted from MGS archives that were collected in 2020 from the east-side road reconnaissance study (Gauthier and Hodder, 2020, 2021).

F.D. No. 5 pegmatite

The till sample collected 150 m southwest of the F.D. No. 5 Li-bearing pegmatite recovered 35 spodumene [$LiAl(Si_2O_6)$] grains within the MDMC (sample 112-22-503-A01; Figure GS2023-12-5; e.g., Figure GS2023-12-6a). The recovery of spodumene from till using a mid-density mineral separation indicates that this novel technique developed at ODM is another tool that can be used in the exploration of Li-bearing pegmatites in the province. Additional till samples were collected in the vicinity of the Li-bearing pegmatites (F.D. No. 5 and Eagle) near Cat Lake (Martins et al., 2023; Roush et al., 2023) during the 2023 field season to gain further understanding of the till composition around these occurrences.

Surprisingly, within the HMC, seven quartz with gahnite ($ZnAl_2O_4$) grains (e.g., Figure GS2023-12-6b) and six scheelite ($CaWO_4$) grains (e.g., Figure GS2023-12-6c) were recovered. There are no known occurrences of zinc or tungsten to the northeast (which is the up-ice direction based on local ice-flow indicators; Figure GS2023-12-5b) of this sample site (Martins et al., 2023).

Importantly, there were also 63 gold grains recovered from this sample (e.g., Figure GS2023-12-6d), including 23 pristine grains (Figure GS2023-12-5). This is a significant amount of gold grains and is nearly double the previous high (n = 35 total grains) recovered from surficial till sampled during the NATMAP projects in southeastern Manitoba (n = 350 samples; Thorleifson et al., 2009). A comparison with visible gold concentrations in the province-wide till dataset (n = 6709 samples; Gauthier, 2020) indicates that this sample ranks in the >99th percentile. The bedrock source of these gold grains is unknown and the closest known gold occurrence is situated 10 km to the northeast (which is up-ice based on the dominant regional ice-flow direction) of this sample site (Martins et al., 2023). The till-matrix geochemistry of this sample is being analyzed alongside the 2023 samples and results are pending.

East-side road

Two till samples collected along the east-side road recovered REE minerals of interest from the HMC: euxenite [$(Y, Ca, Ce, U, Th)(Nb, Ta, Ti)_2O_6$] and parisite [$Ca(Ce, La)_2(CO_3)_3F_2$]. These two samples are situated 30.7 km apart (samples 112-20-011-A01 and 122-20-057-B01; Figure GS2023-12-5) and the bedrock source of the REE minerals recovered is uncertain. Euxenite can be found associated with U-Th-REE–rich granitic pegmatites as described by Bannatyne (1985) for dikes in the Shatford Lake area, Manitoba, or by Simmons et al. (2012) in north-central and southwestern United States. Euxenite is also found in other mineralized systems such as placer deposits (radioactive black sand deposits, Idaho, United States; Kiilsgaard and Hall, 1986), alkaline complexes (Strange Lake deposit, northern Labrador; Miller, 2021) or carbonatites (Aley complex, northeastern British Columbia; Chakhmouradian et al., 2015). Parisite has been described as a rare accessory mineral in the Strange Lake Main Zone deposit (McClenaghan et al., 2019), which hosts Zr-Nb-Y-REE mineralization, associated with a peralkaline granite intrusion in northern Labrador.

Within the MDMC of sample 112-20-027-A01, two spodumene grains were recovered (Figure GS2023-12-5). This is interesting since there are no known Li-bearing pegmatites in this region. To verify this occurrence in till, picked spodumene grains were analyzed with Raman spectroscopy (Figure GS2023-12-7; Table GS2023-12-1) as a follow up from SEM analyses. This analysis looked at the Raman spectra of a spodumene reference material, two picked grains recovered from till sampled down-ice of the F.D. No. 5 pegmatite (sample 112-22-503-A01) and the two grains recovered from till sampled along the east-side road (sample 112-20-027-A01). This analysis confirmed that all four of the picked grains analyzed from till are spodumene and an example of the Raman spectra of one grain from sample 112-20-027-A01 is presented alongside the spodumene reference material in Figure GS2023-12-7 and Table GS2023-12-1.

Elevated Li and Cs concentrations in till matrix

The reconnaissance-scale survey of the east-side road was the first publicly available dataset of till composition for this region (Gauthier and Hodder, 2021). Given the surprising presence of spodumene grains, the Li and Cs partial digestion (aqua regia) concentrations were plotted alongside the province-wide dataset (Gauthier, 2022). Three till samples from the east-side road have >99th percentile Li concentrations and >95th percentile Cs concentrations (Figure GS2023-12-8a, b); these data are also plotted spatially on Figure GS2023-12-5. One of these sites is situated 10.7 km to the northwest of the site where two spodumene grains were recovered from the till sample, and the other two elevated Li-concentration samples are from sites situated 9 km to the north of Bloodvein (Figure GS2023-12-5). Again, there is no known source for Li or Cs in this area.

To the west of Lake Winnipeg, a till-sampling survey was conducted in 2003 within the Fisher Branch (NTS 62P) area. This data was resurrected from digital archives and published in 2016 (Hodder and Bater, 2016). The geochemical data cannot be directly compared with the east-side road data because a different size fraction of the till matrix was analyzed (<177 µm) using a different digestion (four-acid, near-total digestion). However, the Fisher Branch till samples (n = 46) were analyzed alongside the reanalysis of a large number of archived samples (n = 1509) from northwestern Manitoba (Lenton and Kaszycki, 2005). The dataset from the Fisher Branch area (NTS 62P) contains two samples with elevated Li values and two samples with elevated Cs values (Figure GS2023-12-8c, d). When compared to the larger dataset

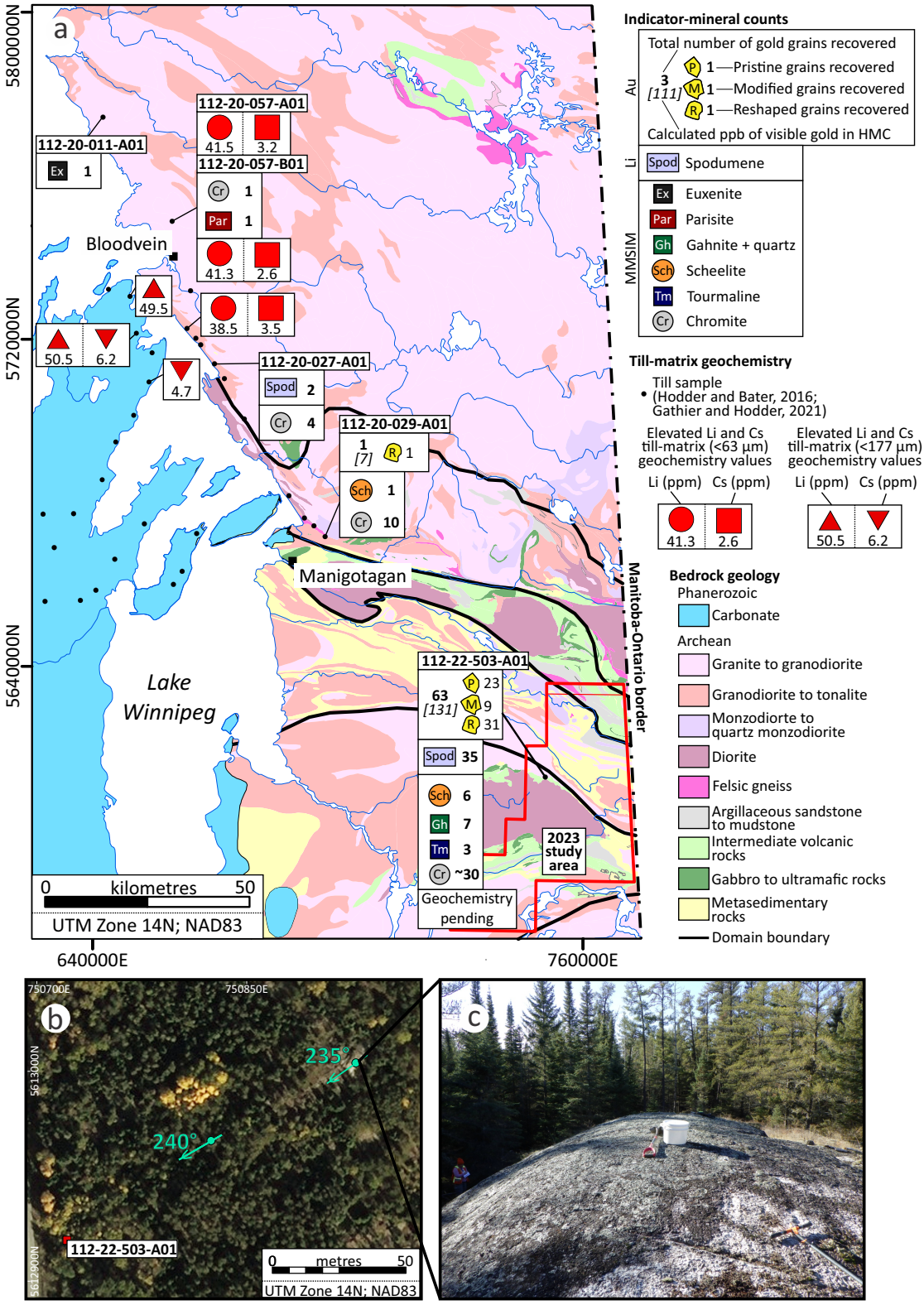

Figure GS2023-12-5: *Pilot study indicator-mineral results and till-matrix geochemistry data from the reconnaissance-scale east-side road (Gauthier and Hodder, 2021) and Fisher Branch area (Hodder and Bater, 2016) studies:* ***a)*** *till-matrix geochemistry values, gold grain counts and selected indicator minerals recovered from till sampled along the road connecting Manigotagan to Berens River (east-side road) and down-ice of the F.D. No. 5 pegmatite (sample 112-22-503-A01); Precambrian bedrock geology is modified from Manitoba Geological Survey (2022) and Phanerozoic bedrock geology is from Nicolas et al. (2010);* ***b)*** *aerial view of the area around the F.D. No. 5 pegmatite with the locations of till sample 112-22-503-A01 and ice-flow indicators measured;* ***c)*** *ground view of the outcropping F.D. No. 5 pegmatite looking down-ice (southwest) with visible ice-flow indicators (grooves) on top. Basemap imagery in b) was created using ArcGIS® software by Esri. ArcGIS® and ArcMap™ are the intellectual property of Esri and are used herein under license. Copyright © Esri. All rights reserved. For more information about Esri software please visit <https://esri.ca/>. Abbreviations: HMC, heavy density mineral concentrate; MMSIM®, metamorphic massive-sulphide–indicator minerals.*

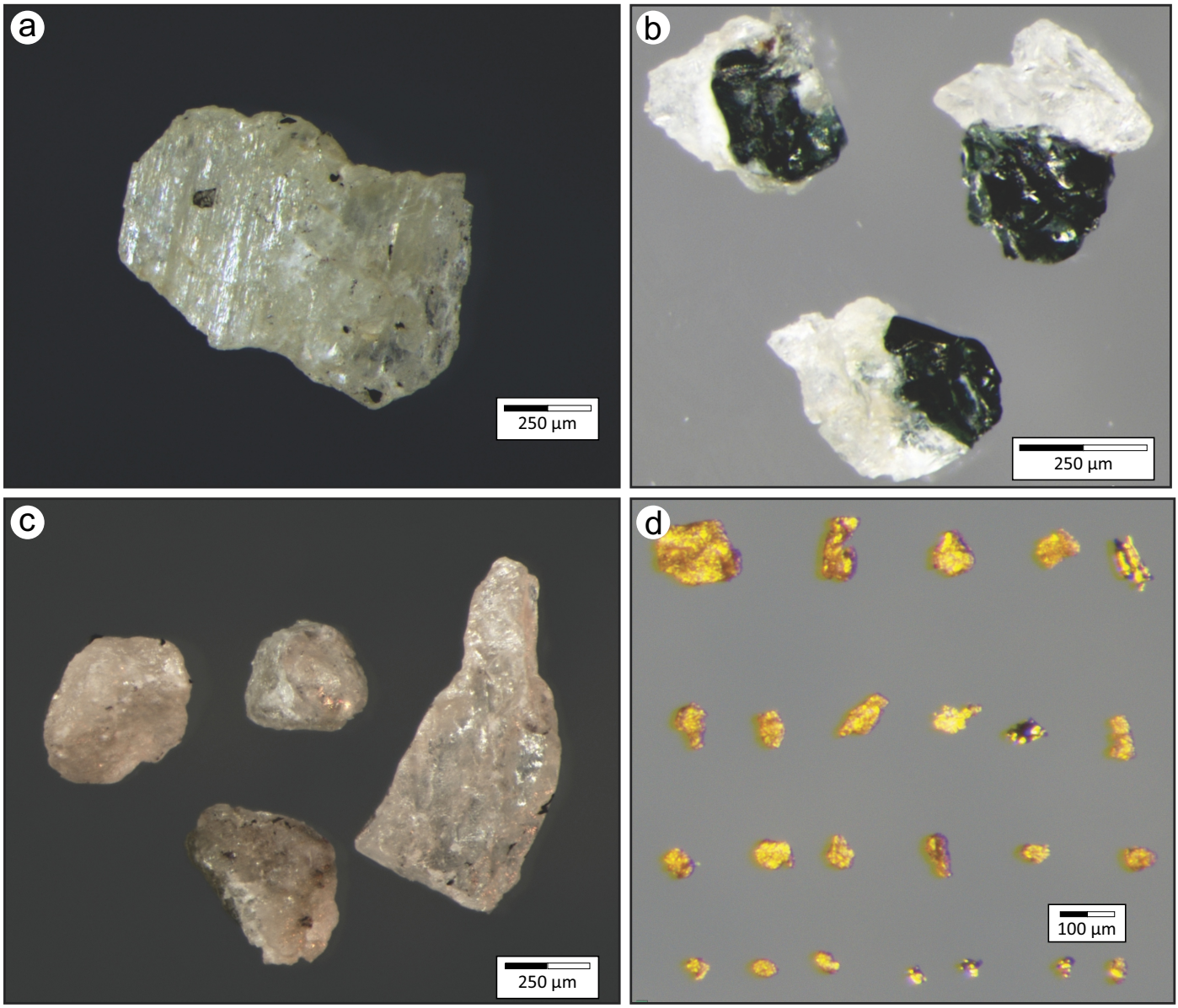

Figure GS2023-12-6: *Example of indicator minerals and gold recovered from sample 112-22-503-A01, which was sampled 150 m down-ice of the F.D. No. 5 Li-bearing pegmatite:* ***a)*** *spodumene grain;* ***b)*** *quartz and gahnite grains;* ***c)*** *scheelite grains;* ***d)*** *gold grains.*

from northwestern Manitoba, the Fisher Branch Li values are in the >98th percentile and the Cs values are in the >97th percentile. This indicates that these Li and Cs values are significant from a regional-scale perspective. These till samples with elevated concentrations are situated 13–30 km southwest of Bloodvein, in close proximity to the elevated Li and Cs samples from the east-side road reconnaissance survey (Figure GS2023-12-5).

The occurrence of elevated Li and Cs values from two different surveys that are spatially coincident, coupled with the recovery of spodumene grains from an indicator-mineral sample from this study, suggests that there is potential for Li-bearing pegamatite mineralization in the region. The dominant ice-flow direction in the region is toward the southwest (220–250°; Gauthier and Hodder, 2020), thus additional till sampling to the east and northeast of Bloodvein could help elucidate the bedrock source.

Suitability of published surficial mapping to guide drift prospecting

Successful drift-prospecting surveys using glacial sediments must use till and not other surficial sediments (McClenaghan et al., 2001, 2020). The Bird River study area is covered by two surficial geology maps that were published at a 1:100 000 scale (Mann, 2004a, b). It is important to note that the fieldwork component of this mapping was primarily restricted to road and trail access, with limited fixed-wing air support (Matile et al., 1998). As a result, there is not an equal distribution of field stations across the mapped area with large regions that have no field-based observations to verify the airphoto interpretations (Figure GS2023-12-9). The surficial geology maps indicate a landscape that is dominated by glacial-derived sediments and bedrock (Figure GS2023-12-9). For the glacial-derived sediments, it

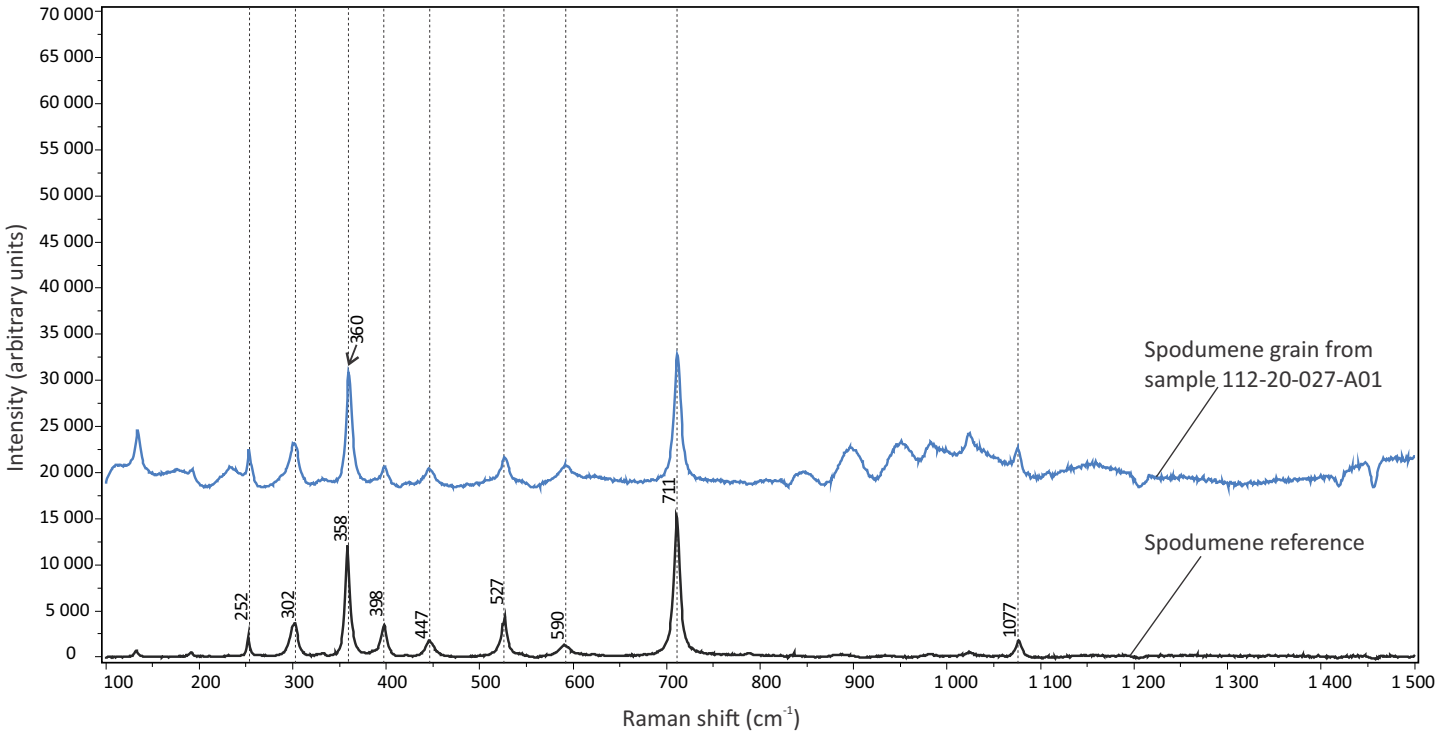

Figure GS2023-12-7: *Raman spectra of spodumene reference material (black) and from one of the spodumene grains recovered from sample 112-20-027-A01 (blue). Note the fluorescence effect after the 850 cm^{-1} range for the spodumene grain from sample 112-20-027-A01 not allowing for a clear match to the peak at approximately 1077 cm^{-1}.*

Table GS2023-12-1: Raman shift of spodumene (reference material and sample 112-20-027-A01) compared to the literature.

Spodumene reference material	Sample 112-20-027-A01	Sharma and Simons (1981)	Raman shift
		225	M-O stretch/bend
252		247	
302	302	296	
		326	
358	360	356	
398	398	389	
		412	
447	447	436	
527	527	512	O-Si-O bend
		542	
590	590	583	
		614	
711	711	707	Si-O_{br} stretch
		782	
		884	
		973	
1077		1012	Si-O_{nbr} stretch
		1066	
		1095	

Abbreviations: br, bridging stretching; nbr, nonbridging stretching; O, oxygen; Si, silicon.

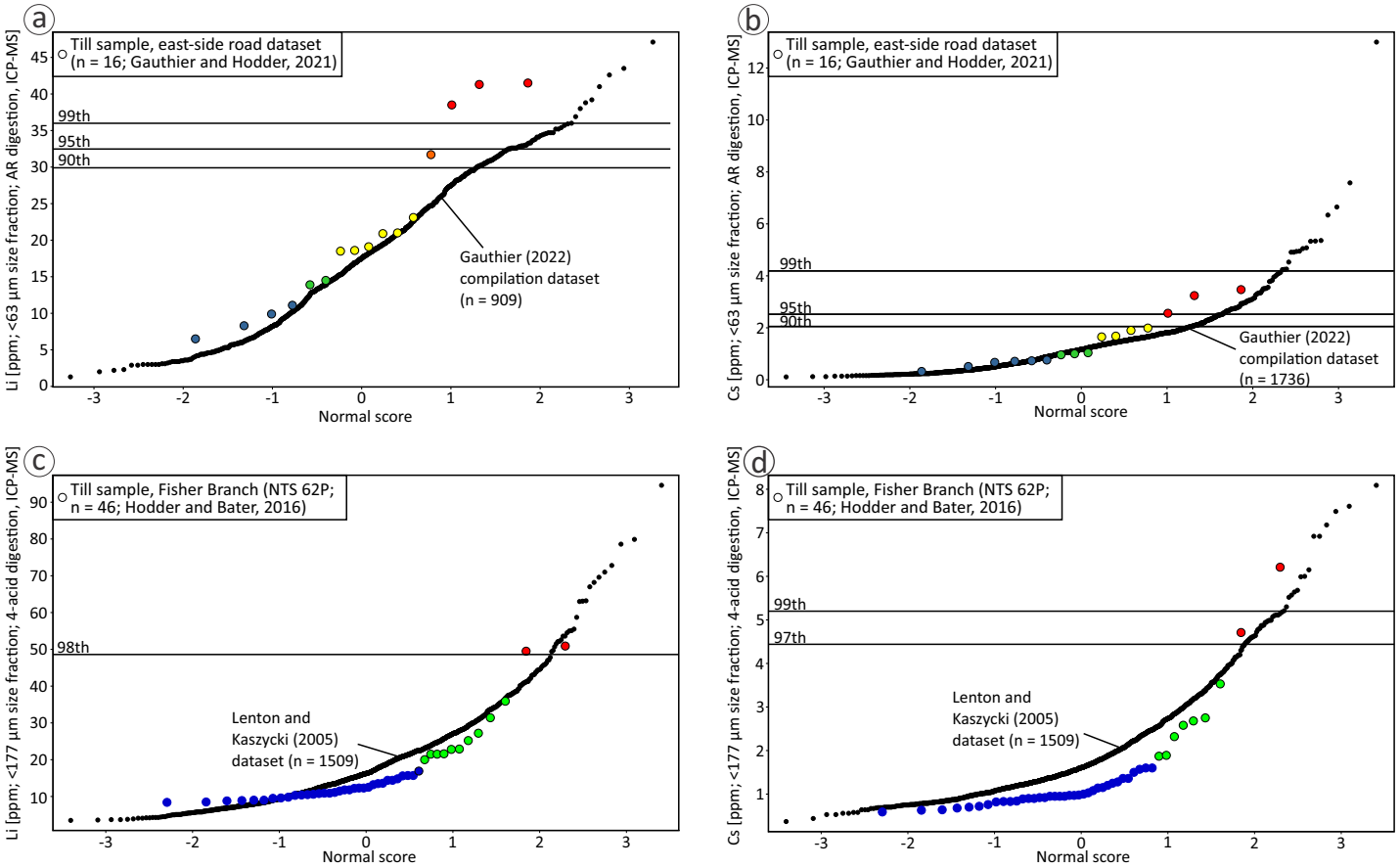

Figure GS2023-12-8: *Till-matrix geochemistry probability plots (Li and Cs) for east-side road and Fisher Branch till samples, compared to regional-scale datasets. Sample symbols have been coloured according to natural breaks, which have been qualitatively identified. Elevated values (red) are plotted spatially on Figure GS2023-12-5:* ***a, b)*** *Li and Cs values from the east-side road study (Gauthier and Hodder, 2021) are compared to values from the province-wide compilation dataset (Gauthier, 2022);* ***c, d)*** *Li and Cs values from the Fisher Branch area (Hodder and Bater, 2016) are compared to reanalyzed till samples from northwestern Manitoba (Lenton and Kaszycki, 2005), which were analyzed at the same time using similar analytical methodologies. Abbreviations: AR, aqua-regia; ICP-MS, inductively coupled plasma–mass spectrometry.*

is important to highlight that by definition these polygons can only be used as guide to where to look for till to sample for drift-prospecting. The legend states that these polygons comprise "gravelly silt to sandy diamicton, sand and gravel; 1–30 m thick; low-relief deposits between outcrops making up 25–75% of the area" (Mann, 2004a, b). Furthermore, these polygons comprise "sandy till interbedded and interspersed with nearly equal and often greater amounts of sandy glaciofluvial sediments, as well as minor glaciolacustrine sediments" (Mann, 2004a, b). These vague and all-encompassing descriptions were the best attempt at the time to acknowledge the scale of mapping, the boreal forest cover, the largely discontinuous sediment cover and the lack of regional field sites. Any future mapping efforts, by the MGS or mineral exploration companies looking for till, will require detailed digital elevation models, such as those derived from light detection and ranging (LiDAR) data, to better understand and map the surficial geology.

Map inaccuracies

The field-station data collected at the time these surficial geology maps were made is now published (Matile et al., 2023c). When comparing these field-based sediment interpretations with the mapped polygons, there are significant discrepancies. To highlight this, two areas are shown with the mapped polygons and field stations plotted together (Figure GS2023-12-10). In the first example (Figure GS2023-12-10a), the area is primarily mapped as discontinuous till and associated glaciofluvial sediments or organic deposits. Yet, the original field station observations indicate that this a bedrock-dominated terrain; confirmed in the field this year and clearly discernible from satellite imagery (Figure GS2023-12-10a). At the one station where till was observed in the field, the area was subsequently mapped as organics. The surficial materials at this location were confirmed as part of this study to be till with a prominent cobble and boulder lag at surface (Figure GS2023-12-10b). In the second example (Figure GS2023-12-10c), all of the field-based observations were of sorted sediments, organics or bedrock, but the subsequent mapping portrays a landscape dominated by discontinuous till and associated glaciofluvial sediments. Even though some of these sediments may have been deposited in a glaciofluvial environment, it is more likely that the majority of these sorted sediments were deposited within glacial Lake Agassiz, which cov-

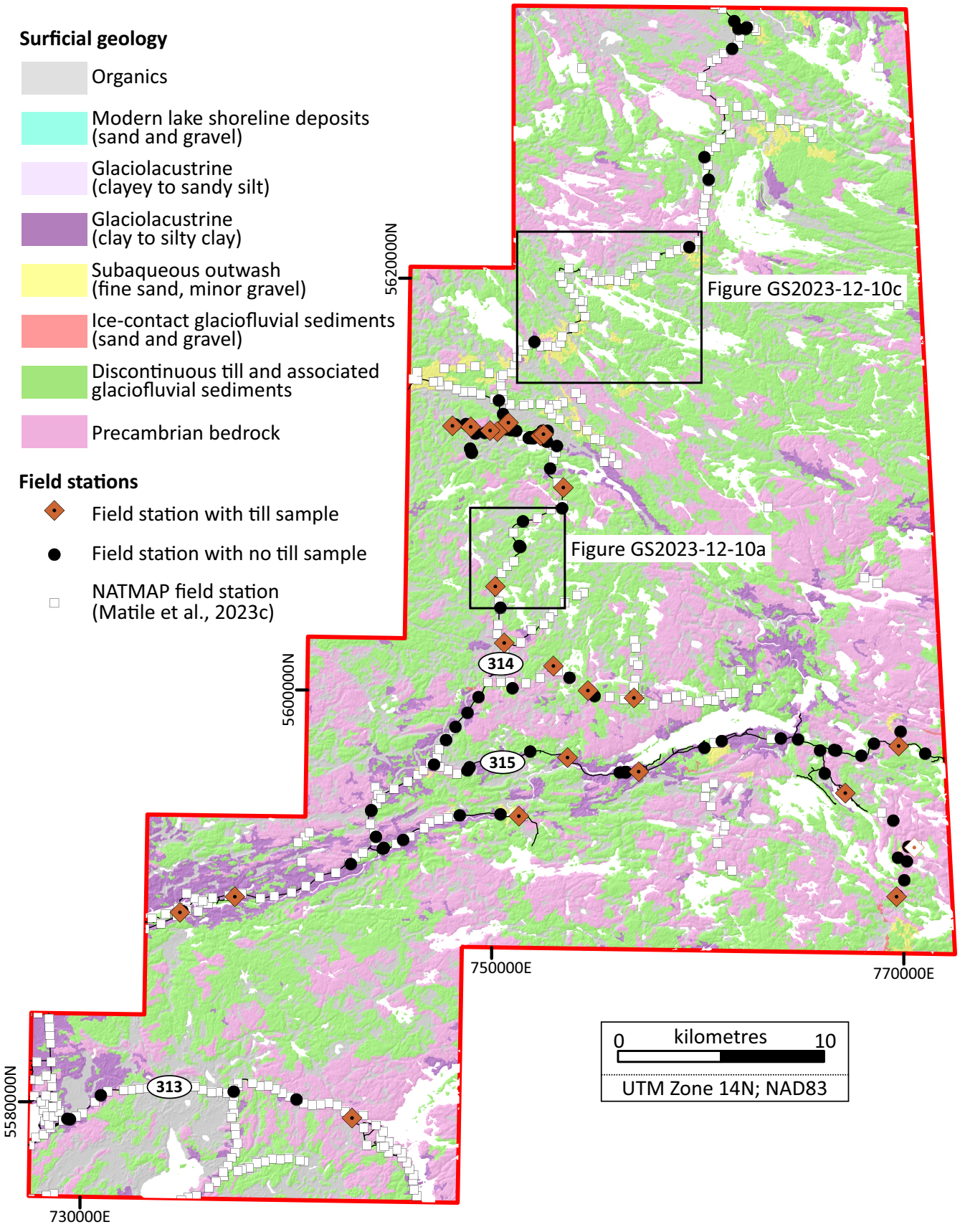

Figure GS2023-12-9: *Surficial geology of the Bird River study area (Mann, 2004a, b). The locations of the field stations, observations from which were used to produce these surficial maps, are displayed alongside 2022 and 2023 field stations. Abbreviation: NATMAP, National Geoscience Mapping Program.*

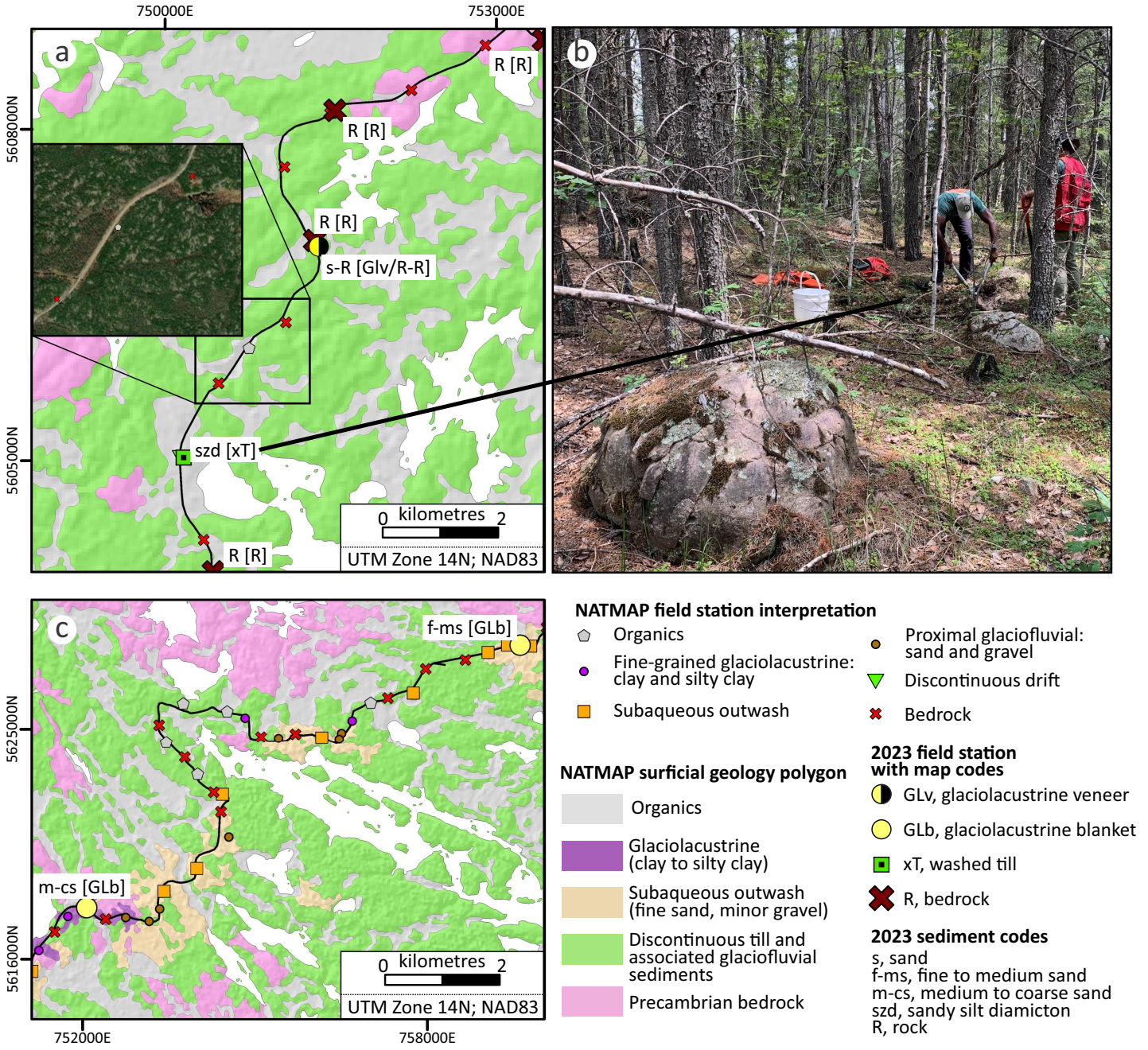

Figure GS2023-12-10: *A comparison between the surficial geology polygons and field-station data from the National Geoscience Mapping Program (NATMAP; Mann, 2004b; Matile et al., 2023c) for two areas in the Bird River study area. Stations from 2023 are presented and labelled with their sediment code and interpreted map code:* ***a)*** *an example of mismatched field-station observations and map polygons and misinterpretation of imagery (see inset);* ***b)*** *ground view of station 112-23-005, location shown in a);* ***c)*** *an example where the field-station data indicated only sorted sediments, organics or bedrock but the area has been mapped primarily as discontinuous till and associated glaciofluvial sediments. Basemap imagery in a) was created using ArcGIS® software by Esri. ArcGIS® and ArcMap™ are the intellectual property of Esri and are used herein under license. Copyright © Esri. All rights reserved. For more information about Esri software please visit <https://esri.ca/>.*

ered this area during several phases of the lake (e.g., Thorleifson, 1996; Fisher and Breckenridge, 2022). Surficial geology maps are typically made using field-station data as 'true', and then interpreting the sediment cover beyond that. The two examples shown here, in addition to many others, highlight that the surficial geology maps are not a reflection of the field-based observations in places.

The published surficial geology maps for the Bird River area overrepresent the proportion of glacial-derived sediments in the area (e.g., diamicton), and underrepresent the proportion of glaciolacustrine sediments (e.g., sand). Furthermore, the mapped polygons do not accurately reflect field-based observations. These issues need to be considered when planning a drift-prospecting survey. To find and sample till in the Bird River area, it is

recommended to use the field-based observations in combination with detailed digital elevation models and orthophotography, and not the published surficial geology maps.

Economic considerations

Spodumene was successfully recovered from till sampled 150 m down-ice of the outcropping F.D. No. 5 Li-bearing pegmatite. Till sampled along the east-side road recovered euxenite, parisite and spodumene grains, which highlights the potential for unrecognized U-Th-REE and Li mineralized systems in the area. Nearby where the two spodumene grains were recovered, till samples have regionally elevated values of Li and Cs in the till matrix, which supports the potential for Li-bearing mineralization in this largely unexplored area. These preliminary results indicate that the use of a MDMC to recover spodumene grains can be a useful exploration tool for Li-bearing pegmatites in Manitoba, especially when coupled with till-matrix geochemistry analysis. These methods are being further tested on till samples collected in the summer of 2023. The recovery of elevated gold grain counts, spodumene, scheelite and gahnite from a single till sample in the Bird River study area is a reflection of the region's diverse mineral potential, including critical minerals.

Acknowledgments

The authors thanks J. Bautista, N. Mesich, H. Adediran, H. Chow and J. Roush for field assistance. Logistical support from C. Epp and P. Belanger is truly appreciated. Acknowledgments are due to A. Chakhmouradian at the University of Manitoba for helping in the collection of Raman spectra. M. Gauthier and M. Nicolas are thanked for reviewing this report.

References

Bannatyne, B.B. 1985: Industrial minerals in rare-element pegmatites of Manitoba; Manitoba Energy and Mines, Geological Services, Economic Geology Report ER84-1, 94 p.

Chakhmouradian, A.R., Reguir, E.P., Kressall, R.D., Crozier, J., Pisiak, L.K., Sidhu, R. and Yang, P. 2015: Carbonatite-hosted niobium deposit at Aley, northern British Columbia (Canada): mineralogy, geochemistry and petrogenesis; Ore Geology Reviews, v. 64, p. 642–666.

Earth Observation Research Center and Japanese Aerospace Exploration Agency 2022: ALOS Global Digital Surface Model; Earth Observation Research Center and Japanese Aerospace Exploration Agency, ALOS World 3D - 30m, URL <https://www.eorc.jaxa.jp/ALOS/en/dataset/aw3d30/aw3d30_e.htm> [March 2022].

Fisher, T.G. and Breckenridge, A. 2022: Relative lake level reconstructions for glacial Lake Agassiz spanning the Herman to Campbell levels; Quaternary Science Review, v. 294, art. 107760, URL <https://doi.org/10.1016/j.quascirev.2022.107760>.

Garrett, R.G., Thorleifson, L.H., Matile, G. and Adcock, S.W. 2008: Till geochemistry, mineralogy and lithology, and soil geochemistry data from the 1991–1992 prairie kimberlite study; Geological Survey of Canada, Open File 5582, 1 CD-ROM.

Gauthier, M.S. 2020: Manitoba till-matrix geochemistry compilation 4: visible gold grains in the heavy mineral (<2 mm; –10 mesh) size-fraction; Manitoba Agriculture and Resource Development, Manitoba Geological Survey, Open File OF2020-6, 3 p.

Gauthier, M.S. 2022: Manitoba till-matrix geochemistry compilation: silt plus clay (<63 µm) size-fraction by inductively coupled plasma–mass spectrometry after an aqua-regia or modified aqua-regia digestion; Manitoba Natural Resources and Northern Development, Manitoba Geological Survey, GeoFile 2-2022, Microsoft® Excel® file.

Gauthier, M.S. and Hodder, T.J. 2020: Surficial geology mapping from Manigotagan to Berens River, southeastern Manitoba (parts of NTS 62P1, 7, 8, 10, 15, 63A2, 7); *in* Report of Activities 2020, Manitoba Agriculture and Resource Development, Manitoba Geological Survey, p. 41–46.

Gauthier, M.S. and Hodder, T.J. 2021: Till geochemistry from Manigotagan to Berens River, southeastern Manitoba (parts of NTS 62P1, 7, 8, 10, 15, 63A2, 7); Manitoba Agriculture and Resource Development, Manitoba Geological Survey, Data Repository Item DRI2021006, Microsoft® Excel® file.

Henderson, P.J. 1994: Surficial geology and drift composition of the Bissett-English Brook area, Rice Lake greenstone belt, southeastern Manitoba; Geological Survey of Canada, Open File 2910, 43 p.

Hodder, T.J. 2023: Gold and indicator-mineral data derived from glacial sediments (till) in southeastern Manitoba (parts of NTS 52L, 62P, 63A): 2022 pilot study results; Manitoba Economic Development, Investment, Trade and Natural Resources, Manitoba Geological Survey, Data Repository Item DRI2023011, Microsoft® Excel® file.

Hodder, T.J. and Bater, C.W. 2016: Till-matrix (<177 µm) geochemistry analytical results from the Lynn Lake (parts of NTS 64C14, 64F3, 4), Southern Indian Lake (parts of NTS 64G8, 9), Churchill River (parts of NTS 64F14, 64K3, 6, 11) and Fisher Branch (NTS 62P) areas, Manitoba; Manitoba Growth, Enterprise and Trade, Manitoba Geological Survey, Data Repository Item DRI2016004, Microsoft® Excel® file.

Hodder, T.J. and Gauthier, M.S. 2023: Field-based ice-flow–indicator data collected during 2023 field season in southeastern Manitoba (parts of NTS 52L, M); Manitoba Economic Development, Investment, Trade and Natural Resources, Manitoba Geological Survey, Data Repository Item DRI2023012, Microsoft® Excel® file.

Holmes, C.D. 1941: Till fabric; Geological Society of America, Bulletin 52, p. 1299–1354.

Kiilsgaard, T.H. and Hall, W.E. 1986: Radioactive black sand placer deposits of the Challis 1° x 2° quadrangle, Idaho; U.S. Geological Survey, Open-File Report 86-633, 13 p.

Lenton, P.G. and Kaszycki, C.A. 2005: Till geochemistry in northwestern Manitoba (NTS 63N, 64B, 64F and 64G and parts of 63K, 63O, 64A and 64C); Manitoba Industry, Economic Development and Mines, Manitoba Geological Survey, Open File Report OF2005-2, 1 CD-ROM.

Manitoba Geological Survey 2022: New edition of the 1:250 000 scale Precambrian bedrock geology compilation map of Manitoba; Manitoba Natural Resources and Northern Development, Manitoba Geological Survey, GeoFile 3-2022.

Manitoba Geological Survey 2023: Surficial geology map index; Manitoba Economic, Development and Trade, Manitoba Geological Survey, URL <https://manitoba.ca/iem/geo/surficial/sg_gf.html> [September 2023].

Mann, J.D. 2004a: Surficial geology, Big Whiteshell Lake, Manitoba–Ontario; Geological Survey of Canada, Map 2054A and Manitoba Industry, Economic Development and Mines, Manitoba Geological Survey, Geoscientific Map MAP2003-6, scale 1:100 000.

Mann, J.D. 2004b: Surficial geology, Nopiming, Manitoba–Ontario; Geological Survey of Canada, Map 2051A and Manitoba Industry, Economic Development and Mines, Manitoba Geological Survey, Geoscientific Map MAP2003-3, scale 1:100 000.

Martins, T., Rinne, M.L., Breasley, C. and Adediran, H. 2023: Preliminary results from field investigations in the Bird River domain of the Archean Superior province, Manitoba (parts of NTS 52L5, 6, 11, 12); *in* Report of Activities 2023, Manitoba Economic Development, Investment, Trade and Natural Resources, Manitoba Geological Survey, p. 4–13.

Matile, G.L.D. and Fulton, R.J. 1994: Southern prairies NATMAP, a progress report (NTS 62F, 62H); *in* Report of Activities 1994, Manitoba Energy and Mines, Geological Services, p. 182–183.

Matile, G.L.D., Thorleifson, L.H., Grant, N., Burt, A. and Mann, J. 1998: Geology of the Winnipeg region NATMAP project (NTS 62H/W, 62I and 52L/W); *in* Report of Activities 1998, Manitoba Energy and Mines, Geological Services, p. 161–171.

Matile, G.L.D., Thorleifson, L.H., Hodder, T.J. and Martin, A.B. 2023a: Field-based ice-flow data collected during the 1998 NATMAP field season, southeastern Manitoba (parts of NTS 52L, 62I); Manitoba Economic Development, Investment and Trade, Manitoba Geological Survey, Data Repository Item DRI2023002, Microsoft® Excel® file.

Matile, G.L.D., Thorleifson, L.H., Martin, A.B. and Hodder, T.J. 2023: Quaternary field site data collected during the 1993–1994 NATMAP field seasons, southeastern Manitoba (parts of NTS 52E, 62A, H); Manitoba Economic Development, Investment, Trade and Natural Resources, Manitoba Geological Survey, Data Repository Item DRI2023009, Microsoft® Excel® file.

Matile, G.L.D., Thorleifson, L.H., Martin, A.B. and Hodder, T.J. 2023: Quaternary field site data collected during the 1997–1998 NATMAP field seasons, southeastern Manitoba (parts of NTS 52L, 62H, I); Manitoba Economic Development, Investment, Trade and Natural Resources, Manitoba Geological Survey, Data Repository Item DRI2023010, Microsoft® Excel® file.

McClenaghan, M.B., Bobrowsky, P.T., Hall, G.E.M. and Cook, S.J., ed. 2001: Drift Exploration in Glaciated Terrain; Geological Society, London, Special Publication no. 185, 350 p.

McClenaghan, M.B., Brushett, D.M., Paulen, R.C., Beckett-Brown, C.E., Rice, J.M., Haji Egeh, A. and Nissen, A. 2023: Critical metal indicator mineral studies of till samples collected around the Brazil Lake LCT pegmatite, southwest Nova Scotia; Geological Survey of Canada, Open File 8960, 12 p., URL <https://doi.org/10.4095/331537>.

McClenaghan, M.B., Paulen, R.C. and Kjarsgaard, I.M. 2019: Rare metal indicator minerals in bedrock and till at the Strange Lake peralkaline complex, Quebec and Labrador, Canada; Canadian Journal of Earth Sciences, v. 56, p. 857–869, URL <https://doi.org/10.1139/cjes-2018-0299>.

McClenaghan, M.B., Spirito, W.A., Plouffe, A., McMartin, I., Campbell, J.E., Paulen, R.C., Garrett, R.G., Hall, G.E.M., Pelchat, P. and Gauthier, M.S. 2020: Till-sampling and analytical protocols: from field to archive, 2020 update; Geological Survey of Canada, Open File OF8591, 73 p.

McMartin, I. and Paulen, R.C. 2009: Ice-flow indicators and the importance of ice-flow mapping for drift prospecting; *in* Application of Till and Stream Sediment Heavy Mineral and Geochemical Methods to Mineral Exploration in Western and Northern Canada, R.C. Paulen and I. McMartin (ed.), Geological Association of Canada, Short Course Notes 18, p. 15–34.

Miller, M. 2021: Hunting for rare-earth-element (REE)-bearing minerals in northern Labrador: MLA-SEM analysis of surficial sediments within the glacial dispersion zone from the Strange Lake main zone deposit; M.Sc. thesis, Memorial University of Newfoundland, St. John's, Newfoundland and Labrador, 327 p.

Nicolas, M.P.B., Matile, G.L.D., Keller, G.R. and Bamburak, J.D. 2010: Phanerozoic geology of southern Manitoba; Manitoba Innovation, Energy and Mines, Manitoba Geological Survey, Stratigraphic Map SM2010-1, 2 sheets, scale 1:600 000.

Roush, J., Martins, T., McFarlane, C.R.M., Rinne, M.L. and Groat, L. 2023: Preliminary examination of the Tappy, Eagle and F.D. No. 5 pegmatites in the Cat Lake–Winnipeg River pegmatite field, southeastern Manitoba (parts of NTS 52L5, 11); *in* Report of Activities 2023, Manitoba Economic Development, Investment, Trade and Natural Resources, Manitoba Geological Survey, p. 20–26.

Sharma, S.K. and Simmons, B. 1981: Raman study of crystalline polymorphs and glasses of spodumene composition quenched from various pressures; American Mineralogist, v. 66, p. 118–126.

Simmons, W.B., Hanson, S.L., Falster, A.U. and Webber, K.L. 2012: A comparison of the mineralogical and geochemical character and geological setting of Proterozoic REE-rich granitic pegmatites of the north-central and southwestern US; The Canadian Mineralogist, v. 50, p. 1695–1712, URL <https://doi.org/10.3749/canmin.50.6.1695>.

Thorleifson, L.H. 1996: Review of Lake Agassiz history; *in* Sedimentology, Geomorphology and History of the Central Lake Agassiz Basin, J.T. Teller, L.H. Thorleifson, G.L.D. Matile and W.C. Brisbin (ed.), Geological Association of Canada–Mineralogical Association of Canada, Joint Annual Meeting, Winnipeg, Manitoba, May 27–29, 1996, Field Trip Guidebook B2, p. 55–84.

Thorleifson, L.H. and Garrett, R.G. 1993: Prairie kimberlite study - till matrix geochemistry, and preliminary indicator mineral data; Geological Survey of Canada, Open File 2745, 1 diskette.

Thorleifson, L.H., Matile, G.L.D., Keller, G.R. and Hauck, S.A. 2009: Till geochemical and indicator mineral reconnaissance of southeastern Manitoba (west half of NTS 52E and 52L and all of 62H and 62I): final results; Manitoba Science, Technology, Energy and Mines, Manitoba Geological Survey, Open File OF2009-13, 5 p.

GS2023-13

Quaternary stratigraphic investigations along the Gods and Yakaw rivers, northeastern Manitoba (parts of NTS 54C2, 7)

by N. Mesich[1], M.S. Gauthier, T.J. Hodder, J. Hathaway[2], M. Schaarschmidt[3], O.B. Lian[3] and M. Ross[1]

In Brief:

- Study of the Quaternary stratigraphy along the Gods and Yakaw rivers, near the confluence with the Hayes River
- Till samples collected to determine provenance and explore the economic potential of the region
- Intertill nonglacial sediments sampled for geochronology and paleoenvironment characterization

Citation:
Mesich, N., Gauthier, M.S., Hodder, T.J., Hathaway, J., Schaarschmidt, M., Lian, O.B. and Ross, M. 2023: Quaternary stratigraphic investigations along the Gods and Yakaw rivers, northeastern Manitoba (parts of NTS 54C2, 7); *in* Report of Activities 2023, Manitoba Economic Development, Investment, Trade and Natural Resources, Manitoba Geological Survey, p. 120–123.

Summary

In August 2023, the Quaternary stratigraphy of eight sections situated on the Gods and Yakaw rivers, in the Hudson Bay Lowland of northeastern Manitoba, were investigated. The goals of this remote fieldwork were to establish a more complete understanding of the Quaternary history of the region and to collect indicator-mineral samples to assist with drift exploration efforts. This data will enable better mineral-potential assessment for the region, and help to interpret the provenance of tills in this glacially complex area. Ninety-eight till samples were collected for both clast lithological and geochemical analyses, with an additional 33 samples collected for indicator-mineral analysis. Additionally, till-clast fabric measurements were conducted at 55 sample sites to interpret paleo–ice-flow direction during deposition. Intertill sorted sediments were documented and sampled whenever possible, using a variety of methods to establish paleoenvironmental conditions and geochronology constraints.

Introduction

The Manitoba Geological Survey (MGS) studied the Quaternary stratigraphy of eight sections along the Gods and Yakaw rivers in northeastern Manitoba in August 2023. These sites were accessed via helicopter and the fieldwork was conducted over the span of two weeks. The objectives of this study were to

- observe and document the Quaternary stratigraphy of exposed sections;
- collect till samples and clast-fabric measurements within till, to interpret paleo–ice-flow directions;
- assess the economic potential of the region using newly acquired till composition datasets; and
- collect geochronological and paleobotanical samples to help establish stratigraphic correlations in the Hudson Bay Lowland (HBL).

Previous work

In 1967, the Geological Survey of Canada initiated Operation Winisk to better understand the geology of the HBL region of Quebec, Ontario and Manitoba (Craig, 1969; McDonald, 1969). Operation Winisk was the first reconnaissance-level survey of the study area, and included preliminary observations of numerous sites along the Hayes and Gods rivers (Figure GS2023-13-1). Netterville (1974) investigated the Quaternary stratigraphy of 10 sections along Gods River, five of which are close to the study area (Figure GS2023-13-1). Several distinct diamictons, interpreted as till, were noted along with one intertill, organic-bearing, sorted-sediment bed (referred to as Gods River sediments), which was interpreted to have been deposited during an interglacial period (Netterville, 1974). Additional regional studies by Klassen (1986) and Hodder et al. (2017) include descriptions of several sections within the study area (Figure GS2023-13-1). To further investigate a relatively high indicator-mineral concentration identified at a site documented in Hodder et al. (2017), the MGS conducted fieldwork to collect indicator-mineral samples and observe the Quaternary stratigraphy near the confluence of the Hayes and Gods rivers (Hodder and Gauthier, 2022; Figure GS2023-13-1). The reconnaissance-level surficial geology of the region was mapped at a 1:250 000 scale (Klassen and Netterville, 1978).

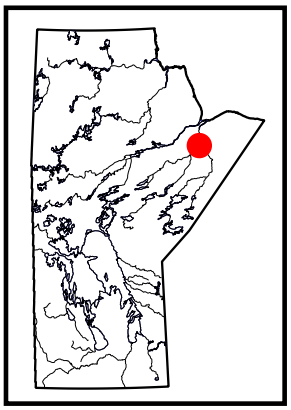

[1] Department of Earth and Environmental Sciences, University of Waterloo, Waterloo, Ontario
[2] Department of Earth Sciences, University of Toronto, Toronto, Ontario
[3] University of the Fraser Valley, Abbotsford, British Columbia

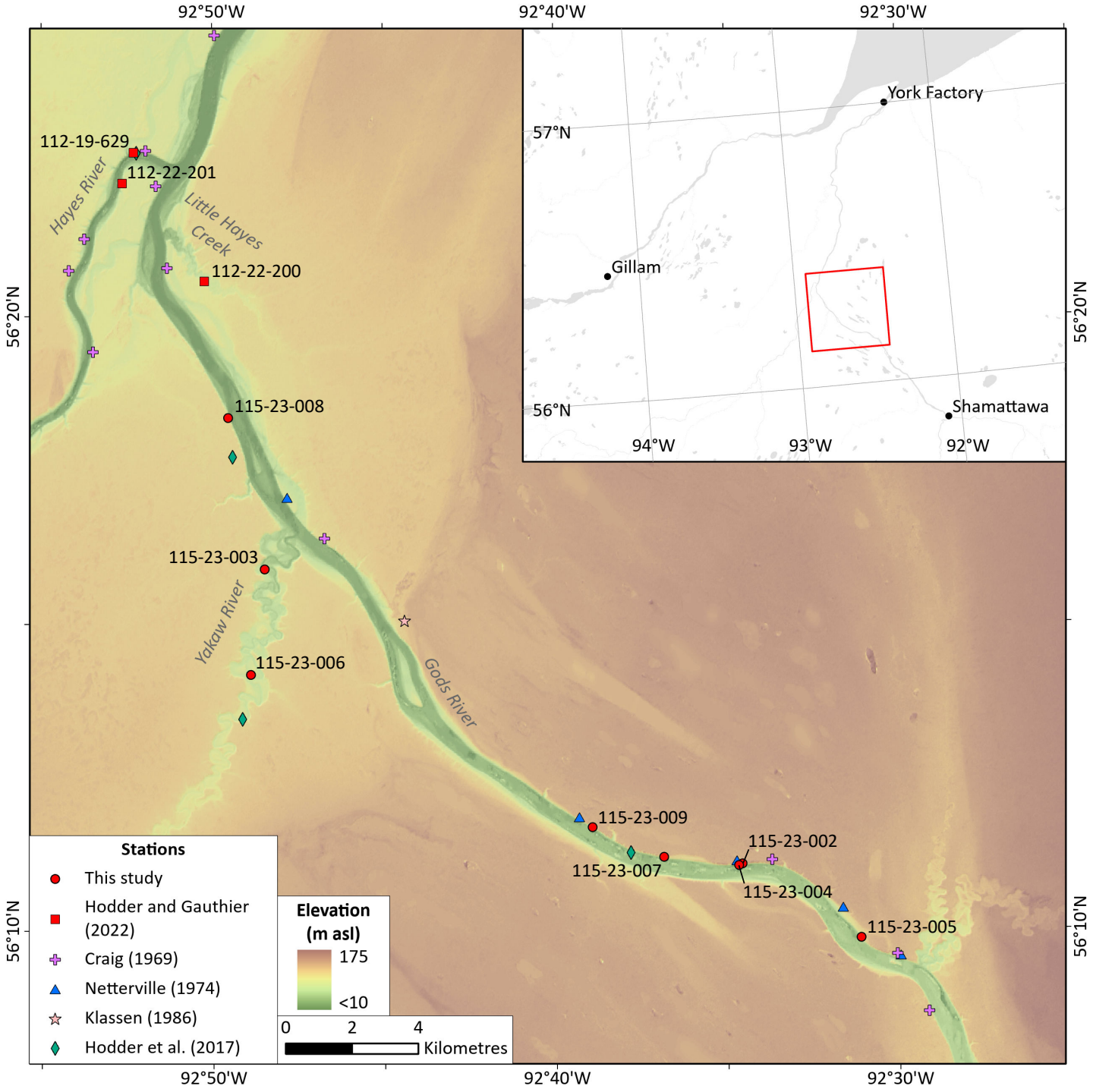

Figure GS2023-13-1: *Location of the 2023 field sites and previously described sections along the Gods, Hayes and Yakaw rivers and Little Hayes Creek, northeastern Manitoba. Inset map shows location of the study area (outlined in red). Background hillshade image was generated from a digital elevation model (Earth Observation Research Center and Japanese Aerospace Exploration Agency, 2022).*

2023 fieldwork

The study area is situated along the Gods and Yakaw rivers, where the region is characterized by a thick (24–92 m) blanket of Quaternary sediments that overlie Paleozoic bedrock of the Hudson Bay Basin (Hodder and Gauthier, 2021). The Quaternary stratigraphy was studied at eight sections; bedrock exposures were not observed. The six sections studied on the Gods River and two on the Yakaw River expose 20–45 m and 20–30 m of Quaternary sediments, respectively. At each section, the overlying slumped materials were first cleared to expose a continuous stratigraphy, which was then documented in detail.

Diamictons at each section, interpreted as formed beneath a glacier (till), were sampled at multiple depths (at ~2 m intervals, if thickness permitted). A total of 98 till samples, each weighing

2–3 kg, were collected in 2023, in addition to the eight till samples collected in 2002 (Gauthier and Hodder, 2023). The 2023 till samples will be split for archiving at the MGS Midland Sample and Core Library (Winnipeg, Manitoba) and then analyzed for grain size, matrix geochemistry (<63 µm size fraction) and clast lithology. An additional 11.4 L till sample was collected for indicator-mineral analysis at 33 sample sites. These samples were submitted to Overburden Drilling Management Limited (Ottawa, Ontario) in collaboration with the Geological Survey of Canada.

Ice-flow data was obtained from the studied sections by measuring the long-axes orientation, or fabric, of clasts within till. The long-axis orientation of elongated clasts was measured, as such clasts tend to rotate within the fine-grained till matrix and orient parallel to the overlying glacier's shear stress direction (Holmes, 1941). Elongated clasts are defined as having a minimum ratio of 1.5:1.0 of their longest axis to their second-longest axis. At 55 sample sites, the orientations (trend and plunge) of a minimum sampled population of 25 elongated clasts were measured in situ for a statistically valid result. Lodged boulders in till, with parallel striae on their polished upper surface, are also paleo–ice-flow indicators. Such indicators were observed at four sites.

Sorted sediments, including those below or between tills, are also of interest for this study as they can indicate nonglacial paleoenvironments and help to provide geochronological constraints (Gauthier et al., 2021). Such intertill sediments were observed at all studied sections along the Gods River. In particular, one section on the Gods River contains three stratigraphically distinct, intertill, sorted-sediment beds, with at least two of these beds interpreted to have been deposited during an interglacial period based on the presence of either marine or organic-rich sediments (Figure GS2023-13-2). Organic-bearing sorted sediments were sampled for pollen and non-pollen palynomorphs. A total of 63 samples from five sections will be analyzed at the Department of Earth Sciences, University of Toronto (Toronto, Ontario); species will be identified and counted to allow for paleoclimate interpretation. These intertill nonglacial beds can be organic-rich in places and contain large amounts of wood, including an in situ log that was uncovered at section 115-23-005 (Figure GS2023-13-3). As part of a project to test the upper age limits of quartz-grain optical dating, bedded nonglacial sands at two sections (sections 115-23-005 and 115-23-009) were sampled for submission to the University of the Fraser Valley Luminescence dating laboratory (Abbotsford, British Columbia). Additionally, four paleomagnetism samples (8 cm^3 each) were collected from a clay facies within a subtill marine bed at one site (section 115-23-004), and are to be analyzed at the Western Paleomagnetic & Petrophysical Laboratory at Western University (London, Ontario).

Economic considerations

Manitoba's far northeast is a remote and largely unexplored frontier, with thick drift covering much of the bedrock in the region. Results from this study will contribute to an improved understanding of the Quaternary stratigraphy, glacial history, and till provenance in the area of the Gods and Yakaw rivers. This is necessary to support drift prospecting efforts in this region of thick drift, which contains a depositional record spanning multiple glaciations.

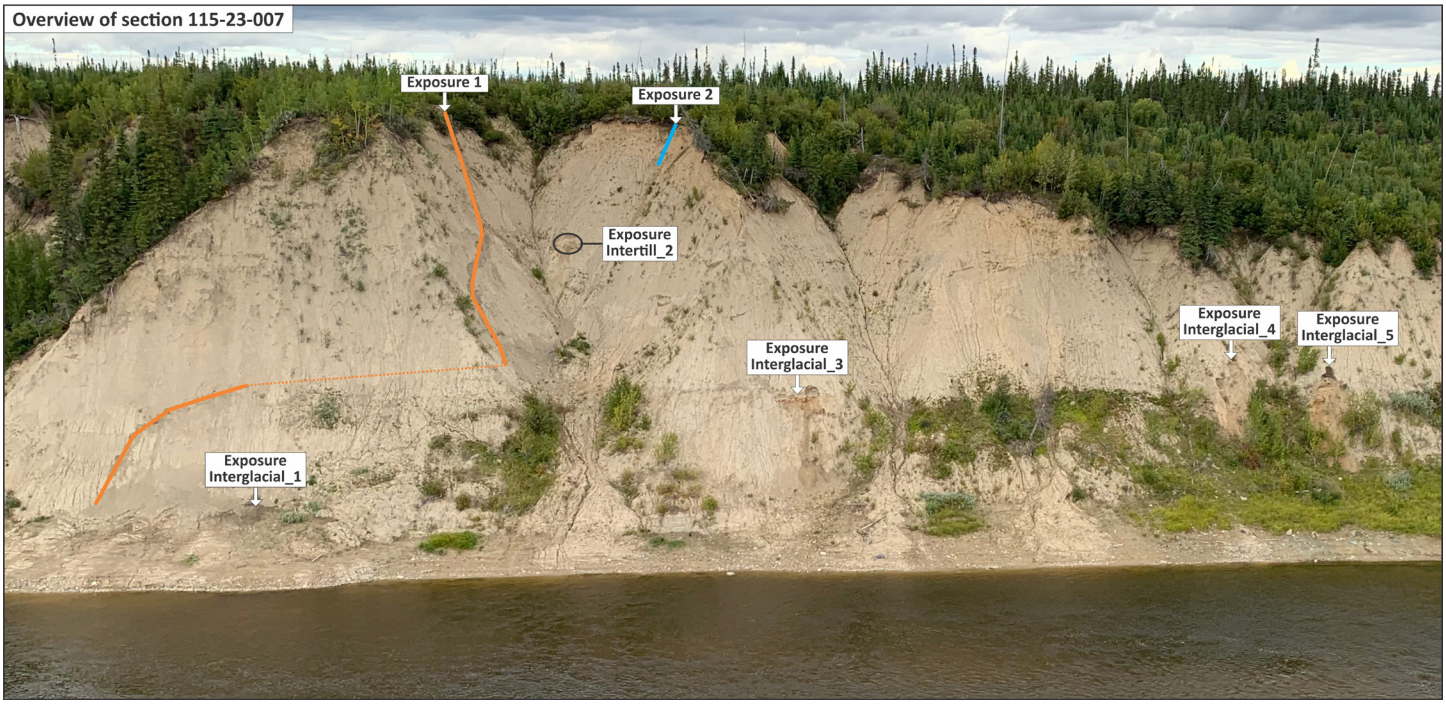

Figure GS2023-13-2: *Section 115-23-007, situated along the Gods River, exposes ~42 m of Quaternary sediments, including three stratigraphically distinct, intertill, sorted-sediment beds.*

Figure GS2023-13-3: *A log was found buried within sand, which is part of a 2.4 m thick bed of nonglacial sediments at section 115-23-005.*

Acknowledgments

The authors thank Prairie Helicopters Inc. for providing excellent air support throughout the fieldwork. This research is funded by the Manitoba Geological Survey and the Geological Survey of Canada's Geo-mapping for Energy and Minerals, GeoNorth program (GEM-GeoNorth). The University of the Fraser Valley Luminescence dating laboratory is supported by funds from Natural Sciences and Engineering Research Council of Canada Discovery and Research Tools and Instruments grants.

References

Craig, B.G. 1969: Late glacial and post-glacial history of the Hudson Bay region; *in* Earth Science Symposium on Hudson Bay, P.J. Hood (ed.), Geological Survey of Canada, Paper 68-83, p. 63–77.

Earth Observation Research Center and Japanese Aerospace Exploration Agency 2022: ALOS Global Digital Surface Model; Earth Observation Research Center and Japanese Aerospace Exploration Agency, ALOS World 3D - 30m, URL <https://www.eorc.jaxa.jp/ALOS/en/dataset/aw3d30/aw3d30_e.htm> [September 2023].

Gauthier, M.S. and Hodder, T.J. 2023: Till geochemistry and heavy mineral analyses (gold, MMSIM®, visual KIM) from three sections near the confluence of the Hayes and Gods rivers, northeastern Manitoba (part of NTS 54C7); Manitoba Economic Development, Investment, Trade and Natural Resources, Manitoba Geological Survey, Data Repository Item DRI2023008, Microsoft® Excel® file.

Gauthier, M.S., Hodder, T.J., Lian, O.B., Finkelstein, S.A., Dalton, A.S. and Paulen, R.C. 2021: Stratigraphic, paleoenvironmental and geochronological investigations of intertill nonglacial deposits in northeastern Manitoba (parts of NTS 54B-F, K, L, 64A, H, I); *in* Report of Activities 2021, Manitoba Agriculture and Resource Development, Manitoba Geological Survey, p. 71–76.

Hodder, T.J. and Gauthier, M.S. 2021: Quaternary stratigraphic and depth to bedrock data compilation for northeastern Manitoba; *in* Report of Activities 2021, Manitoba Agriculture and Resource Development, Manitoba Geological Survey, p. 66–70.

Hodder, T.J. and Gauthier, M.S. 2022: Quaternary stratigraphic investigations near the confluence of the Hayes and Gods rivers, northeastern Manitoba (part of NTS 54C7); *in* Report of Activities 2022, Manitoba Natural Resources and Northern Development, Manitoba Geological Survey, p. 110–120.

Hodder, T.J., Gauthier, M.S. and Nielsen, E. 2017: Quaternary stratigraphy and till composition along the Hayes, Gods, Nelson, Fox, Stupart, Yakaw, Angling and Pennycutaway rivers, northeast Manitoba (parts of NTS 53N, 54C, 54D, 54F); Manitoba Growth, Enterprise and Trade, Manitoba Geological Survey, Open File OF2017-4, 20 p.

Holmes, C.D. 1941: Till fabric; Bulletin of the Geological Society of America, v. 52, p. 1299–1354.

Klassen, R.W. 1986: Surficial geology of north-central Manitoba; Geological Survey of Canada, Memoir 419, 57 p.

Klassen, R.W. and Netterville, J.A. 1978: Surficial geology, Hayes River, Manitoba; Geological Survey of Canada, Preliminary Map 2-1978, scale 1:250 000.

McDonald, B.C. 1969: Glacial and interglacial stratigraphy, Hudson Bay Lowland; *in* Earth Science Symposium on Hudson Bay, P.J. Hood (ed.), Geological Survey of Canada, Paper 68-83, p. 78–99.

Netterville, J.A. 1974: Quaternary stratigraphy of the lower Gods River region, Hudson Bay Lowlands, Manitoba; M.Sc. thesis, University of Calgary, Calgary, Alberta, 79 p.

GS2023-14

Manitoba's aggregate program: past, present, future

by J.W. Rentz

Summary

The Manitoba Geological Survey is updating the assessment of aggregate resources in the province. Initial studies were primarily published between the 1970s and mid-1990s, with a few publications in the 2000s. The initial areas selected for updating are the Winnipeg Metropolitan Region and the Arden area. The aggregate resource maps in these areas are being re-evaluated to determine the accuracy of the existing maps and identify new potential deposits. Additionally, a database will be created that incorporates both historical and new data. This is being accomplished by reviewing historical information, more recently acquired field-based data, the latest high-resolution digital elevation models and available imagery (satellite and orthorectified).

In Brief:

- History of Manitoba's aggregate exploration/mapping program and comparison of historic to current methodologies
- Aggregate maps for the Winnipeg capital region and Arden area are being updated

Citation:
Rentz, J.W. 2023: Manitoba's aggregate program: past, present, future; *in* Report of Activities 2023, Manitoba Economic Development, Investment, Trade and Natural Resources, Manitoba Geological Survey, p. 124–130.

Introduction

Aggregates are a combination of rock fragments, and are typically derived by extracting sand and gravel from surficial deposits or crushing bedrock. The current understanding of aggregate resources in Manitoba is based on mapping efforts that were largely completed 30–50 years ago. Since these initial mapping efforts, there has been little to no record about what material has been extracted and where resources have been depleted. There have also been technological advances since these initial mapping efforts, such as high-resolution digital elevation models and satellite imagery, which allow for a more accurate mapping of surficial features. The initial paper-based maps have been digitally captured and are in the process of being updated within a Geographic Information System (GIS) environment to remove inaccuracies in the dataset. The inaccuracies in the maps are important to correct since Policy Area 8 of the Provincial Planning Regulation of Manitoba dictates that economically valuable mineral deposits shall be protected from land uses that limit mineral exploration and development (Government of Manitoba, 2011), meaning that development on such lands is restricted.

In 2023, mapping of aggregate resources in Manitoba was restarted with the current goals of this program being to

- re-evaluate and update the previous mapping efforts within a GIS environment and identify new potential deposits using new data and high-resolution imagery; and
- create a database structure that can incorporate legacy datasets and newly acquired data.

The initial focus for updating the aggregate resource mapping is the Winnipeg Metropolitan Region and the Arden area (NTS 62J6).

Previous work

Prior to the 1970s, Manitoba's public aggregate information was extracted from 1:250 000 scale Quaternary geology maps (Groom, 1999). These small-scale maps were very broad in their content, resulting in reduced accuracy in the geographic positioning of sites and data, and did not include smaller, yet significant, deposits. To address this, the Department of Energy and Mines in the early 1970s undertook a mapping and resource evaluation program to gain a better understanding of the aggregate resource within the province of Manitoba. This program was completed by a combination of provincial geologists and external consulting and engineering firms.

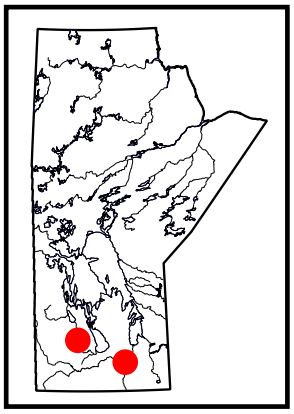

In the 1970s, the priority for aggregate mapping was to cover the southern portion of Manitoba at a scale of 1:50 000 (Groom, 1999). Aggregate deposits were mapped and evaluated by examining airphotos, stereoscopic imagery, backhoe test pits, hand-augured or hand-dug holes, geophysics surveys, boreholes, roadcuts and borrow or gravel pits. When possible, sand and gravel samples were collected to analyze for particle size and if possible, lithology (e.g., granite, limestone and less desirable lithologies such as chert and shale). Aggregate data collected from both remote observation and fieldwork were subsequently published in aggregate reports, open file reports or consulting company reports. In 1988, twelve compilation aggregate maps of the southern portion of the province were published at a 1:250 000 scale, which captured the state of knowledge at the time (Manitoba Energy

and Mines, 1988a–l). By the mid-1990s, aggregate mapping had been completed for most of southern Manitoba (Figure GS2023-14-1) and the program was largely disbanded.

Aggregate mapping and inventory assessment continued in the summer of 1999 with updating of the Winnipeg capital region and the Ochre River area (Groom, 1999). These mapping efforts were completed by one geologist (H. Groom) and further efforts continued until 2008 (Groom, 2008). The details of this work were primarily published in the Manitoba Geological Survey's (MGS) Report of Activities series with limited publication of maps.

In 2018, with the goal to modernize access to the aggregate maps and associated data, as well as to prepare for their update, the MGS undertook a project to digitally capture all the previous mapping efforts and create a single database that could be used for aggregate resource mapping purposes in the future (Hodder et al., 2019).

Current work

There have been many technological advancements since the initial aggregate program commenced, which allow the identification of potential surface aggregate deposits in a more

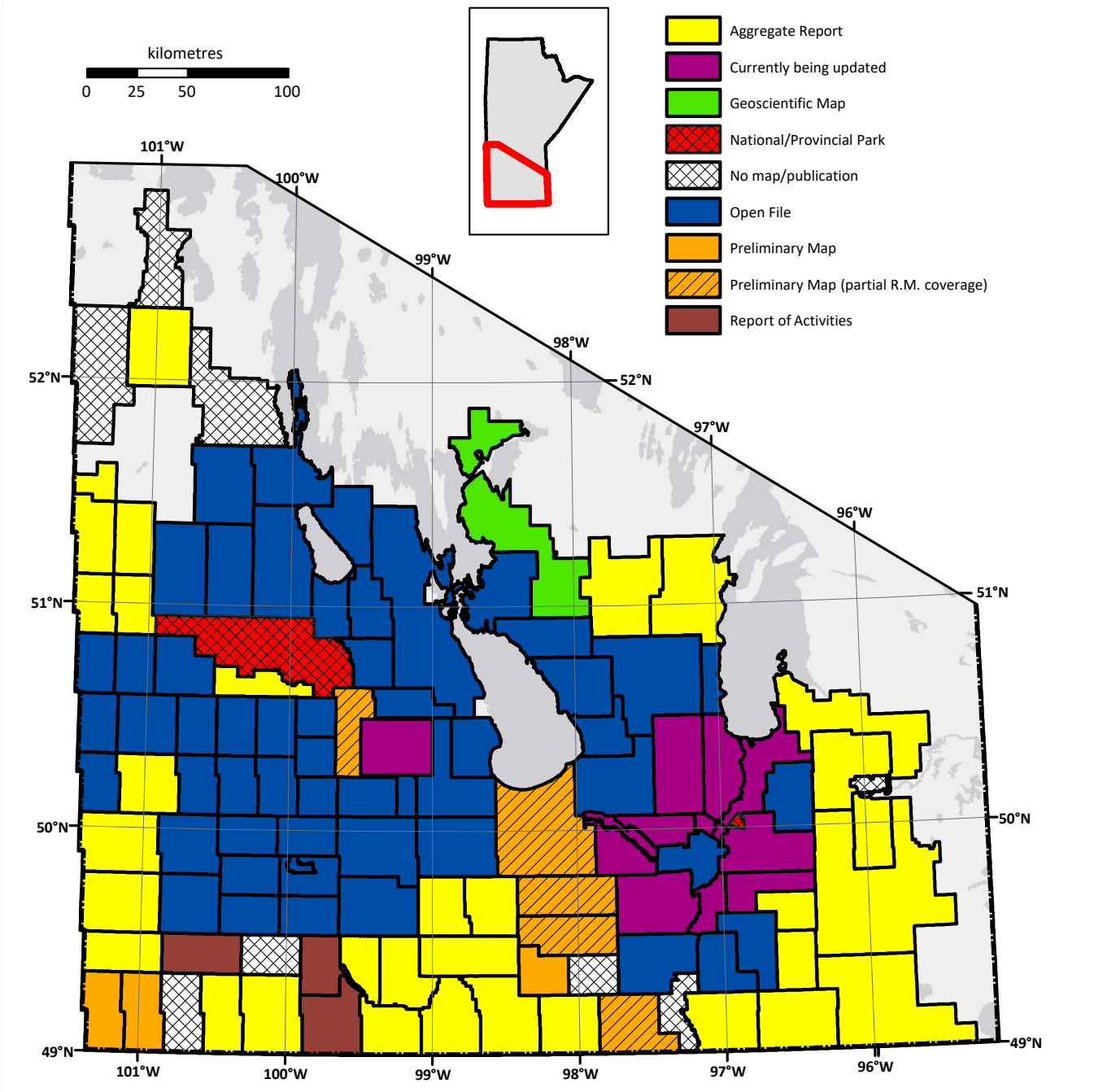

Figure GS2023-14-1*: Updated map showing the state of aggregate mapping in southern Manitoba. The original map is available online (https://manitoba.ca/iem/geo/surficial/aggregate.html) as an interactive bibliography for each rural municipality (R.M.).*

efficient manner. Global positioning system (GPS) capability has increased the accuracy of sample and site locations, and GIS software allows mapping within a digital environment. Perhaps most importantly, publicly available light detection and ranging (LiDAR) digital elevation models (Government of Manitoba, 2023) can delineate elevation changes at 1–5 m horizontal resolution and 0.09–0.15 m vertical resolution (with resolutions being area dependent), which allows the identification of changes in topography that may be related to aggregate deposits (i.e., Figure GS2023-14-2). The availability of digital high-resolution orthophotography (e.g., Google Earth, Esri® Maps and Bing Maps) allows land cover to be easily viewed in greater detail, particularly in areas where LiDAR data may not exist, and provides a tool to track the size and locations of existing pits/quarries.

Using the more detailed digital elevation models (Government of Manitoba, 2023) allows the MGS to update the historical deposit outlines and polygons (e.g., Figure GS2023-14-3) and to identify new surface deposits.

As a part of this new project, a centralized field site database is being updated and brought to modern digital standards for public access. The database will house all pertinent data for the deposits including location, site and sample descriptions, stratigraphic information and general deposit information. Currently, the available information is found within the original reports and maps; an index of these maps is located on the MGS website at https://manitoba.ca/iem/geo/surficial/aggregate.html. Data from the initial digital data capture of previous mapping are also available for download in Hodder et al. (2019).

Future work

Preliminary work will include digitization of historical data, incorporation of data from various governmental departments and reinterpretation of remote sensing imagery. A cross-jurisdictional review is currently underway to inform how information is best presented and what type of information should be captured. As part of this review, all stakeholders are encouraged to contact the author with questions or comments.

The initial mapping will be focused on both the Winnipeg Metropolitan Region, as well as the Arden area, which was previously mapped for surficial geology by Hodder and Trommelen (2015) and Hodder and Gauthier (2020). An example of the updated Arden map area is shown in Figure GS2023-14-4.

Economic considerations

Aggregate is an essential resource within the engineering and construction industries and is commonly used for road construction, foundation construction, railroad base and concrete/asphalt formation. The increasing demand for aggregate, especially from the metropolitan region, requires that the inventory of this important resource be updated. Furthermore, additional resources need to be identified, and areas that have a high resource potential need to be protected from future development. Past estimations predicted that high quality aggregate deposits within the metropolitan region may be depleted as early as the year 2026 (The UMA Group, 1976) and there is currently no up-to-date aggregate inventory for this region. Therefore, it is imperative that all aggregate resources be identified in order to inform land-use planning and be available for future growth in the metropolitan region.

Acknowledgments

The author thanks M. Gauthier for providing guidance and support during site visits and N. Mesich for participating and providing assistance during the 2023 field season site visits.

References

ATLIS Geomatics Inc. 2016: Cooks Creek LiDAR DEM; Manitoba Infrastructure, URL <https://mli.gov.mb.ca/dems/index_external_lidar.html> [June 2023].

GeoManitoba 2006: Fisher River 5m LiDAR grid; Manitoba Conservation and Water Stewardship, GeoManitoba, URL <https://mli.gov.mb.ca/dems/index_external_lidar.html> [July 2023].

Government of Manitoba 2011: Provincial Planning Regulation, M.R. 81/2011; Government of Manitoba, URL <https://web2.gov.mb.ca/laws/regs/current/081-2011.php?lang=en> [October 2023].

Government of Manitoba 2023: Manitoba LiDAR data; Government of Manitoba, URL <https://mli.gov.mb.ca/dems/index.html> [June 2023].

Groom, H.D. 1999: Updating aggregate maps in R.M. of Ochre River and the Capital Region; *in* Report of Activities 1999, Manitoba Industry, Trade and Mines, Geological Services, p. 123–124, URL <https://manitoba.ca/iem/geo/field/roa99pdfs/gs-29-99.pdf> [August 2023].

Groom, H.D. 2008: Aggregate resources in the rural municipalities of Dauphin, Ethelbert, Gilbert Plains, Grandview and Mossey River, Manitoba (parts of NTS 62N1, 2, 7, 8, 9, 10, 62O4, 5, 12); *in* Report of Activities 2008, Manitoba Science, Technology, Energy and Mines, Manitoba Geological Survey, p. 159–170, URL <https://manitoba.ca/iem/geo/field/roa08pdfs/GS-15.pdf> [September 2023].

Groupe Info Consult 2018: Whitemud River Watershed LiDAR; Manitoba Infrastructure, URL <https://mli.gov.mb.ca/dems/index_external_lidar.html> [June 2023].

Hodder, T.J. and Gauthier, M.S. 2020: Surficial geology of the Arden area, Manitoba (NTS 62J6); Manitoba Agriculture and Resource Development, Manitoba Geological Survey, Geoscientific Map MAP2020-1, scale 1:50 000, URL <https://manitoba.ca/iem/info/libmin/MAP2020-1.zip> [June 2023].

Hodder, T.J. and Trommelen, M.S. 2015: Quaternary geology of the Arden NTS area (62J6), southwestern Manitoba; *in* Report of Activities 2015, Manitoba Mineral Resources, Manitoba Geological Survey, p. 115–123, URL <https://manitoba.ca/iem/geo/field/roa15pdfs/GS-10.pdf> [July 2023].

Hodder, T.J., Keller, G., Santucci, A. and Lee, S.K.Y. 2019: Manitoba aggregate data capture – release 1.0; Manitoba Growth, Enterprise and Trade, Manitoba Geological Survey, zipped Esri® shapefile, URL <https://manitoba.ca/iem/geo/surficial/mb_aggregate_potential_poly.zip> [June 2023].

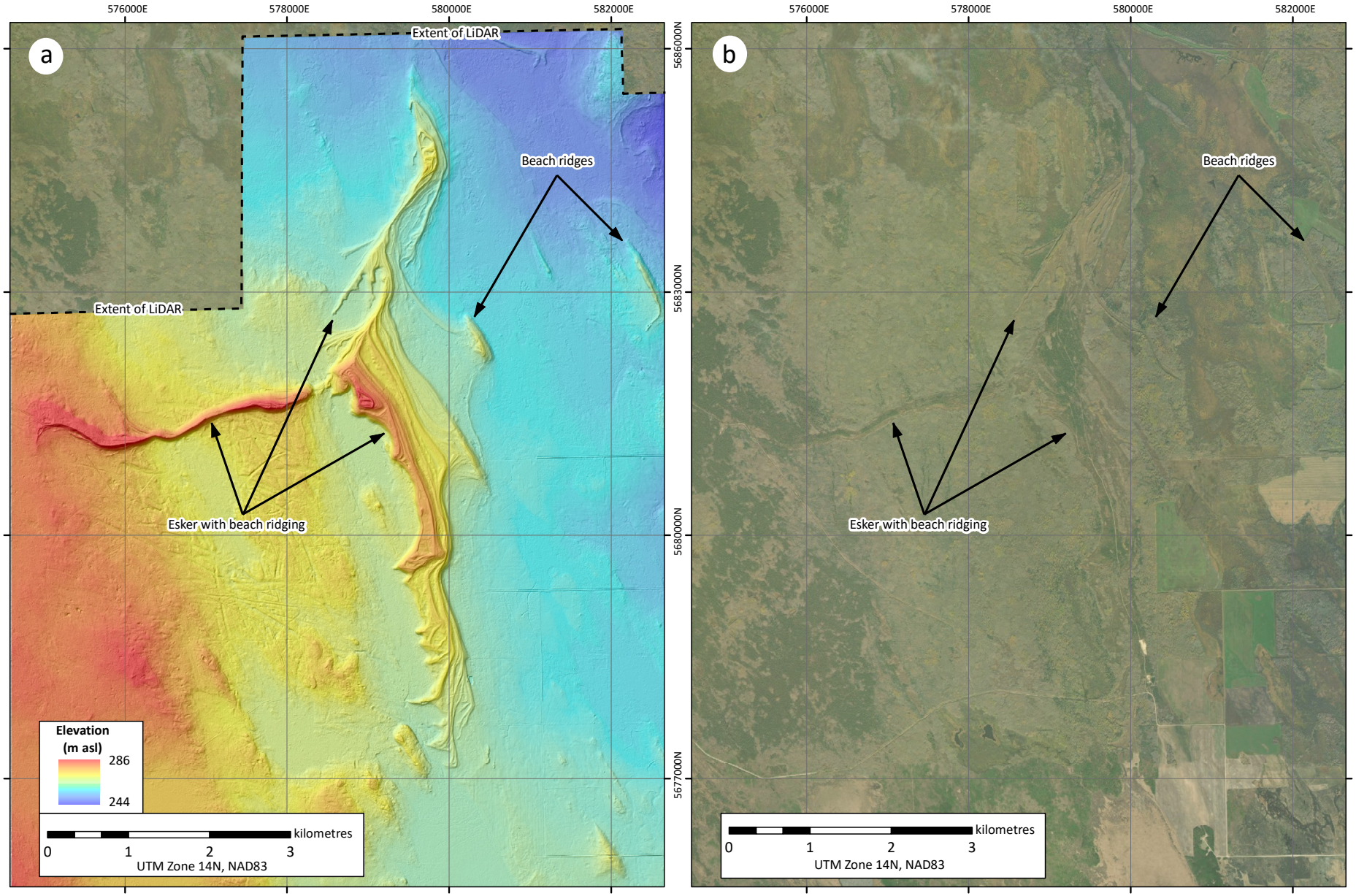

Figure GS2023-14-2: *Example of high-resolution digital elevation models and imagery available to map aggregate resources, Rural Municipality of Fisher, Manitoba:* ***a)*** *light detection and ranging (LiDAR) hillshade image (GeoManitoba, 2006) shows elevation changes at 5 m horizontal resolution and 0.09–0.15 m vertical resolution, in approximate 3-D, which allows geologists to better identify landforms that may contain sand and gravel (eskers and beach ridges);* ***b)*** *orthoimagery of the same location shows the effects of vegetation and land use that may have contributed to poor mapping accuracy. Basemaps were created using ArcGIS® software by Esri. ArcGIS® and ArcMap™ are the intellectual property of Esri and are used herein under license. Copyright © Esri. All rights reserved. For more information about Esri software, please visit <https://esri.ca/>.*

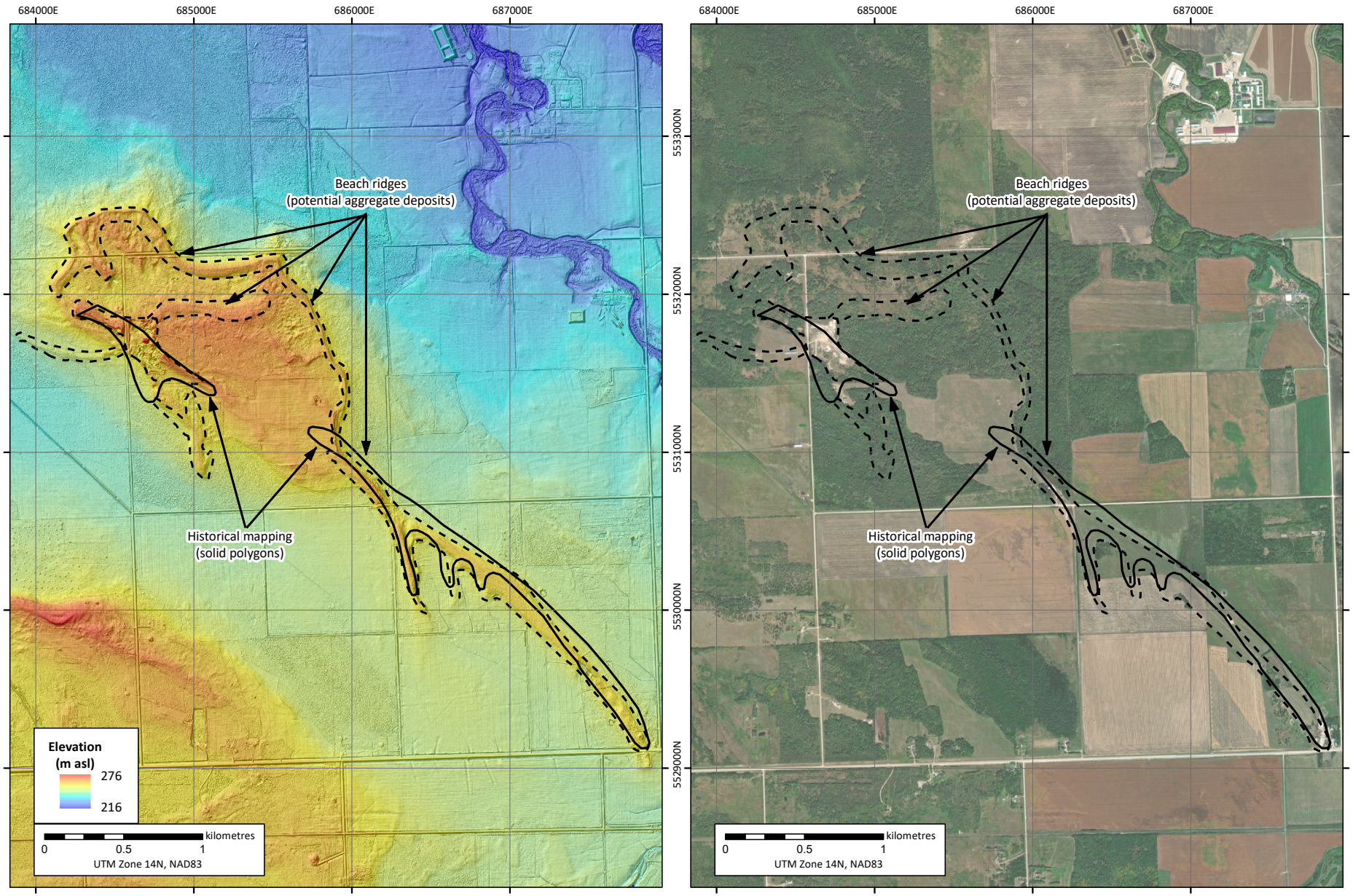

Figure GS2023-14-3: *Example of high-resolution digital elevation models and imagery available to map aggregate resources, near Vivian, Manitoba:* ***a)*** *light detection and ranging (LiDAR) hillshade image (ATLIS Geomatics Inc., 2016) with 1 m horizontal resolution and 0.03–0.05 m vertical resolution; both historical mapped deposits and corrected and newly mapped potential deposits are shown;* ***b)*** *orthoimagery of the same location shows the effects of vegetation and farming that may have contributed to poor mapping accuracy. Historical mapping polygons from Hodder et al. (2019). Basemaps were created using ArcGIS® software by Esri. ArcGIS® and ArcMap™ are the intellectual property of Esri and are used herein under license. Copyright © Esri. All rights reserved. For more information about Esri software, please visit <https://esri.ca/>.*

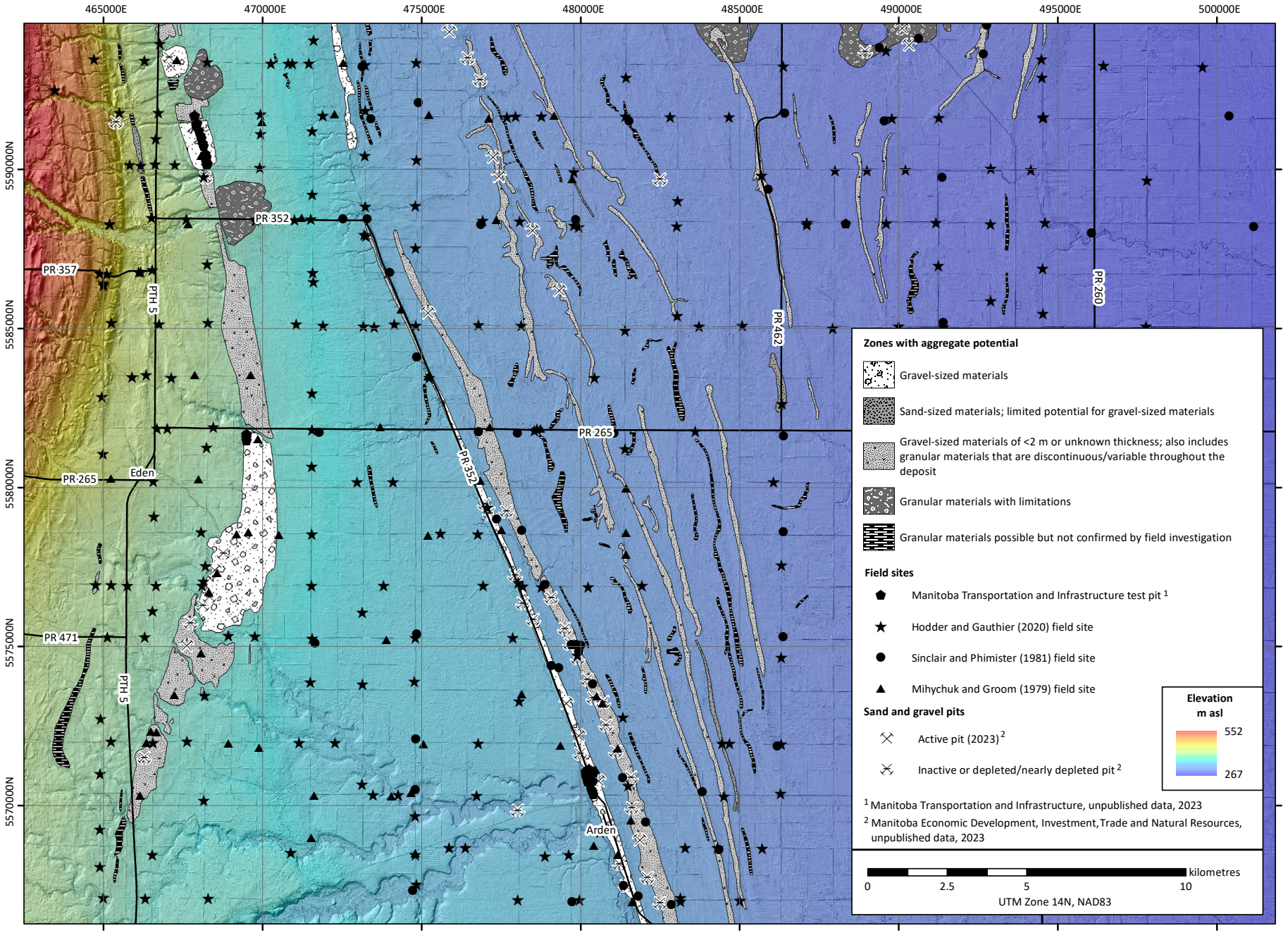

Figure GS2023-14-4: *Preliminary interpretation of the aggregate potential within the Arden area, Manitoba, using a light detection and ranging (LiDAR) hillshade image (Groupe Info Consult, 2018), field station and pit data. The legend is preliminary and adapted from Ricketts (2014); it is an example of the type of legend that may be used on the final maps.*

Manitoba Energy and Mines 1988a: Brandon, NTS 62G; Manitoba Energy and Mines, Mines Branch, Aggregate Resources Compilation Map AR88-1-3, UMA Engineering Limited (comp.), scale 1:250 000, URL <https://manitoba.ca/iem/info/libmin/ar/MAP_AR88-1-3.pdf> [September 2023].

Manitoba Energy and Mines 1988b: Dauphin Lake, NTS 62O; Manitoba Energy and Mines, Mines Branch, Aggregate Resources Compilation Map AR88-1-10, UMA Engineering Limited (comp.), scale 1:250 000, URL <https://manitoba.ca/iem/info/libmin/ar/MAP_AR88-1-10.pdf> [September 2023].

Manitoba Energy and Mines 1988c: Duck Mountain, NTS 62N; Manitoba Energy and Mines, Mines Branch, Aggregate Resources Compilation Map AR88-1-11, UMA Engineering Limited (comp.), scale 1:250 000, URL <https://manitoba.ca/iem/info/libmin/ar/MAP_AR88-1-11.pdf> [September 2023].

Manitoba Energy and Mines 1988d: Hecla, NTS 62P; Manitoba Energy and Mines, Mines Branch, Aggregate Resources Compilation Map AR88-1-9, UMA Engineering Limited (comp.), scale 1:250 000, URL <https://manitoba.ca/iem/info/libmin/ar/MAP_AR88-1-9.pdf> [September 2023].

Manitoba Energy and Mines 1988e: Kenora, NTS 52E; Manitoba Energy and Mines, Mines Branch, Aggregate Resources Compilation Map AR88-1-1, UMA Engineering Limited (comp.), scale 1:250 000, URL <https://manitoba.ca/iem/info/libmin/ar/MAP_AR88-1-1.pdf> [September 2023].

Manitoba Energy and Mines 1988f: Neepawa, NTS 62J; Manitoba Energy and Mines, Mines Branch, Aggregate Resources Compilation Map AR88-1-7, UMA Engineering Limited (comp.), scale 1:250 000, URL <https://manitoba.ca/iem/info/libmin/ar/MAP_AR88-1-7.pdf> [September 2023].

Manitoba Energy and Mines 1988g: Pointe Du Bois, NTS 52L; Manitoba Energy and Mines, Mines Branch, Aggregate Resources Compilation Map AR88-1-5, UMA Engineering Limited (comp.), scale 1:250 000, URL <https://manitoba.ca/iem/info/libmin/ar/MAP_AR88-1-5.pdf> [September 2023].

Manitoba Energy and Mines 1988h: Riding Mountain, NTS 62K; Manitoba Energy and Mines, Mines Branch, Aggregate Resources Compilation Map AR88-1-8, UMA Engineering Limited (comp.), scale 1:250 000, URL <https://manitoba.ca/iem/info/libmin/ar/MAP_AR88-1-8.pdf> [September 2023].

Manitoba Energy and Mines 1988i: Selkirk, NTS 62I; Manitoba Energy and Mines, Mines Branch, Aggregate Resources Compilation Map AR88-1-6, UMA Engineering Limited (comp.), scale 1:250 000, URL <https://manitoba.ca/iem/info/libmin/ar/MAP_AR88-1-6.pdf> [September 2023].

Manitoba Energy and Mines 1988j: Swan Lake, NTS 63C; Manitoba Energy and Mines, Mines Branch, Aggregate Resources Compilation Map AR88-1-12, scale 1:250 000, URL <https://manitoba.ca/iem/info/libmin/ar/MAP_AR88-1-12.pdf> [September 2023].

Manitoba Energy and Mines 1988k: Virden, NTS 62F; Manitoba Energy and Mines, Mines Branch, Aggregate Resources Compilation Map AR88-1-4, UMA Engineering Limited (comp.), scale 1:250 000, URL <https://manitoba.ca/iem/info/libmin/ar/MAP_AR88-1-4.pdf> [September 2023].

Manitoba Energy and Mines 1988l: Winnipeg, NTS 62H; Manitoba Energy and Mines, Mines Branch, Aggregate Resources Compilation Map AR88-1-2, scale 1:250 000, URL <https://manitoba.ca/iem/info/libmin/ar/MAP_AR88-1-2.pdf> [September 2023].

Mihychuk, M.A. and Groom, H.D. 1979: Quaternary geology of the Neepawa area–Arden (NTS 62J/5E and 62J/6W); Manitoba Department of Mines, Natural Resources and Environment, Mineral Resources Division, Preliminary Map 1979 PN-2, scale 1:50 000.

Ricketts, M.J. 2014: Granular-aggregate resources of the Stakit Lake map sheet (NTS 23J10); Government of Newfoundland and Labrador, Department of Natural Resources, Geological Survey, Map 2014-15, Open File 023J/10/0376, URL <https://www.gov.nl.ca/iet/files/mines-maps-surflab-images-map2014-15.pdf> [August 2023].

Sinclair, R.D. and Phimister, J.P. 1981: Sand and gravel inventory of the Westlake area; Manitoba Department of Energy and Mines, Mineral Resources Division, Open File Report OF81-2, 60 p., 7 maps, scale 1:50 000.

The UMA Group 1976: Aggregate resources of the Winnipeg region; Manitoba Mines, Resources and Environmental Management, Mineral Resources Division, Open File Report 77/4, URL <https://manitoba.ca/iem/info/libmin/OF77-4.pdf> [June 2023].

PUBLICATIONS

Data Repository Items

DRI2014001 (re-release)

Whole-rock geochemical data from pegmatites at South Bay, Southern Indian Lake and Partridge Breast Lake, and fluorine granite at Thorsteinson Lake, Manitoba (parts of NTS 64G3–6, 8, 9, 64B11)

by T. Martins

Microsoft® Excel® file supplements:

Martins, T. and Kremer, P.D. 2013: Rare-metals scoping study of the Trans-Hudson orogen, Manitoba (parts of NTS 64G3–6, 8, 9, 64B11); *in* Report of Activities 2013, Manitoba Mineral Resources, Manitoba Geological Survey, p. 114–122.

DRI2022002 (re-release)

Bedrock geochemistry from the Stuart Bay–Chickadee Lake area (east of Wekusko Lake), north-central Manitoba (parts of NTS 63J12, 13)

by K.D. Reid

Microsoft® Excel® file supplements:

Reid, K.D. 2019: Bedrock geological mapping of the Puella Bay area (Wekusko Lake), north-central Manitoba (part of NTS 63J12); *in* Report of Activities 2019, Manitoba Natural Resources and Northern Development, Manitoba Geological Survey, p. 42–51.

Reid, K.D. 2021: Results of bedrock geological mapping in the Stuart Bay–Chickadee Lake area (east of Wekusko Lake), north-central Manitoba (parts of NTS 63J12, 13); *in* Report of Activities 2021, Manitoba Natural Resources and Northern Development, Manitoba Geological Survey, p. 29–39.

DRI2023001

Sediment gold grain count data from the Little Bear Lake property (AFN 74096), southeastern Manitoba

By T.J. Hodder

DRI2023002

Field-based ice-flow data collected during the 1998 NATMAP II field season, southeastern Manitoba (parts of NTS 52L, 62I)

By G.L.D. Matile, L.H. Thorleifson, T.J. Hodder and A.B. Martin

DRI2023003

Sandilands rotosonic drillcore data, southeastern Manitoba (parts of NTS 52E, 62H)

By G.L.D. Matile, M.S. Gauthier and M.P.B. Nicolas

DRI2023004

Till-matrix geochemistry data from the Gillam area, northeastern Manitoba: additional 2022 data (NTS 54D5–8, 64A2)

By M.S. Gauthier and T.J. Hodder

DRI2023005

Rotosonic borehole stratigraphy, southeastern Manitoba (parts of NTS 52E, 62H)

By G.L.D. Matile, H. Thorleifson and M.S. Gauthier

DRI2023006

Salvaged diamond-drillcore at the Thompson Facility and Compound, from east-central Manitoba (parts of NTS 54C, 63P, 64A)

by C.G. Couëslan

Microsoft® Excel® file supplements:

Couëslan, C.G. 2023: Thompson Facility and Compound core recovery project, east-central Manitoba (parts of NTS 54C, 63P, 64A); *in* Report of Activities 2023, Manitoba Economic Development, Investment, Trade and Natural Resources, Manitoba Geological Survey, p. 90–92.

DRI2023008

Till geochemistry and heavy mineral analyses (gold, MMSIM®, visual KIM) from three sections near the confluence of the Hayes and Gods rivers, northeastern Manitoba (part of NTS 54C7)

by M.S. Gauthier and T.J. Hodder

DRI2023009

Quaternary field site data collected during the 1993–1994 NATMAP field seasons, southeastern Manitoba (parts of NTS 52E, 62A, H)

by G.L.D. Matile, L.H. Thorleifson, A.B. Martin and T.J. Hodder

DRI2023010

Quaternary field site data collected during the 1997–1998 NATMAP field seasons, southeastern Manitoba (parts of NTS 52L, 62H, I)

by G.L.D. Matile, L.H. Thorleifson, A.B. Martin and T.J. Hodder

DRI2023011

Gold and indicator-mineral data derived from glacial sediments (till) in southeastern Manitoba (parts of NTS 52L, 62P, 63A): 2022 pilot study results

by T.J. Hodder

Microsoft® Excel® file supplements:

Hodder, T.J. and Martins, T. 2023: Current Quaternary geology investigations in southeastern Manitoba and implications for mineral exploration (parts of NTS 52L, 62P, 63A); *in* Report of Activities 2023, Manitoba Economic Development, Investment, Trade and Natural Resources, Manitoba Geological Survey, p. 105–119.

DRI2023012

Field-based ice-flow–indicator data collected during 2023 field season in southeastern Manitoba (parts of NTS 52L, M)

by T.J. Hodder and M.S. Gauthier

Microsoft® Excel® file supplements:

Hodder, T.J. and Martins, T. 2023: Current Quaternary geology investigations in southeastern Manitoba and implications for mineral exploration (parts of NTS 52L, 62P, 63A); *in* Report of Activities 2023, Manitoba Economic Development, Investment, Trade and Natural Resources, Manitoba Geological Survey, p. 105–119.

DRI2023013

Geochemical data of gabbroic rocks from the Lynn Lake greenstone belt, northwestern Manitoba (parts of NTS 64C10–12, 14–16)

by X.M. Yang

Microsoft® Excel® file supplements:

Yang, X.M. 2023: Field relationships, geochemical characteristics and metallogenic implications of gabbroic intrusions in the Paleoproterozoic Lynn Lake greenstone belt, northwestern Manitoba (parts of NTS 64C10–12, 14–16); *in* Report of Activities 2023, Manitoba Economic Development, Investment, Trade and Natural Resources, Manitoba Geological Survey, p. 73–89.

DRI2023014

Rock Volatiles Stratigraphy data from drill cuttings from three oil wells in southwestern Manitoba (parts of NTS 62F2, K3)

by M.P.B. Nicolas, C.M. Smith and M.P. Smith

Microsoft® Excel® file supplements:

Nicolas, M.P.B., Smith, C.M. and Smith, M.P. 2023: Volatiles analysis of drill cuttings to evaluate the helium prospectivity of southwestern Manitoba (parts of NTS 62F2, K3); *in* Report of Activities 2023, Manitoba Economic Development, Investment, Trade and Natural Resources, Manitoba Geological Survey, p. 93–104.

GeoFile

GeoFile 6-2023

Manitoba radiocarbon ages

by M.S. Gauthier

Geoscientific Paper

GP2023-1

Metamorphic map of the Flin Flon domain, west-central Manitoba (parts of NTS 63J, K, N, O)

by M. Lazzarotto, D.R.M. Pattison, S. Gagné and C.G. Couëslan

Open Files

OF2022-2 (re-release)

Bedrock geology of Manitoba

by Manitoba Geological Survey (scale 1:1 000 000)

OF2022-3

Progress report on the study of granitoids in Manitoba: petrogenesis and metallogeny

by X.M. Yang

OF2023-1

Indicator mineral and gold grain data from till sampled in the Churchill to Little Churchill rivers area, northeastern Manitoba

by T.J. Hodder and M.S. Gauthier

OF2023-2

Age and petrology of zirconium- and light rare-earth element–enriched quartz monzonite in drillcore from the Huzyk Creek property, sub-Phanerozoic Kisseynew domain, central Manitoba (NTS 63J6)

by C.G. Couëslan

OF2023-3

Quaternary site data, till composition and ice-flow indicators in the Roseau River area, southeastern Manitoba (parts of NTS 62H2, 7)

by M.S. Gauthier and T.J. Hodder

Breasley, C.M., Groat, L.A., Martins, T., Linnen, R.L., Moser, D., Landry, E., Hutchins, A., Deveau, C. and Barker, I. 2023: Trace element geochemistry, quantitative analyses, and origins of spodumene and quartz intergrowth textural groups at the Tanco pegmatite, Manitoba; Geological Association of Canada–Mineralogical Association of Canada, Joint Annual Meeting, May 24–29, 2023, Sudbury, Ontario, oral presentation.

Breasley, C.M., Martins, T., Deveau, C., Hutchins, A., Linnen, R.L., Groat, L.A., Landry, E.M.K. and Moser, D. 2023: Mining and processing of micro spodumene-quartz intergrowths at the Tanco pegmatite, Manitoba; Prospectors & Developers Association of Canada, PDAC 2023, March 5–8, 2023, Toronto, Ontario, poster presentation.

Breasley, C.M., Martins, T., Deveau, C., Hutchins, A., Linnen, R.L., Groat, L.A., Landry, E.M.K. and Moser, D. 2023: The geochemistry, origins and implications for mining and processing of micro spodumene-quartz intergrowths at the Tanco pegmatite, Manitoba; Association for Mineral Exploration, AME Roundup, January 23–26, 2023, Vancouver, British Columbia, poster presentation.

Chinaglia, S., Miles, A., Martins, T., Groat, L. and Goodenough, K. 2023: Field observations on pegmatites from Araçuaí (Brazil): structural control and mineralogy; Geological Association of Canada–Mineralogical Association of Canada, Joint Annual Meeting, May 24–29, 2023, Sudbury, Ontario, Program with Abstracts, v. 46, and poster presentation.

Couëslan, C.G. 2023: The Pikwitonei Granulite Domain, Manitoba: a large-hot orogen along the northwestern margin of the Superior craton; Geological Association of Canada–Mineralogical Association of Canada, Joint Annual Meeting, May 24–29, 2023, Sudbury, Ontario, Program with Abstracts, v. 46.

Dias, F., Lima, A., Roda-Robles, E. and Martins, T. 2023: Li-exploration and processing: the case study of spodumene from the Barroso-Alvão field, northern Portugal; Geological Association of Canada–Mineralogical Association of Canada, Joint Annual Meeting, May 24–29, 2023, Sudbury, Ontario, Program with Abstracts, v. 46.

Dias, F., Lima, A., Roda-Robles, E. and Martins, T. 2023: Textural and mineralogical characterization of one lithium deposit, from the Barroso-Alvão aplite-pegmatite field: preliminary study; Society of Economic Geologists, SEG 2023 Conference, August 26–29, 2023, London, England, poster presentation.

Dias, F., Ribeiro, R., Gonçalves, F., Lima, A., Roda-Robles, E. and Martins, T. 2023: Calibrating a handheld LIBS for Li exploration in the Barroso–Alvão aplite-pegmatite field, northern Portugal: textural precautions and procedures when analyzing spodumene and petalite; Minerals, v. 13, art. 470, URL <https://doi.org/10.3390/min13040470>.

Dias, F., Ribeiro, R., Soares, F., Lima, A., Roda-Robles, E. and Martins, T. 2023: Calibrating a handheld LIBS SciAps Z300 to analyze spodumene and petalite for Li-exploration in the Barroso-Alvão aplite-pegmatite field, northern Portugal; EMS LIBS 2023, September 4–7, 2023, Porto, Portugal, poster presentation.

Dias, F., Ribeiro, R., Soares, F., Lima, A., Roda-Robles, E. and Martins, T. 2023: Evaluating the purity of the NIST standard reference material 182 (petalite) when compared with the petalite from the Barroso-Alvão field, Portugal; Mineral Deposits Studies Group, Annual Meeting, January 4–6, 2023, Leicester, England, poster presentation.

Errandonea-Martin, J., Roda-Robles, E., Garate-Olave, I., Menuge, J.F., Müller, A., Pesquera, A., Martins, T. and Lima, A. 2023: Exometasomatism prompted by spodumene-bearing pegmatites and its implications in lithium exploration: the case study from Alijó (northern Portugal); Geological Association of Canada–Mineralogical Association of Canada, Joint Annual Meeting, May 24–29, 2023, Sudbury, Ontario, poster presentation.

Hart, B.S., Hofmann, M., Plint, G. and Nicolas, M. 2022: Shale compositional trends in the Cenomanian–Turonian Cretaceous Western Interior Seaway: facies and sequence stratigraphic models; *in* The Cenomanian-Turonian Stratigraphic Interval across the Americas: Argentina to Alaska, J. Macquaker, P. Markwick, K.J. Whidden and J. Suter (ed.), Proceedings of the 38th annual GCSSEPM Foundation Perkins-Rosen Research Conference and Core Workshop, December 5–9, 2022, Houston, Texas, p. 105–119.

Hodder, T.J., Gauthier, M.S., Ross, M. and Grunsky, E. 2023: Discriminating tills of mixed provenance in central Canada to decipher the influence of two major ice dispersal centres of the Laurentide Ice Sheet; International Union for Quaternary Research, XXI Inqua Congress, July 14–20, 2023, Rome, Italy, poster presentation.

Hodder, T.J., Gauthier, M.S., Ross, M. and Lian, O.B. 2023: Was there a nonglacial episode in the western Hudson Bay Lowland during Marine Isotope Stage 3?; Quaternary Research, v. 116, p. 148–161, URL <https://doi.org/10.1017/qua.2023.35>.

Hodder, T.J., Gauthier, M.S., Ross, M., Lian, O.B., Schaarschmidt, M. and Dalton, A.S. 2023: Constraining the evolution of the Laurentide Ice Sheet through multiple glacial-interglacial cycles in central Canada; International Union for Quaternary Research, XXI Inqua Congress, July 14–20, 2023, Rome, Italy, oral presentation.

Koopmans, L., Martins, T., Linnen, R., Gardiner, N.J., Breasley, C.M., Palin, R.M., Groat, L., Silva, D. and Robb, L.J. 2023: The formation of lithium-rich pegmatites through multi-stage melting; Geological Society of America, Geology, URL <https://doi.org/10.1130/G51633.1>.

Lawley, C.J.M., Schneider, D.A., Camacho, A., McFarlane, C.R.M., Davis, W.J. and Yang, X.M. 2023: Post-orogenic exhumation triggers gold mineralization in the Trans-Hudson orogen: new geochronology results from the Lynn Lake greenstone belt, Manitoba, Canada; Precambrian Research, v. 395, art. 107127, URL <https://doi.org/10.1016/j.precamres.2023.107127>.

Martins, T. 2023: Lithium in Manitoba, production and exploration potential; Society of Economic Geologists, SEG 2023 Conference, August 26–29, 2023, London, England, abstract and oral presentation.

Martins, T. 2023: Pegmatites: concepts and exploration techniques; Critical Minerals Conference, June 26–27, 2023, Kelowna, British Columbia, oral presentation.

McMartin, I., Gauthier, M.S. and Page, A.V. 2022: Updated post-glacial marine limits along western Hudson Bay, central mainland Nunavut and northern Manitoba; Geological Survey of Canada, Open File 8921, 19 p.

Nicolas, M.P.B. 2023: Bakken and Torquay formations in southwestern Manitoba; American Association of Petroleum Geologists, Rocky Mountain Section, 2023 Williston Basin Core Workshop, June 3–4, 2023, Bismarck, North Dakota, program book, p. 173–185.

Nicolas, M.P.B. 2023: Helium potential of southwestern Manitoba, Canada; Rocky Mountain Association of Geologists, 2023 North American Helium Conference, March 22–23, 2023, Westminster, Colorado, Program Book 3.7.23, p. 49–50.

Ren, Y., Yang, X.Y., Yang, X.M., Ling, M. and Liu, Y. 2023: Mineralogical study on the distribution regularity of niobium in various types of ores in the giant Bayan Obo Fe-REE-Nb deposit; Ore Geology Reviews, v. 161, art. 105602, URL <https://doi.org/10.1016/j.oregeorev.2023.105602>.

Ribeiro, R., Dias, F., Soares, F., Lima, A., Roda-Robles, E. and Martins, T. 2023: Handheld LIBS analysis in Li-minerals from the Barroso-Alvão Field, in Portugal; International Workshop on the Characterisation and Quantification of Lithium, from the Micro- to the Nano-Scale, from Mining to Energy, June 26–27, 2023, Paris, France, poster presentation.

Schaarschmidt, M., Lian, O.B., Hodder, T.J., Gauthier, M.S., Ross, M., Brewer, V. and Ferguson, N. 2023: Assessing the timing of the extent of the Laurentide Ice Sheet using optical dating of quartz, Hudson Bay Lowland, Manitoba, Canada; 17th International Luminescence and Electron Spin Resonance Dating Conference, June 25–30, 2023, Copenhagen, Denmark, oral presentation.

Silva, D., Groat, L., Martins, T. and Linnen, R. 2023: Structural controls on the origin and emplacement of lithium-bearing pegmatites; The Canadian Journal of Mineralogy and Petrology, v. 61.

Silva, D., Martins, T., Groat, L. and Linnen, R., 2023: Emplacement controls of Li pegmatites in Wekusko Lake pegmatite field, Manitoba; Association for Mineral Exploration, AME Roundup, January 23–26, 2023, Vancouver, British Columbia, poster presentation.

Silva, D., Martins, T., Groat, L. and Linnen, R. 2023: Preliminary observations on emplacement controls and Li mineral partition of pegmatite dikes from the Wekusko Lake pegmatite field, central Manitoba; Geological Association of Canada–Mineralogical Association of Canada, Joint Annual Meeting, May 24–29, 2023, Sudbury, Ontario, Program with Abstracts, v. 46, and oral presentaion.

Zhao, Y., Lyu, J., Han, X., Lin, S., Zhang, P., Yang, X.M. and Chen, C. 2023: Geochronology and geological implications of Paleoproterozoic post-collisional monzogranitic dykes in the Ne Jiao-Liao-Ji Belt, North China Craton; Minerals, v. 13, art. 928, URL <https://doi.org/10.3390/min13070928>.